eman ta zabal zazu

Universidad del País Vasco
Euskal Herriko Unibertsitatea

REGULATION OF INFLAMMATORY PROCESSES BY CERAMIDE KINASE AND PHOSPHATIDYLETHANOLAMINE *N*-METHYLTRANSFERASE IN LUNG CELLS, ADIPOCYTES AND LIVER TISSUE

DOCTORAL THESIS
"INTERNATIONAL DOCTOR MENTION"

Natalia Presa Torre

MAY 2019

Index

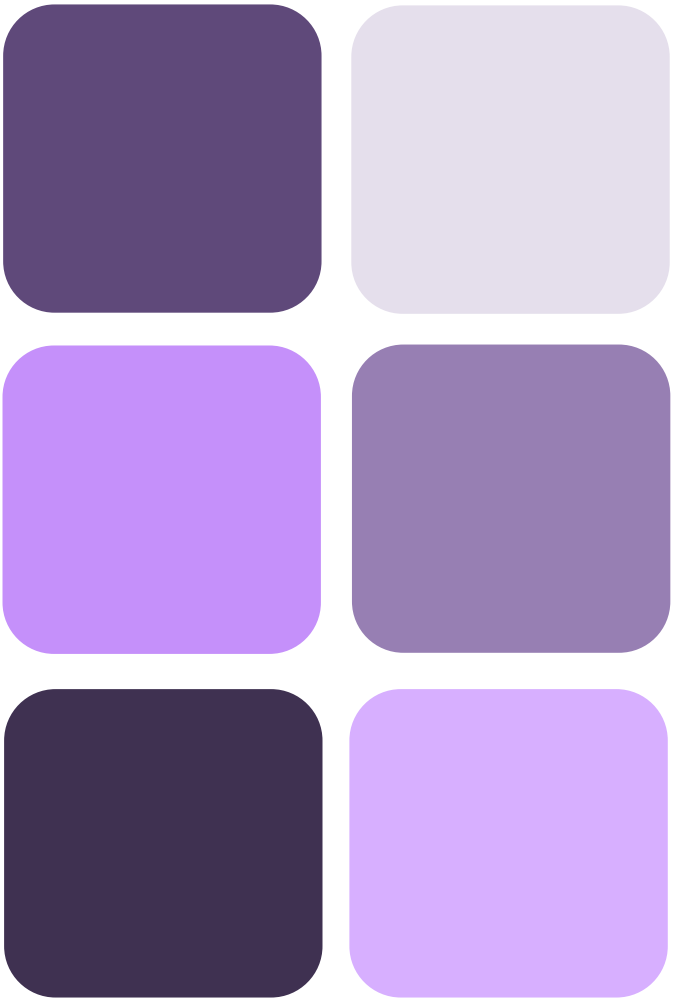

Index

Abstract

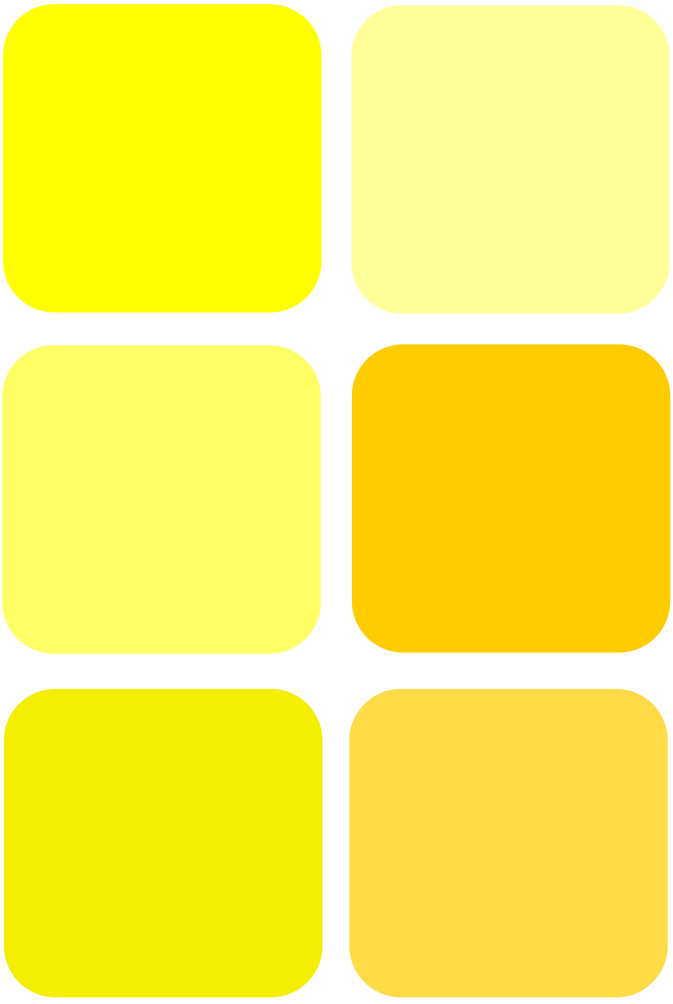

Abstract

The World Health Organization (WHO) ranks chronic inflammatory diseases as the greatest threat to human health, and their prevalence is estimated to increase constantly for the next 30 years. Nowadays, around 60% of the world's population dies from chronic inflammatory conditions, such as chronic respiratory diseases, obesity, fatty liver disease and cancer. All of these pathologies are associated with alterations in sphingolipid metabolism. Thus, understanding the mechanisms responsible for the establishment and evolution of those diseases may be useful for developing novel strategies to control their development and progression. In this thesis, we demonstrate that ROCK1 is a key regulatory enzyme necessary for cigarette smoke extract (CSE)-induced monocyte chemoattractant protein-1 (MCP-1) release in lung epithelial cells, and that AKT2 and the Ceramide Kinase (CerK)/ ceramide 1-phosphate (C1P) axis elicit opposite effects; this points to an anti-inflammatory role of C1P in the lungs. Also, this work provides evidence suggesting that adipogenesis is associated with an increase in phosphatidylethanolamine *N*-methyltransferase-2 (PEMT-2) protein expression, whose depletion leads to impaired adipocyte differentiation, as can be deduced from the observed decrease of adipogenic markers expression, and reduced lipid droplet formation, triglyceride (TG) content and leptin release. It is also demonstrated in this thesis that inhibition of adipocyte differentiation by exogenous C1P occurs through modulation of PEMT expression. Additionally, an abnormal sphingolipid metabolism in *Pemt*$^{-/-}$ mice fed a HFD, with elevation of ceramides, sphingomyelin, sphinganine, sphingosine, 1-deoxyceramides, and C26:1 C1P, as well as higher expression of mRNAs for acid ceramidase (Asah1) and ceramide kinase (CerK) has been observed. Interestingly, treatment with vitamin E (0.5 g/kg) for 3 weeks improved VLDL-TG secretion and normalized cholesterol metabolism, although it failed to reduce hepatic TG content. Vitamin E treatment also reduced hepatic oxidative stress, inflammation and fibrosis, and restored Asah1 and CerK mRNA and sphingolipid levels, suggesting that vitamin E treatment can efficiently prevent the progression from simple steatosis to steatohepatitis in mice lacking PEMT, and that sphingolipid metabolites and Asah1 and CerK may be important factors in this action.

Abbreviations

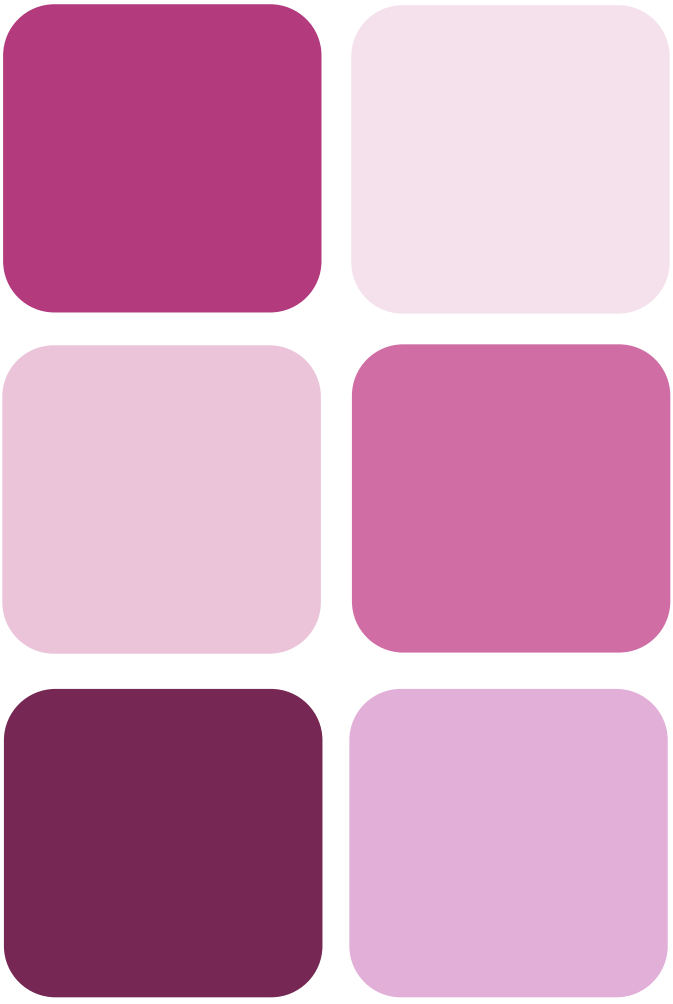

Abbreviations

AA	Arachidonic acid
ABTS	2,2'-Azino-bis(3-ethylbenzothiazoline-6-sulfonic acid)
ADP	Adenosine diphosphate
AIM	Adipogenesis induction medium
ANOVA	Analysis of variance
Apo	Apolipoprotein
Asah	Acid ceramidase
ASMase	Acidic sphingomyelinase
ATP	Adenosine triphospate
Bad	Bcl-2-associated death
BAL	Bronchoalveolar lavage
Bcl2	B-cell lymphoma-2
BiP	Binding immunoglobulin protein
BMDM	Bone marrow-derived macrophages
BMI	Body mass index
BSA	Bovine serum albumin
C/EBP	CCAAT/enhancer binding protein
C1P	Ceramide 1-phosphate
C1PP	Ceramide 1-phosphate phosphatase
CD	Cluster of differentiation
CDase	Ceramidase
CEPT	1,2-diacylglycerol choline/ethanolamine phosphotransferase
Cer	Ceramide
CerK	Ceramide kinase
CerS	Ceramide synthase
CERT	Ceramide transfer protein

CHOP	CCAAT-enhancer-binding protein homologous protein
CK	Choline kinase
CM	Conditioned medium
CoA	Coenzyme A
COL1A1	Alpha-1 type I collagen
COPD	Chronic obstructive pulmonary disease
cPLA	Group IV cytosolic phospholipase A2
CPTP	Ceramide-1-phosphate transfer protein
CREB	cAMP response element-binding protein
CS	Cigarette smoke
CSE	Cigarette smoke extract
CTP	1,2-diacylglycerol cholinephosphotransferase
DAG	Diacylglycerol
DAOS	3,5-Dimethoxy-N-athyl-N-(2-hydroxy-3-sulfopropyl)-aniline sodium salt
DES	Desaturase
dhCer	Dihydroceramide
dhSph	Dihydrosphingosine
DNA	Deoxyribonucleic acid
DNAse	Deoxyribonuclease
dNTP	Deoxynucleotide triphosphate
DTT	Dithiothreitol
ECM	Extracellular matrix
EDTA	Ethylenediaminetetraacetic acid
ELISA	Enzyme-linked immunosorbent assay
EMT	Epithelial to mesenchymal transition
ER	Endoplasmic reticulum
ERK	Extracellular signal-regulated kinase
FABP	Fatty acid binding protein
FBS	Fetal bovine serum
GAPDH	Glyceraldehide 3-phosphate dehydrogenase
GLUT	Glucose transporter
GM	Growth medium
GPCR	G-protein-coupled receptor

GPx	Glutathione peroxidase
GR	Glutathione reductase
GSH	Glutathione
GSK3β	Glycogen synthase kinase 3 β
GSL	Glycosphingolipid
GSSG	Oxidized glutathion
HDL	High density lipoprotein
HEPES	4-(2-hydroxyethyl)-1-piperazineethanesulfonic acid
HFD	High fat diet
HMOX	Heme oxygenase
HPLC	High-performance liquid chromatography
HRP	Horseradish peroxidase
IBMX	3-isobutyl-1-methylxanthine
IL	Interleukin
INF	Interferon
iNOS	Inducible nitric oxide synthase
IU	International unit
JAK	Janus Kinase
JNK	c-Jun N-terminal kinase
KLF	Kruppel-like factor
KO	Knock out
LDL	Low-density lipoprotein
LPL	Lipoprotein lipase
LPP	Lipid phosphate phosphatase
LPS	Lipopolysaccharide
MAPK	Mitogen-activated protein kinase
MCE	Mitotic clonal expansion
MCP-1	Monocyte chemoattractant protein 1
MDA	Malondialdehyde
MEK	Mitogen-activated kinase
MHC	Major histocompatibility complex
MMP	Matrix metalloproteinase
mRNA	Messenger ribonucleic acid
mTOR	Mammalian target of rapamycin

MTS	[3-(4,5-dimethyl-2-yl)-5-(3-carboxymethoxyphenyl)-2-(4-sulfophenyl)-2H-tetrazolium
NADPH	Nicotinamide adenine dinucleotide
NAFLD	Non-alcoholic fatty liver disease
NASH	Non-alcoholic steatohepatitis
NBCS	Newborn Calf Serum
NBD	7-nitro-2,1,3-benzoxadiazol-4-yl
NFκB	Nuclear factor kappa-light-chain-enhancer of activated B cells
NK cells	Natural Killer cells
NO	Nitric oxide
NOX	NADPH oxidase
NSCLC	Non-small-cell lung cancer
NSMase	Neutral sphingomyelinase
OptiMEM	Modification of Eagle's minimal essential medium
PA	Phosphatidic acid
PAGE	Polyacrylamide gel electrophoresis
PARP	Poly (ADP-ribose) polymerase
PBS	Phosphate-buffered saline
PC	Phosphatidylcholine
PCR	Polymerase chain reaction
PDI	Protein disulfide-isomerase
PE	Phosphatidylethanolamine
PEMT	Phosphatidylethanolamine *N*-Methyltransferase
PI3K	Phosphatidylinositol-4,5-bisphosphate 3-kinase
PIC	Pretease inhibitior cocktail
PKB/Akt	Protein kinase B
PKC	Protein kinase C
PMSF	Phenylmethylsulfonyl fluoride
PP	Protein phosphatase
PPAR	Proliferator-activated receptor
Ptx	Pertussis toxin
PVDF	Polyvinylidene difluoride
qPCR	Quantitative polymerase chain reaction
RhoA	Ras homolog A

RISCs	RNA-induced silencing complexes
RNA	Ribonucleic acid
RNAi	Ribonucleic acid interference
RNAse	Ribonuclease
ROCK	Rho-associated protein kinase
ROS	Reactive oxygen species
RT-PCR	Retrotranscription polymerase chain reaction
S1P	Sphingosine 1-phosphate
S1PR	S1P receptor
SCLC	Small-cell lung cancer
SDS	Sodium dodecyl sulphate
SEM	Standard error of the mean
siRNA	Small interfering ribonucleic acid
SM	Sphyngomyelin
SMase	Sphyngomyelinase
SMS	Sphingomyelin synthase
Spa	Sphinganine
Sph	Sphingosine
SphK	Sphingosine kinase
SPP	Sphingosine phosphatases
SPT	Serine palmitoyltransferase
SR-B1	Scavenger receptor, class B type 1
STAT	Signal transducer and activator of transcription
T2D	Type 2 diabetes
TBA	Thiobarbituric acid
TBARS	Thiobarbituric acid reactive substances
TBS	Tris-buffered saline
TG	Triglyceride
TGFβ	Transforming growth factor β
TIMP	Tissue inhibitor of metalloproteinase
TLC	Thin layer chromatography
TMB	3,3′,5,5′-Tetramethylbenzidine
TNFα	Tumor necrosis factor α
UCP	Uncoupled protein

VEGF	Vascular endothelial growth factor
Vit	Vitamin
VLDL	Very low-density lipoprotein
WHO	World Health Organization
WT	Wild type

Introduction

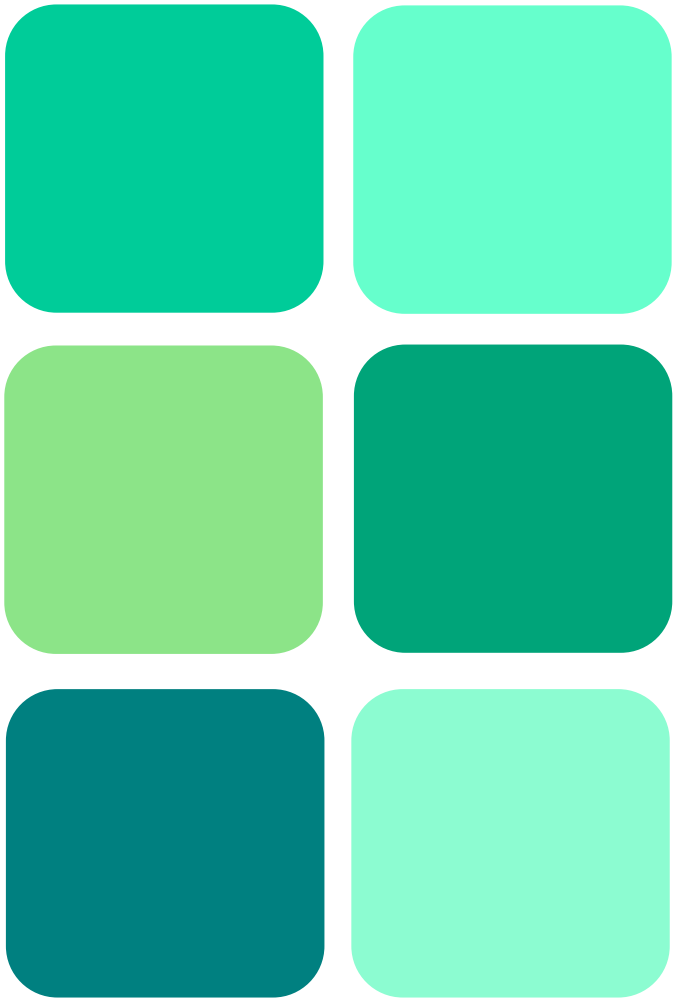

Introduction

1. Cell homeostasis

When all forces in a system are balanced to the point where no change occur the system is said to be in a state of *static equilibrium*. This fully obeys the laws of thermodynamics, which establish that all systems in the universe tend imperatively to increase their equilibrium, or absolute stability. In contrast to stable systems that are in thermodynamic equilibrium, systems that are far from equilibrium are inherently unstable.

Living organisms are open systems that are never at equilibrium until they die, so the understanding of death is the absolute stability. Living organisms create internal organization thanks to a continuous flow of energy known as *dynamic equilibrium* or steady state. This dynamic equilibrium is actively regulated by living systems in order to avoid being affected by external changes. The difference between a living and a non-living organism is the ability to regulate its internal environment. This active regulation is also known as homeostasis. Homeostasis is the condition of dynamic equilibrium between at least two system variables, and it is an indispensable ability for the continuance of life. The capacity of maintaining the internal organization and characteristics despite the always-varying external environment is what discerns life from death.

Living organisms must be able to detect internal or external changes and activate the control mechanisms by which they can restore homeostasis. Strictly regulated and highly complex cellular signaling processes make homeostasis possible. Alterations in any of these processes lead to metabolic dysfunctions and health disorders as a result of homeostatic imbalance or an inability of the body to restore a functional and stable internal environment [1, 2].

In multicellular organisms, the immune system is a key factor for controlling tissue and cell homeostasis.

2. The immune system

Inflammation is one of the best-known pathophysiological processes and represents a well-conserved mechanism evolved by vertebrates as an adaptive and defensive response to tissue injury and invasion of microorganisms that might attempt to colonize the host. The immune reaction comprises a series of events triggered in response to recognition of pathogens or tissue damage, involving cells and soluble mediators, such as cytokines, of the innate and adaptive immune system. The main purpose of this inflammatory response is to remove the foreign agent disturbing tissue homeostasis. In the normal physiological context, after tissue repair or pathogen elimination, inflammation is resolved and the homeostatic state is recovered.

All cells of the immune system originate from hematopoietic stem cell in the bone marrow, which gives rise to two major lineages: a myeloid progenitor cell and a lymphoid progenitor cell. These two progenitors give rise to the myeloid cells (megakaryocytes, monocytes, macrophages, granulocytes and dendritic cells) and lymphoid cells (T and B-lymphocytes and natural killer (NK) cells), respectively. These cells conform the cellular components of the innate (non-specific) and adaptive (specific) immune systems.

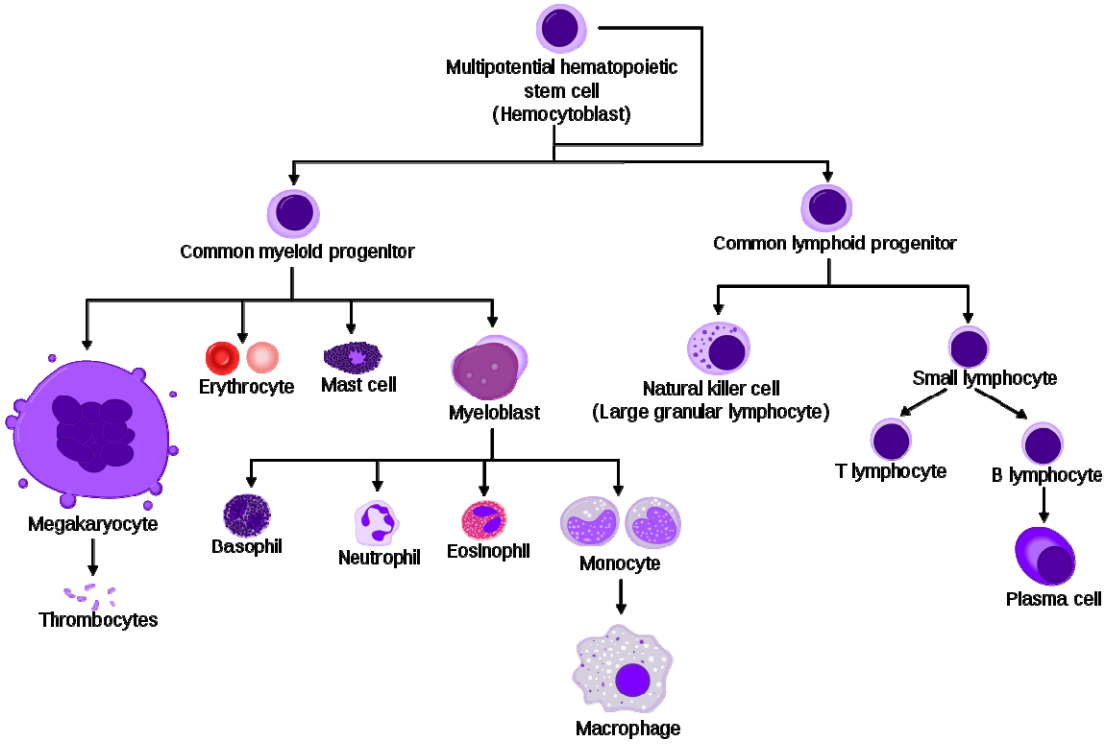

Figure 1: Normal human hematopoietic process.

2.1. The innate immune system

The innate immune system is a general defense against pathogens or damage stimuli that acts in a non-specific way. The elements of the innate immune system include the skin and mucous membranes in the body openings that act as anatomical barriers, secreted molecules that can be found in the blood and in body fluids, and cellular components, mainly leukocytes. Production of chemokines, activation of the complement cascade and activation of adaptive immune cells by antigen presentation are the most important functions of innate immune system.

When, despite body barriers, pathogens make it pass the skin or mucous membranes and enter the body, the second line of defense comes into action. Inflammatory cells move to the site of infection and are activated. Soluble protein substances are activated too and help to protect the organism. This leads to an inflammatory reaction that promotes swelling and heat. If bacteria or viruses manage to enter the body, macrophages and granulocytes enclose and digest them in their interior.

The natural killer cells are the third important part of the innate immune system. These cells are specialized in detecting virus-infected or tumorous cells by looking for changes in their cell surface and dissolving them using cytotoxins.

2.2. The adaptive immune system

When the innate immune system is unsuccessful in destroying the pathogens, the adaptive immune response sets in. Adaptive immune system is composed of specialized cells and mechanisms able to recognize and eliminate pathogens efficiently. Even though it takes longer than the innate response, adaptive immune response targets the pathogen more accurately and specifically, and it is able to create memory cells for each eliminated pathogen so that a second exposure to the same antigen will originate a faster, stronger and more efficient response.

Adaptive immune system has several parts that react in different ways, depending on the site of the organism where the infection occurs. The parts of adaptive defense include T-lymphocytes, B-lymphocytes, antibodies and soluble proteins in the blood, and cytokines. Lymphocytes are the central core of all immune responses. They originate from stem cells in the bone marrow and mature either in the bone marrow (B-lymphocytes) or in the thymus (T-lymphocytes). B-lymphocytes will develop to form

plasmatic cells and are responsible for the production of specific antibodies. T-lymphocytes will then give rise to two different populations: cytotoxic lymphocytes, responsible for cell-mediated immune responses, and helper T-lymphocytes, which regulate the immune system, governing the quality and strength of all immune responses.

3. Chronic inflammation

Overall, a normal acute inflammatory response begins with the production of chemical agents by cells in the infected, injured or diseased tissue. These agents will cause redness, swelling, heat and loss of function. Inflamed tissues will then create additional signals that recruit leukocytes to the site of inflammation, which will destroy any infective or injurious agent, and will remove cellular debris from damaged tissue. Acute inflammation is active for a short period of few days. In first instance, inflammation is a beneficial process, serving to immobilize the area of injury as the rest of the immune system mobilizes to heal. However, regardless of the underlying initiating cause, when an infectious or assaulting agent is inadequately cleared and persists in tissue, or inflammation is not properly extinguished due to impaired resolution and a tissue is subjected to ingoing damage, it turns into chronic inflammation, resulting in aberrant tissue remodeling and organ dysfunction [3]. In chronic inflammation, the inflammation becomes the problem rather than the solution to infection, injury or disease. Chronically inflamed tissues continue to generate signals that attract leukocytes from the bloodstream. When leukocytes migrate from the bloodstream into the tissue, they amplify the inflammatory response, and this chronic inflammatory response can break down healthy tissue in a misdirected attempt at repair and healing.

Chronic inflammatory diseases are the most significant cause of death in the world. The World Health Organization (WHO) ranks chronic diseases as the greatest threat to human health. The prevalence of diseases associated with chronic inflammation is estimated to increase constantly for the next 30 years. In fact, worldwide, 3 out of 5 people die due to chronic inflammatory diseases such as neurological disorders, including Parkinson's or Alzheimer's diseases, inflammatory bowel disease, rheumatoid arthritis, atherosclerosis, obesity, type II diabetes, chronic obstructive pulmonary disease, asthma, or cancer [4-6].

Endogenous lipids are possibly the most important mediators not only to be implicated in all phases of inflammation, but also to be involved in the regulation of its course and ending. Indeed, many lipids besides being major constituents of cell membranes and very efficient sources of energy, can also act as key physiological mediators of several intercellular and intracellular processes. Thus, during the past two decades, they have been termed 'bioactive lipids' due to their pivotal role in immune regulation, inflammation and maintenance of tissue homeostasis. Thus, it seems that bioactive lipids are largely involved in managing inflammation, acting as either activators or repressors of the inflammatory response.

4. Sphingolipids

Discovered in 1884, sphingolipids were described as enigmatic compounds just like the Greek sphinx, as neurochemist J.L.W Thudichum thought. Most of them were first discovered in the brain, thus giving rise to names such as sphingomyelin and cerebrosides. Now we know that sphingolipids are ubiquitous in eukaryotic cells as fundamental components of the cell membranes [7]. Research from late 1980's and 1990's provided unequivocal evidence that sphingolipids, besides having an structural role, also function as vital signaling molecules [8]. Sphingolipids are defined by the presence of a backbone called sphingoid base, a long chain amino alcohol (Fig. 2). They are long-chain aliphatic amines, containing two or three hydroxyl groups, and often a distinctive trans-double bond in position 4. The most regular type of sphingolipid bases in animal tissues and humans are sphingosines (Sph) and its saturated analogue dihydrosphingosine (dhSph) or sphinganine (Spa). There are some patterns that define the association between specific components of these sphingoid bases, but the potential number of combinations gives an idea of the complexity that these lipids can reach [9].

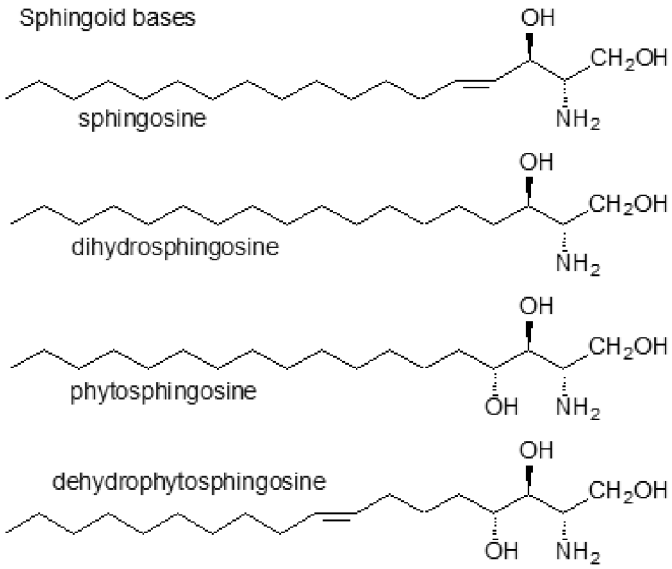

Figure 2: Structure of four different sphingoid bases. Taken from AOCS Lipid Library.

4.1. Metabolism of sphingolipids

The central core of sphingolipid metabolism is ceramide (Cer). Despite being essential in cell membrane architecture, it also plays a fundamental role as signaling molecule in different processes such as proliferation, differentiation, adhesion, migration or apoptosis. Ceramides are composed of a sphingosine backbone with a fatty acid residue usually ranging from 16 to 24 carbons in length, and thus, they can be classified according to the length of the fatty acid residue and the number of unsaturations [10]. Besides, each organism or tissue can synthesize different ceramide species.

Ceramides can be synthesized by four different pathways involving different cell compartments: the *de novo* synthesis pathway, the sphingomyelinase (SMase) pathway, the salvage pathway, and the neutral ceramidase pathway.

a) The *de novo* synthesis pathway:

This anabolic pathway takes place in the endoplasmic reticulum (ER) [11] and begins with the condensation of serine and pamitoyl-CoA to form 3-ketosphinganine in a reaction catalyzed by serine palmitoyltransferase (SPT), the rate limiting enzyme of this pathway. This reaction is followed by a rapid reduction to form sphinganine, through the action of 3-ketosphingosine reductase. Upon N-acylation by ceramide synthase (CerS), sphinganine is transformed into dihydroceramide (dhCer). Then a desaturase (DES) catalyzes the last step of this pathway by the introduction of a double

bond in position 4-5 trans into dihydroceramide molecule to generate ceramide. Once synthesized, ceramides have to be transported to the Golgi apparatus, where the synthesis of complex sphingolipids, such as sphingomyelin (SM) and glycosphingolipids (GSLs), takes place.

b) The sphingomyelinase (SMase) pathway:

The second major mechanism for ceramide formation is a catabolic pathway that generates phosphorylcholine and ceramide directly from degradation of sphingomyelin at the plasma membrane or in lysosomes. This reaction is catalyzed by one of several sphingomyelinases (SMases). Five types of sphingomyelinases can be distinguished by their pH optima, metal ion requirement for activity, and subcellular distribution: acid lysosomal SMase (ASMase), Zn^{2+} dependent secreted form of ASMase, neutral Mg^{2+} dependent SMase (NSMase), neutral Mg^{2+} independent SMase, and alkaline SMase [12, 13]. Since sphingomyelin is the most abundant sphingolipid in mammalian cells, its ability to form ceramides in considerably high. The opposite reaction is catalyzed by the enzyme sphingomyelin synthase (SMS), which is fundamental to maintain ceramide and sphingomyelin levels in cells.

c) The salvage pathway:

The third most important mechanism for ceramide synthesis is the salvage pathway, in which complex sphingolipids are degraded to sphingosine that can then be converted back to ceramide by the action of ceramide synthases.

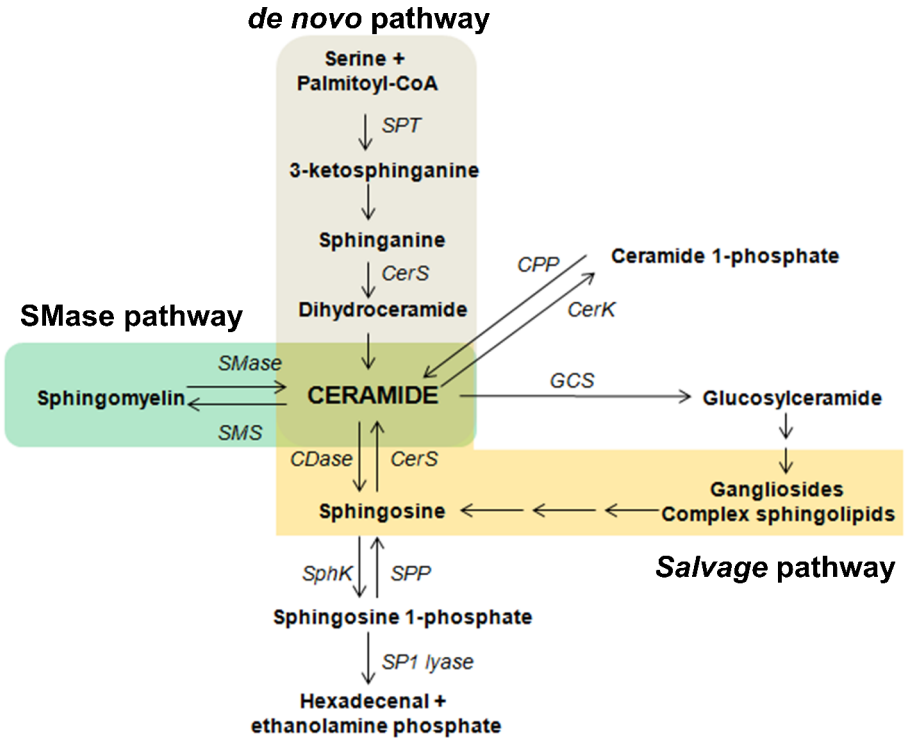

Figure 3: General metabolism of sphingolipids.

d) The neutral ceramidase pathway:

Alternatively, in liver mitochondria, a fourth pathway for ceramide synthesis takes place. The key regulator enzyme in this pathway is neutral ceramidase, which catalyzes the condensation of sphingosine and acyl-CoA, a reaction that occurs in two steps. First, palmitoyl-CoA is hydrolyzed in mitochondria to palmitate and CoA by a thioesterase; then neutral ceramidase condenses palmitate and sphingosine to form ceramide in a reverse ceramidase reaction [14].

Once generated, ceramides can undergo further processing to generate more complex sphingolipids, such as glycosylceramides or complex glycosphingolipids, which in turn, upon their breakdown by specific glucosidases and galactosidades, can once again generate ceramides. Ceramides can also be metabolized by ceramidases (CDases), which cleave the amide-linked fatty acid residue to form sphingosine. Thus, sphingosine can be available either for recycling into ceramides or for phosphorylation by one of the two sphingosine kinase (SphK) enzymes. The product of this reaction, sphingosine 1-phosphate (S1P), can lose the phosphate group through the action of sphingosine phosphatases (SPPases) or be metabolized by S1P lyase to phosphoethanolamine and a fatty aldehyde. Finally, ceramides can undergo

phosphorylation by the action of Ceramide Kinase (CerK) to generate ceramide 1-phosphate (C1P), which can be converted back to ceramide by the action of ceramide 1-phosphate phosphatase (C1PP), or lipid phosphate phosphatases (LPP).

4.2. Bioactive sphingolipids

It is well known that sphingolipids can serve both as structural and signaling or regulatory molecules in eukaryotic cells. The sphingolipid metabolites ceramide, S1P and C1P are major signaling molecules implicated in the regulation of key physiologic processes including cell proliferation, survival, embryo development, organogenesis, autophagy, immune cell trafficking or steroidogenesis. In addition, they have been found to be implicated in variety of pathological processes, mainly those related to inflammatory responses or inflammation-associated diseases [8, 15].

4.2.1. Ceramides

Ceramides consist of a sphingosine backbone covalently linked to a fatty acid via an amide bond. Unlike sphingoid precursors, ceramides are highly hydrophobic molecules and are located in membrane compartments, including the plasma membrane, where they participate in raft formation. These ceramide platforms are an important class of membrane domains with relevant biological roles, including participation in apoptotic signaling cascades and viral or bacterial entry into the cells [16, 17].

It has been reported that ceramides induce cell cycle arrest and promote apoptosis [18, 19]. Besides, they can also play key roles in the regulation of autophagy, cell differentiation, survival, and inflammatory responses [20-28]. Ceramides can function through direct activation of protein phosphatases PP1A and PP2A, which can perform critical responses, such as the induction of apoptosis through the inactivation of the anti-apoptotic targets Akt and Bcl2, and activating pro-apoptotic proteins Bad and Bax [29]. It has also been shown that ceramide can regulate the activity of different members of the Protein Kinase C (PKC) family. Another binding target for ceramide is the cellular protease cathepsin D, which may regulate the actions of lysosomally-generated ceramides [30].

In addition, ceramide and its downstream metabolites have been suggested to play decisive roles in a number of pathological states, including microbial pathogenesis,

inflammation, obesity, neurodegeneration, diabetes, cardiovascular disease, and cancer.

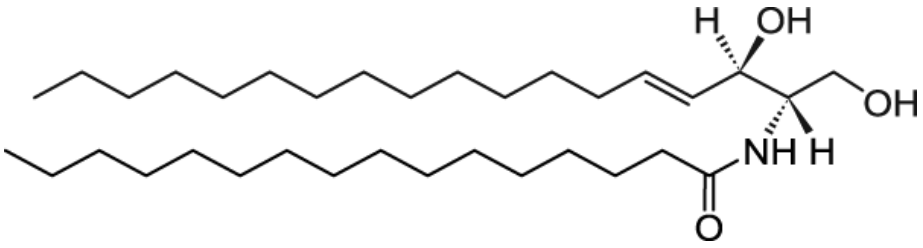

Figure 4: C-16 ceramide.

4.2.2. Sphingosines

Sphingosine (Sph) is an 18-carbon amino alcohol with an unsaturated hydrocarbon chain. Sph has been connected to cellular processes such as induction of cell cycle arrest and apoptosis by modulation of protein kinases and other signaling pathways. It has also been involved in the regulation of the actin cytoskeleton and endocytosis and it has been shown to inhibit PKC [31]. Kinase targets for sphingoid bases have also been found in yeast, suggesting their involvement in the regulation of endocytosis, cell cycle arrest and protein synthesis [29].

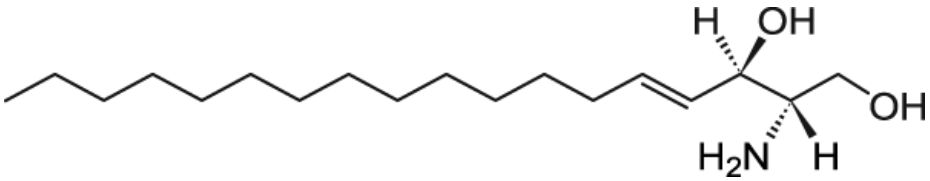

Figure 5: Sphingosine.

4.2.3. Sphingosine 1-phosphate

Phosphorylation of sphingosine by sphingosine kinases 1 and 2 (SphK1 and SphK2) leads to the production of sphingosine 1-phosphate (S1P). S1P can be found intracellularly where it is produced, but it is also present in serum at relatively high concentrations, where it can be found attached to lipoproteins or albumin [32]. S1P and Sph are easily inter-convertible by specific intracellular S1P phosphatases (SPP) [33, 34]. Even though many of the effects of S1P are exerted intracellularly, a family of specific G-protein-coupled receptors (GPCRs), S1P receptors (S1PR), have been described [35], and most of the S1P actions have been associated to stimulation of these receptors.

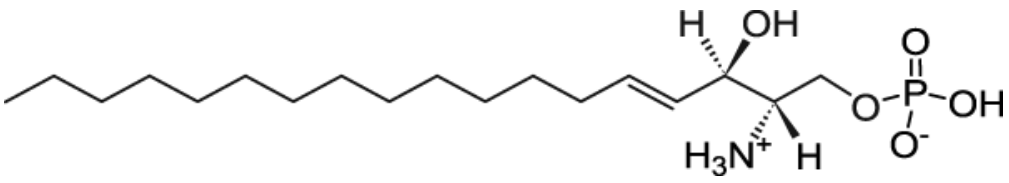

Figure 6: Sphingosine 1-phosphate.

S1P can regulate a variety of cellular functions including proliferation, differentiation, cell survival, migration, angiogenesis, and immune responses [36]. For these reasons it can be classified as a tumor-promoting lipid, therefore showing antagonizing effects to those of ceramide and sphingosine [37]. These pleiotropic effects grant S1P a key role in several diseases, including cancer, inflammation, autoimmunity, atherosclerosis and fibrotic disorders [38-40].

4.2.4. Ceramide 1-phosphate and Ceramide Kinase

Ceramide 1-phosphate (C1P) is a major metabolite of ceramide. It is synthesized through direct phosphorylation of ceramide by Ceramide Kinase (CerK), a reaction that takes place in the trans-Golgi network where the enzyme uses ceramide that is transported from the ER to the Golgi apparatus by CERT [41]. C1P was first identified as the product of a new kinase activity found in rat brain tissue [42], and it was later confirmed in human leukemia cells [43]. Since then, CerK activity has been described in a broad number of cell types.

Once synthesized, C1P is transported to the plasma membrane or to other cell compartments by the specific ceramide phosphate transfer protein (CPTP), where it can be released for autocrine or paracrine signaling. CPTP resides in the cytosol but can connect with the trans-Golgi network, nucleus and plasma membrane to deliver C1P. The CerK pathway is the only pathway described for C1P biosynthesis in mammalian cells. Nevertheless, significant levels of C1P have been found in bone marrow-derived macrophages (BMDM) isolated from CerK null mice, suggesting that other mechanisms for C1P biosynthesis in mammals might exist [44]. Alternative pathways for C1P synthesis may involve the transfer of fatty acyl chains to S1P, or cleavage of sphingomyelin by phospholipase D type SMase (SMase D) activity. However, although SMase D activity has been detected in the toxins of some bacteria and the venom of some arthropods, there is no evidence of SMase D activity in mammalian cells [45].

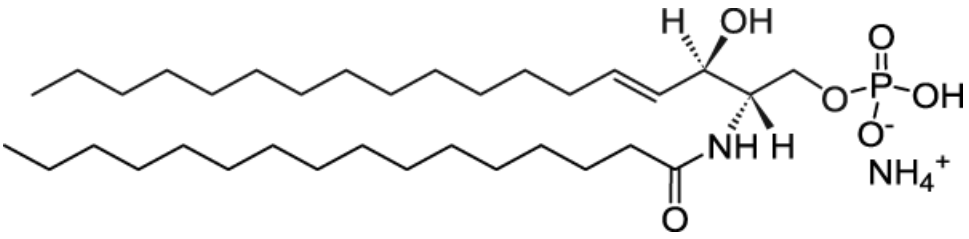

Figure 7: C16 ceramide 1-phosphate

Our group was the first to demonstrate that C1P is a bioactive molecule. C1P was then described as a pro-survival agent capable of stimulating proliferation and inhibited apoptosis in different cell types, including fibroblasts, macrophages and myoblasts [46-50]. Using different cell types and mass spectrometric analysis, it was found that the major intracellular C1P species was palmitoyl (C16) C1P [51]. The mitogenic effects of C1P included stimulation of MEK/ERK, PI3K/Akt, c-JNK, the mammalian target of rapamycin (mTOR), PKC, ROCK/RhoA, GSK3β, and NFκB [52-59]. Regarding its function in cell survival, C1P was demonstrated to block apoptosis through the inhibition of ASMase and SPT activities, as well as by increasing the production of nitric oxide (NO) by the stimulation of the inducible form of nitric oxide synthase (iNOS), and by activating PI3K/Akt pathway.

More recently, our group showed that not all the effects of C1P can be achieved by increasing its intracellular levels. For instance, C1P can stimulate glucose uptake [60] or induce cell migration in Raw 264.7 cells [61], but these effects cannot be accomplished by increasing intracellular C1P concentration [62]. These findings led to the identification of a specific C1P membrane binding site, possibly a receptor. The putative receptor did not bind other sphingolipids including ceramides, S1P, or SM, and resulted to be a G_i protein-coupled receptor (GPCR). Ligation of C1P to its receptor was necessary for triggering glucose metabolism and cell migration [60-62].

5. Sphingolipids in inflammation

Sphingolipids participate in numerous inflammatory processes and are responsible for controlling intracellular trafficking and signaling, cell growth, adhesion, vascularization, survival and apoptosis [15, 63]. The sphingolipid metabolites ceramide, sphingosine 1-phosphate (S1P) and ceramide 1-phosphate (C1P) are major signaling molecules implicated in inflammatory responses and inflammation-related diseases [15]. The role of these three sphingolipids in chronic inflammation has been extensively investigated in the past years, and they have been associated mainly with immune-

dependent and vascular-related chronic inflammatory diseases, including diabetes, obesity, chronic obstructive pulmonary disease (COPD), inflammatory bowel disease, neuroinflammatory disorders and cancer. While ceramides have been associated with pro-inflammatory responses, S1P and C1P have both pro- and anti-inflammatory properties depending upon the cell type in which they are generated.

5.1. Ceramides

Once generated, ceramides can induce the expression and activation of the pro-inflammatory transcription factor NFκB, which is ubiquitously expressed in mammalian cells. This transcription factor regulates the expression of more than 150 inflammation-related genes, such as interleukins, chemokines and pro-inflammatory enzymes involved in the synthesis of prostaglandins [64]. They can also regulate the overexpression of CCAAT/enhancer binding proteins (c/EBP), another family of transcription factors closely associated with inflammation. This up-regulation promotes the expression of several inflammatory proteins [65, 66].

An excessive ceramide signaling is related with adipose tissue inflammation and insulin resistance, leading to obesity and type II diabetes, by inducing over activation of immune cells such as macrophages and B cells. Ceramides participate in signal transduction processes by the activation of specific serine/threonine protein kinases or phosphatases, including PP1, PP2A, and PP2C. Stimulation of PP2A promotes the inactivation by dephosphorylation of Akt, the downstream target of PI3K, a crucial pathway involved in the promotion of cell survival. Since PI3K/Akt pathway is the most important pathway by which insulin exerts its metabolic effects, inhibition of this pathway by ceramides would contribute to insulin resistance and the development of type II diabetes [67]. Ceramides have also been found elevated in the plasma and mediastinal human adipose tissue [68], thus it seems obvious that obesity, diabetes, and inflammation are interconnected by ceramides.

Ceramides have also become relevant in the pathogenesis of lung diseases, including asthma, chronic obstructive pulmonary disease (COPD), pulmonary fibrosis and pulmonary infections [69-72]. Ceramides can also be found in biological fluids, like plasma or bronchoalveolar lavage fluid (BALF), where they bind to carrier proteins or lipid microvesicles that originate from the cell plasma membrane. Exogenous ceramides have been shown to induce ASMase activity and to stimulate the *de novo* synthesis pathway to produce more ceramides, thus creating a paracrine amplification

loop to increase ceramide levels within the cell. Ceramides accumulate in cystic fibrosis lungs and mediate increased cell death, susceptibility to infections, and inflammation. Regarding COPD, it has been demonstrated that exposure to cigarette smoke promotes ceramide accumulation in lungs, which is sufficient to cause alveolar endothelial and epithelial cell apoptosis, activation of macrophages, and matrix proteolysis, thus promoting emphysema [70, 73, 74].

Of note, some of the pro-inflammatory activities of ceramides may be attributed to further metabolism to S1P and C1P.

5.2. Sphingosine 1-phosphate

Sphingosine 1-phosphate (S1P) may be the best studied molecule of this family of bioactive lipids and most of its effects are mediated by five identified receptors (S1PR1-5) [75]. S1P is a key mediator for lymphocyte trafficking between lymphoid and non-lymphoid tissues, favoring the exit of effector T and B-lymphocytes from lymph nodes, thymus, and bone marrow and blocking the ability of immature dendritic cells to migrate. This effect of S1P is particularly important in the development of chronic inflammatory conditions and autoimmune diseases, in which T and B-lymphocytes play a key role.

S1P levels are elevated in individuals with inflammatory arthritis, inflammatory bowel disease, and asthma. S1P has been shown to stimulate the activation of NFκB, which is a key transcription factor implicated in inflammatory responses [76]. However, S1P has also been reported to act as anti-inflammatory molecule in some cases. For instance, S1P may exert anti-inflammatory actions in the skin, and may also promote the switch from the pro-inflammatory M1 to the anti-inflammatory M2 macrophage subtype.

S1P can also be seen as a tumor-promoting lipid involved in the regulation of proliferation, cell growth, cell survival, cell migration, inflammation, angiogenesis, vasculogenesis, and resistance to apoptotic cell death, and therefore shows antagonizing effects to those of ceramides [77].

5.3. Ceramide 1-phosphate and Ceramide Kinase

As indicated above, C1P has both pro- and anti-inflammatory properties depending upon the cell type in which it is generated or act. Initial studies pointed to pro-

inflammatory effects of C1P. It was shown, for instance, that C1P was able to stimulate arachidonic acid (AA) release and subsequent production of pro-inflammatory eicosanoids, including prostaglandins, upon the direct activation of group IV cytosolic phospholipase A2 ($cPLA_2$) [78, 79]. C1P has also been described as a regulator of cytokine secretion, specifically TNF-α, the major mediator of systemic and acute inflammation, which is a pro-inflammatory event occurring in response to invading microbes [80]. TNF-α deregulation results in hyper-activation of the immune response accompanied by lethal tissue damage most commonly described as septic shock, and it has also been linked to rheumatoid arthritis and cancer [81, 82]. Besides, it has also been shown that the interaction of C1P to its receptor results in the stimulation of cell migration and increases glucose uptake in macrophages [60, 61]. Another interesting observation related to the pro-inflammatory actions of C1P is that CerK deficiency decreases diet-induced obesity and insulin resistance by reducing body weight in mice fed a high fat diet [83]. Moreover, CerK-null mice showed decreased MCP-1 signaling in macrophages infiltrating the adipose tissue, a process that is thought to be a crucial factor for the development of inflammation in obese animals. Thus, CerK deficiency resulted in attenuation of inflammatory responses in adipocytes, which might otherwise promote obesity and diabetes. C1P has also been reported as a potent inductor or cell migration in different cell types, including macrophages. Cell migration is also stimulated in response to inflammation and it is critical for chronic inflammatory diseases, such as asthma, rheumatoid arthritis, multiple sclerosis, or inflammatory bowel disease, where the constant infiltration of immune cells into inappropriate sites promotes progressive and severe tissue damage [84, 85]. Besides, cell migration is also associated with cardiovascular disease and establishment and progression of atherosclerosis [86].

However, accumulating evidence suggest that C1P can also exert anti-inflammatory effects under certain circumstances, or that it can specifically induce both pro- and anti-inflammatory responses depending on cell type. In this context, C1P potently inhibited cigarette smoke-induced airway inflammation. Noteworthy, C1P has been shown to be able to counteract the inflammatory effects of ceramides, which triggered apoptosis of pulmonary epithelial cells, thus promoting emphysema [87]. This effect was mediated by the inhibition of the activity and expression of N-SMase, and NFκB, and the inhibition of several pro-inflammatory cytokine release in mice lungs and human airway epithelial cells and neutrophils.

6. Phosphatidylethanolamine *N*-methyltransferase (PEMT)

Phosphatidylcholine (PC) is the most abundant phospholipid of all mammalian cells and subcellular organelles. In general, PC comprises 40–50% of total cellular phospholipids. The second most abundant phospholipid in mammalian membranes is phosphatidylethanolamine (PE), which is enriched in mitochondrial inner membranes (~40% of total phospholipids) compared to other organelles (15–25% of total phospholipids). In all nucleated mammalian cells PC is synthesized by the CDP-choline pathway, also called the Kennedy pathway [88, 89]. When dietary choline enters the cell, it is rapidly phosphorylated to phosphocholine via the cytosolic enzyme choline kinase (CK). Then, CTP and phosphocholine are converted to CDP-choline via the enzyme CTP phosphocholine cytidylyltransferase (CT), which is the rate-limiting reaction for this PC synthesis pathway [90]. The final reaction in the CDP-choline pathway is catalyzed by the integral membrane protein CDP-choline: 1,2-diacylglycerol cholinephosphotransferase (CPT) and the dual-specificity protein, CDP-choline:1,2-diacylglycerol choline/ethanolamine phosphotransferase (CEPT). These proteins are tightly embedded in the endoplasmic reticulum (ER) membrane and transfer phosphocholine from CDP-choline to DAG thereby generating PC. In addition to the CDP-choline pathway for PC synthesis, the liver uses an alternative pathway, the phosphatidylethanolamine *N*-methyltransferase (PEMT) pathway [91]. PEMT is a small integral membrane protein (~ 22 kDa isoform 1, and ~ 27 kDa isoform 2), which catalyzes the conversion of phosphatidylethanolamine (PE) to phosphatidylcholine (PC) by the transfer of 3 methyl groups from S-adenosylmethionine to PE.

In rodents, approximately 30% of PC biosynthesized in the liver is derived from the PEMT pathway with the remaining 70% of PC being generated by the CDP-choline pathway [92]. Despite being predominantly expressed in the liver, relatively low PEMT activities have been found in other tissues such as heart and adipocytes [93]. Nonetheless, there is now evidence that PEMT activity might be important in lipid droplet biosynthesis in adipocyte cells and white adipose tissue [94].

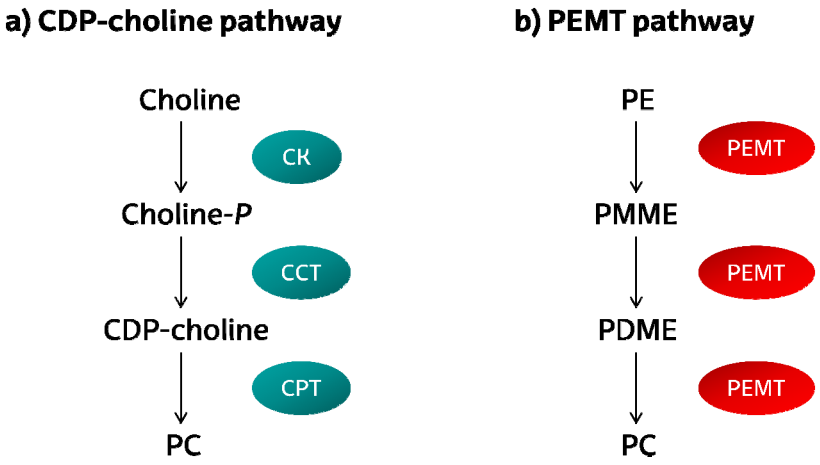

Figure 8: Phosphatidylcholine synthesis pathways.

In several mouse models and in human studies, a change in not only the absolute concentrations of these phospholipids, but more critically in the molar ratio between PC and PE, is a key determinant of liver health. Changes in the hepatic PC/PE molar ratio have been linked to development of non-alcoholic fatty liver disease (NAFLD) in humans [95], as well as in liver failure [96], impaired liver regeneration [97], and the severity of alcoholic fatty liver disease [98].

The present thesis explores the role of CerK/C1P and PEMT in inflammatory processes in different cell types including lung cells, adipocytes and liver, so as to increase our knowledge on the molecular mechanisms of related diseases.

7. References

[1] M.E. Kotas, R. Medzhitov, Homeostasis, inflammation, and disease susceptibility, Cell 160 (5) (2015) 816-827.

[2] D.F. Marks, Homeostatic theory of obesity, Health Psychol Open 2 (1) (2015) 2055102915590692.

[3] C. Nathan, A. Ding, Nonresolving inflammation, Cell 140 (6) (2010) 871-882.

[4] A. Gomez-Munoz, N. Presa, A. Gomez-Larrauri, I.G. Rivera, M. Trueba, M. Ordonez, Control of inflammatory responses by ceramide, sphingosine 1-phosphate and ceramide 1-phosphate, Prog Lipid Res 61 (2016) 51-62.

[5] J.N. Fullerton, D.W. Gilroy, Resolution of inflammation: a new therapeutic frontier, Nat Rev Drug Discov 15 (8) (2016) 551-567.

[6] T. Aoki, S. Narumiya, Prostaglandins and chronic inflammation, Trends Pharmacol Sci 33 (6) (2012) 304-311.

[7] M. Levy, A.H. Futerman, Mammalian ceramide synthases, IUBMB Life 62 (5) (2010) 347-356.

[8] Y.A. Hannun, Functions of ceramide in coordinating cellular responses to stress, Science 274 (5294) (1996) 1855-1859.

[9] A.H. Merrill, Jr., Y.A. Hannun, R.M. Bell, Introduction: sphingolipids and their metabolites in cell regulation, Adv Lipid Res 25 (1993) 1-24.

[10] E. Fahy, S. Subramaniam, H.A. Brown, C.K. Glass, A.H. Merrill, Jr., R.C. Murphy, C.R. Raetz, D.W. Russell, Y. Seyama, W. Shaw, T. Shimizu, F. Spener, G. van Meer, M.S. VanNieuwenhze, S.H. White, J.L. Witztum, E.A. Dennis, A comprehensive classification system for lipids, J Lipid Res 46 (5) (2005) 839-861.

[11] E.C. Mandon, I. Ehses, J. Rother, G. van Echten, K. Sandhoff, Subcellular localization and membrane topology of serine palmitoyltransferase, 3-dehydrosphinganine reductase, and sphinganine N-acyltransferase in mouse liver, J Biol Chem 267 (16) (1992) 11144-11148.

[12] F.M. Goni, A. Alonso, Sphingomyelinases: enzymology and membrane activity, FEBS Lett 531 (1) (2002) 38-46.

[13] N. Marchesini, Y.A. Hannun, Acid and neutral sphingomyelinases: roles and mechanisms of regulation, Biochem Cell Biol 82 (1) (2004) 27-44.

[14] S.A. Novgorodov, B.X. Wu, T.I. Gudz, J. Bielawski, T.V. Ovchinnikova, Y.A. Hannun, L.M. Obeid, Novel pathway of ceramide production in mitochondria: thioesterase and neutral ceramidase produce ceramide from sphingosine and acyl-CoA, J Biol Chem 286 (28) (2011) 25352-25362.

[15] Y.A. Hannun, L.M. Obeid, Principles of bioactive lipid signalling: lessons from sphingolipids, Nat Rev Mol Cell Biol 9 (2) (2008) 139-150.

[16] C.R. Bollinger, V. Teichgraber, E. Gulbins, Ceramide-enriched membrane domains, Biochim Biophys Acta 1746 (3) (2005) 284-294.

[17] E. Gulbins, S. Dreschers, B. Wilker, H. Grassme, Ceramide, membrane rafts and infections, J Mol Med (Berl) 82 (6) (2004) 357-363.

[18] Y.A. Hannun, L.M. Obeid, The Ceramide-centric universe of lipid-mediated cell regulation: stress encounters of the lipid kind, J Biol Chem 277 (29) (2002) 25847-25850.

[19] W. Zheng, J. Kollmeyer, H. Symolon, A. Momin, E. Munter, E. Wang, S. Kelly, J.C. Allegood, Y. Liu, Q. Peng, H. Ramaraju, M.C. Sullards, M. Cabot, A.H. Merrill, Jr., Ceramides and other bioactive sphingolipid backbones in health and disease: lipidomic analysis, metabolism and roles in membrane structure, dynamics, signaling and autophagy, Biochim Biophys Acta 1758 (12) (2006) 1864-1884.

[20] R. Kolesnick, D.W. Golde, The sphingomyelin pathway in tumor necrosis factor and interleukin-1 signaling, Cell 77 (3) (1994) 325-328.

[21] Y.A. Hannun, The sphingomyelin cycle and the second messenger function of ceramide, J Biol Chem 269 (5) (1994) 3125-3128.

[22] Y.A. Hannun, L.M. Obeid, Ceramide: an intracellular signal for apoptosis, Trends Biochem Sci 20 (2) (1995) 73-77.

[23] K.A. Dressler, S. Mathias, R.N. Kolesnick, Tumor necrosis factor-alpha activates the sphingomyelin signal transduction pathway in a cell-free system, Science 255 (5052) (1992) 1715-1718.

[24] A. Gomez-Munoz, Modulation of cell signalling by ceramides, Biochim Biophys Acta 1391 (1) (1998) 92-109.

[25] S. Mathias, K.A. Dressler, R.N. Kolesnick, Characterization of a ceramide-activated protein kinase: stimulation by tumor necrosis factor alpha, Proc Natl Acad Sci U S A 88 (22) (1991) 10009-10013.

[26] S. Mathias, R. Kolesnick, Ceramide: a novel second messenger, Adv Lipid Res 25 (1993) 65-90.

[27] T. Okazaki, A. Bielawska, R.M. Bell, Y.A. Hannun, Role of ceramide as a lipid mediator of 1 alpha,25-dihydroxyvitamin D3-induced HL-60 cell differentiation, J Biol Chem 265 (26) (1990) 15823-15831.

[28] D.S. Menaldino, A. Bushnev, A. Sun, D.C. Liotta, H. Symolon, K. Desai, D.L. Dillehay, Q. Peng, E. Wang, J. Allegood, S. Trotman-Pruett, M.C. Sullards, A.H. Merrill, Jr.,

Sphingoid bases and de novo ceramide synthesis: enzymes involved, pharmacology and mechanisms of action, Pharmacol Res 47 (5) (2003) 373-381.

[29] L.A. Cowart, Y.A. Hannun, Selective substrate supply in the regulation of yeast de novo sphingolipid synthesis, J Biol Chem 282 (16) (2007) 12330-12340.

[30] M. Maceyka, S.G. Payne, S. Milstien, S. Spiegel, Sphingosine kinase, sphingosine-1-phosphate, and apoptosis, Biochim Biophys Acta 1585 (2-3) (2002) 193-201.

[31] E.R. Smith, A.H. Merrill, L.M. Obeid, Y.A. Hannun, Effects of sphingosine and other sphingolipids on protein kinase C, Methods Enzymol 312 (2000) 361-373.

[32] K. Watterson, H. Sankala, S. Milstien, S. Spiegel, Pleiotropic actions of sphingosine-1-phosphate, Prog Lipid Res 42 (4) (2003) 344-357.

[33] D.W. Waggoner, A. Gomez-Munoz, J. Dewald, D.N. Brindley, Phosphatidate phosphohydrolase catalyzes the hydrolysis of ceramide 1-phosphate, lysophosphatidate, and sphingosine 1-phosphate, J Biol Chem 271 (28) (1996) 16506-16509.

[34] D.N. Brindley, D. English, C. Pilquil, K. Buri, Z.C. Ling, Lipid phosphate phosphatases regulate signal transduction through glycerolipids and sphingolipids, Biochim Biophys Acta 1582 (1-3) (2002) 33-44.

[35] S. Pyne, S.C. Lee, J. Long, N.J. Pyne, Role of sphingosine kinases and lipid phosphate phosphatases in regulating spatial sphingosine 1-phosphate signalling in health and disease, Cell Signal 21 (1) (2009) 14-21.

[36] M. Tabasinezhad, N. Samadi, P. Ghanbari, M. Mohseni, A.A. Saei, S. Sharifi, N. Saeedi, A. Pourhassan, Sphingosin 1-phosphate contributes in tumor progression, J Cancer Res Ther 9 (4) (2013) 556-563.

[37] S. Spiegel, S. Milstien, Functions of the multifaceted family of sphingosine kinases and some close relatives, J Biol Chem 282 (4) (2007) 2125-2129.

[38] M. Knapp, Cardioprotective role of sphingosine-1-phosphate, J Physiol Pharmacol 62 (6) (2011) 601-607.

[39] M. Maceyka, K.B. Harikumar, S. Milstien, S. Spiegel, Sphingosine-1-phosphate signaling and its role in disease, Trends Cell Biol 22 (1) (2012) 50-60.

[40] Y. Takuwa, H. Ikeda, Y. Okamoto, N. Takuwa, K. Yoshioka, Sphingosine-1-phosphate as a mediator involved in development of fibrotic diseases, Biochim Biophys Acta 1831 (1) (2013) 185-192.

[41] D.K. Simanshu, R.K. Kamlekar, D.S. Wijesinghe, X. Zou, X. Zhai, S.K. Mishra, J.G. Molotkovsky, L. Malinina, E.H. Hinchcliffe, C.E. Chalfant, R.E. Brown, D.J. Patel, Non-vesicular trafficking by a ceramide-1-phosphate transfer protein regulates eicosanoids, Nature 500 (7463) (2013) 463-467.

[42] S.M. Bajjalieh, T.F. Martin, E. Floor, Synaptic vesicle ceramide kinase. A calcium-stimulated lipid kinase that co-purifies with brain synaptic vesicles, J Biol Chem 264 (24) (1989) 14354-14360.

[43] R.N. Kolesnick, M.R. Hemer, Characterization of a ceramide kinase activity from human leukemia (HL-60) cells. Separation from diacylglycerol kinase activity, J Biol Chem 265 (31) (1990) 18803-18808.

[44] A. Boath, C. Graf, E. Lidome, T. Ullrich, P. Nussbaumer, F. Bornancin, Regulation and traffic of ceramide 1-phosphate produced by ceramide kinase: comparative analysis to glucosylceramide and sphingomyelin, J Biol Chem 283 (13) (2008) 8517-8526.

[45] I.G. Rivera, M. Ordonez, N. Presa, A. Gomez-Larrauri, J. Simon, M. Trueba, A. Gomez-Munoz, Sphingomyelinase D/Ceramide 1-Phosphate in Cell Survival and Inflammation, Toxins (Basel) 7 (5) (2015) 1457-1466.

[46] A. Gomez-Munoz, P.A. Duffy, A. Martin, L. O'Brien, H.S. Byun, R. Bittman, D.N. Brindley, Short-chain ceramide-1-phosphates are novel stimulators of DNA synthesis and cell division: antagonism by cell-permeable ceramides, Mol Pharmacol 47 (5) (1995) 833-839.

[47] A. Gomez-Munoz, L.M. Frago, L. Alvarez, I. Varela-Nieto, Stimulation of DNA synthesis by natural ceramide 1-phosphate, Biochem J 325 (Pt 2) (1997) 435-440.

[48] A. Gomez-Munoz, J.Y. Kong, B. Salh, U.P. Steinbrecher, Ceramide-1-phosphate blocks apoptosis through inhibition of acid sphingomyelinase in macrophages, J Lipid Res 45 (1) (2004) 99-105.

[49] P. Mitra, M. Maceyka, S.G. Payne, N. Lamour, S. Milstien, C.E. Chalfant, S. Spiegel, Ceramide kinase regulates growth and survival of A549 human lung adenocarcinoma cells, FEBS Lett 581 (4) (2007) 735-740.

[50] O. Pastukhov, S. Schwalm, U. Zangemeister-Wittke, D. Fabbro, F. Bornancin, L. Japtok, B. Kleuser, J. Pfeilschifter, A. Huwiler, The ceramide kinase inhibitor NVP-231 inhibits breast and lung cancer cell proliferation by inducing M phase arrest and subsequent cell death, Br J Pharmacol 171 (24) (2014) 5829-5844.

[51] N.F. Lamour, R.V. Stahelin, D.S. Wijesinghe, M. Maceyka, E. Wang, J.C. Allegood, A.H. Merrill, Jr., W. Cho, C.E. Chalfant, Ceramide kinase uses ceramide provided by ceramide transport protein: localization to organelles of eicosanoid synthesis, J Lipid Res 48 (6) (2007) 1293-1304.

[52] P. Gangoiti, M.H. Granado, S.W. Wang, J.Y. Kong, U.P. Steinbrecher, A. Gomez-Munoz, Ceramide 1-phosphate stimulates macrophage proliferation through

activation of the PI3-kinase/PKB, JNK and ERK1/2 pathways, Cell Signal 20 (4) (2008) 726-736.

[53] P. Gangoiti, C. Bernacchioni, C. Donati, F. Cencetti, A. Ouro, A. Gomez-Munoz, P. Bruni, Ceramide 1-phosphate stimulates proliferation of C2C12 myoblasts, Biochimie 94 (3) (2012) 597-607.

[54] T.J. Kim, Y.J. Kang, Y. Lim, H.W. Lee, K. Bae, Y.S. Lee, J.M. Yoo, H.S. Yoo, Y.P. Yun, Ceramide 1-phosphate induces neointimal formation via cell proliferation and cell cycle progression upstream of ERK1/2 in vascular smooth muscle cells, Exp Cell Res 317 (14) (2011) 2041-2051.

[55] L. Arana, P. Gangoiti, A. Ouro, I.G. Rivera, M. Ordonez, M. Trueba, R.S. Lankalapalli, R. Bittman, A. Gomez-Munoz, Generation of reactive oxygen species (ROS) is a key factor for stimulation of macrophage proliferation by ceramide 1-phosphate, Exp Cell Res 318 (4) (2012) 350-360.

[56] P. Gangoiti, M.H. Granado, L. Arana, A. Ouro, A. Gomez-Munoz, Involvement of nitric oxide in the promotion of cell survival by ceramide 1-phosphate, FEBS Lett 582 (15) (2008) 2263-2269.

[57] A. Gomez-Munoz, J.Y. Kong, K. Parhar, S.W. Wang, P. Gangoiti, M. Gonzalez, S. Eivemark, B. Salh, V. Duronio, U.P. Steinbrecher, Ceramide-1-phosphate promotes cell survival through activation of the phosphatidylinositol 3-kinase/protein kinase B pathway, FEBS Lett 579 (17) (2005) 3744-3750.

[58] M.H. Granado, P. Gangoiti, A. Ouro, L. Arana, A. Gomez-Munoz, Ceramide 1-phosphate inhibits serine palmitoyltransferase and blocks apoptosis in alveolar macrophages, Biochim Biophys Acta 1791 (4) (2009) 263-272.

[59] G.E. Miranda, C.E. Abrahan, D.L. Agnolazza, L.E. Politi, N.P. Rotstein, Ceramide-1-phosphate, a new mediator of development and survival in retina photoreceptors, Invest Ophthalmol Vis Sci 52 (9) (2011) 6580-6588.

[60] A. Ouro, L. Arana, P. Gangoiti, I.G. Rivera, M. Ordonez, M. Trueba, R.S. Lankalapalli, R. Bittman, A. Gomez-Munoz, Ceramide 1-phosphate stimulates glucose uptake in macrophages, Cell Signal 25 (4) (2013) 786-795.

[61] L. Arana, M. Ordonez, A. Ouro, I.G. Rivera, P. Gangoiti, M. Trueba, A. Gomez-Munoz, Ceramide 1-phosphate induces macrophage chemoattractant protein-1 release: involvement in ceramide 1-phosphate-stimulated cell migration, Am J Physiol Endocrinol Metab 304 (11) (2013) E1213-1226.

[62] M.H. Granado, P. Gangoiti, A. Ouro, L. Arana, M. Gonzalez, M. Trueba, A. Gomez-Munoz, Ceramide 1-phosphate (C1P) promotes cell migration Involvement of a specific C1P receptor, Cell Signal 21 (3) (2009) 405-412.

[63] M. El Alwani, B.X. Wu, L.M. Obeid, Y.A. Hannun, Bioactive sphingolipids in the modulation of the inflammatory response, Pharmacol Ther 112 (1) (2006) 171-183.

[64] G.F. Nixon, Sphingolipids in inflammation: pathological implications and potential therapeutic targets, Br J Pharmacol 158 (4) (2009) 982-993.

[65] N.V. Giltiay, A.A. Karakashian, A.P. Alimov, S. Ligthle, M.N. Nikolova-Karakashian, Ceramide- and ERK-dependent pathway for the activation of CCAAT/enhancer binding protein by interleukin-1beta in hepatocytes, J Lipid Res 46 (11) (2005) 2497-2505.

[66] Y.H. Cho, C.H. Lee, S.G. Kim, Potentiation of lipopolysaccharide-inducible cyclooxygenase 2 expression by C2-ceramide via c-Jun N-terminal kinase-mediated activation of CCAAT/enhancer binding protein beta in macrophages, Mol Pharmacol 63 (3) (2003) 512-523.

[67] J.A. Chavez, S.A. Summers, A ceramide-centric view of insulin resistance, Cell Metab 15 (5) (2012) 585-594.

[68] J. Gertow, S. Kjellqvist, M. Stahlman, L. Cheung, J. Gottfries, O. Werngren, J. Boren, A. Franco-Cereceda, P. Eriksson, R.M. Fisher, Ceramides are associated with inflammatory processes in human mediastinal adipose tissue, Nutr Metab Cardiovasc Dis 24 (2) (2014) 124-131.

[69] E.L. Smith, E.H. Schuchman, The unexpected role of acid sphingomyelinase in cell death and the pathophysiology of common diseases, FASEB J 22 (10) (2008) 3419-3431.

[70] I. Petrache, V. Natarajan, L. Zhen, T.R. Medler, A.T. Richter, C. Cho, W.C. Hubbard, E.V. Berdyshev, R.M. Tuder, Ceramide upregulation causes pulmonary cell apoptosis and emphysema-like disease in mice, Nat Med 11 (5) (2005) 491-498.

[71] I. Petrache, D.N. Petrusca, R.P. Bowler, K. Kamocki, Involvement of ceramide in cell death responses in the pulmonary circulation, Proc Am Thorac Soc 8 (6) (2011) 492-496.

[72] A.P. Seitz, H. Grassme, M.J. Edwards, Y. Pewzner-Jung, E. Gulbins, Ceramide and sphingosine in pulmonary infections, Biol Chem 396 (6-7) (2015) 611-620.

[73] I. Petrache, T.R. Medler, A.T. Richter, K. Kamocki, U. Chukwueke, L. Zhen, Y. Gu, J. Adamowicz, K.S. Schweitzer, W.C. Hubbard, E.V. Berdyshev, G. Lungarella, R.M. Tuder, Superoxide dismutase protects against apoptosis and alveolar enlargement induced by ceramide, Am J Physiol Lung Cell Mol Physiol 295 (1) (2008) L44-53.

[74] M. Levy, E. Khan, M. Careaga, T. Goldkorn, Neutral sphingomyelinase 2 is activated by cigarette smoke to augment ceramide-induced apoptosis in lung cell death, Am J Physiol Lung Cell Mol Physiol 297 (1) (2009) L125-133.

[75] S. Spiegel, S. Milstien, The outs and the ins of sphingosine-1-phosphate in immunity, Nat Rev Immunol 11 (6) (2011) 403-415.

[76] S.E. Alvarez, K.B. Harikumar, N.C. Hait, J. Allegood, G.M. Strub, E.Y. Kim, M. Maceyka, H. Jiang, C. Luo, T. Kordula, S. Milstien, S. Spiegel, Sphingosine-1-phosphate is a missing cofactor for the E3 ubiquitin ligase TRAF2, Nature 465 (7301) (2010) 1084-1088.

[77] S. Spiegel, S. Milstien, Sphingosine-1-phosphate: an enigmatic signalling lipid, Nat Rev Mol Cell Biol 4 (5) (2003) 397-407.

[78] B.J. Pettus, A. Bielawska, P. Subramanian, D.S. Wijesinghe, M. Maceyka, C.C. Leslie, J.H. Evans, J. Freiberg, P. Roddy, Y.A. Hannun, C.E. Chalfant, Ceramide 1-phosphate is a direct activator of cytosolic phospholipase A2, J Biol Chem 279 (12) (2004) 11320-11326.

[79] B.J. Pettus, A. Bielawska, S. Spiegel, P. Roddy, Y.A. Hannun, C.E. Chalfant, Ceramide kinase mediates cytokine- and calcium ionophore-induced arachidonic acid release, J Biol Chem 278 (40) (2003) 38206-38213.

[80] N.F. Lamour, D.S. Wijesinghe, J.A. Mietla, K.E. Ward, R.V. Stahelin, C.E. Chalfant, Ceramide kinase regulates the production of tumor necrosis factor alpha (TNFalpha) via inhibition of TNFalpha-converting enzyme, J Biol Chem 286 (50) (2011) 42808-42817.

[81] M. Feldmann, S.R. Maini, Role of cytokines in rheumatoid arthritis: an education in pathophysiology and therapeutics, Immunol Rev 223 (2008) 7-19.

[82] G. Sethi, B. Sung, B.B. Aggarwal, TNF: a master switch for inflammation to cancer, Front Biosci 13 (2008) 5094-5107.

[83] S. Mitsutake, T. Date, H. Yokota, M. Sugiura, T. Kohama, Y. Igarashi, Ceramide kinase deficiency improves diet-induced obesity and insulin resistance, FEBS Lett 586 (9) (2012) 1300-1305.

[84] A.D. Luster, R. Alon, U.H. von Andrian, Immune cell migration in inflammation: present and future therapeutic targets, Nat Immunol 6 (12) (2005) 1182-1190.

[85] J.B. Beltman, A.F. Maree, R.J. de Boer, Analysing immune cell migration, Nat Rev Immunol 9 (11) (2009) 789-798.

[86] U.P. Steinbrecher, A. Gomez-Munoz, V. Duronio, Acid sphingomyelinase in macrophage apoptosis, Curr Opin Lipidol 15 (5) (2004) 531-537.

[87] K. Baudiss, C.K. Ayata, Z. Lazar, S. Cicko, J. Beckert, A. Meyer, A. Zech, R.P. Vieira, R. Bittman, A. Gomez-Munoz, I. Merfort, M. Idzko, Ceramide-1-phosphate inhibits cigarette smoke-induced airway inflammation, Eur Respir J 45 (6) (2015) 1689-1680.

[88] E.P. Kennedy, S.B. Weiss, The function of cytidine coenzymes in the biosynthesis of phospholipides, J Biol Chem 222 (1) (1956) 193-214.

[89] E.P. Kennedy, Metabolism of lipides, Annu Rev Biochem 26 (1957) 119-148.

[90] P.C. Choy, S.B. Farren, D.E. Vance, Lipid requirements for the aggregation of CTP:phosphocholine cytidylyltransferase in rat liver cytosol, Can J Biochem 57 (6) (1979) 605-612.

[91] D.E. Vance, Phospholipid methylation in mammals: from biochemistry to physiological function, Biochim Biophys Acta 1838 (6) (2014) 1477-1487.

[92] C.J. DeLong, Y.J. Shen, M.J. Thomas, Z. Cui, Molecular distinction of phosphatidylcholine synthesis between the CDP-choline pathway and phosphatidylethanolamine methylation pathway, J Biol Chem 274 (42) (1999) 29683-29688.

[93] D.E. Vance, N.D. Ridgway, The methylation of phosphatidylethanolamine, Prog Lipid Res 27 (1) (1988) 61-79.

[94] G. Horl, A. Wagner, L.K. Cole, R. Malli, H. Reicher, P. Kotzbeck, H. Kofeler, G. Hofler, S. Frank, J.G. Bogner-Strauss, W. Sattler, D.E. Vance, E. Steyrer, Sequential synthesis and methylation of phosphatidylethanolamine promote lipid droplet biosynthesis and stability in tissue culture and in vivo, J Biol Chem 286 (19) (2011) 17338-17350.

[95] Z. Li, L.B. Agellon, T.M. Allen, M. Umeda, L. Jewell, A. Mason, D.E. Vance, The ratio of phosphatidylcholine to phosphatidylethanolamine influences membrane integrity and steatohepatitis, Cell Metab 3 (5) (2006) 321-331.

[96] C.J. Walkey, L. Yu, L.B. Agellon, D.E. Vance, Biochemical and evolutionary significance of phospholipid methylation, J Biol Chem 273 (42) (1998) 27043-27046.

[97] J. Ling, T. Chaba, L.F. Zhu, R.L. Jacobs, D.E. Vance, Hepatic ratio of phosphatidylcholine to phosphatidylethanolamine predicts survival after partial hepatectomy in mice, Hepatology 55 (4) (2012) 1094-1102.

[98] K.K. Kharbanda, M.E. Mailliard, C.R. Baldwin, H.C. Beckenhauer, M.F. Sorrell, D.J. Tuma, Betaine attenuates alcoholic steatosis by restoring phosphatidylcholine generation via the phosphatidylethanolamine methyltransferase pathway, J Hepatol 46 (2) (2007) 314-321.

Rationale of thesis and Objectives

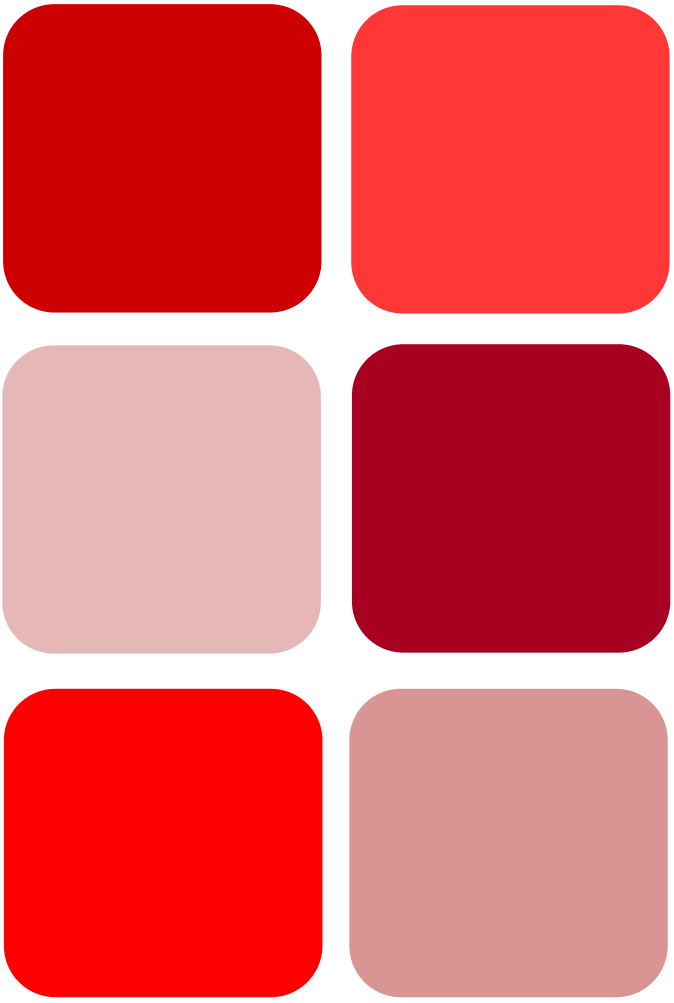

Rationale

Chronic inflammatory diseases are a major cause of mortality in human beings. Worldwide 3 out of 5 people die due to chronic inflammatory diseases including, chronic respiratory illnesses, obesity, fatty liver diseases and cancer. Many lung diseases develop as chronic inflammatory responses to inspired irritants, namely cigarette smoke. Obesity is a local and systemic chronic state of low-grade adipose tissue inflammation, which leads to the development of serious diseases such as type II diabetes, cardiovascular disease, non-alcoholic fatty liver disease (NAFLD), and even certain forms of cancer. Although these pathologies are dissimilar, they have a common link: alterations in sphingolipid metabolism. Therefore, understanding the molecular pathways involved in the formation and degradation of sphingolipid metabolites may help to elucidate the mechanisms responsible for the establishment and progression of these diseases.

In this connection, bioactive sphingolipids have been shown to regulate important biological functions including cell proliferation, cell survival, organogenesis, or immune cell trafficking, and some of them are implicated in inflammatory responses. In particular, ceramide 1-phosphate (C1P) and the enzyme responsible for its biosynthesis, ceramide kinase (CerK), have been implicated in the regulation of inflammatory responses associated with lung disease, obesity, NAFLD and cancer. Interestingly, recent evidence suggests that phosphatidylethanolamine *N*-methyltransferase (PEMT), an enzyme that regulates the biosynthesis of phosphatidylcholine (PC) through methylation of phosphatidylethanolamine (PE), also participates in the development of inflammatory diseases that are associated with NAFLD, obesity and cancer, pathologies in which ceramide metabolism also plays critical roles.

Therefore, the present thesis was undertaken to examine the possible role of CerK and PEMT in inflammatory processes in lung cells, adipocytes and liver.

Objectives

Accordingly, the objectives proposed in this thesis were:

1. To study the implication of CerK/C1P in inflammatory responses elicited by CSE in lung epithelial cells.

2. To determine the implication of PEMT in inflammatory processes in major PEMT expressing tissues (adipocytes and liver).

    2.1. To determine the possible implication of PEMT in adipogenesis and a possible interaction with C1P actions in this process.

    2.2. To study the possible relationship between PEMT and bioactive sphingolipids in NAFLD in PEMT knock-out mice, and the possible therapeutic effect of vitamin E.

Materials and Methods

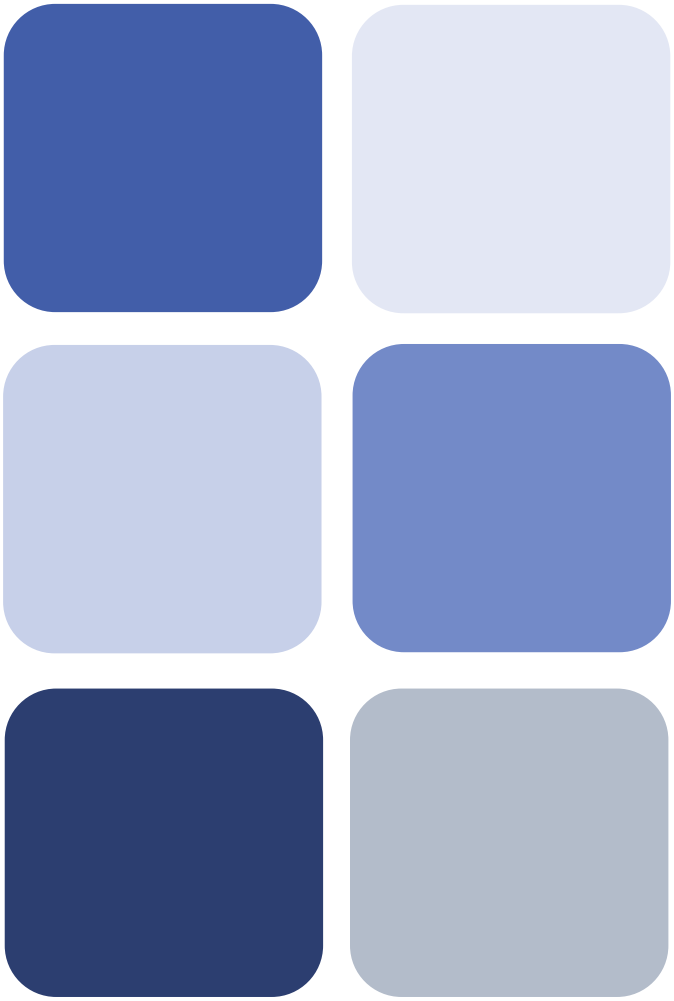

Materials and Methods

1. MATERIALS

1.1. Reagents

Supplier	Reactive
Abcam	CD36 Ab (#ab133625) GSH/GSSG Ratio Detection Assay Kit
Abnova	Adipogenesis assay kit
Applied Biosystems (Ambion)	CERK siRNA P85α siRNA MAPK1 siRNA MAPK3 siRNA ROCK1 siRNA ROCK2 siRNA AKT1 siRNA AKT2 siRNA PEMT siRNA Negative siRNA
Avanti Polar Lipids	C16 Ceramide 1-phosphate
Biorad	BCA protein assay kit PVDF membranes Protein markers
Cayman Chemical	C6-NBD-ceramide
Cell Signaling Technology	ERK1/2 Ab (#9102) Phospho-ERK1/2 Ab (#9101) AKT Ab (#9272) Phospho-AKT Ab (#9271) AKT1 Ab (#2938)

	AKT2 Ab (#3063) ROCK1 Ab (#4035) ROCK2 Ab (#9029) PI3K (p85) Ab (#4292) E-Cadherin Ab (#3195) PPARγ Ab (#2430) Adiponectin Ab (#2789) Perilipin Ab (#3470)
Gibco (Thermofisher Scientific)	Fetal Bovine Serum Newborn Calf Serum Opti-MEM® Reduced Serum Media 0,05% Trypsin-EDTA
Invitrogen	Oligofectamine ™ Transfection Reagent Lipofectamine® 2000 Transfection Reagent Hygromycin B Gentamicin Solution Human IL-8 ELISA kit Human IL-6 ELISA kit Human TGF-β1 ELISA kit Human MCP-1 ELISA kit
LifeSpan BioSciences	PEMT Ab (#LS-C80583)
Lonza	DMEM medium 4.5 g/l glucose RPMI medium
PeproTech	Human VEGF ELISA kit Mouse Leptin ELISA kit
Polyplus Transfection	jetPRIME® DNA & siRNA Transfection Reagent
Promega	Cell Titer 96® Aqueous Non-Radioactive Cell Proliferation Assay
R&D Systems	TBARS Parameter Assay Kit
Santa Cruz Biotechnology, Inc.	GAPDH Ab
Sigma Aldrich	Ampicillin Sodim Salt Acrylamide/Bis-acrylamide, 30% solution

	Ammonium persulfate Bovine Serum Albumin Fibronectin L-glutamine Protease Inhibitor Cocktail Tween-20 Pertussis toxin Crystal violet Dexamethasone Insulin IBMX Rosiglitazone Oil Red O
Thermofisher Scientific	SuperSignal® West femto Maximum Sensitivity Substrate

1.2. Cell lines

1.2.1. 3T3-L1 cell line

The 3T3-L1 cell line is a murine fibroblast cell line purchased from American Type Culture Collection (ATCC®CL-173) and cultured following the manufacturer's indications. Cells were grown in DMEM (4.5 g glucose/l) supplemented with 10% heat inactivated NBCS, 50 mg/l gentamicin and 4 mM L-glutamine. Cells were incubated in a humidified 5% CO_2 incubator at 37ºC and subcultured every 3-4 days.

3T3-L1 cells undergo a pre-adipose to adipose like conversion as they progress from a rapidly dividing to a confluent and contact inhibited state. High serum content in the medium enhances fat accumulation.

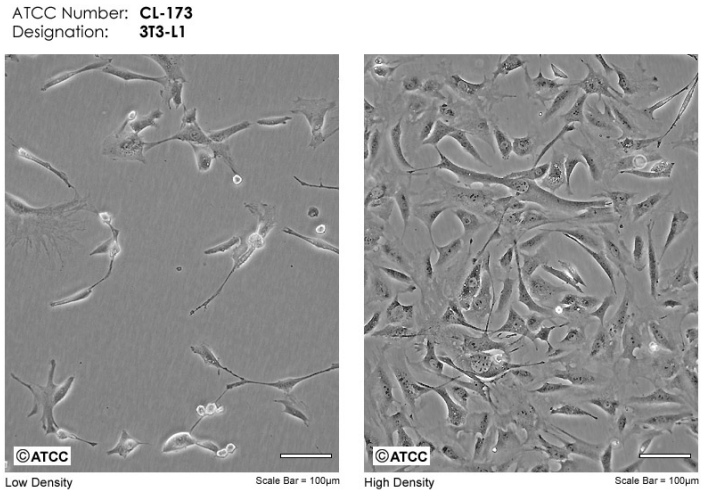

Figure 1: Micrograph of 3T3-L1 cells taken from ATCC website.

1.2.2. A549 cell line

The A549 cell line, originally from ATCC, was kindly provided by the laboratory of Dr. Sergio Moya (CICbiomaGUNE, San Sebastian, Basque Country, Spain) and cultured following the manufacturer's indications. The A549 cell line is an alveolar basal epithelial cell line derived from an explant culture of lung carcinomatous tissue from a 58-year-old Caucasian male.

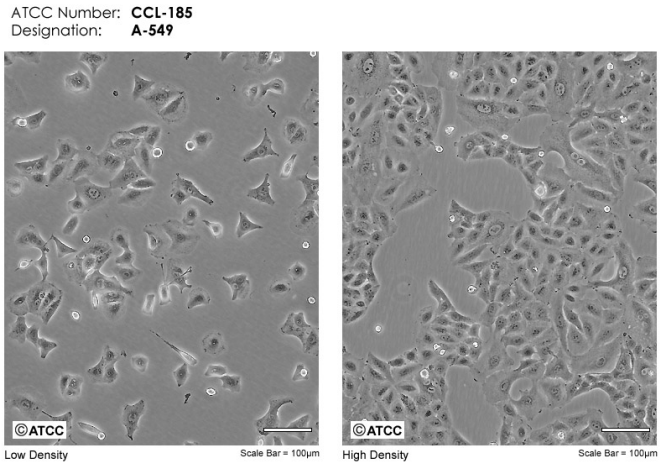

Figure 2: Micrograph of A549 cells taken from ATCC website.

Cells were grown in 75 cm^2 flasks in RPMI medium supplemented with 10% heat-inactivated FBS, 2 mM L-glutamine and 50 mg/l gentamicin. Cells were cultured in a humidified 5% CO_2 incubator at 37ºC and subcultured every 3-4 days maintaining at a cell concentration between 6 x 10^3 and 6 x 10^4 cell/cm^2.

1.2.3 THP-1 cell line

The THP-1 cell line, originally from ATCC, was kindly provided by the laboratory of Dr. Ana Zubiaga (Department of Genetics, EHU-UPV, Basque Country, Spain) and cultured following the indications dictated by ATCC. This cell line is a human monocytic cell line derived from peripheral blood of a 1-year old acute monocytic leukemia patient.

Cells were grown in 100 mm plates in RPMI medium supplemented with 10% heat-inactivated FBS, 2 mM L-glutamine, 50mg/L gentamicin and 0.05 mM 2-mercaptoethanol. Cells were cultured in a humidified 5% CO_2 incubator at 37ºC and maintained by the addition of fresh medium or replacement of medium every 2-3 days. Alternatively, cells can be subcultured by centrifugation with subsequent resuspension at 2-4 x 10^5 cells/ml.

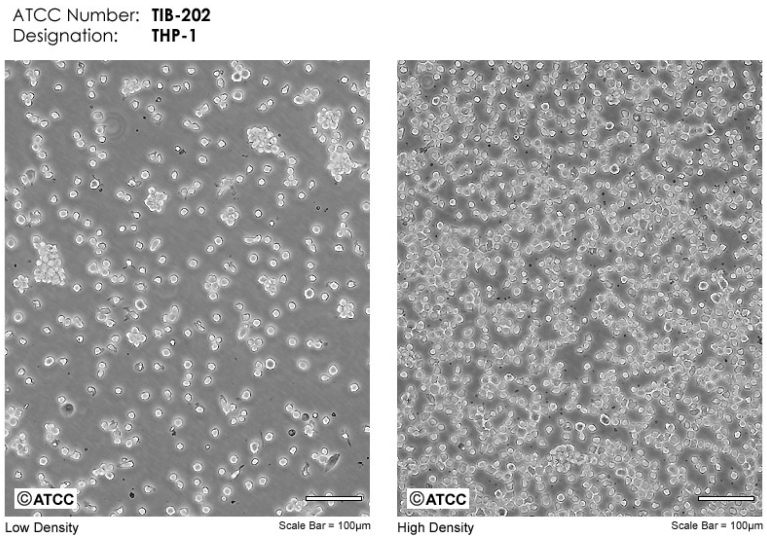

Figure 3: Micrograph of THP-1 cells taken from ATCC website.

2. ANIMAL HANDLING AND DIETS

All experimental procedures were approved by the University of Alberta's Institutional Animal Care Committee in accordance with guidelines of Canadian Council on Animal Care. Male *Pemt*$^{+/+}$ and *Pemt*$^{-/-}$ mice (backcrossed into C57B1/6 for seven generations), were fed a semi-synthetic HFD (catalog no.F3282, Bio-Serv, Flemington, NJ; 60% kcal fat) or HFD supplemented with vitamin E (0.5 g/kg) for 3 weeks. This concentration of vitamin E results in an approximate dose of 133 IU/kg/day, which is equivalent to the recommended dose for human vitamin E

supplements. Animals were fasted for 12 h before collection of different tissues. Blood was collected from the heart to an EDTA-containing tube, mixed, separated by centrifugation, and the plasma was stored at –80 °C. The liver was rinsed with ice-cold saline, weighed, immediately frozen in liquid nitrogen, and stored at –80 °C until further analyses. Formalin-fixed paraffin-embedded livers were sectioned for histological analysis using hematoxylin-eosin staining. Fibrillar collagen was visualized by Picro-Sirius red staining (5-μm sections, formalin-fixed livers) and confocal microscopy.

3. METHODS

3.1. Delivery of C1P to cells in culture

An aqueous dispersion in the form of liposomes of C1P was added to cultured cells as previously described [1]. Specifically, stock solutions of C1P were prepared by sonicating 5 mg C1P in 3 ml of sterile nanopure water on ice using a probe sonicator until a clear dispersion was obtained. The final concentration in the stock solution was 2.62 mM. This procedure is considered preferable to dispersions prepared by adding C1P in organic solvents such as methanol, ethanol or DMSO because droplet formation is minimized and there are no organic solvent effects on the cells. C1P was then added to the culture medium in the micromolar range.

3.2. Preparation of cigarette smoke extract (CSE) and delivery to cells

Fresh cigarette smoke extract (CSE) was prepared using a modification of the method described by Aoshiba [2]. Briefly, the smoke from fifteen half-filtered commercial cigarettes (Marlboro; Philips Morris GmbH, Munich, Germany) was bubbled through 150 ml warm RPMI medium. The obtained extract was immediately adjusted to a pH of 7.4, and filtered through a 0.22 μm filter to sterilize and remove particulate matter. This solution was considered the 100% of CSE and was aliquoted and stored at -80ºC until used.

When needed, CSE was melted and cells were treated between 0-72 hours with CSE in the presence or absence of agonists or inhibitors as indicated.

3.3. Cell viability assay (Crystal violet method)

Adherent cells detach from cell culture plates during cell death. This characteristic can be used for the indirect quantification of cell death and to determine differences in

proliferation upon stimulation with death-inducing agents. A simple method to detect maintained adherence of cells is the staining of attached cells with crystal violet dye, which binds to proteins and DNA. Cells that undergo cell death lose their adherence and are subsequently lost from the population of cells, reducing the amount of crystal violet staining in a culture.

- **A549 cells** were seeded at a density of 10^4 cells/well in 96-well plates in triplicates (100 µl). Cells were then incubated overnight in RPMI medium supplemented with 10% FBS. Then, the medium was replaced with fresh medium without serum in the presence or absence of agonists or inhibitors and further incubated, as indicated.

After the indicated incubation time periods, cells were washed twice with distilled water and 50 µl of 0.5% crystal violet in 20% methanol were added to each well. Cells were stained for 20 minutes at room temperature while shaking. After this time cells were washed three times with distilled water and the plate was left air-dry overnight. The next day 200 µl of methanol were added to each well and plate was incubated with its lid on for 20 minutes at room temperature on a bench rocker. The absorbance was measured at 570 nm and absorbance of the blank (stained wells without cells) was subtracted from all absorbance values. The control values were indicated as 100% of cell viability.

3.4. Western Blotting

A549 cells were seeded in a 6-well plates at 2 x 10^5 cells/well and grown overnight in RPMI medium containing 10% FBS. Then, the medium was replaced with fresh medium without serum in the presence or absence of agonists or inhibitors further incubated, as indicated.

Cells were washed twice with cold PBS and harvested with ice-cold lysis buffer (0.1 M Tris pH 8, 0.685 M NaCl, 2.5 mM EDTA, 1% (v/v) igepal, 10% (v/v) glycerol and 1µg/ml Protease Inhibitor Cocktail (PIC). Samples were lysed by sonication and protein concentration was determined using a protein assay commercial kit (BioRad).

Samples (10-40 µg protein/sample) were mixed with 4X loading buffer (240 mM Tris pH 6.8, 40% (v/v) glycerol, 8% SDS, 0.04% (p/v) bromophenol and 50 µl/ml β-mercaptoethanol). Samples were then heated at 90ºC for 10 minutes and loaded into polyacrilamide gels (15%, 12% or 7.5% acrylamide) to perform protein separation by

SDS-PAGE. Electrophoresis was run (75V for 30 minutes-125V for 1.5 hours approx.) in electrophoresis buffer (1.92 mM glycin, 0.25 M Tris-HCl and 1% SDS).

Proteins were then transferred intro nitrocellulose or polyvinylidene difluoride (PVDF) membranes. Transference was run at 400 mA for 75 minutes in ice-cold transfer buffer (14.4 g/L glycin, 3 g/L Tris and 20% methanol). In order to avoid unspecific antibody binding, the membrane was blocked for 1 hour with 5% skim milk in Tris-Buffered Saline (TBS) containing 0.1% Tween-20, pH 7.6. The skim milk was then removed and membranes were incubated overnight with primary antibody diluted in TBS/0.1% Tween-20 with 5% BSA (1:1000, unless indicated otherwise) at 4ºC. After three washes with TBS/0.1% Tween-20, membranes were incubated with Horseradish Peroxidase (HRP)-conjugated secondary antibody at 1:5000-1:10000 dilution in 1% skim milk in TBS/0.1%Tween-20 for 1 hour. Bands were visualized by enhanced chemiluminiscence using ChemiDoc™ Imaging System and quantified using ImageLab™ software.

3.5. Quantitative Enzyme-Linked ImmunoSorbent Assay (ELISA)

3.5.1. Determination of VEGF and leptin concentration

A549 cells were seeded in 12-well plates (8 x 10^4 cells/well) and incubated overnight in RPMI medium containing 10% FBS. The next day cells were washed twice with PBS and the medium was replaced with RPMI medium without serum. Cells were further incubated in serum deprivation conditions for 2 hours. After this period, agonists and/or inhibitors were added and cells were incubated for the indicated periods of time. The medium was then collected into microcentrifuge tubes and centrifuged at 10000 g for 5 minutes at 4ºC to remove any cell residues and the supernatant was collected and stored at -80ºC until used. Remaining cells in the wells were washed twice with ice-cold PBS and harvested, and the pellet was resuspended in 80 μl lysis buffer (0.1 M Tris pH 8, 0.685 M NaCl, 2.5 mM EDTA, 1% (v/v) igepal, 10% (v/v) glycerol and 1μg/ml Protease Inhibitor Cocktail (PIC)). Samples were lysed by sonication and protein concentration was determined by a protein concentration commercial kit (BioRad) for later normalization of the results.

3T3-L1 cells were seeded in 24-well plates (2.5 x 10^4 cells/well) and incubated overnight in DMEM supplemented with 10% NBCS. The next day siRNA protocol was performed and cells were further incubated for 2 days. Then, adipogenesis was induced

and cells were differentiated until day 7. At day 7 after differentiation cells supernatant was collected and stored at -80ºC until used.

Once supernatants were collected as described above, the VEGF and leptin concentration was determined using a Human Standard ELISA development Kit (*Peprotech*) for each cytokine following the manufacturer's indications.

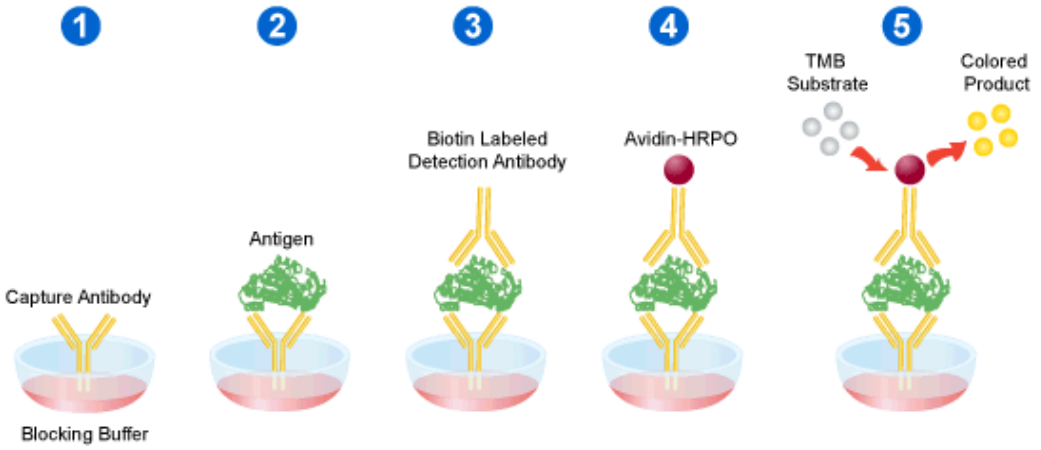

Figure 4: Schematic representation of sandwich ELISA format experiment.

Briefly, a 96-well high reactivity plate was pre-coated with specific antibodies for VEGF or leptin and incubated overnight at 4ºC. The next day, the wells were washed and blocked with 1% bovine serum albumin (BSA) in PBS for 1 hour at room temperature. 100 µl of each sample were added in duplicate to the wells without previous dilution. Along with the samples, serial dilutions of a standard solution for each cytokine were also added to the plate. Samples were incubated for 2 hours at room temperature and then the biotinylated-detection antibody was added. This antibody binds to the VEGF/leptin capture antibody complexes. After 1 hour incubation and subsequent washes, an Avidin-HRP solution was added to each well and reactions with biotinylated-detection antibody were allowed to occur for 30 minutes. Finally, after the last wash step, a 2,2'-Azino-bis(3 ethylbenzothiazoline-6-sulfonic acid) diammonium salt (ABTS) solution was added as a substrate. The reaction catalyzed by the enzyme in the presence of ABTS substrate produces a chromophoric product that enables a colorimetric change. The absorbance was then read at 405 and 650 nm using a PowerWave™ XS (*Biotek*) microplate reader provided with Gen5 software. For analyzing the data absorbance values obtained at 650 nm were subtracted from the ones obtained at 405 nm in order to avoid possible interference, and the standard solutions were used to perform a calibration curve. Sample concentration values

(pg/ml) obtained by the calibration curve were normalized considering total volume of supernatants collected and by the total protein determined in each well (pg/mg total protein).

3.5.2. Determination of MCP-1,TGF-β1, IL-6 and IL-8 concentration

A549 cells were seeded in 12-well plates (1 x 10^5 cells/well and incubated overnight in RPMI medium containing 10% FBS. The next day cells were washed twice with PBS and the medium was replaced with RPMI medium without serum. Cells were further incubated in serum deprivation conditions for 2 hours. After this period, agonists and/or inhibitors were added and cells were incubated for the indicated periods of time. The medium was then collected into microcentrifuge tubes and centrifuged at 10000 g for 5 minutes at 4ºC to remove any cell residues and the supernatant was collected and stored at -80ºC until used. Remaining cells in the wells were washed twice with ice-cold PBS and harvested with 80 µl lysis buffer (0.1 M Tris pH 8, 0.685 M NaCl, 2.5 mM EDTA, 1% (v/v) igepal, 10% (v/v) glycerol and 1µg/ml Protease Inhibitor Cocktail (PIC)). Samples were lysed by sonication and protein concentration was determined by a protein concentration commercial kit (BioRad) for later normalization of the results.

The MCP-1, TGF-β, IL-6 and IL-8 concentration was determined using a Human ELISA Ready-Set-Go! Kit (eBioscience) for each cytokine and the manufacturer's instructions were followed.

Briefly, a 96-well high reactivity plate was precoated with a specific antibody against each cytokine and incubated overnight at 4ºC. The next day the wells were washed and blocked with diluent buffer for 1 hour at room temperature. 100 µl of each sample were then added in duplicate to the wells.

- **MCP-1** samples were added without previous dilution.
- **TGF-β1** samples had to be activated with HCl for 10 minutes and neutralized with NaOH to analyze latent TGF-β1 amount. To determine activated TGF-β1 amount, no activation is required.
- **IL-6** samples were added without previous dilution.
- **IL-8** samples were added without previous dilution.

Along with the samples, serial dilutions of a standard solution for each cytokine were also added to the plate. Samples were incubated for 2 hours at room temperature and then the biotinylated-detection antibody was added. This antibody binds to the MCP-1, TGF-β1, IL-6 or IL-8 capture antibody complexes. After 1 hour of incubation and subsequent washes, an Avidin-HRP solution was added to each well and reactions with biotinylated-detection antibody were allowed to occur for 30 minutes. Finally, after the last wash step, a 3',3',5,5'-tetramethylbenzidine (TMB) solution was added as a substrate and the reaction produced a chromophoric product that prompted a colorimetric change. The reaction was then stopped with 2 N H_2SO_4 solution and the absorbance was read at 450 and 570 nm using PowerWave™ XS (Biotek) microplate reader provided with Gen5 software.

For analyzing the data, absorbance values obtained at 570 nm were subtracted to the ones obtained at 450 nm in order to avoid possible interference, and the standard solutions were used to perform a calibration curve. Sample concentration values (pg/ml) obtained by the calibration curve were normalized considering total volume of supernatants collected and by the total protein determined in each well (pg/mg total protein).

3.6. Determination of cell migration. Boyden chamber assay (Transwell)

Cell migration was measured using a Boyden chamber-based cell migration assay, also called transwell migration assay. 24-well chemotaxis chambers with 5.0 µm pore diameter (Transwell, *Corning Costar*) were used for the experiments. Transwell chambers were precoated with 30 µl of fibronectin (0.2 µg/µl) to allow cell attachment in the experiments with THP-1 cells. THP-1 cell suspension (100 µl, 1 x 10^5 cells) were then added to the upper wells of the 24-well chemotaxis chambers in a serum free 0.2% fatty-acid free Bovine Serum Albumin (BSA) medium. Agonists were added to the lower wells diluted in 300 µl of the same medium. When used, inhibitors were added to the upper and lower wells and preincubated for 1 hour prior to agonist addition. The chambers holding the cells were then moved into agonist containing lower compartments.

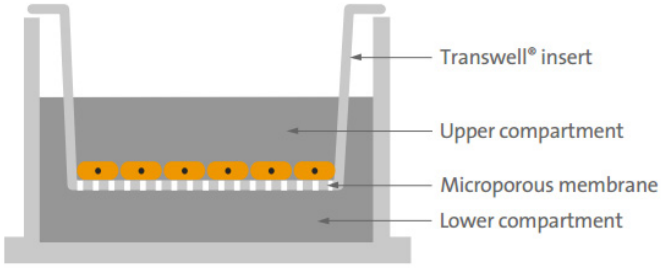

Figure 5: Schematic representation of a Boyden chamber based cell migration assay, from *Corning* 'instructions for use' guide.

After the indicated incubation time, non-migrated cells were removed with a cotton swab, and the filters were fixed with para-formaldehyde (5% in phosphate-buffered saline (PBS)) for 30 minutes. Then, para-formaldehyde was removed and the filters were stained with crystal violet solution (0.1% in PBS) for 20 minutes. After removing the dye with water, the filters were cleaned again with a cotton swab to remove any remaining non-migrated cells. Filters were then placed on microscope slides using mineral oil, avoiding bubbles between slides and coverslips. Cell migration was measured by counting the number of migrated cells in a Nikon Elipse 90i microscope equipped with the NIS-Elements 3.0 software. Cells were counted in 8 randomly selected microscope fields per well, at 100x magnification. The number of migrated cells was normalized to the number of migrated cells in the control chambers.

3.7. Small interfering RNA (siRNA) transfection

Small interfering RNAs (siRNAs) assemble into endoribonuclease containing complexes known as RNA-induced silencing complexes (RISCs). RISC is a multiprotein complex that incorporated one strand of small interfering RNA to be used as a template for recognizing complementary mRNA. When it finds a complementary strand, RISC activates a ribonuclease and cleaves the RNA. Cleavage of cognate RNA takes place near the middle of the bounded region by the siRNA strand.

After the cleavage of targeted mRNA, translation process cannot occur so that the expression of the targeted protein is inhibited or silenced.

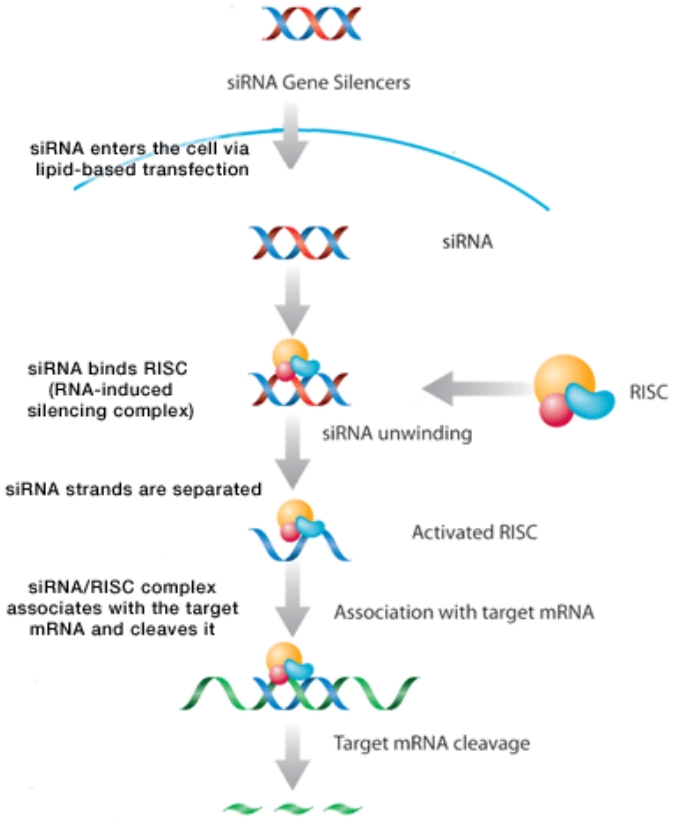

Figure 6: The mechanism of RNA interference (RNAi) from Santa Cruz Biotechnology Inc. website.

siRNA protocols were performed following the manufacturer's instructions.

2.7.1. A549 siRNA transfection with Oligofectamine

A549 cells were seeded in 60 mm plates (2 x 10^5 cells/well) in RPMI medium containing 10% FBS. After 5-6 hours, when cells were attached, the medium was replaced with 1600 μL Opti-MEM and cells were further incubated overnight. Then the siRNA was added following the procedure below:

Solution A: 8 μl of Oligofectamine + 30 μl of Opti-MEM (mixed and incubated for 10 minutes).

Solution B: 20 μl of specific siRNA (20 μM stock) + 360 μl of Opti-MEM.

Solution A was added to solution B and mixed gently by pipetting. The mixture was incubated at room temperature for 15 minutes and 400 μl of the siRNA mixture were then added into each well. Cells were incubated for 5 hours and then 2 ml of Opti-MEM containing 20% FBS was added, without removing the transfection mixture. Cells were

incubated in these conditions overnight. Finally medium was replaced by fresh RPMI medium supplemented with 10% FBS for some hours before cells were harvested and seeded for further experiments. Cells that had not been used were collected and lysed for protein quantification. The silencing efficiency was determined by western blot assay using specific antibodies against the silenced protein.

2.7.2. 3T3-L1 siRNA transfection with Jetprime

3T3-L1 pre-adipocytes were transfected with siRNA using Jetprime transfection reagent from Polyplus-transfection. Cells were seeded in 24-well (2.5 x 10^4 cells/well), 12-well (5 x 10^4 cells/well) or 6-well (1.5 x 10^5 cells/well) plates in DMEM supplemented with 10% NBCS and incubated overnight. The next day siRNA transfection protocol was performed following manufacturer's instructions transfecting 50 nM siRNA per well. Briefly, siRNA was mixed with reaction buffer and Jetprime reagent and incubated for 10 minutes at room temperature before adding it to the cells. Cells were further incubated for 48 hours without medium removal and then adipogenesis was induced. At day 4 after the induction of adipogenesis cell samples were collected and gene silencing was analyzed by western blot using specific antibodies.

3.8. Determination of CerK activity using NBD-Ceramide as a substrate

A549 cells were seeded in 6-well plates (2 x 10^6 cells/well) and grown overnight in RPMI medium supplemented with 10% FBS. The next day, the medium was replaced with serum free medium and incubated for 2 hours. After that time the experiment conditions were set and cells were further incubated for the indicated time. Cells were washed twice with PBS, trypsinized and centrifuged at 200 g for 5 minutes. Cell pellet was then resuspended in 80 µl of homogenization buffer (20 mM HEPES pH 7.4; 150 mM NaCl; 1 mM DTT) supplemented with Protease Inhibition Cocktail (PIC) (1000:1). Cells were lysed by 3 freeze-thaw cycles and sonicated for cell disrupting with 4 cycles of 10 seconds at 20% amplitude using Sonics Vibracell™ VCX 130 sonicator. A fluorescent CerK assay, adapted for a microplate reader, was performed using the method described by Don and Rosen [3], with some modifications. Briefly, cell lysates (50-100 µg of total protein) were mixed with 100 µl of reaction buffer 2X (40 mM HEPES; 20 mM KCl, 30 mM $CaCl_2$; 15 mM $MgCl_2$, 20% glycerol; 2 mM DTT; 2 mM ATP; 0.4 mg/ml BSA) containing 20 µM of C6-NBD-Ceramide. The reactions were allowed to proceed for 20 minutes in the dark at 35ºC before lipid extraction. Then, 250 µl chloroform:methanol (2:1) solution were added and samples were vortexed and centrifuged at 16000 g for 1.5

minutes. 100 µl of the upper aqueous phase were transferred to a black opaque 96-well plate and 100 µl dimethylformamide were added to each well. Fluorescence was measured using a Synergy HT (Biotek) plate reader equipped with Gen5 software. NBD fluorescence was quantified with a 495 nm excitation filter and 525 nm emission filter. Results were expressed relative to fluorescence of control samples.

3.9. Tissue homogenization

Approximately 350 mg of liver or lung tissue were put into a 10 ml-Douncer homogenizer along with 1.7 ml of ice-cold homogenization buffer containing 10 mM Tris-HCl, pH 7.4, 150 mM NaCl, 1 mM EDTA, 1 mM DTT, 0.1 mM PMSF and protease inhibitor at a dilution of 1:1000. Each sample was homogenized with 20 strokes with a motorized Potter-Elvehjem homogenizer and stored at -80ºC until used.

3.10. Folch lipid extraction

Tissue homogenates were sonicated to ensure their homogeneity before lipid extraction. About 1-2 mg of protein were extracted in a 15 ml threaded glass tube in 1 ml of water. 4 ml of chloroform:methanol (2:1) were added, tubes were caped and vortexed for 1 minute. After vortexing samples were centrifuged 500 g for 10 minutes to separate organic and aqueous phases. Upper phases (aqueous) were aspirated and lower (organic) phases were transferred to clean tubes. Chloroform was dried down under nitrogen gas, vortexing occasionally to collect residues from the tube walls.

3.11. Triglyceride measurement in plasma and liver tissue

Liver triglycerides (TG) were measured using a commercial kit from Roche Diagnostics following manufacturer's instructions. This assay provides a sensitive and easy way to measure TG concentration converting them to free fatty acids and glycerol. The glycerol is then oxidized using glycerol oxidase, and H_2O_2, one of the reaction products, is measured quantitatively in a peroxidase catalyzed reaction that produces a measurable color that can be read at 540 nm.

Briefly, 200 µl of lipids in chloroform were transferred into a new tube and 1 ml of chloroform 2% Triton-X100 was added. Samples were dried down under nitrogen gas and lipids and detergent were resuspended in 1 ml of water. They were incubated at 37ºC for 15 minutes, with regular vortexing. Around 150 µg of protein (approximately 50 µl of lipid sample) were used for the assay in 96-well plates. After mixing the assay

reagents as indicated in the kit instructions, absorbance was read at 540 nm and TG concentration was determined using the standard curve. Results were then normalized to mg of total protein.

For plasma TG determination 10 µl of plasma samples were put directly into 96-well plates and the assay was performed following the same protocol.

3.12. Thin-layer chromatography of lipids

Chloroform-dissolved lipid samples were applied onto the origin line of 20x20 cm thin layer chromatography (TLC) silica gel 60 plates, which was set at 1.5 cm from the bottom of the plate. TLC plates were developed in Chloroform/Methanol/Acetic acid/Water (25/15/4/2, by vol) until the solvent reached 10 cm from the origin. The excess of solvent was evaporated from the plate and lipid bands were visualized after staining in iodine vapor.

3.13. Sensitive lipid phosphorus assay

After TLC lipid separation, PC and PE bands were scratched from the TLC plate and put into new glass tubes. Standards and any aqueous samples were dried in a 180ºC heating block. 450 µl of 70% perchloric acid were added to each tube, covered, and heated at 180ºC for 1 hour. Later, 2.5 ml of water were added to each tube, along with 0.5 ml of 2.5% (w/v) ammonium molybdate, vortexing samples immediately. Then 0.5 ml of 10% ascorbic acid (w/v) were added, again vortexing each tube immediately after addition of the reagent. Tubes were then incubated in 95ºC water for 15 minutes, and absorbance was read at 820 nm after cooling and spinning down samples for 5 minutes at 400 g. Each phospholipid concentration was calculated using the standard curve.

3.14. Total RNA isolation

2.14.1. Total RNA isolation from cell cultures

After the indicated treatment, cells were trypsinized, washed with PBS and collected by centrifugation. Henceforth, the whole protocol must be done at 4ºC to ensure the correct RNA extraction. 800 µl of Easy blue reagent were added to the cell pellet, homogenized by pipetting up and down vigorously and incubated at room temperature for 5 minutes. 200 µl of chloroform were added to each sample and mixed by vortexing. After a 15 minute-centrifugation at 14000 g phases were separated and 400 µl of the upper aqueous phase were collected in a new tube. The same volume of

isopropanol was added and RNA was precipitated by incubating the samples for 20 minutes at -80ºC and centrifuging for 10 minutes at 14000 g. An additional wash step with ethanol 75% was done to remove any remaining salt from the sample. Finally, the RNA was dried, 25 µl of nuclease-free water were added and samples were quantified on Nanodrop. Samples were kept at -80ºC until used.

2.14.2. Total RNA isolation from tissue

RNA was isolated from mouse lung tissue using tryzol. Briefly, after mice were euthanized, tissue was harvested using Polytron tool and trizol. Then the tissue lysates were separated into 1 ml aliquots in RNA-free tubes, placed at room temperature for 5 minutes to ensure the disruption of nucleoprotein complexes and centrifuged at 13000 g for 10 minutes at 4ºC to remove fibrous material. Supernatant was then transferred to a clean nuclease-free tube and 200 µl of chloroform were added to each sample. Lysates were then vortexed and incubated at room temperature for 5 minutes. After that, samples were centrifuged again at 13000 g for 15 minutes at 4 ºC. The upper aqueous phase was transferred to an RNAse-free tube and an equal volume of isopropanol was added to the collected aqueous phase. Then, tubes were vortexed and kept on ice for at least 15 minutes to allow RNA precipitation. The samples were then centrifuged at 13000 g for 15 minutes at 4 ºC. Supernatant was then carefully removed by pipetting, 1 ml of 75% ethanol prepared in nuclease-free water was added and samples were then gently mixed by pipetting. Samples were then centrifuged again at 13000 g for 10 minutes at 4ºC. Supernatant was then removed and tubes were left to air dry for 5 minutes. Finally, 50 µl of nuclease-free water were added and samples were vortexed and kept on ice for 10 minutes. Isolated RNA was quantified using the ND-1000 spectrophotometer (*NanoDrop*) and samples were then stored at -80 ºC until used.

2.15. RT-PCR assay (cDNA synthesis)

For retrotranscription protocol 1000 ng of RNA of each sample were used. 3 µl of random primers were added and the samples were incubated 5 minutes at 65ºC to let them anneal and then left on ice. Each RNA sample was then mixed in PCR tubes with 4.3 µl of Reverse Transcription Master Mix solution, containing 2 µl of retrotranscription buffer (10x), 0.8 µl dNTP mix (25 mM), 0.5 µl of RNAse inhibitor and 1 µl retrotranscriptase. The samples were incubated 10 minutes at room temperature. Then, the retrotranscription step was performed for 1 hour at 42ºC and an extra step of 10 minutes at 70ºC was done. Samples were then stored at -80ºC until used.

2.16. PCR assay

For PCR assay 1 µl of each sample was added to 49 µl of master mix reaction containing: 5 µl of PCR buffer (10 x), 0.5 µl of Paq polymerase; 1 µl of each primer (from 10 µM stock), 0.4 µl of dNTP mix (25 mM), and nuclease-free water to a total volume of 50 µl.

The PCR protocol was run as follows:

Initial Denaturation	95ºC	10 min
25-35 cycles	95ºC 55-65ºC 72ºC	30 seg 20 seg 20 seg
Final extension	72ºC	10 min
Storage	4ºC	hold

The samples were then run in a gel red-stained 1% agarose gel for 30 minutes at 100 V and the fragments were analyzed using a Chemidoc MP Imaging System (BioRad). The intensity of the band of each sample was normalized to the intensity of the GAPDH band.

2.17. Quantitative PCR (qPCR) assay

For q-PCR, a cDNA template was diluted (1/100) in sterile dH_2O and a master mix reaction was prepared. Each reaction contained: 0.8 µl forward and 0.8 µl reverse primers (from 10 µM stock), 10 µl qPCR Supermix containing SYBR Green, and 4.4 µl of sterile dH_2O. The master mix solution was vortexed and 16 µl of this solution was dispensed into the wells of the PCR plate, which was placed in the aluminum PCR set up block, chilled on ice. 4 µl of diluted cDNA template was added into each well and a clear adhesive cover was positioned over the PCR plate so that it covered all the wells. The plate was then mixed using Eppendorf MixMate plate mixer for 1 minute. After mixing, the plates were centrifuged at 250 g for 30 seconds in the Eppendorf desktop centrifuge using plate spinner buckets. Finally, quantitative real-time PCR (qPCR) was performed using Step One Plus qPCR system following a 3 step cycling protocol, which consists of an initial step at 94 ºC for 4 minutes, a cycling step at 94 ºC for 30 seconds (denaturation), 60 ºC for 30 seconds (annealing) and 72 ºC for 30 seconds (extension) and a final step at 72 ºC. The last cycle was followed by a melting curve analysis to

ensure that a reaction free of products has been performed. Diluted standard curves were used as external standards. The level of fluorescence emitted from SYBR green dye when incorporated to double-stranded DNA was detected.

The mRNA expression of the samples was normalized to cyclophilin expression, and qPCR data were directly exported from Step One Plus qPCR machine.

The following genes were measured:

Target template	FORWARD SEQUENCE	REVERSE SEQUENCE
CD36	TGGCTAAATGAGACTGGGACC	ACATCACCACTCCAATCCCAAG
NOX2	GACTGGACGGAGGGGCTAT	ACTTGAGAATGGAGGCAAAGG
HMOX1	AGGCTAAGACCGCCTTCCT	TGTGTTCCTCTGTCAGCATCA
CD68	GCGGCTCCCTGTGTGTCTGAT	GGGCCTGTGGCTGGTCGTAG
COL1A1	AGACATGTTCAGCTTTGTGGAC	GCAGCTGACTTCAGGGATG
ASMase	TGCTGAGAATCGAGGAGACA	GACCGGCCAGAGTGTTTTC
CerS2	TGGCCCTGCTCTTTCTCGT	GCTTGCCGCTGGTCTGGT
CerS6	GGAGCTGTCATTTTATTGGTCTTT	GGAACATAATGCCGAAGTCC
Asah1	ACATTTGTGCCAAGTGGAAA	TCAGGAAGGCTGCCAATC
CerK	ACGAGCAGCTGTGTCACCT	GCAAGTGCTTCGGTCTTGA
SPT1	GCTCCTTCGTGGTTGAC	CTTATGGATGTTCTGGCATT
UCP2	CATTGGCCTCTACGACTCTG	GCCTGGAAGCGGACCTTTAC
Cyclophilin	TCCAAAGACAGCAGAAAACTTTCG	TCTTCTTGCTGGTCTTGCCATTCC

2.18. TBARS assay

Oxidizing agents can alter lipid structure, creating lipid peroxides that result in the formation of malondialdehyde (MDA), which can be measured as Thiobarbituric Acid Reactive Substances (TBARS). The measure of TBARS is a commonly used method of determining the relative lipid peroxide content of samples. In the presence of heat and acid, MDA reacts with TBA to produce a colored end product that absorbs light at 530-540 nm. The intensity of the color at 532 nm corresponds to the level of lipid peroxidation in the sample.

After liver tissue homogenization (described above) liver samples were diluted 1:20 in homogenization buffer (10 mM Tris-HCl, pH 7.4, 150 mM NaCl, 1 mM EDTA, 1 mM DTT, 0.1 mM PMSF and protease inhibitor at a dilution of 1:1000) to have approximately 1-1.5 mg protein/ml. For TBARS measurement manufacturer's instructions were followed. First, all samples were acid treated to make a clear solutions by precipitating interfering proteins and other substances for removal by centrifugation, and also to catalyze the TBARS reaction. Then, MDA standard curve was prepared. 150 µl of standards or samples were added to each well of a 96-well plate plus 75 µl of TBA reagent. The optical density of the microplate was pre-read at 532 nm. Then, the plate was covered and incubated at 45°C for 2-3 hours for color development. After that time, the optical density of each well was read again at 532 nm. Pre-reading values were subtracted from the final reading values to correct for the sample's contribution to the final absorption at 532 nm, and results were expressed as nmol TBARS/mg protein in each sample.

2.19. Cholesterol measurement

Cholesterol esters in the serum are hydrolyzed to free cholesterol and fatty acids in a reaction catalyzed by cholesterol ester hydrolase. The cholesterol produced and the free cholesterol already present in the serum are oxidized in a reaction catalyzed by cholesterol oxidase that generates hydrogen peroxide. The formed hydrogen peroxide participates in quantitative oxidative condensation between 3,5-Dimethoxy-N-athyl-N-(2-hydroxy-3-sulfopropyl)-aniline sodium salt (DAOS) and 4-aminoantipyrine in the presence of peroxidase. The product of the reaction is a blue pigment. The total amount of cholesterol in the sample is determined by measurement of the absorbance of the blue color at 600 nm.

For total cholesterol measurement, manufacturer's instructions were followed. Briefly, standard curve was prepared and 5 µl of either standard or plasma sample were added to a 96-well plate in duplicate. Then, 200 µl of assay color reagent (containing cholesterol ester hydrolase, cholesterol oxidase, peroxidase, 4-aminoantipyrine, ascorbate oxidase and DAOS) were added to each well and the plate was incubated at 37°C for 10 minutes. Then, absorbance was measured at 600 nm and 700 nm. 700 nm reading values were subtracted from 600 nm reading values and total cholesterol concentration was calculated using the standard curve. Results were expressed as mM of cholesterol in each sample.

2.20. Glutathione status measurement

Glutathione (GSH) is a tripeptide that contains L-cysteine, L-glutamic acid and glycine. It is the smallest intracellular protein thiol molecule in the cells, which prevents cell damage caused by reactive oxygen species such as free radicals and peroxides. Glutathione exists in reduced (GSH) and oxidized (GSSG) states. GSH is a major tissue antioxidant that provides reducing equivalents for the glutathione peroxidase (GPx) catalyzed reduction of lipid hydroperoxides to their corresponding alcohols and hydrogen peroxide to water. In the GPx catalyzed reaction, the formation of a disulfide bond between two GSH molecules generates oxidized glutathione (GSSG). Glutathione reductase (GR) recycles GSSG to GSH with the simultaneous oxidation of β-nicotinamide adenine dinucleotide phosphate (β-NADPH2). In healthy cells, ›90% of the total glutathione pool is in the reduced form (GSH). When cells are exposed to increased levels of oxidative stress, GSSG accumulates and the ratio of GSSG to GSH increases. An increased ratio of GSSG-to-GSH is an indication of oxidative stress.

Approximately 20 mg of liver or lung tissue were put into a 400 μl of ice-cold PBS/0.5% NP-40 and homogenized using a Dounce homogenizer with 10-15 passes. Samples were then centrifuged for 15 minutes at 4ºC at maximum speed to remove any insoluble material. Samples were kept on ice until used. For GSSG/GSH measurement manufacturer's instructions were followed. Total glutathione, reduced glutathione and oxidized glutathione concentrations were obtained using the fluorimetric values obtained by reading the fluorescence of each sample at 490 nm excitation and 520 nm emission wavelengths using a fluorescence plate reader. Results were expressed as GSSG-to-GSH ratio as an indicator of oxidative stress.

2.21. Adipocyte differentiation

For effective differentiation of 3T3-L1 cells to mature adipocytes a previously described protocol was followed [4] .

Briefly, cells were seeded in 96, 24, 12 or 6-well plates in normal growth medium (DMEM high glucose containing 10% of NBCS and 50 mg/l gentamicin). The next day, when the medium was replaced with fresh medium, cells had already reached confluence. 48 hours later, cell differentiation was induced by changing the medium to DMEM high glucose containing 10% of FBS, 50 mg/l gentamicin, 0.5 mM 3-isobutyl-1-methylxanthine (IBMX), 0.25 μM dexamethasone, 1 μg/ml insulin, and 2 μM

rosiglitazone. After 48 hours, on day 2 after the induction of differentiation, the medium was changed to DMEM high glucose containing 10% FBS, 50 mg/l gentamicin and 1 μg/ml insulin, and maintained for another 48 hours. This medium was further refreshed on days 5, 7 and 9 after the induction of differentiation. For undifferentiated 3T3-L1 pre-adipocytes (control), the normal growth medium (DMEM containing 10% of NBCS and 50 mg/l gentamicin) was refreshed on days 2, 4, 5, 7 and 9.

The differentiation process is easily visible. Intracellular lipid droplets start to appear at around day 4 after induction of adipogenesis and increased in both number and size over the following days. After 10 days almost all of cells cultured following the differentiation protocol contained lipid droplets of different sizes. In normal culture medium used for undifferentiated pre-adipocytes, only very few single cells showed small visible lipid droplets that did not change their size over time.

2.22. Triglyceride measurement in cell culture

3T3-L1 pre-adipocytes were cultured in 96-well plates (7 x 10^3 cells/well) and grown in DMEM supplemented with 10% NBCS. After the induction of adipogenesis triacylglicerides content was measured using an adipogenesis assay kit from Abnova. In this assay, triglycerides are efficiently solubilized, then hydrolyzed to glycerol, which is subsequently oxidized to convert the probe to generate color that absorbs at 570nm.

For triglyceride (TG) testing, the manufacturer's instructions were followed. Briefly, after differentiation, cells were washed with PBS and 100 μl of the lipid extraction solution per well were added. Then, plates were cover with an adhesive film to avoid evaporation and they were incubated in a heating block at 95°C for 30 minutes. In order to ensure that triglycerides were completely dissolved in the lipid extraction buffer, plates were cooled while shaking. 50 μl/well of standard dilutions and 15 μl of the lipid extracts were transferred to the 96-well plate and assay buffer was added in order to bring the volume up to 50 μl. Then 2 μl of lipase were added to each well containing either sample or standard, mixed and incubated 10 minutes at room temperature so that TGs will be converted to glycerol and fatty acids. Then, 50 μl of the reaction mix (46 μl adipogenesis assay buffer+ 2 μl probe + 2 μl enzyme mix) were added to each well and incubated at 37°C for 30 minutes in the dark. Finally, the absorbance values were read at 570 nm in a plate reader and TG concentration of each sample was calculated.

2.23. Oil Red O staining

3T3-L1 pre-adipocytes were seeded in 24-well plates (6 x 10^4 cells/well) and grown in DMEM supplemented with 10% NBCS. After the induction of adipogenesis, in order to quantify accumulation of intracellular lipid droplets, an Oil Red O stock solution (3 mg/ml of Oil Red O in isopropanol) was prepared. Cells were washed with PBS and 500 µl of previously diluted Oil Red O solution (3 parts of Oil Red O stock solution mixed with 2 parts of H_2O) were added to each well, including control well without cells. Cells were then incubated with Oil Red O solution for 20 minutes at room temperature while gentle shaking. Then, cells were washed with water and after removal of the last wash stained plates were photographed under a conventional light microscope. Finally, 200 µl of isopropanol (dye extraction solution) per well were added and shaken for 30 minutes. Then, 50 µl of extracted dye were transferred into a 96-well plate and quantified by reading the absorbance at 510 nm in a plate reader. The dye extracted from the controls (wells without cells) represents non-specific binding of the dye to the plate. Thus, this value must be subtracted from the absorbance of experimental wells to obtain more accurate assessment of specific staining.

2.24. Statistical analyses

Results are expressed as the mean ± SEM of the number of independent experiments performed in duplicate or triplicate, as indicated in each case. Differences between means of each group were analyzed using two-tailed Student's *t*-test or two-way ANOVA with Tukey's post-hoc test for multiple comparison test, with level of significance set at $p<0.05$.

Significance and symbols used:

Symbol	Significance
n.s.	p>0,05; not significant
*	P<0,05; significant
**	P<0,01; significant
***	P<0,001; significant

symbol has been used instead of * symbol to compare inhibitor/agonist-treated conditions versus agonist-treated ones.

3. References

[1] P. Gangoiti, M.H. Granado, S.W. Wang, J.Y. Kong, U.P. Steinbrecher, A. Gomez-Munoz, Ceramide 1-phosphate stimulates macrophage proliferation through activation of the PI3-kinase/PKB, JNK and ERK1/2 pathways, Cell Signal 20 (4) (2008) 726-736.

[2] K. Aoshiba, J. Tamaoki, A. Nagai, Acute cigarette smoke exposure induces apoptosis of alveolar macrophages, Am J Physiol Lung Cell Mol Physiol 281 (6) (2001) L1392-1401.

[3] A.S. Don, H. Rosen, A fluorescent plate reader assay for ceramide kinase, Anal Biochem 375 (2) (2008) 265-271.

[4] K. Zebisch, V. Voigt, M. Wabitsch, M. Brandsch, Protocol for effective differentiation of 3T3-L1 cells to adipocytes, Anal Biochem 425 (1) (2012) 88-90.

Chapter 1

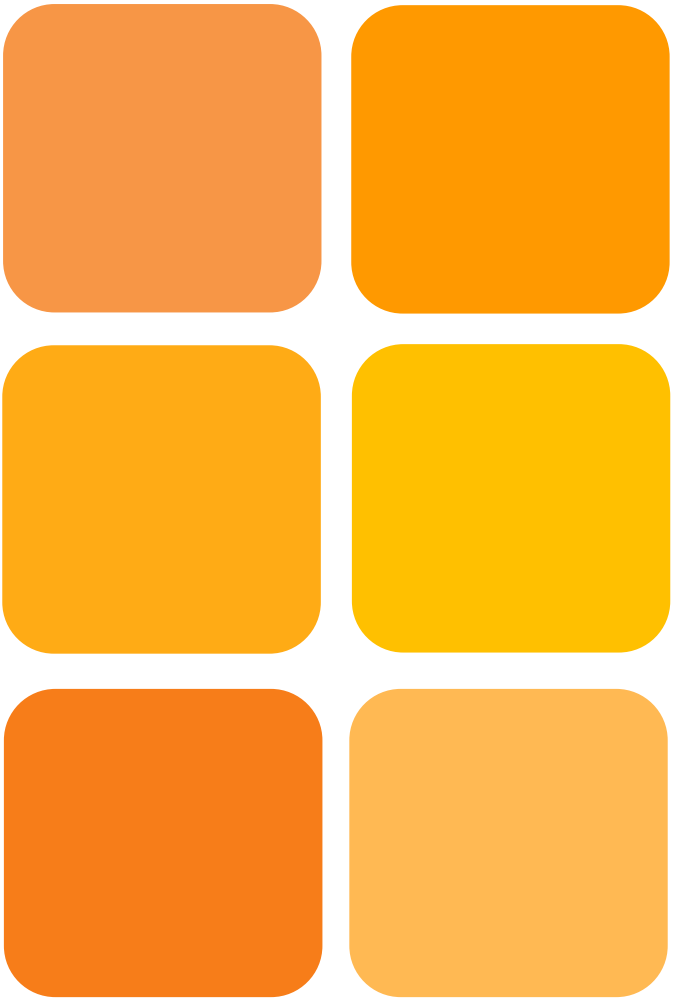

CHAPTER 1:

Role of CerK/C1P in cigarette smoke-induced deleterious effects in lung cells

1. INTRODUCTION

1.1. Cigarette smoke and lung diseases

Cigarette smoking has reached epidemic proportions worldwide and it is the most prevalent cause of many serious health disorders including respiratory diseases, cancer, and other pathologies related to kidney, liver, pancreas, and the cardiovascular system.

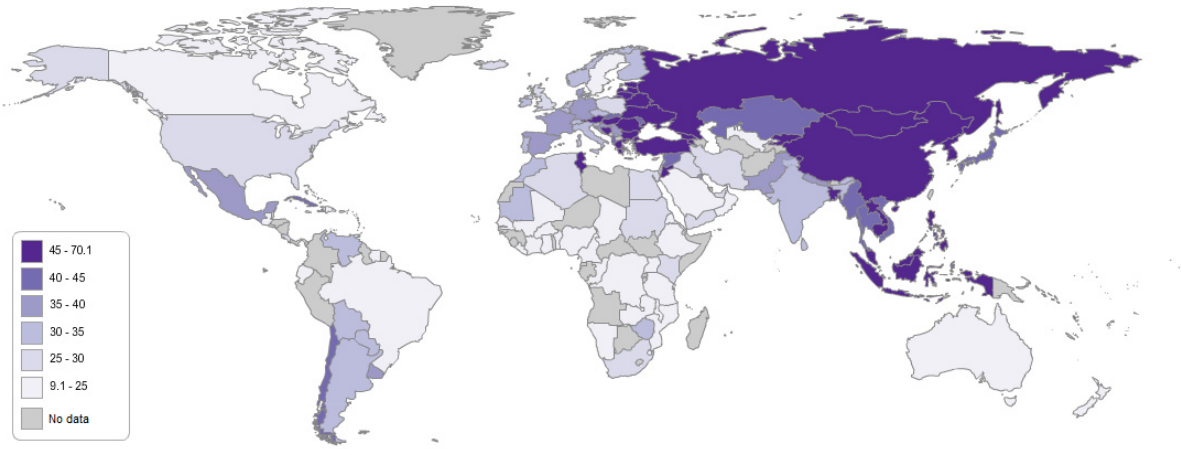

Figure 1: **Prevalence of tobacco smoking worldwide.** Image taken from FUNDADEPS website.

Cigarette smoke (CS) is a complex, dynamic and reactive mixture containing more than 7000 different chemicals. In spite of uncertainties concerning whether particular cigarette smoke constituents are responsible for specific adverse health outcomes, there is broad scientific agreement in several of the major classes of chemicals in the combustion emissions of burned tobacco are toxic and carcinogenic [1]. This toxic and

carcinogenic mixture is one of the leading causes of death and an important risk factor for several systemic and respiratory diseases. According to World Health Organization (WHO) estimates, 5.4 million premature deaths are related to tobacco smoking worldwide, and by 2025, if current trends continue, 10 million smokers are expected to die.

Chronic CS exposure causes structural and functional changes in the respiratory tract but the mechanisms leading to those effects remain unclear. Long-lasting smoking can generate different pathologies including chronic obstructive pulmonary disease (COPD), epithelial cell tumors, cardiovascular disease, as well as an increased incidence of asthma and respiratory infections [2].

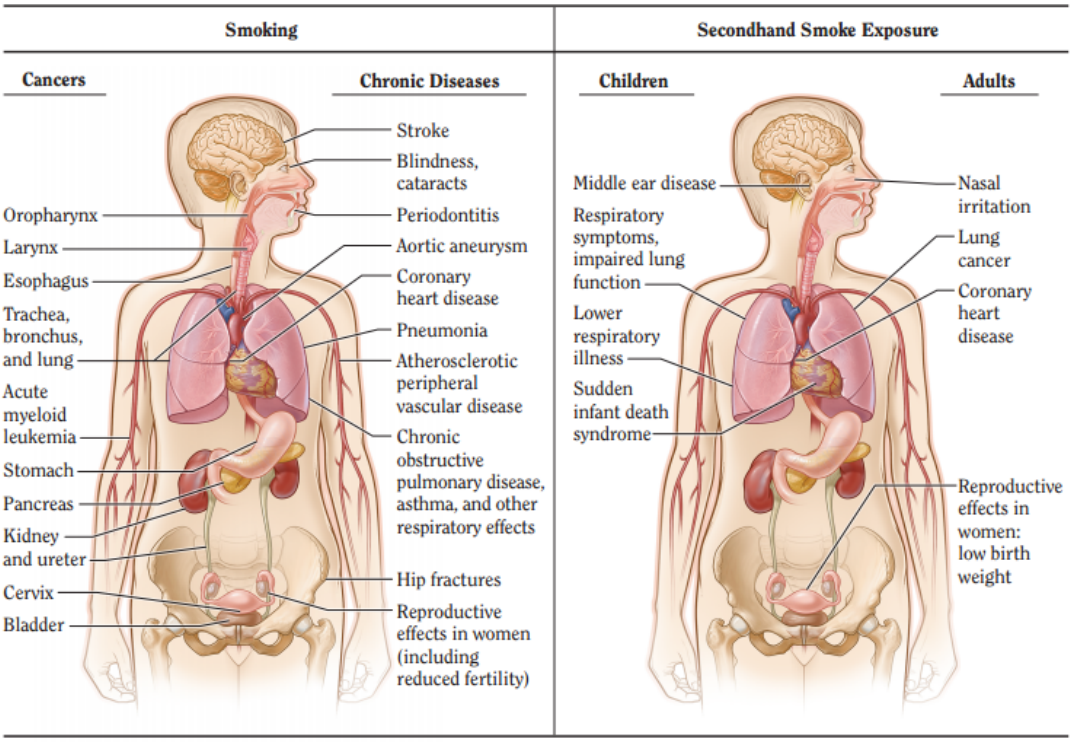

Figure 2: The health consequences causally linked to smoking and exposure to secondhand smoke. Image taken from The U.S. Department of Health and Human Services (USDHHS).

The respiratory epithelium is the main target of highly toxic CS. Chronic inhalation of CS alters the function of both the innate and the adaptive immune response. It has been shown that epithelial integrity and immunity is significantly affected by smoke exposure. CS is clearly detrimental to lung epithelium and mobilizes and activates alveolar macrophages producing pro-inflammatory mediators, reactive oxygen species, and proteolytic enzymes.

1.2. Chronic obstructive pulmonary disease (COPD)

Chronic obstructive pulmonary disease (COPD) is characterized by persistent and progressive airflow limitation caused by chronic inflammation of the airways and lung parenchyma. The airflow limitation is associated with an enhanced chronic inflammatory response in the airways and lung tissue to harmful particles or gases [3], and is caused by the combination of chronic bronchitis and emphysema. Typically, the terms of chronic bronchitis and emphysema have been used to describe the two major clinical features of COPD. Chronic bronchitis results from chronic inflammation of the small and medium-size airways and leads to airflow limitation, dyspnea, chronic cough, and sputum production. Emphysema, on the other hand, is the result of the inflammatory processes that destroy elastic tissue in the terminal airspaces and lung parenchyma, resulting in loss of lung elastic recoil, airflow limitation, dyspnea, and hypoxemia. Depending on the anatomic location of lung tissue destruction, emphysema can be further characterized into panlobular emphysema, which involves predominantly lower lobes, or centrilobular emphysema, which involves the upper lobes, as a result of inflammatory destruction of the respiratory bronchioles. This last type of emphysema is most commonly associated with tobacco smoking [4].

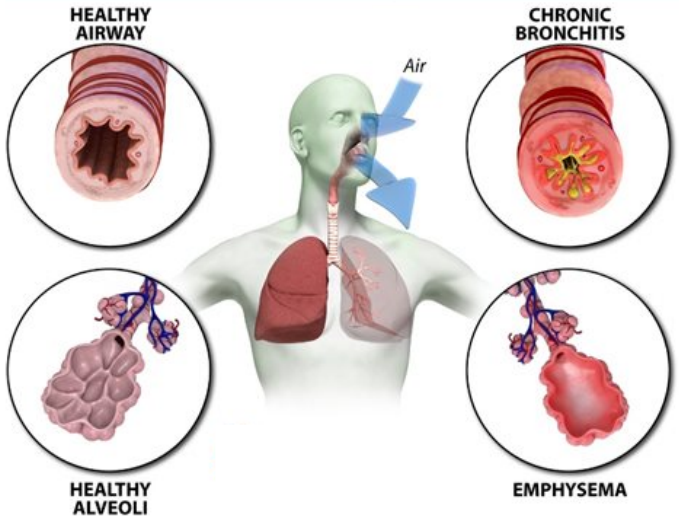

Figure 3: Schematic representation of chronic bronchitis and emphysema. Taken from National Jewish Health website.

Closely linked to smoking, COPD is a public health problem of epic proportions as it is the third leading cause of mortality and morbidity in the world [5]. Among smokers,

COPD and lung cancer commonly coexist, and the presence of COPD increases the risk of developing lung cancer [6].

1.3. Cell migration

Cell migration is part of the inflammatory response. It is a complex process that requires strict coordination of the following steps: cell polarization, protrusion and cell adhesion. These processes are regulated by complex signaling networks initiated by integrins and other receptors. The regulation occurs through local, transient signals that retain polarity of the cell and drive local remodeling like actin polymerization, adhesion, actomyosin bundling and contraction, and microtubule dynamics. Actin filaments, microtubules, and cycling lipid vesicles span the cell and contribute to integrate the processes that mediate migration.

Cell migration is a key component for the homeostasis of the adult individual. Therefore, any cell migration failure, or inappropriate migratory movements, can result in severe defects such as immunosuppression, autoimmune diseases, defective wound repair, or tumor dissemination. Thus, understanding the mechanisms that support cell migration is essential for the development of new strategies for inflammation and cancer therapy.

1.4. Monocyte chemoattractant protein-1 (MCP-1/CCL2)

The monocyte chemoattractant protein-1 (MCP-1 or CCL2) was the first discovered human C-C chemokine. Located on chromosome 17, human MCP-1 is a 13 kDa-protein composed of 76 amino-acids [7]. However, it can acquire different molecular mass by O-glycosylations. These changes on the MCP-1 molecule have been shown to slightly reduce its chemotactic potency. Although monocyte/macrophages are thought to be the major MCP-1 source [8], this chemokine can also be produced by a variety of cell types, including endothelial cells, fibroblasts, smooth muscle cells, astrocytes, microglial cells and epithelial cells [9-12]. The expression of MCP-1 can be constitutive or induced by oxidative stress, cytokines, or growth factors.

MCP-1 regulates the migration and infiltration of monocytes, memory T lymphocytes, and natural killer (NK) cells, and thereby it is a potential intervention point for the treatment of various diseases, including multiple sclerosis, rheumatoid arthritis, atherosclerosis, insulin-resistance and diabetes [13-16]. MCP-1 mediates its effects through interaction with its receptor CCR2, and, unlike MCP-1, CCR2 expression is quite

restricted to certain cells types. There are two alternatively spliced forms of CCR2, named CCR2A and CCR2B, which differ only in their C-terminal tails. CCR2A is the major isoform expressed by mononuclear cells and vascular smooth muscle cells, whereas monocytes and activated NK cells express predominantly the CCR2B isoform [17].

Macrophages have been found to be increased in airways, lung parenchyma, bronchoalveolar lavage fluid (BALF), and sputum in patients with COPD, which correlates with the severity of the disease [18-20]. The increased number of macrophages in the lungs of patients with COPD are caused by increased recruitment of monocytes from the circulation in response to the monocytes-selective chemokines MCP-1 and CXCL1, which are increased in sputum and BALF in those patients [21].

1.5. Lung cancer

Cancer is a hyperproliferative disorder that involves morphological cellular transformation, dysregulation of apoptosis, uncontrolled cellular proliferation, invasion, angiogenesis, and metastasis. Worldwide lung cancer is most commonly occurring cancer in men and the third most common cancer in women. About 2 million new cases were reported in 2018, which represents the 13.5% of all new cases of cancer, and it accounted for 1.8 million deaths in 2018 [22]. Small-cell (SCLC) and non-small-cell lung cancer (NSCLC) are the two main types of lung cancer. NSCLC accounts for up to 85% of all lung cancer cases and it can be divided into three major subtypes: squamous cell carcinoma, adenocarcinoma and large-cell carcinoma [23, 24]. SCLC, on the other hand, accounts for up to 15% of all lung cancers, and it is characterized by aggressive biology, propensity for early metastasis and overall poor prognosis.

Smoking and secondary exposure to tobacco smoke are the main causes of lung cancer. Carcinogens in tobacco smoke and other inhaled particles can interact directly with the DNA of lung cells. Because the whole lung is exposed to inhaled carcinogens, several sites may accumulate different cancerous changes, leading to multiple cancers originating in different types of cells. Besides, clinical and epidemiologic studies suggest a strong association between chronic inflammation and the development of lung cancer, as it increases the risk of malignant transformation [25], as a response to exposure to irritants and repeated injury. Chronic cigarette smoking retard mucociliary clearance of foreign particulates and secretions that contribute to persistent inflammation, whereas the inhaled particles evoke strong lung and airway inflammatory responses [26].

1.6. Epithelial-to-mesenchymal transition (EMT)

Epithelial to mesenchymal transition (EMT) is a biologic process by which an epithelial cell undergoes biochemical changes that promote the acquisition of a mesenchymal phenotype in response to external stressors or specific growth factors. A particular characteristic of EMT is the loss of cell adhesion, driven by the down regulation of epithelial markers, such as adherence protein E-cadherin, and the up regulation of mesenchymal markers including vimentin, fibronectin, and N-cadherin. Cells undergoing EMT gain functional characteristics of mesenchymal cells, like acquiring invasive potential and the ability to secrete matrix metalloproteinases (MMPs) and extracellular matrix (ECM) proteins.

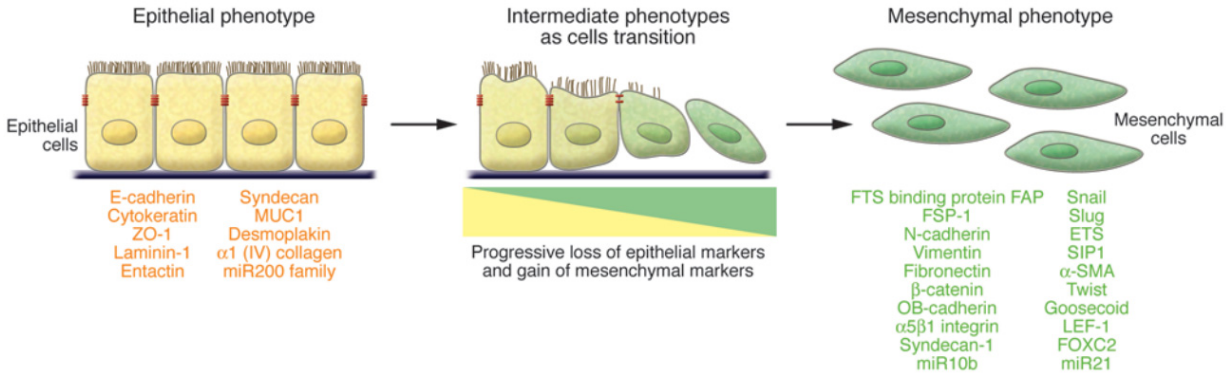

Figure 4: Epithelial-to-mesenchymal transition (EMT) process. Taken from [27].

EMT is recognized as a central feature of normal tissue development. It takes part in different developmental and repair processes like implantation, embryo formation, and organ development as well as wound healing, tissue regeneration, and organ fibrosis. However, this process also occurs during tumor invasion and metastasis [28]. On progression to more aggressive tumor, cancer cells acquire qualities that enable them to invade neighboring tissues and to metastasize. The steps involved in metastatic dissemination include loss of cell-cell adhesion, increased motility and invasiveness, entry into and survival in the circulation, dispersion to distant anatomic sites, extravasation, and colonization of a distant organ [27]. Therefore, the mesenchymal and thereby more invasive phenotype and the subsequent colonization of distant tissues, far from the tissue of origin, have been areas of intensive research.

Although the EMT process can be induced and regulated by different growth and differentiation factors [29-32], transforming growth factor β1 (TGF-β1) has been identified as the major EMT inducer during embryogenesis, fibrosis and cancer

progression in different cancer cells [33]. Upon TGF-β1 treatment, epithelial cells change from cuboidal to elongated spindle shape, and show decreased expression of epithelial markers and enhanced expression of mesenchymal markers. These changes are accompanied by increased motility. Cancer cells often increase their production of active TGF-β1, which not only triggers EMT and allows the cells to become more invasive, but also enhances angiogenesis in close proximity to the tumor microenvironment, providing an exit route for migratory mesenchymal cells [34].

In this chapter, we sought to examine the deleterious effects elicited by CS in lung epithelial cells. More specifically, we sought to determine the implication of CerK/C1P in CS-induced inflammatory responses and EMT process, two of the main effects of cigarette smoking in lung tissue.

2. RESULTS

2.1. Exposure to CSE promotes MCP-1 but not VEGF, IL-8 or IL-6 cytokine release in A549 cells

The effects of CS in cells were studied using CS extracts (CSE) that were prepared as outlined in the *Materials and Methods* section. To establish the optimal non-toxic concentration of CSE to be used in experiments, cell viability assays were performed using increasing concentrations of CSE and crystal violet to stain and count the cells. We wanted to expose cells to CSE as longer as possible avoiding toxicity, so we decided to test low concentrations in a 48-h treatment, since A549 cells maintained in a serum –free medium for longer time periods started to die. As seen in figure 5, low concentrations of CSE for 48 h had no significant effect on cell viability. Based on these results, we decided to test the effect of 3% CSE on a 48-h treatment.

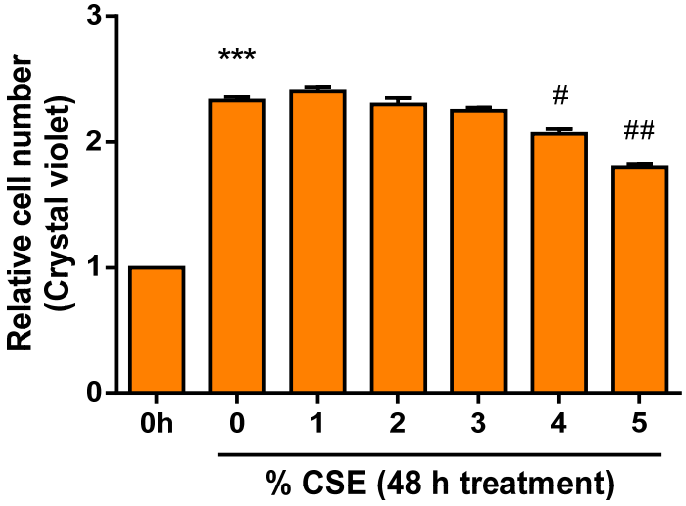

Figure 5: Low concentrations of CSE for 48 h have no effect on cell viability. A549 cells were seeded in 96-well plates (8000 cells/well) and treated with increasing concentrations of CSE for 48 h. The cells were then stained with a solution of crystal violet as described in *Materials and Methods*. Results are expressed as the absorbance at 570 nm relative to control at 0 h and they are the mean ± SEM of 3 different experiments performed in triplicate. (***p‹0.001; #p‹0.05; ##p‹0.01).

Cigarette smoke has been described as the main cause for several inflammatory diseases, such as COPD or asthma. To test the pro-inflammatory ability of CSE A549 cells were treated with 3% CSE for 48 h and the concentration of different secreted cytokines were analyzed by ELISA. We observed that the release of vascular endothelial growth factor (VEGF), interleukin-8 (IL-8) or interleukin-6 (not shown) increased over time but CSE (3%) had no significant effect (Figure 6).

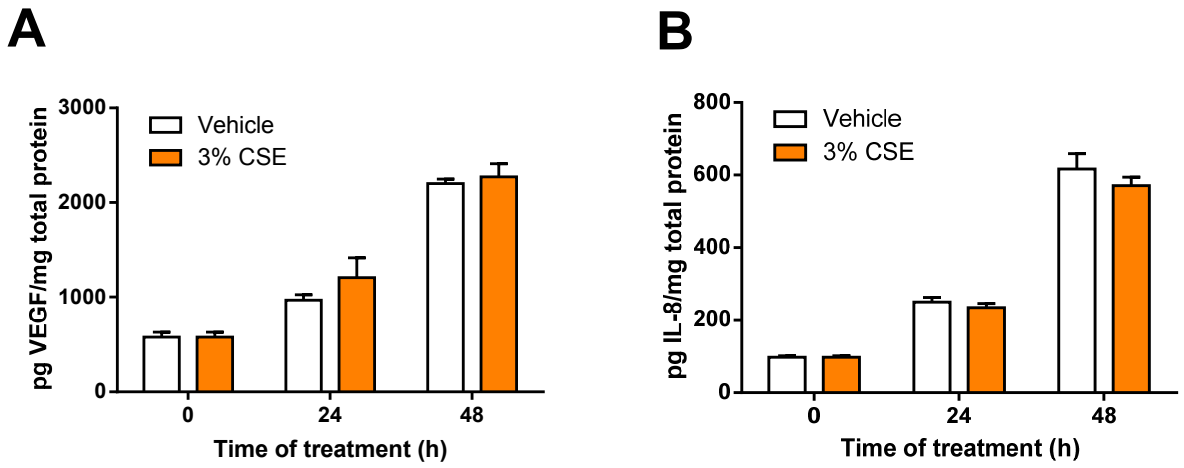

Figure 6: CSE does not alter VEGF or IL-8 cytokine release in A549 cells. Cells were seeded in 12-well plates (80000cells/well) and treated with 3% CSE for the indicated time. Cytokine release was measured using commercial ELISA kits as described in *Materials and Methods*. A) VEGF and B) IL-8 release of 3% CSE-treated cells. Results were normalized to total protein content in each well and they are expressed as mean ± SEM of 3 independent experiments performed in duplicate.

An important chemokine also involved in inflammatory responses is monocyte chemoattractant protein-1 (MCP-1). Therefore, we tested to evaluate whether CSE had any significant effect on MCP-1 release. Figure 7 shows that MCP-1 release also increases with time, and interestingly CSE significantly enhanced MCP-1 release.

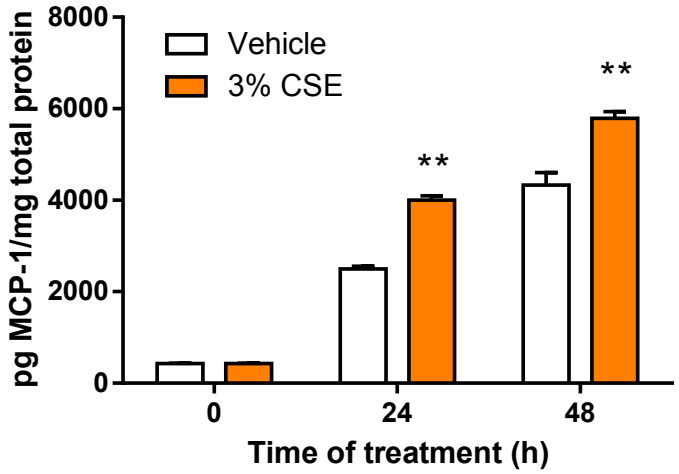

Figure 7: CSE (3%) enhances MCP-1 release in A549 cells. Cells were seeded in 12-well plates (80000 cells/well) and treated with 3% CSE for the indicated times. MCP-1 release was measured using a commercial ELISA kit as described in *Materials and Methods*. Results were normalized to the total protein content in each well and they are expressed as mean ± SEM of 3 independent experiments performed in duplicate. (**p‹0.01).

2.2. CSE-treated A549 cells promote THP-1 monocyte migration

Given the importance of MCP-1 as a chemoattractant cytokine for monocytes, we tested to see whether conditioned medium from CSE-treated A549 cells was able to stimulate monocyte migration. For this, human THP-1 monocytes were used. Cell migration was determined using a Boyden-chamber migration assay in which conditioned medium from untreated and CSE-treated A549 cells were placed in the lower chambers whereas THP-1 monocytes suspended in regular medium were seeded in the upper chambers. Cell migration was determined after 24 h of incubation. Figure

8 shows that A549 cell conditioned medium significantly stimulated THP-1 cell migration, thereby supporting our observation that CSE-induced MCP-1 release was causing the migration of THP-1 monocytes.

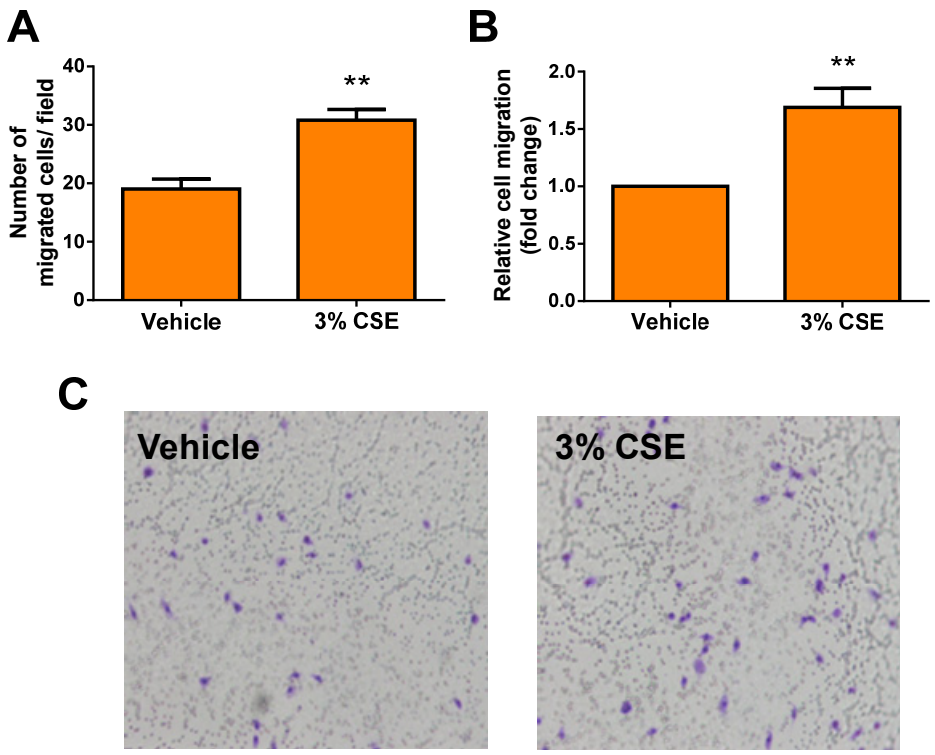

Figure 8: Conditioned medium from CSE (3%)-treated A549 cells promotes THP-1 cell migration. A549 cells were seeded in 12-well plates (80000 cells/well) and treated with 3% CSE for 48 h, as described in *Materials and Methods*. A549 cell conditioned medium was placed in the lower chambers of 24-well Boyden chamber plates, and THP-1 cells were seeded in regular medium in the upper chambers. Cell migration was assessed after 24 h of incubation. A) Number of THP-1 migrated cells per well using A549 untreated and 3% CSE-treated A549 cell conditioned medium as chemoattractant. B) THP-1 cell migration relative to controls. C) Representative micrographs of THP-1 migrated cells. All values are expressed as mean ± SEM of 7 independent experiments performed in duplicate. (**$p<0.01$).

We next sought to determine whether conditioned medium from CSE-treated A549 cells was able to induce THP-1 monocyte differentiation into macrophages. For this, THP-1 cells were treated either with medium from non-treated A549 (vehicle) or with cell conditioned medium from cells treated with 3% CSE for 48 h. Macrophage differentiation was analyzed by determining the expression of the CD36 macrophage marker by Western-blotting. As shown in figure 9, conditioned medium from non-treated A549 cells were already able to stimulate THP-1 macrophage differentiation but

this was significantly enhanced when conditioned medium from CSE (3%)-treated A549 cells was used.

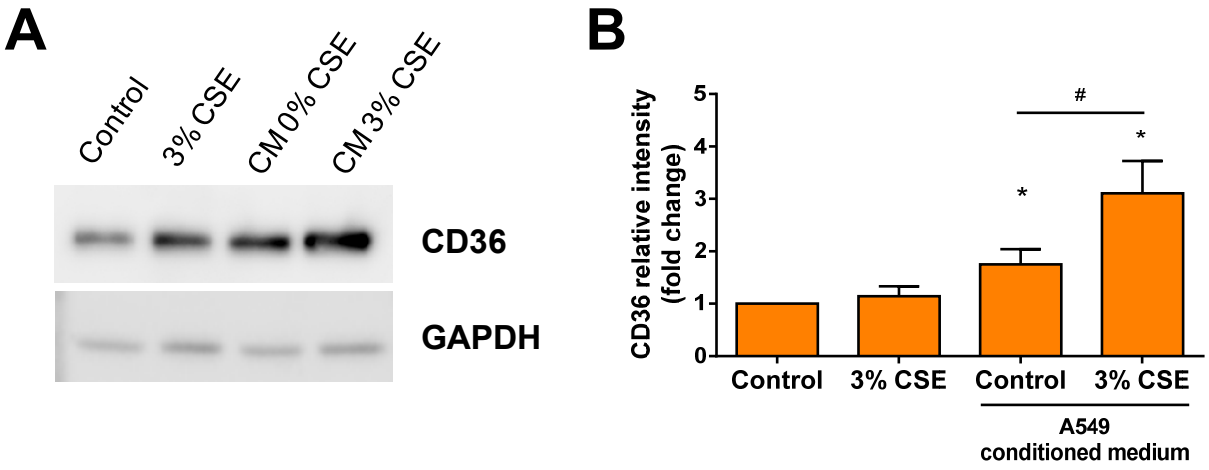

Figure 9: Conditioned medium from CSE (3%)-treated A549 cells promotes THP-1 monocyte differentiation into macrophages. THP-1 cells were treated with 3% CSE or with conditioned medium from non-treated or CSE (3%)-treated A549 cells for 48 h. CD36 macrophage marker expression levels were analyzed by Western-blotting using specific antibodies. Equal loading of protein was assessed with an antibody against GAPDH. A) Representative western blot results. Similar results were obtained in each of 7 independent experiments. B) Quantification of A relative to control. All results are expressed as mean ± SEM of 7 independent experiments. (*p‹0.05, #p‹0.05).

2.3. Signaling pathways implicated in CSE-enhanced MCP-1 release

Previous work from our laboratory showed that MEK-ERK, PI3K-AKT, and ROCK1-2 are relevant pathways implicated in MCP-1 release [35]. Therefore, we sought to determine whether these routes were important for regulation of MCP-1 release by CSE.

To determine the implication of the MEK-ERK pathway in CSE-induced MCP-1 release in A549 cells we performed gene silencing for MAPK1 (ERK2) and MAPK3 (ERK1) using gene specific siRNA for each independent kinase, as detailed in the *Materials and Methods* section. siRNA-targeted cells were seeded in 12-well plates and treated with 3% CSE for 48 h. The culture medium was then analyzed for MCP-1 release using an ELISA kit. The results shown in figure 10 indicate that neither MAPK1 nor MAKP3 were implicated in CSE-induced MCP-1 release in these cells.

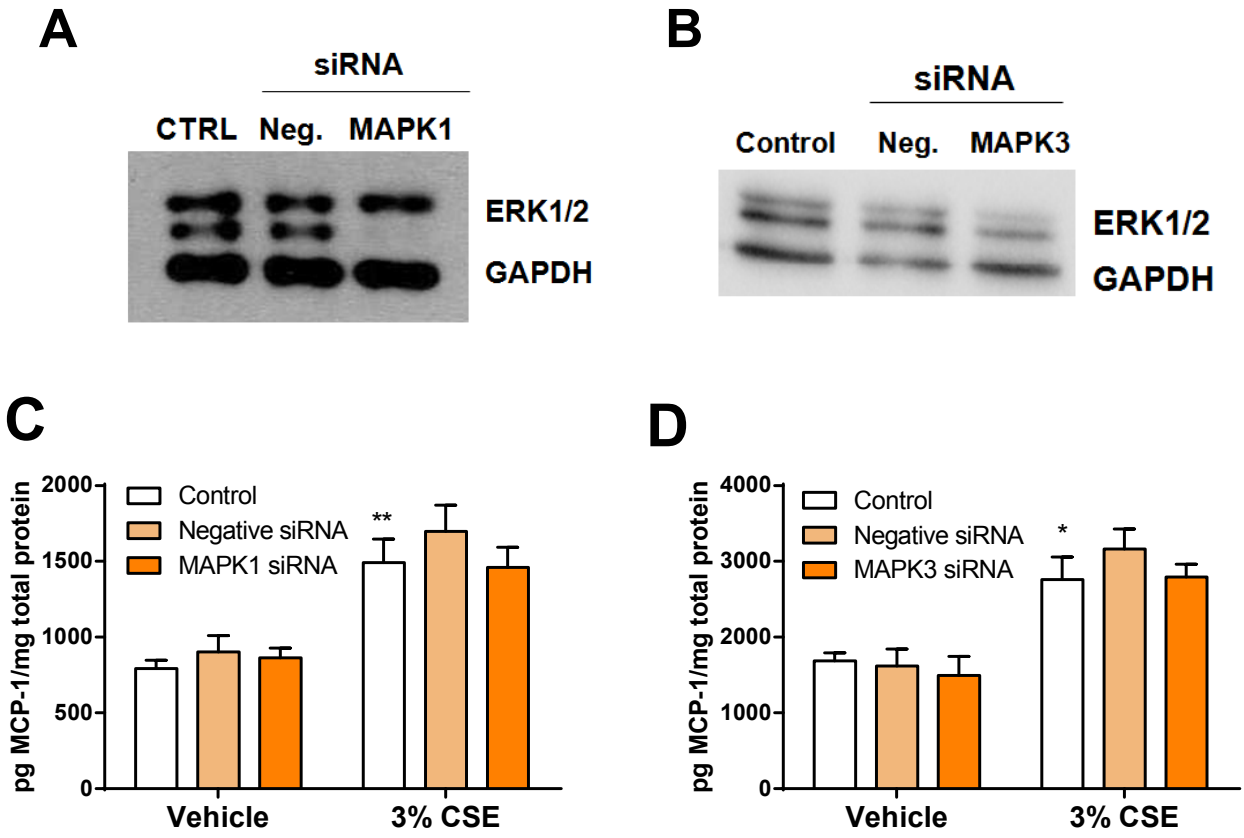

Figure 10: Neither MAPK1 nor MAKP3 are implicated in CSE-enhanced MCP-1 release in A549 cells. Cells were seeded in 60-mm dishes and siRNA treatment was performed using oligofectamine as transfection reagent as described in *Materials and Methods*. Cells were then trypsinized and counted. Gene silencing was checked by Western blotting. siRNA-targeted cells were seeded in 12-well plates (80000 cells/well) and treated with either vehicle or 3% CSE for 48 h. After that time, the supernatants were collected for determination of MCP-1 release using an ELISA kit. A) and B) Representative western blot results showing the effective gene silencing by siRNA. Similar results were obtained in each of 4 experiments. C) and D) MCP-1 quantification by ELISA assay normalized to total protein. Results are expressed as mean ± SEM of 5 (for C) or 4 (for D) independent experiments performed in duplicate. (*$p<0.05$, ***$p<0.001$).

To determine the implication of the PI3K-AKT pathway in CSE-induced MCP-1 release we performed gene silencing for p85α (PI3K regulatory subunit α), AKT1 and AKT2 in A549 cells. siRNA-targeted cells were then seeded in 12-well plates and treated with either vehicle or 3% CSE for 48 h. The culture medium was then analyzed for MCP-1 release as indicated above. Figure 11A shows that p85α silencing did not significantly affect CSE-enhanced MCP-1 release. By contrast, knockdown of AKT2 significantly enhanced MCP-1 release both in non-treated and CSE-treated cells, suggesting that

AKT2 may have an inhibitory role in MCP-1 release (Figure 11C). However, silencing of AKT1 had no significant effect.

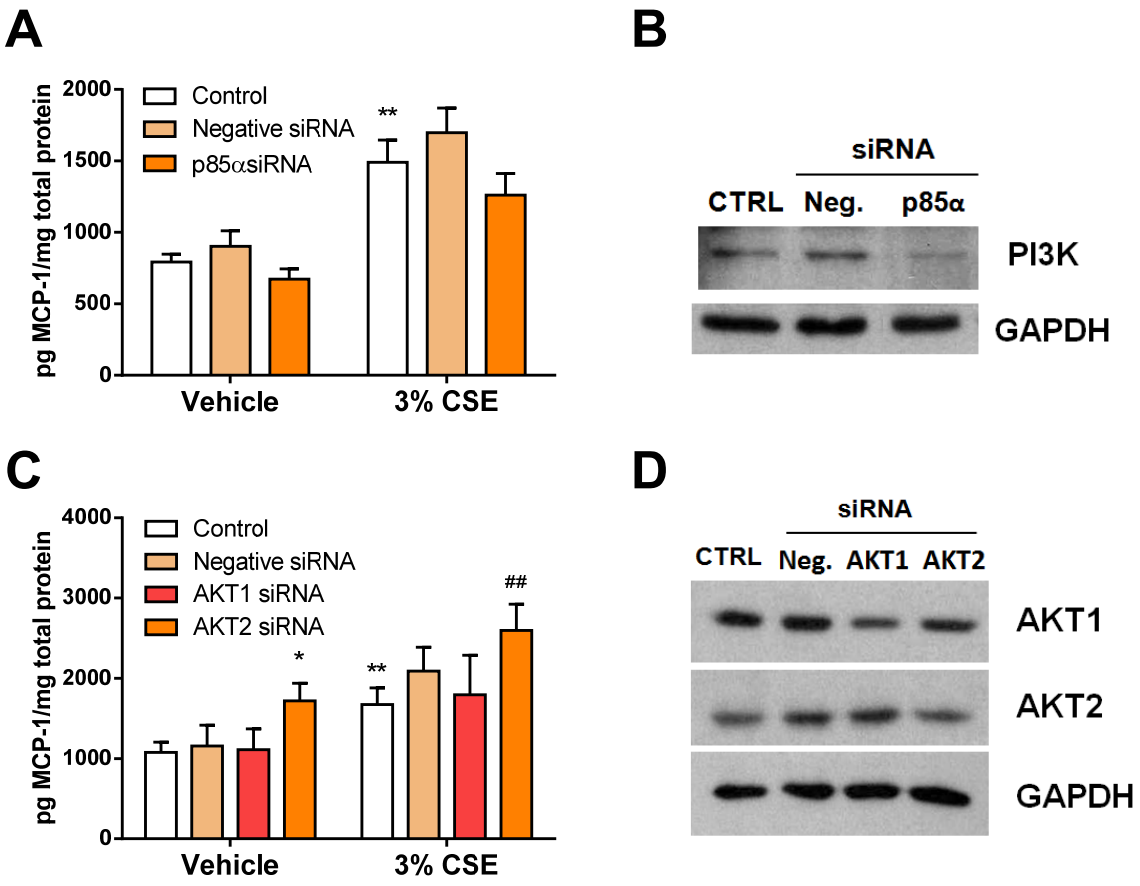

Figure 11: AKT2 is implicated in CSE-enhanced MCP-1 release in A549 cells. Cells were seeded in 60-mm dishes and siRNA treatment was performed using specific siRNAs to silence the gene encoding p85α, AKT1and AKT2, as described in *Materials and Methods*. Cells were then trypsinized and counted. siRNA-targeted cells were seeded in 12-well plates (80000 cells/well) and treated with either vehicle or 3% CSE for 48 h. After that time, the supernatants were collected and MCP-1 was analyzed using an ELISA kit. A) MCP-1 quantification by ELISA assay normalized to total protein in p85α siRNA-targeted cells. Similar results were obtained in each of 5 experiments performed in duplicate B) Representative western blot of the effective p85α silencing. GAPDH was used as protein loading control. Similar results were obtained in each experiment. C) MCP-1 quantification by ELISA assay normalized to total protein in AKT1 and AKT2 siRNA-targeted cells. D) Representative western blot showing the effective AKT1 and AKT2 silencing by siRNA. GAPDH was used as protein loading control. Similar results were obtained in each experiment. Results are expressed as mean ± SEM of 5 independent experiments performed in duplicate. (*$p<0.05$, **$p<0.01$).

We also studied the implication of ROCK1-2, as this is also a key regulatory pathway of cell migration. To determine the implication of this pathway in CSE-induced MCP-1 release we silenced both ROCK1 and ROCK2, and performed an ELISA assay to quantify cytokine levels after 3% CSE treatment for 48 h. As it can be observed in figure 12A, ROCK1 but not ROCK2 inhibition strongly blocked MCP-1 release in A549 cells, suggesting that ROCK1 is necessary for regulation of this process.

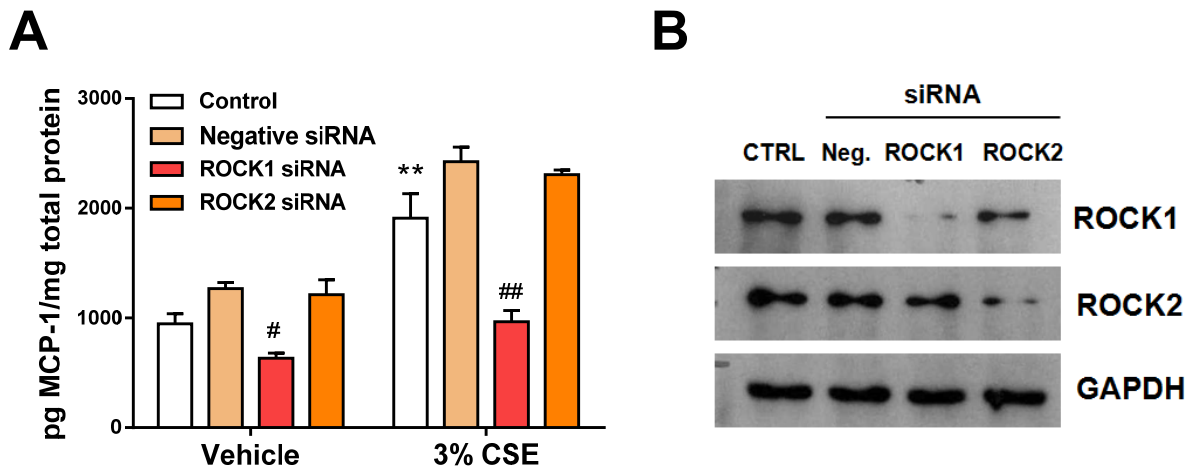

Figure 12: ROCK1 but not ROCK2 is implicated in CSE-enhanced MCP-1 release in A549 cells. Cells were seeded in 60-mm dishes and gene silencing was performed using oligofectamine as transfection reagent as described in *Materials and Methods*. Cells were then trypsinized and counted. siRNA-targeted cells were seeded in 12-well plates (80000 cells/well) and treated with either vehicle or 3% CSE for 48 h. After that time, the supernatants were collected and MCP-1 was analyzed using an ELISA kit. A) MCP-1 quantification by ELISA assay normalized to total protein in ROCK1 and ROCK2 siRNA-targeted cells. B) Representative western blot of ROCK1 and ROCK2 showing the effective gene silencing by siRNA. GAPDH was used as protein loading control. Similar results were obtained in each of 4 experiments. Results are expressed as mean ± SEM of 4 independent experiments performed in duplicate. (*$p<0.05$, **$p<0.01$).

Besides the classical inflammatory components, our laboratory and others have previously shown that the Ceramide Kinase (CerK)/ceramide 1-phosphate (C1P) axis plays a critical role in inflammation. C1P is synthesized in the Golgi apparatus through phosphorylation of ceramide by CerK. Interestingly, both C1P and CerK have been demonstrated to exert both pro- and anti-inflammatory actions, depending on cell type [36]. To test if CerK/C1P was implicated in the enhancement of MCP-1 release by CSE, the CerK gene was silenced with specific siRNA. As seen in figure 13, CerK knockdown significantly enhanced MCP-1 release both in non-treated and CSE-treated cells,

suggesting that CerK may play an inhibitory role in MCP-1 release, thereby suggesting that it might act as anti-inflammatory factor under these conditions.

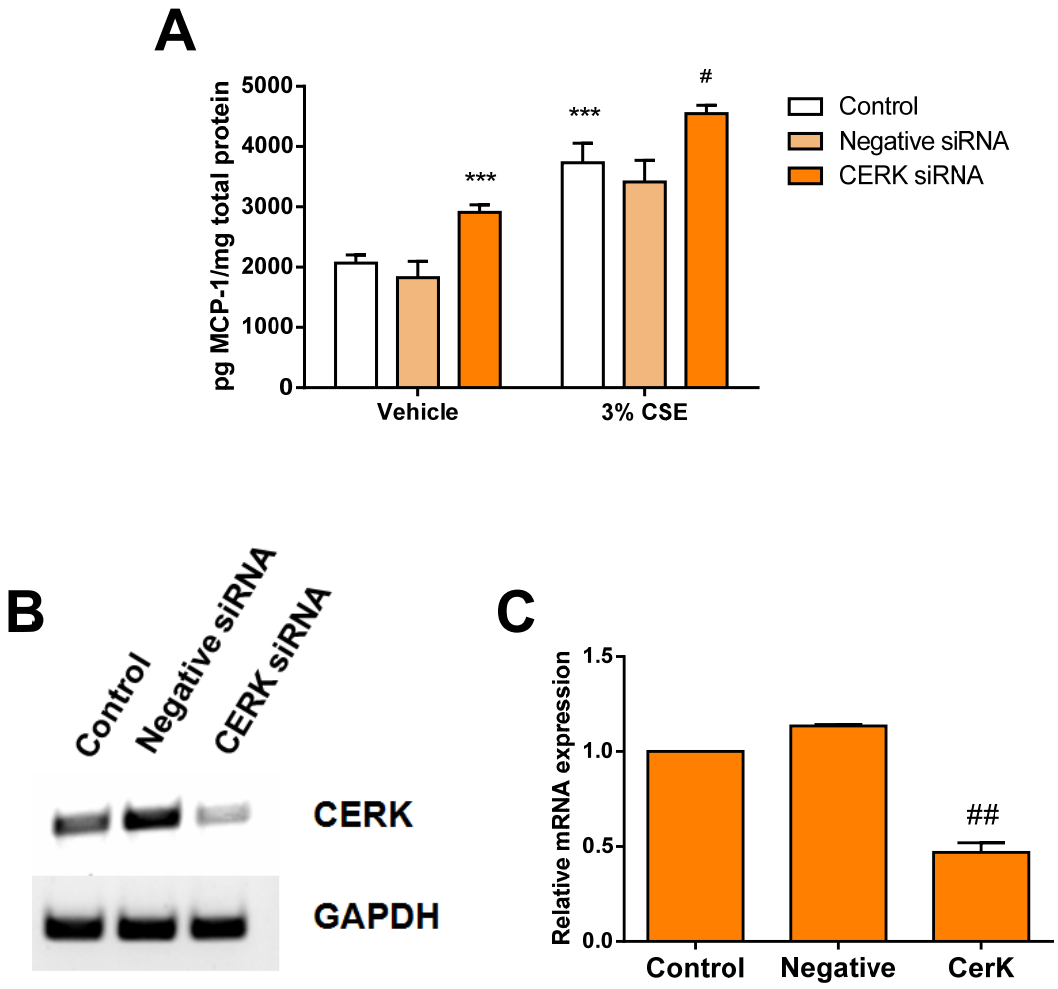

Figure 13: Ceramide Kinase (CerK) is negatively implicated in CSE-enhanced MCP-1 release in A549 cells. Cells were seeded in 60 mm dishes and gene silencing was performed using oligofectamine as transfection reagent as described in *Materials and Methods*. Cells were then trypsinized and counted. RNA extraction was performed cells, followed by retrotranscription step and CerK gen silencing was confirmed by PCR. siRNA-targeted cells were seeded in 12-well plates (80000 cells/well) and treated with either vehicle or 3% CSE for 48 h. After that time, the supernatants were collected and MCP-1 was analyzed using an ELISA kit. A) MCP-1 quantification by ELISA assay normalized to total protein in CerK siRNA-targeted cells. B) Separation in 1% agarose gel of PCR products using specific CerK primers showing effective CerK silencing. Expression of GAPDH was used as a protein loading control. Results are expressed as mean ± SEM of 4 independent experiments performed in duplicate. (*$p<0.05$, **$p<0.01$).

To support the hypothesis that CerK/C1P inhibits CSE-enhanced MCP-1 release, we pretreated the cells with exogenous C1P for 1 h prior to incubation with CSE. After 48 h, we performed an ELISA assay and quantified MCP-1 levels. Figure 14 shows that exogenous C1P was able to block CSE-enhanced MCP-1 release in A549 cells, pointing to an anti-inflammatory role of C1P in these cells, as previously suggested.

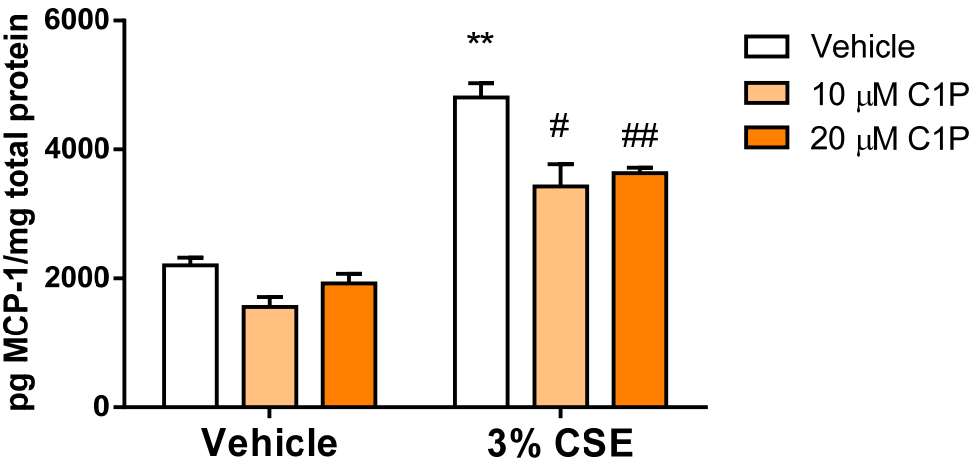

Figure 14: Exogenous C1P blocks CSE-induced MCP-1 release in A549 cells. Cells were seeded in 12-well plates (80000 cells/well) and treated with either vehicle or exogenous C1P at different concentrations 1 h prior to 3% CSE induction. After 48 h, supernatant was collected and ELISA assays were assessed. MCP-1 quantification by ELISA assay normalized to total protein in A549 cells. Results are expressed as mean ± SEM of 4 independent experiments performed in duplicate. (*$p<0.05$, **$p<0.01$).

Our group previously demonstrated the existence of a specific receptor for C1P. Binding of C1P to its receptor stimulated cell migration, and this effect was completely abolished by pretreatment of cells with pertussis toxin (Ptx), (a toxin from *Bordetella pertussis*) [37], suggesting that the receptor belongs to the G_i protein-coupled receptor family (GPCR). To test whether the inhibition of CSE-enhanced MCP-1 release by C1P was a receptor mediated effect A549 cells were pretreated cells overnight with Ptx before CSE addition. Figure 15 shows that this toxin partially reversed the inhibitory effect of C1P on MCP-1 release, suggesting that C1P was acting through interaction with a Gi protein-coupled receptor.

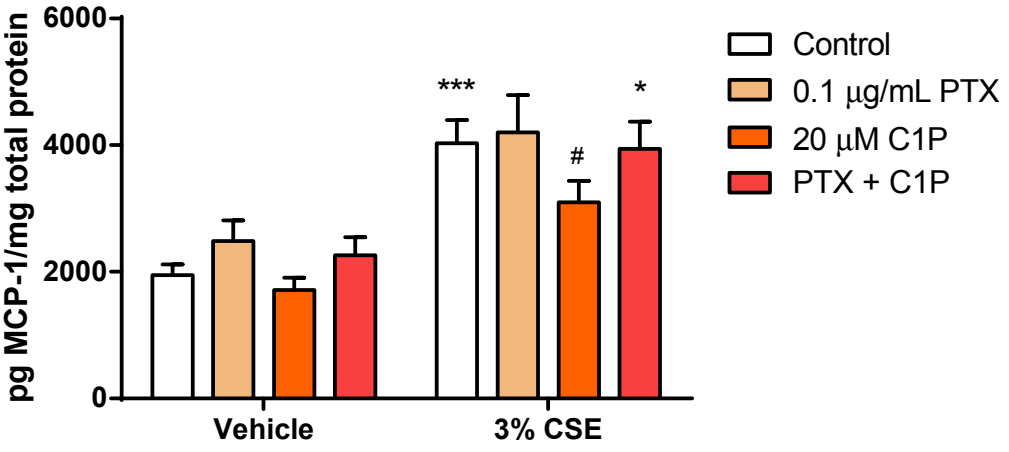

Figure 15: Ptx partially reverses the inhibitory effect of C1P on CSE-induced MCP-1 release in A549 cells. Cells were seeded in 12-well plates (40000 cells/well) and treated with either vehicle or 0.1 μg/ml Ptx overnight. The next day exogenous C1P was added 1 hour prior to 3% CSE induction. After 48 h, supernatant was collected and ELISA assays were assessed. MCP-1 quantification by ELISA assay normalized to total protein. Similar results were obtained in each experiment. Results are expressed as mean ± SEM of 6 independent experiments performed in duplicate. (*p‹0.05, ***p‹0.001).

2.4. CSE treatment downregulates the expression of the epithelial marker E-cadherin

The transmembrane adhesion receptor E-cadherin is a transmembrane glycoprotein that establishes interactions with adjacent E-cadherin molecules expressed by neighboring cells, thereby forming the core of the epithelial adherent junctions (AJ). AJ are located adjacent to the tight junctions in the basolateral surface of epithelial cells, and connect to cytoskeletal microfilaments. AJ form a belt-like structure at the lateral interface of epithelial cells [38]. The cytoplasmic domains of E-cadherin bind tightly to β-catenin, a cytoplasmic protein that interacts with α-catenin, which in turn anchors to the actin cytoskeleton [39]. Loss of E-cadherin is considered a hallmark event of the epithelial-mesenchymal transition (EMT) process, as it enables metastasis. E-cadherin acts by disrupting intercellular contacts thereby becoming an early step in metastatic cancer cell dissemination [40, 41]. However, loss of E-cadherin should not be considered, as the sole pivotal event in EMT, since blocking its expression does not induce full EMT [42, 43]. Regardless, loss or decrease of E-cadherin expression has recurrently been associated with poor prognosis and poor overall survival of

different types of cancer including gastric cancer [44], colon cancer [45] and breast cancer [46].

Since exposure to tobacco smoke is one of the main causes of lung cancer, we sought to explore whether the exposure of A549 cells to CSE had any significant effect on the expression of E-cadherin. To do this, the cells were treated with 3% CSE for 24 and 48 h and E-cadherin expression was analyzed by Western-blotting. As it can be observed in figure 16, treatment with 3% CSE significantly decreased E-cadherin expression in A549 cells, both at 24 and 48 h.

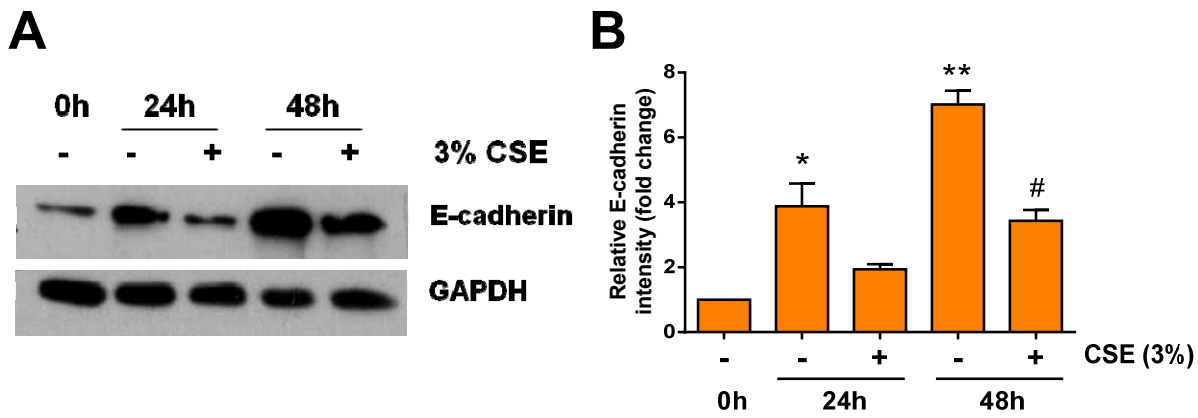

Figure 16: CSE downregulates E-cadherin expression. Cells were seeded in 6-well plates (200000 cells/well) and treated with either vehicle or 3% CSE for the indicated time periods. E-cadherin expression levels were analyzed by Western-blotting using specific antibodies. Equal loading of protein was assessed with an antibody against GAPDH. A) Representative western blot results. Similar results were obtained in each experiment. B) Quantification of A relative to control at the beginning of the experiment. All results are expressed as mean ± SEM of 3 independent experiments. (*p‹0.05, **p‹0.01).

Loss of E-cadherin is an early step of the EMT process and, as pointed out previously, transforming growth factor-β1 (TGF-β1) is a major EMT inducer [33]. Hence, we tested to evaluate whether CSE-induced downregulation of E-cadherin was due to an increased secretion of TGF-β1 in CSE treated cells. To achieve this, TGF-β1 levels were measured in the supernatant of cells treated or not with 3% CSE. Both active and latent TGF-β1 levels were measured, but treatment with CSE did not stimulate TGF-β1 secretion (Figure 17).

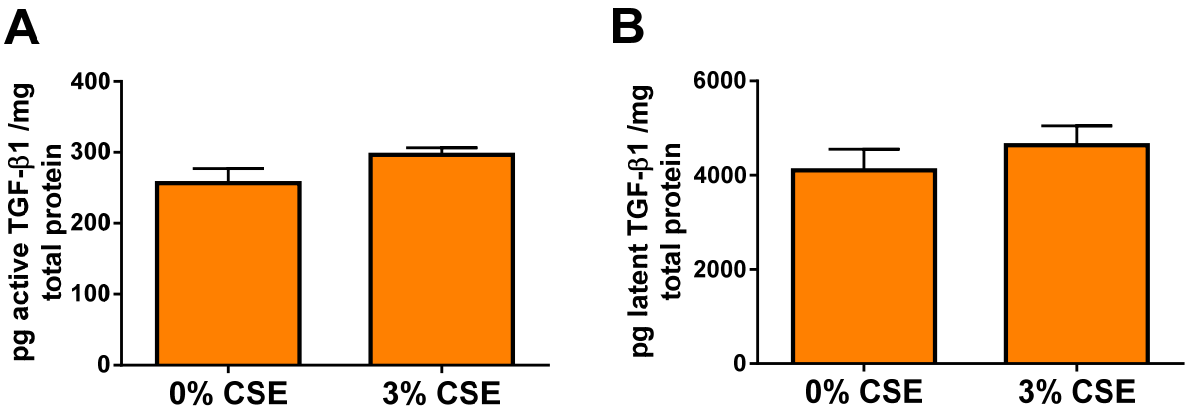

Figure 17: CSE does not stimulate TGF-β1 secretion in A549 cells. A549 cells were seeded in 12-well plates (80000 cells/well) and treated with 3% CSE for the indicated time. Active (A) and latent (B) TGF-β1 secretion was measured using a commercial ELISA kit as described in *Materials and Methods*. Results were normalized to total protein content in each well. Results are expressed as mean ± SEM of 3 independent experiments performed in duplicate.

2.5. Signaling pathways implicated in the loss of E-cadherin expression induced by CSE

To investigate into the mechanisms by which CSE induces E-cadherin downregulation we studied the possible implication of various signaling pathways. Specifically, the MEK-ERK, PI3K-AKT, ROCK1-2 and CerK-C1P pathways were tested. Figure 18 shows that treatment with 3% CSE induced rapid phosphorylation of ERK1/2.

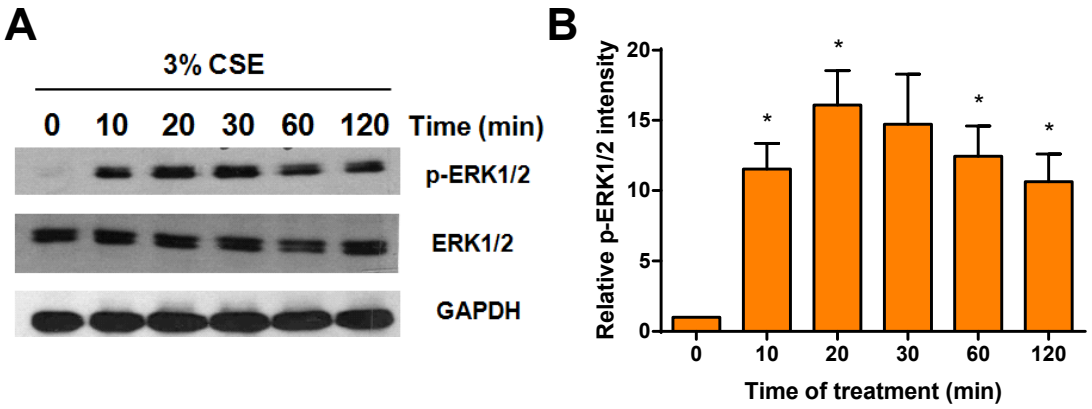

Figure 18: CSE promotes rapid activation of ERK1/2 in A549 cells. Cells were seeded in 6-well plates (200000 cells/well) and grown overnight. The next day, CSE (3%) was added to cells in culture and at the indicated time points, cells were harvested. ERK and p-ERK protein expression levels were analyzed by Western-blotting using specific antibodies. Equal protein loading was

assessed with an antibody against GAPDH. A) Representative western blot results. Similar results were obtained in each of 3 independent experiments. B) Quantification of A relative to control condition. All results are expressed as mean ± SEM of 3 independent experiments. (*p<0.05).

In addition, CSE was able to sustain ERK1/2 phosphorylation at longer time periods. In particular, it was observed that ERK phosphorylation was still elevated at 24 and 48 h after treatment with CSE. This late activation of ERK is in agreement with the downregulation of E-cadherin shown in figure 16.

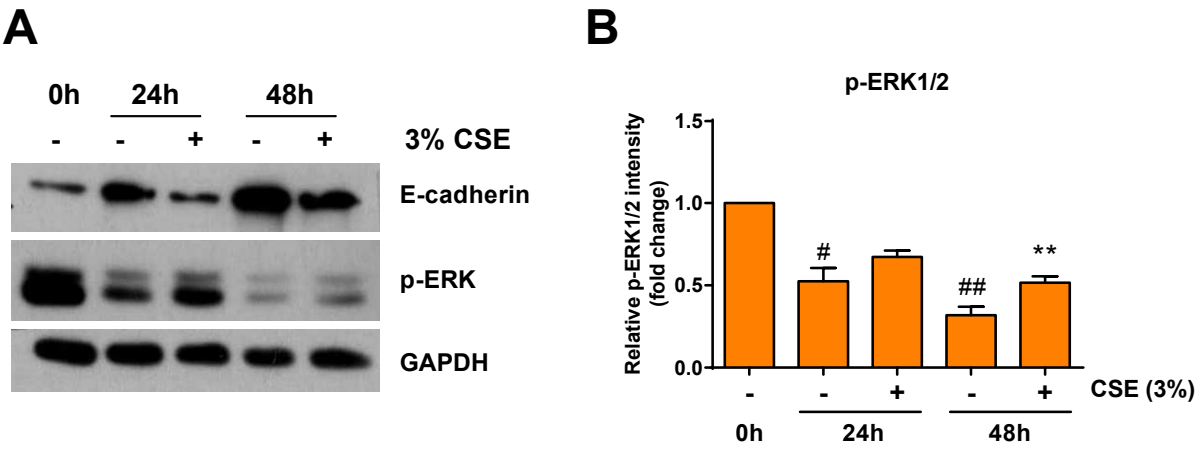

Figure 19: Treatment of A549 cells with CSE causes sustained ERK phosphorylation and this is concomitant with the loss of E-cadherin expression. Cells were seeded in 6-well plates (200000 cells/well) and treated with either vehicle or 3% CSE for the indicated time periods. E-cadherin and p-ERK expression levels were analyzed by western blot using specific antibodies. Equal loading of protein was assessed with an antibody against GAPDH. A) Representative western blot results. Similar results were obtained in each of 3 independent experiments. B) Quantification of A relative to control at the beginning of the experiment. All results are expressed as mean ± SEM of 3 independent experiments. (*p<0.05, **p<0.01).

To further confirm that ERK activation downregulates E-cadherin, the cells were pretreated with specific siRNAs to silence the genes encoding MAPK1 (ERK2) and MAPK3 (ERK1). The siRNA-treated cells were then seeded in 6-well plates and incubated with 3% CSE for 48 h. We found that MAPK1, but not MAPK3, was implicated in the loss of E-cadherin that was caused by treatment with CSE (Figure 20), suggesting that MAPK1 (ERK2) activation is necessary for CSE-induced loss of E-cadherin.

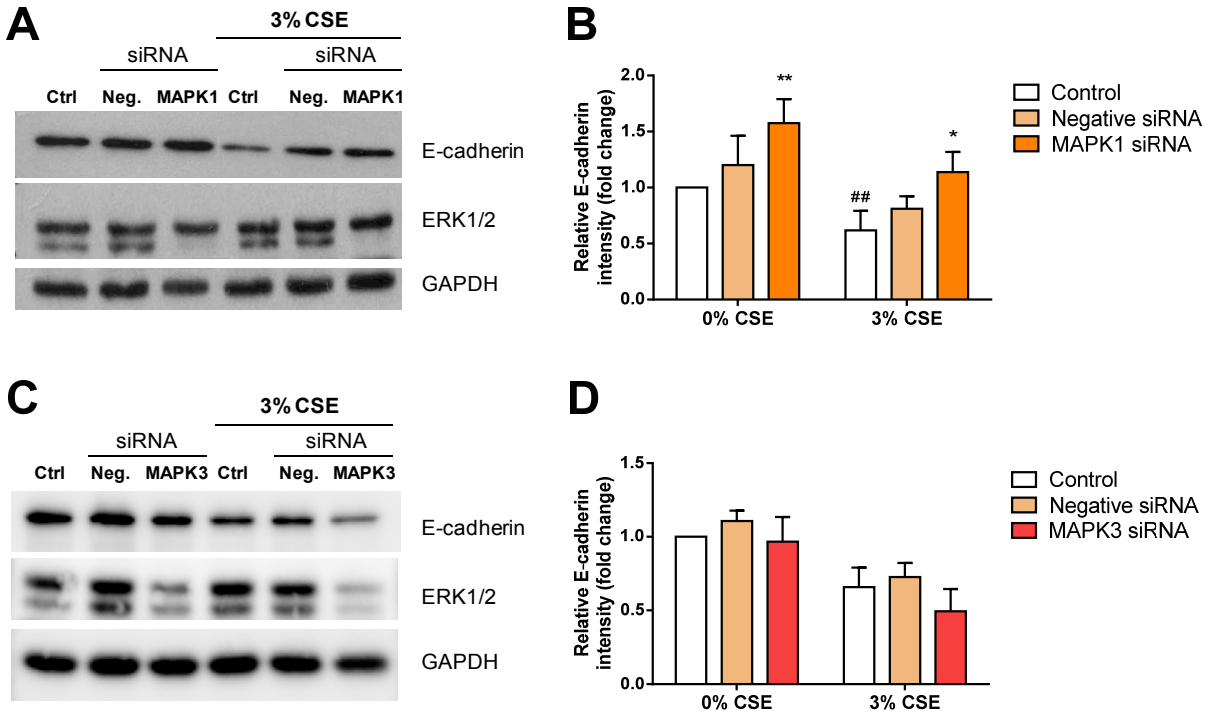

Figure 20: MAPK1, but not MAPK3, is necessary for CSE-induced loss of E-cadherin in A549 cells. Cells were seeded in 60 mm dishes and gene silencing was performed using specific siRNAs to knockdown MAPK1 or MAPK3, as described in *Materials and Methods*. Cells were then trypsinized and counted. siRNA-targeted cells were seeded in 6-well plates (200000 cells/well) and treated with either vehicle or 3% CSE for 48 h. After that time cells were harvested and E-cadherin expression levels were analyzed by Western-blotting. Gene silencing was confirmed by measuring total ERK expression. Equal loading of protein was assessed with an antibody against GAPDH. A) and C) Representative western blot of E-cadherin and total ERK. GAPDH was used as protein loading control. Similar results were obtained in each experiment. B) and D) Quantification of A and C, respectively, relative to control. All results are expressed as mean ± SEM of 3 independent experiments. (*p‹0.05, **p‹0.01).

We next sought to determine whether the PI3K-AKT pathway was involved in downregulation of E-cadherin. To do this, A549 cells were pretreated with specific siRNA to silence the genes encoding p85α, which is the regulatory subunit of PI3K, as well as the genes encoding AKT1 and AKT2. siRNA-targeted cells were then seeded in 6-well plates and incubated with 3% CSE for 48 h. As shown in figure 21, when both p85α and AKT2 were silenced CSE-induced E-cadherin downregulation was more dramatic, indicating that the PI3K/AKT2 pathway favors the expression of E-cadherin.

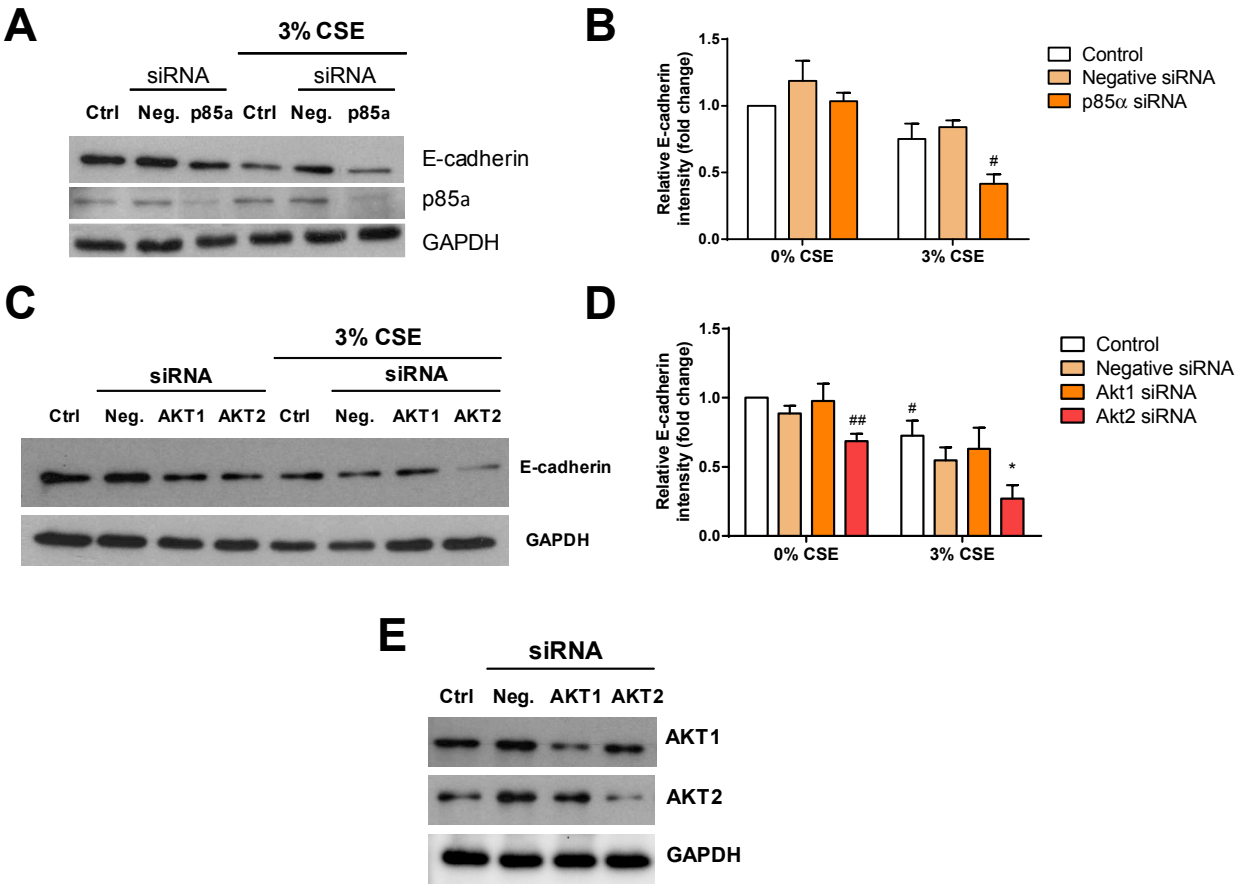

Figure 21: The PI3K/AKT2 pathway is involved in the maintenance of E-cadherin expression in A549 cells. Cells were seeded in 60-mm dishes and gene silencing was performed using specific siRNAs to knockdown p85-α, AKT1 and AKT2, as described in *Materials and Methods*. Cells were then trypsinized and counted. siRNA-targeted cells were then seeded in 6-well plates (200000 cells/well) and treated with either vehicle or 3% CSE for 48 h. After that time cells were harvested and E-cadherin expression levels were analyzed by Western-blotting. Gene silencing was confirmed by measuring total p85α, AKT1 and AKT2 expression. Equal loading of protein was assessed with an antibody against GAPDH. A) Representative western blot of E-cadherin and p85α. GAPDH was used as protein loading control. B) Quantification of A relative to control. C) Representative western blot of E-cadherin. GAPDH was used as protein loading control. D) Quantification of C relative to control. E) Representative western blot to confirm the AKT1 and AKT2 gene silencing. GAPDH was used as protein loading control. Similar results were obtained in 3 independent experiments performed in triplicate. All results are expressed as mean ± SEM of 3 independent experiments. (*p‹0.05, **p‹0.01).

Another pathway that could be implicated in CSE-induced E-cadherin expression is the ROCK pathway. To study this possibility both ROCK1 and ROCK2 genes were silenced using specific siRNAs prior to treatment of the cells with 3% CSE for 48 h.

However, figure 22 shows that neither ROCK1 nor ROCK2 are necessary for CSE-induced loss of E-cadherin in A549 cells.

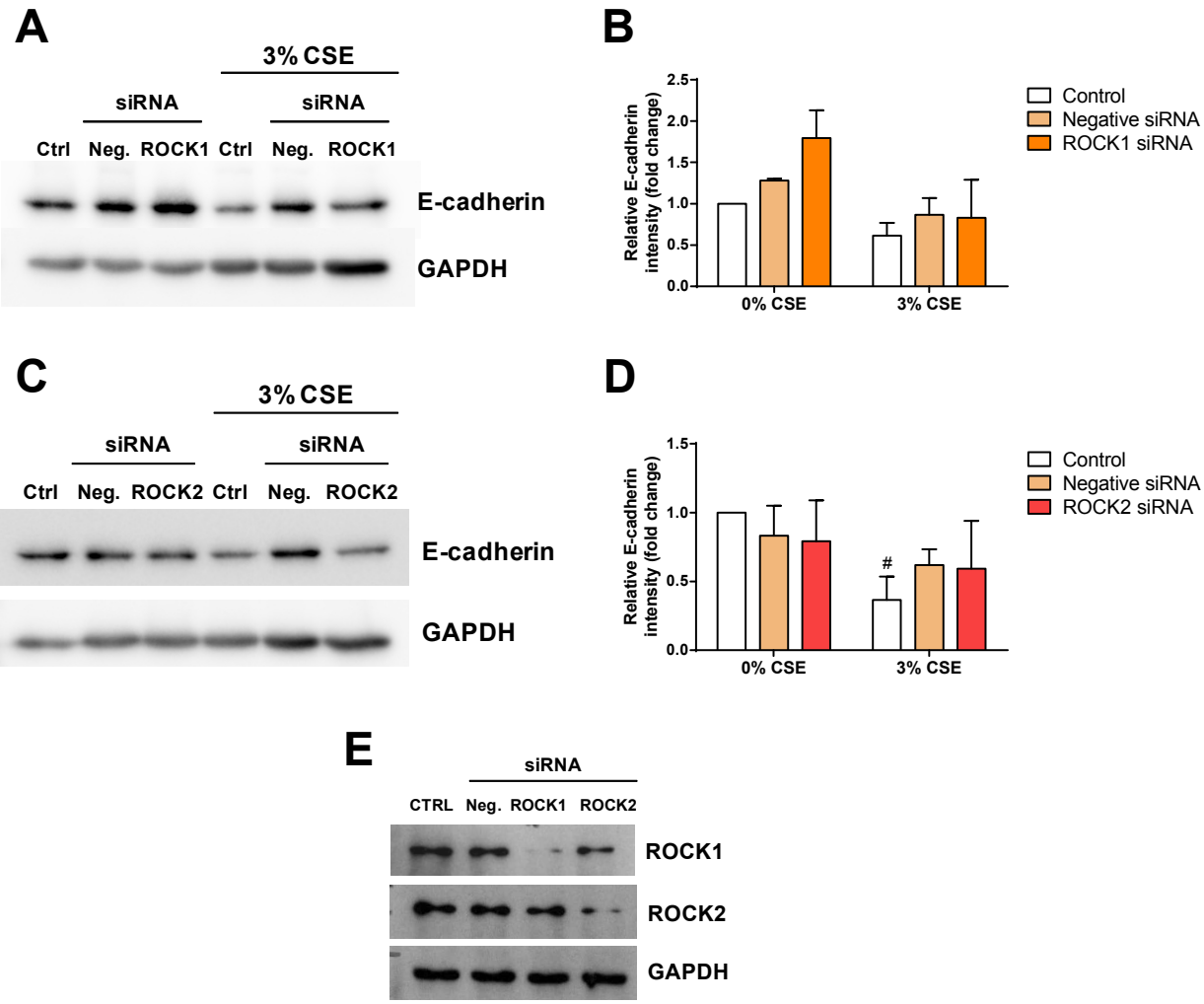

Figure 22: Neither ROCK1 nor ROCK2 are necessary for CSE-induced loss of E-cadherin in A549 cells. Cells were seeded in 60-mm dishes and gene silencing was performed using oligofectamine as transfection reagent as described in *Materials and Methods*. Cells were then trypsinized and counted. siRNA-targeted cells were seeded in 6-well plates (200000 cells/well) and treated with either vehicle or 3% CSE for 48 h. Cells were then harvested and E-cadherin expression levels were analyzed by Western-blotting. Gene silencing was confirmed by measuring ROCK1 and ROCK2 expression. Equal loading of protein was assessed with an antibody against GAPDH. A) Representative western blot of E-cadherin in ROCK1 siRNA-targeted cells. GAPDH was used as protein loading control. B) Quantification of A relative to control. C) Representative western blot of E-cadherin in ROCK2 siRNA-targeted cells. GAPDH was used as protein loading control. D) Quantification of C relative to control. E) Representative western blot to confirm ROCK1 and ROCK2 gene silencing. GAPDH was used as protein loading control. All results are expressed as mean ± SEM of 3 (for A) or 4 (for C) independent experiments. (# $p<0.05$)

Finally, we determine whether CerK was implicated in the loss of E-cadherin induced by CSE. Using specific siRNA to silence the gene encoding CerK it was observed that, it does not take part in CSE-induced loss of E-cadherin (Figure 23).

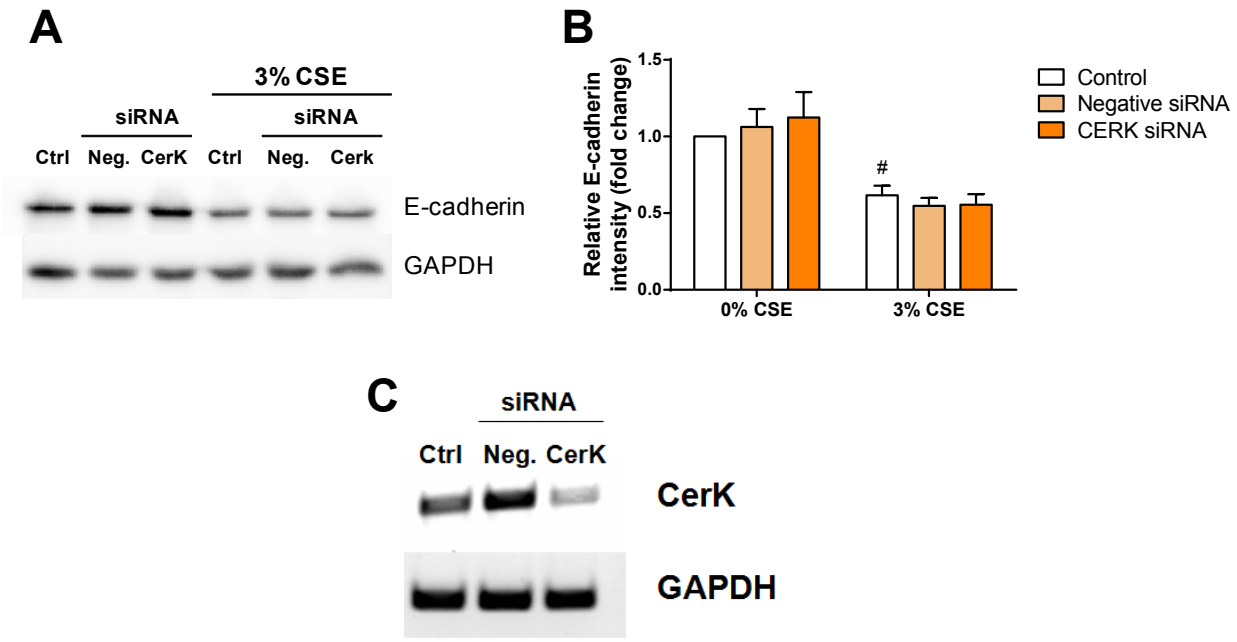

Figure 23: CerK does not participate in CSE-induced loss of the E-cadherin in A549 cells. Cells were seeded in 60 mm dishes and gene silencing was performed using oligofectamine as transfection reagent as described in *Materials and Methods*. Cells were then trypsinized and counted. siRNA-targeted cells were seeded in 6-well plates (200000 cells/well) and treated with either vehicle or 3% CSE for 48 h. After that time cells were harvested and E-cadherin expression levels were analyzed by Western blotting. Gene silencing was confirmed by PCR using specific primers for CerK. A) Representative western blot of E-cadherin in CerK siRNA-targeted cells. GAPDH expression was used as protein loading control. B) Quantification of A relative to control. C) Confirmation of CerK silencing by PCR using specific primers against CerK. GAPDH expression was used as protein loading control. All results are expressed as mean ± SEM of 3 independent experiments. (# $p<0.05$).

Altogether, the data presented in this chapter demonstrate that CSE promotes MCP-1 release by lung epithelial cells leading to recruitment of monocytes. CSE-induced MCP-1 release is mediated through the ROCK pathway. Interestingly, AKT2 and CerK may act as anti-inflammatory intermediates, as knockdown of any of these kinases enhances MCP-1 release in response to CSE. In this connection, exogenous C1P also blocks CSE-induced MCP-1 release, an action that occurs through interaction of C1P with a putative Gi protein-coupled receptor. On the other hand, treatment of A549

cells with CSE causes downregulation of the epithelial marker E-cadherin. This effect seems to be mediated through the ERK pathway, and more specifically through MAPK1, which has been demonstrated to be essential for E-cadherin repression. By contrast, the PI3K/AKT2 pathway acts favoring the expression of E-cadherin in A549 lung epithelial cells.

3. DISCUSSION

Inflammation is a combination of cellular and humoral reactions that defend the organism from infection and tissue damage. In response to tissue injury, a multifactorial network of chemical signals starts and maintains a host response designed to restore the affected tissue. This involves the activation and directed migration of leukocytes to sites of damage.

COPD is an obstructive disease of the lungs that progresses leading to death from respiratory failure or comorbidities such as cardiovascular disease and lung cancer. It is associated with an enhanced chronic inflammatory response in the airways and lung tissue to harmful particles or gases, mainly the chronic exposure to CS or, particularly in developing countries, the inhalation of smoke from burning biomass fuels or other inhaled irritants. The inflammatory response in COPD involves both innate immunity (neutrophils, macrophages, eosinophils, mast cells, natural killer cells, and dendritic cells) and adaptive immunity (T- and B- lymphocytes) but also implicates the activation of structural cells, including alveolar epithelial cells, endothelial cells, and fibroblasts. In fact, many inflammatory mediators derived from inflammatory cells and structural cells of the airways and lungs are increased in COPD [47]. It seems that the primary event in CS cytotoxicity involves epithelial cells, which further activate immune cells to produce inflammation and a variety of time-dependent, morphological and functional alterations. Thus, CS and other irritants inhaled into the respiratory tract activate surface macrophages and airway epithelial cells to release multiple chemotactic mediators, specially chemokines, which attract and activate circulating neutrophils, monocytes, and lymphocytes into the lungs [48]. The profile of cytokine/chemokines persisting at an inflammatory site is important in the development of chronic disease.

In this thesis we have explored the effects of cigarette smoke extracts (CSE) on the behavior of lung epithelial cells maintained in culture. We have demonstrated that cigarette smoke exposure promotes the release of MCP-1 by A549 lung epithelial cells. This action promotes the migration of THP-1 monocytes, which is associated with the inflammatory response. This observation has been previously reported [49-52]. However, we failed to observe the release of other pro-inflammatory cytokines.

We found that liberation of MCP-1 to the culture medium was mediated by the ROCK pathway. The RhoA/ROCK pathway has attracted considerable attention in

various fields of research, especially in the cardiovascular field. In a study by Li *et al*. [53], the inhibition of ROCK by Fasudil, attenuated the high glucose-induced increase in MCP-1 expression in human umbilical vein endothelial cells (HUVECs), indicating that the inhibition of the Rho/ROCK pathway has the potential to protect against the diabetic inflammatory process in vessels. In another work by Rao *et al*. [54] the use of Fasudil ameliorated the accumulation of adhesion and infiltration of inflammatory cells in the glomerulus, indicating that inhibition of the RhoA/ROCK pathway had a protective effect on glomerular inflammation. Thus, it seems that this metabolic pathway contributes to the expression of chemokines relative to the inflammatory response.

Another relevant observation in this thesis is that AKT2 and CerK may act as anti-inflammatory intermediates, as silencing of the genes encoding these kinases enhances the release of MCP-1 in response to CSE. In this connection, exogenous C1P also blocked CSE-induced MCP-1 release by the A549 cells, suggesting that it is an essential factor in the regulation of MCP-1 release. Interestingly, the effect of exogenous C1P could be inhibited by Ptx thereby indicating the intervention of a G_i protein-coupled receptor in this process. These findings indicate that C1P and CerK, the enzyme responsible for its biosynthesis, may act as anti-inflammatory agents in the lung. Although C1P has been mainly associated with pro-inflammatory responses in different cell types [35, 37, 55-58], there is a growing body of evidence pointing to an anti-inflammatory action of exogenous C1P in the lung. In the work by Baudiss *et al*. [59] exogenous C1P was demonstrated to inhibit CS-induced airway inflammation in mice. In human peripheral blood mononuclear cells C1P prevented the production of pro-inflammatory IL-6, IL-8 and IL-1β, thereby indicating that exogenous C1P also acts as an anti-inflammatory lipid mediator of some immune responses [60]. Moreover, the anti-inflammatory role of C1P has been recently highlighted in a model of dextran sodium-induced murine colitis, in which depletion of CerK enhanced the pathology of colitis and lethal responses in these animals [61-63]. Therefore, CerK/C1P may exert both pro- and anti-inflammatory depending on cell type.

Clinical and epidemiologic studies have suggested a strong association between chronic infection, inflammation, and cancer [64-66]. Such observations suggest that chronic inflammation is involved in tumor initiation (the process by which normal cells are genetically altered to become malignant), promotion (the process by which small clusters of malignant cells are stimulated to grow), and progression (the process by

which growing tumors become more aggressive). Recent data from mouse models of human cancer have established that inflammation is a critical component of both tumor promotion and progression. The process by which a tumor cell becomes more aggressive is the epithelial to mesenchymal transition (EMT) course. This process is characterized by the loss of epithelial features such as the loss of the E-cadherin marker of epithelial cells, and the acquisition of mesenchymal features such as overexpression of the mesenchymal markers vimentin, fibronectin, or N-cadherin. In this context, we found that CSE is able to downregulate the expression of E-cadherin, although somehow surprising, this effect was not associated with increased TGF-β1 production. The implication of TGF-β1 in CSE-induced EMT is not fully established, as some reports show a direct link [67] and some others demonstrate the opposite [68]. The effect on E-cadherin downregulation by CSE seems to be mediated by the ERK pathway, and more specifically through activation of MAPK1, whose depletion leads to increased levels of the epithelial marker. A similar observation has been previously reported by Tashiro *et al*. [69], who showed that the MEK inhibitor U0126 suppressed EGF-induced E-cadherin expression at the transcriptional level. Moreover, Li *et al*. [70] showed that decreased expression of MAPK1 could alter the EMT process by interfering with the expression of E-cadherin in HeLa cells, thereby inhibiting invasion and metastasis of these malignant cells. Similarly, constitutively active ERK inhibited E-cadherin promoter activity in SW480 colon cancer cells [71], and *in vivo* experiments demonstrated that lack of MAPK activity leads to stabilization of E-cadherin to adherent junctions, thereby strengthening intracellular adhesions in renal branching in mice [72]. Regarding the effects of cigarette smoke, it has also been shown that ERK1/2 inhibitors effectively attenuate CS-induced EMT in both human urothelial cells and mouse bladder tissue [73]. On another hand, the role of AKT in cell migration and metastases is not clear because of conflicting studies suggesting either positive or negative regulatory roles [74, 75]. In this thesis we have evidence suggesting that the, PI3K/AKT2 pathway acts favoring E-cadherin expression and stabilization in A549 lung epithelial cells, as knockdown of the genes encoding these kinases resulted in enhanced CSE-induced E-cadherin downregulation.

Taken together, the results presented in this chapter demonstrate that CSE promotes the release of the pro-inflammatory chemokine MCP-1, which attracts monocytes and facilitates their activation, thereby promoting an inflammatory response. In this context, ROCK1, but not ROCK2, seems to be a key regulatory enzyme necessary for CSE-induced MCP-1 release. However, AKT2 and CerK elicit opposite

effects, suggesting that they may act as anti-inflammatory intermediates. The results using exogenous C1P reinforce the notion that C1P inhibits inflammatory responses in the lungs. Moreover, it is demonstrated here that CSE promotes the loss of the epithelial marker E-cadherin, which would facilitate metastasis. This action is mediated by MAPK1 (ERK-2) but not MAPK3 (ERK-1). By contrast, the PI3K/AKT2 pathway promotes the maintenance of E-cadherin expression in A549 lung epithelial cells. It is now necessary to establish the anti-inflammatory role of exogenous C1P in the lung in order to develop novel therapeutic strategies to treat inflammation-associated lung diseases. In this context, our group previously showed that exogenous C1P reduced inflammation and emphysema in a chronic model of CS-induced lung inflammation in mice [59] and suggested that C1P may be used both as prophylactic and therapeutic agent [76].

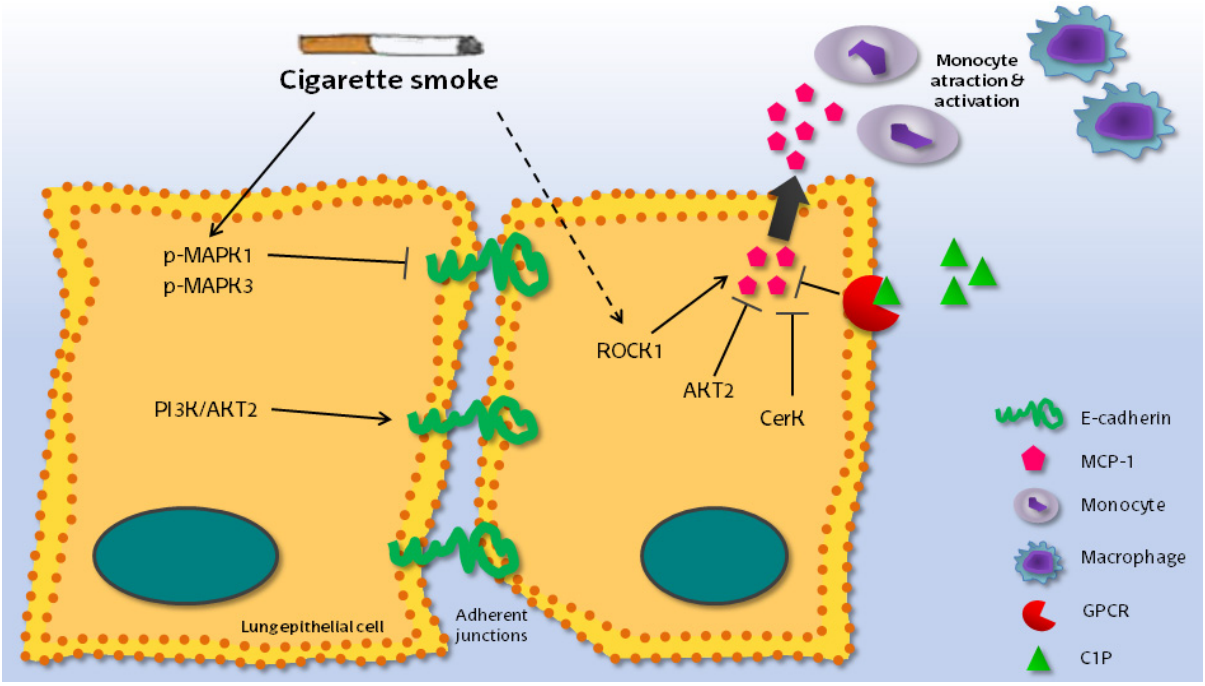

Figure 24: Working model for the effect of CSE in A549 lung epithelial cells.

4. REFERENCES

[1] R. Talhout, T. Schulz, E. Florek, J. van Benthem, P. Wester, A. Opperhuizen, Hazardous compounds in tobacco smoke, Int J Environ Res Public Health 8 (2) (2011) 613-628.

[2] C.M. Chang, C.G. Corey, B.L. Rostron, B.J. Apelberg, Systematic review of cigar smoking and all cause and smoking related mortality, BMC Public Health 15 (2015) 390.

[3] J. Vestbo, S.S. Hurd, A.G. Agusti, P.W. Jones, C. Vogelmeier, A. Anzueto, P.J. Barnes, L.M. Fabbri, F.J. Martinez, M. Nishimura, R.A. Stockley, D.D. Sin, R. Rodriguez-Roisin, Global strategy for the diagnosis, management, and prevention of chronic obstructive pulmonary disease: GOLD executive summary, Am J Respir Crit Care Med 187 (4) (2013) 347-365.

[4] J.C. Hogg, R.M. Senior, Chronic obstructive pulmonary disease - part 2: pathology and biochemistry of emphysema, Thorax 57 (9) (2002) 830-834.

[5] R. Lozano, M. Naghavi, K. Foreman, S. Lim, K. Shibuya, V. Aboyans, J. Abraham, T. Adair, R. Aggarwal, S.Y. Ahn, M. Alvarado, H.R. Anderson, L.M. Anderson, K.G. Andrews, C. Atkinson, L.M. Baddour, S. Barker-Collo, D.H. Bartels, M.L. Bell, E.J. Benjamin, D. Bennett, K. Bhalla, B. Bikbov, A. Bin Abdulhak, G. Birbeck, F. Blyth, I. Bolliger, S. Boufous, C. Bucello, M. Burch, P. Burney, J. Carapetis, H. Chen, D. Chou, S.S. Chugh, L.E. Coffeng, S.D. Colan, S. Colquhoun, K.E. Colson, J. Condon, M.D. Connor, L.T. Cooper, M. Corriere, M. Cortinovis, K.C. de Vaccaro, W. Couser, B.C. Cowie, M.H. Criqui, M. Cross, K.C. Dabhadkar, N. Dahodwala, D. De Leo, L. Degenhardt, A. Delossantos, J. Denenberg, D.C. Des Jarlais, S.D. Dharmaratne, E.R. Dorsey, T. Driscoll, H. Duber, B. Ebel, P.J. Erwin, P. Espindola, M. Ezzati, V. Feigin, A.D. Flaxman, M.H. Forouzanfar, F.G. Fowkes, R. Franklin, M. Fransen, M.K. Freeman, S.E. Gabriel, E. Gakidou, F. Gaspari, R.F. Gillum, D. Gonzalez-Medina, Y.A. Halasa, D. Haring, J.E. Harrison, R. Havmoeller, R.J. Hay, B. Hoen, P.J. Hotez, D. Hoy, K.H. Jacobsen, S.L. James, R. Jasrasaria, S. Jayaraman, N. Johns, G. Karthikeyan, N. Kassebaum, A. Keren, J.P. Khoo, L.M. Knowlton, O. Kobusingye, A. Koranteng, R. Krishnamurthi, M. Lipnick, S.E. Lipshultz, S.L. Ohno, J. Mabweijano, M.F. MacIntyre, L. Mallinger, L. March, G.B. Marks, R. Marks, A. Matsumori, R. Matzopoulos, B.M. Mayosi, J.H. McAnulty, M.M. McDermott, J. McGrath, G.A. Mensah, T.R. Merriman, C. Michaud, M. Miller, T.R. Miller, C. Mock, A.O. Mocumbi, A.A. Mokdad, A. Moran, K. Mulholland, M.N. Nair, L. Naldi, K.M. Narayan, K. Nasseri, P. Norman, M. O'Donnell, S.B. Omer, K. Ortblad, R. Osborne, D. Ozgediz, B. Pahari, J.D. Pandian, A.P. Rivero,

R.P. Padilla, F. Perez-Ruiz, N. Perico, D. Phillips, K. Pierce, C.A. Pope, 3rd, E. Porrini, F. Pourmalek, M. Raju, D. Ranganathan, J.T. Rehm, D.B. Rein, G. Remuzzi, F.P. Rivara, T. Roberts, F.R. De Leon, L.C. Rosenfeld, L. Rushton, R.L. Sacco, J.A. Salomon, U. Sampson, E. Sanman, D.C. Schwebel, M. Segui-Gomez, D.S. Shepard, D. Singh, J. Singleton, K. Sliwa, E. Smith, A. Steer, J.A. Taylor, B. Thomas, I.M. Tleyjeh, J.A. Towbin, T. Truelsen, E.A. Undurraga, N. Venketasubramanian, L. Vijayakumar, T. Vos, G.R. Wagner, M. Wang, W. Wang, K. Watt, M.A. Weinstock, R. Weintraub, J.D. Wilkinson, A.D. Woolf, S. Wulf, P.H. Yeh, P. Yip, A. Zabetian, Z.J. Zheng, A.D. Lopez, C.J. Murray, M.A. AlMazroa, Z.A. Memish, Global and regional mortality from 235 causes of death for 20 age groups in 1990 and 2010: a systematic analysis for the Global Burden of Disease Study 2010, Lancet 380 (9859) (2012) 2095-2128.

[6] I.A. Yang, V. Relan, C.M. Wright, M.R. Davidson, K.B. Sriram, S.M. Savarimuthu Francis, B.E. Clarke, E.E. Duhig, R.V. Bowman, K.M. Fong, Common pathogenic mechanisms and pathways in the development of COPD and lung cancer, Expert Opin Ther Targets 15 (4) (2011) 439-456.

[7] E. Van Coillie, J. Van Damme, G. Opdenakker, The MCP/eotaxin subfamily of CC chemokines, Cytokine Growth Factor Rev 10 (1) (1999) 61-86.

[8] T. Yoshimura, E.A. Robinson, S. Tanaka, E. Appella, E.J. Leonard, Purification and amino acid analysis of two human monocyte chemoattractants produced by phytohemagglutinin-stimulated human blood mononuclear leukocytes, J Immunol 142 (6) (1989) 1956-1962.

[9] S.D. Cushing, J.A. Berliner, A.J. Valente, M.C. Territo, M. Navab, F. Parhami, R. Gerrity, C.J. Schwartz, A.M. Fogelman, Minimally modified low density lipoprotein induces monocyte chemotactic protein 1 in human endothelial cells and smooth muscle cells, Proc Natl Acad Sci U S A 87 (13) (1990) 5134-5138.

[10] T.J. Standiford, S.L. Kunkel, S.H. Phan, B.J. Rollins, R.M. Strieter, Alveolar macrophage-derived cytokines induce monocyte chemoattractant protein-1 expression from human pulmonary type II-like epithelial cells, J Biol Chem 266 (15) (1991) 9912-9918.

[11] Z. Brown, R.M. Strieter, G.H. Neild, R.C. Thompson, S.L. Kunkel, J. Westwick, IL-1 receptor antagonist inhibits monocyte chemotactic peptide 1 generation by human mesangial cells, Kidney Int 42 (1) (1992) 95-101.

[12] B.P. Barna, J. Pettay, G.H. Barnett, P. Zhou, K. Iwasaki, M.L. Estes, Regulation of monocyte chemoattractant protein-1 expression in adult human non-neoplastic

astrocytes is sensitive to tumor necrosis factor (TNF) or antibody to the 55-kDa TNF receptor, J Neuroimmunol 50 (1) (1994) 101-107.

[13] T.L. Sorensen, R.M. Ransohoff, R.M. Strieter, F. Sellebjerg, Chemokine CCL2 and chemokine receptor CCR2 in early active multiple sclerosis, Eur J Neurol 11 (7) (2004) 445-449.

[14] K. Hayashida, T. Nanki, H. Girschick, S. Yavuz, T. Ochi, P.E. Lipsky, Synovial stromal cells from rheumatoid arthritis patients attract monocytes by producing MCP-1 and IL-8, Arthritis Res 3 (2) (2001) 118-126.

[15] K.F. Kusano, K. Nakamura, H. Kusano, N. Nishii, K. Banba, T. Ikeda, K. Hashimoto, M. Yamamoto, H. Fujio, A. Miura, K. Ohta, H. Morita, H. Saito, T. Emori, Y. Nakamura, I. Kusano, T. Ohe, Significance of the level of monocyte chemoattractant protein-1 in human atherosclerosis, Circ J 68 (7) (2004) 671-676.

[16] P. Sartipy, D.J. Loskutoff, Monocyte chemoattractant protein 1 in obesity and insulin resistance, Proc Natl Acad Sci U S A 100 (12) (2003) 7265-7270.

[17] S.L. Deshmane, S. Kremlev, S. Amini, B.E. Sawaya, Monocyte chemoattractant protein-1 (MCP-1): an overview, J Interferon Cytokine Res 29 (6) (2009) 313-326.

[18] W.F. Grashoff, J.K. Sont, P.J. Sterk, P.S. Hiemstra, W.I. de Boer, J. Stolk, J. Han, J.M. van Krieken, Chronic obstructive pulmonary disease: role of bronchiolar mast cells and macrophages, Am J Pathol 151 (6) (1997) 1785-1790.

[19] J.C. Hogg, F. Chu, S. Utokaparch, R. Woods, W.M. Elliott, L. Buzatu, R.M. Cherniack, R.M. Rogers, F.C. Sciurba, H.O. Coxson, P.D. Pare, The nature of small-airway obstruction in chronic obstructive pulmonary disease, N Engl J Med 350 (26) (2004) 2645-2653.

[20] B. Meshi, T.Z. Vitalis, D. Ionescu, W.M. Elliott, C. Liu, X.D. Wang, S. Hayashi, J.C. Hogg, Emphysematous lung destruction by cigarette smoke. The effects of latent adenoviral infection on the lung inflammatory response, Am J Respir Cell Mol Biol 26 (1) (2002) 52-57.

[21] S.L. Traves, S.V. Culpitt, R.E. Russell, P.J. Barnes, L.E. Donnelly, Increased levels of the chemokines GROalpha and MCP-1 in sputum samples from patients with COPD, Thorax 57 (7) (2002) 590-595.

[22] F. Bray, J. Ferlay, I. Soerjomataram, R.L. Siegel, L.A. Torre, A. Jemal, Global cancer statistics 2018: GLOBOCAN estimates of incidence and mortality worldwide for 36 cancers in 185 countries, CA Cancer J Clin 68 (6) (2018) 394-424.

[23] J.R. Molina, P. Yang, S.D. Cassivi, S.E. Schild, A.A. Adjei, Non-small cell lung cancer: epidemiology, risk factors, treatment, and survivorship, Mayo Clin Proc 83 (5) (2008) 584-594.

[24] J. Tang, R. Salama, S.M. Gadgeel, F.H. Sarkar, A. Ahmad, Erlotinib resistance in lung cancer: current progress and future perspectives, Front Pharmacol 4 (2013) 15.

[25] B.N. Ames, L.S. Gold, W.C. Willett, The causes and prevention of cancer, Proc Natl Acad Sci U S A 92 (12) (1995) 5258-5265.

[26] K. Matsumoto, H. Aizawa, H. Inoue, H. Koto, S. Takata, M. Shigyo, H. Nakano, N. Hara, Eosinophilic airway inflammation induced by repeated exposure to cigarette smoke, Eur Respir J 12 (2) (1998) 387-394.

[27] R. Kalluri, R.A. Weinberg, The basics of epithelial-mesenchymal transition, J Clin Invest 119 (6) (2009) 1420-1428.

[28] J.P. Thiery, H. Acloque, R.Y. Huang, M.A. Nieto, Epithelial-mesenchymal transitions in development and disease, Cell 139 (5) (2009) 871-890.

[29] R. Pagan, I. Martin, M. Llobera, S. Vilaro, Epithelial-mesenchymal transition of cultured rat neonatal hepatocytes is differentially regulated in response to epidermal growth factor and dimethyl sulfoxide, Hepatology 25 (3) (1997) 598-606.

[30] N. Ahmed, S. Maines-Bandiera, M.A. Quinn, W.G. Unger, S. Dedhar, N. Auersperg, Molecular pathways regulating EGF-induced epithelio-mesenchymal transition in human ovarian surface epithelium, Am J Physiol Cell Physiol 290 (6) (2006) C1532-1542.

[31] J. Yang, C. Dai, Y. Liu, A novel mechanism by which hepatocyte growth factor blocks tubular epithelial to mesenchymal transition, J Am Soc Nephrol 16 (1) (2005) 68-78.

[32] F. Strutz, M. Zeisberg, F.N. Ziyadeh, C.Q. Yang, R. Kalluri, G.A. Muller, E.G. Neilson, Role of basic fibroblast growth factor-2 in epithelial-mesenchymal transformation, Kidney Int 61 (5) (2002) 1714-1728.

[33] D.M. Gonzalez, D. Medici, Signaling mechanisms of the epithelial-mesenchymal transition, Sci Signal 7 (344) (2014) re8.

[34] J. Seoane, R.R. Gomis, TGF-beta Family Signaling in Tumor Suppression and Cancer Progression, Cold Spring Harb Perspect Biol 9 (12) (2017)

[35] L. Arana, M. Ordonez, A. Ouro, I.G. Rivera, P. Gangoiti, M. Trueba, A. Gomez-Munoz, Ceramide 1-phosphate induces macrophage chemoattractant protein-1 release: involvement in ceramide 1-phosphate-stimulated cell migration, Am J Physiol Endocrinol Metab 304 (11) (2013) E1213-1226.

[36] N. Presa, A. Gomez-Larrauri, I.G. Rivera, M. Ordonez, M. Trueba, A. Gomez-Munoz, Regulation of cell migration and inflammation by ceramide 1-phosphate, Biochim Biophys Acta 1861 (5) (2016) 402-409.

[37] M.H. Granado, P. Gangoiti, A. Ouro, L. Arana, M. Gonzalez, M. Trueba, A. Gomez-Munoz, Ceramide 1-phosphate (C1P) promotes cell migration Involvement of a specific C1P receptor, Cell Signal 21 (3) (2009) 405-412.

[38] C.M. Niessen, C.J. Gottardi, Molecular components of the adherens junction, Biochim Biophys Acta 1778 (3) (2008) 562-571.

[39] M.J. Wheelock, K.R. Johnson, Cadherins as modulators of cellular phenotype, Annu Rev Cell Dev Biol 19 (2003) 207-235.

[40] A. Nagafuchi, Y. Shirayoshi, K. Okazaki, K. Yasuda, M. Takeichi, Transformation of cell adhesion properties by exogenously introduced E-cadherin cDNA, Nature 329 (6137) (1987) 341-343.

[41] B.M. Gumbiner, Regulation of cadherin-mediated adhesion in morphogenesis, Nat Rev Mol Cell Biol 6 (8) (2005) 622-634.

[42] A. Llorens, I. Rodrigo, L. Lopez-Barcons, M. Gonzalez-Garrigues, E. Lozano, A. Vinyals, M. Quintanilla, A. Cano, A. Fabra, Down-regulation of E-cadherin in mouse skin carcinoma cells enhances a migratory and invasive phenotype linked to matrix metalloproteinase-9 gelatinase expression, Lab Invest 78 (9) (1998) 1131-1142.

[43] A. Chen, H. Beetham, M.A. Black, R. Priya, B.J. Telford, J. Guest, G.A. Wiggins, T.D. Godwin, A.S. Yap, P.J. Guilford, E-cadherin loss alters cytoskeletal organization and adhesion in non-malignant breast cells but is insufficient to induce an epithelial-mesenchymal transition, BMC Cancer 14 (2014) 552.

[44] X. Xing, Y.B. Tang, G. Yuan, Y. Wang, J. Wang, Y. Yang, M. Chen, The prognostic value of E-cadherin in gastric cancer: a meta-analysis, Int J Cancer 132 (11) (2013) 2589-2596.

[45] D. Jie, Z. Zhongmin, L. Guoqing, L. Sheng, Z. Yi, W. Jing, Z. Liang, Positive expression of LSD1 and negative expression of E-cadherin correlate with metastasis and poor prognosis of colon cancer, Dig Dis Sci 58 (6) (2013) 1581-1589.

[46] H.N. Horne, M.E. Sherman, M. Garcia-Closas, P.D. Pharoah, F.M. Blows, X.R. Yang, S.M. Hewitt, C.M. Conway, J. Lissowska, L.A. Brinton, L. Prokunina-Olsson, S.J. Dawson, C. Caldas, D.F. Easton, S.J. Chanock, J.D. Figueroa, Breast cancer susceptibility risk associations and heterogeneity by E-cadherin tumor tissue expression, Breast Cancer Res Treat 143 (1) (2014) 181-187.

[47] P.J. Barnes, Mediators of chronic obstructive pulmonary disease, Pharmacol Rev 56 (4) (2004) 515-548.

[48] L.E. Donnelly, P.J. Barnes, Chemokine receptors as therapeutic targets in chronic obstructive pulmonary disease, Trends Pharmacol Sci 27 (10) (2006) 546-553.

[49] M. Checa, J.S. Hagood, R. Velazquez-Cruz, V. Ruiz, C. Garcia-De-Alba, C. Rangel-Escareno, F. Urrea, C. Becerril, M. Montano, S. Garcia-Trejo, J. Cisneros Lira, A. Aquino-Galvez, A. Pardo, M. Selman, Cigarette Smoke Enhances the Expression of Profibrotic Molecules in Alveolar Epithelial Cells, PLoS One 11 (3) (2016) e0150383.

[50] T. Masubuchi, S. Koyama, E. Sato, A. Takamizawa, K. Kubo, M. Sekiguchi, S. Nagai, T. Izumi, Smoke extract stimulates lung epithelial cells to release neutrophil and monocyte chemotactic activity, Am J Pathol 153 (6) (1998) 1903-1912.

[51] T. Mio, D.J. Romberger, A.B. Thompson, R.A. Robbins, A. Heires, S.I. Rennard, Cigarette smoke induces interleukin-8 release from human bronchial epithelial cells, Am J Respir Crit Care Med 155 (5) (1997) 1770-1776.

[52] P.G. Woodruff, A. Ellwanger, M. Solon, C.J. Cambier, K.E. Pinkerton, L.L. Koth, Alveolar macrophage recruitment and activation by chronic second hand smoke exposure in mice, COPD 6 (2) (2009) 86-94.

[53] H. Li, W. Peng, W. Jian, Y. Li, Q. Li, W. Li, Y. Xu, ROCK inhibitor fasudil attenuated high glucose-induced MCP-1 and VCAM-1 expression and monocyte-endothelial cell adhesion, Cardiovasc Diabetol 11 (2012) 65.

[54] J. Rao, Z. Ye, H. Tang, C. Wang, H. Peng, W. Lai, Y. Li, W. Huang, T. Lou, The RhoA/ROCK Pathway Ameliorates Adhesion and Inflammatory Infiltration Induced by AGEs in Glomerular Endothelial Cells, Sci Rep 7 (2017) 39727.

[55] B.J. Pettus, A. Bielawska, S. Spiegel, P. Roddy, Y.A. Hannun, C.E. Chalfant, Ceramide kinase mediates cytokine- and calcium ionophore-induced arachidonic acid release, J Biol Chem 278 (40) (2003) 38206-38213.

[56] B.J. Pettus, A. Bielawska, P. Subramanian, D.S. Wijesinghe, M. Maceyka, C.C. Leslie, J.H. Evans, J. Freiberg, P. Roddy, Y.A. Hannun, C.E. Chalfant, Ceramide 1-phosphate is a direct activator of cytosolic phospholipase A2, J Biol Chem 279 (12) (2004) 11320-11326.

[57] D.S. Wijesinghe, P. Subramanian, N.F. Lamour, L.B. Gentile, M.H. Granado, A. Bielawska, Z. Szulc, A. Gomez-Munoz, C.E. Chalfant, Chain length specificity for activation of cPLA2alpha by C1P: use of the dodecane delivery system to determine lipid-specific effects, J Lipid Res 50 (10) (2009) 1986-1995.

[58] A. Gomez-Munoz, P. Gangoiti, M.H. Granado, L. Arana, A. Ouro, Ceramide-1-phosphate in cell survival and inflammatory signaling, Adv Exp Med Biol 688 (2010) 118-130.

[59] K. Baudiss, C.K. Ayata, Z. Lazar, S. Cicko, J. Beckert, A. Meyer, A. Zech, R.P. Vieira, R. Bittman, A. Gomez-Munoz, I. Merfort, M. Idzko, Ceramide-1-phosphate inhibits cigarette smoke-induced airway inflammation, Eur Respir J 45 (6) (2015) 1689-1680.

[60] J.L. Hankins, K.E. Ward, S.S. Linton, B.M. Barth, R.V. Stahelin, T.E. Fox, M. Kester, Ceramide 1-phosphate mediates endothelial cell invasion via the annexin a2-p11 heterotetrameric protein complex, J Biol Chem 288 (27) (2013) 19726-19738.

[61] S. Suzuki, A. Tanaka, H. Nakamura, T. Murayama, Knockout of Ceramide Kinase Aggravates Pathological and Lethal Responses in Mice with Experimental Colitis, Biol Pharm Bull 41 (5) (2018) 797-805.

[62] E. Shacter, S.A. Weitzman, Chronic inflammation and cancer, Oncology (Williston Park) 16 (2) (2002) 217-226, 229; discussion 230-212.

[63] K.E. de Visser, A. Eichten, L.M. Coussens, Paradoxical roles of the immune system during cancer development, Nat Rev Cancer 6 (1) (2006) 24-37.

[64] L.M. Coussens, Z. Werb, Inflammation and cancer, Nature 420 (6917) (2002) 860-867.

[65] F. Balkwill, K.A. Charles, A. Mantovani, Smoldering and polarized inflammation in the initiation and promotion of malignant disease, Cancer Cell 7 (3) (2005) 211-217.

[66] A. Ben-Baruch, Inflammation-associated immune suppression in cancer: the roles played by cytokines, chemokines and additional mediators, Semin Cancer Biol 16 (1) (2006) 38-52.

[67] H.J. Shen, Y.H. Sun, S.J. Zhang, J.X. Jiang, X.W. Dong, Y.L. Jia, J. Shen, Y. Guan, L.H. Zhang, F.F. Li, X.X. Lin, X.M. Wu, Q.M. Xie, X.F. Yan, Cigarette smoke-induced alveolar epithelial-mesenchymal transition is mediated by Rac1 activation, Biochim Biophys Acta 1840 (6) (2014) 1838-1849.

[68] I.M. Eurlings, N.L. Reynaert, T. van den Beucken, H.R. Gosker, C.C. de Theije, F.M. Verhamme, K.R. Bracke, E.F. Wouters, M.A. Dentener, Cigarette smoke extract induces a phenotypic shift in epithelial cells; involvement of HIF1alpha in mesenchymal transition, PLoS One 9 (10) (2014) e107757.

[69] E. Tashiro, S. Henmi, H. Odake, S. Ino, M. Imoto, Involvement of the MEK/ERK pathway in EGF-induced E-cadherin down-regulation, Biochem Biophys Res Commun 477 (4) (2016) 801-806.

[70] X.W. Li, M. Tuergan, G. Abulizi, Expression of MAPK1 in cervical cancer and effect of MAPK1 gene silencing on epithelial-mesenchymal transition, invasion and metastasis, Asian Pac J Trop Med 8 (11) (2015) 937-943.

[71] M. Conacci-Sorrell, I. Simcha, T. Ben-Yedidia, J. Blechman, P. Savagner, A. Ben-Ze'ev, Autoregulation of E-cadherin expression by cadherin-cadherin interactions: the roles of beta-catenin signaling, Slug, and MAPK, J Cell Biol 163 (4) (2003) 847-857.

[72] A. Ihermann-Hella, M. Lume, I.J. Miinalainen, A. Pirttiniemi, Y. Gui, J. Peranen, J. Charron, M. Saarma, F. Costantini, S. Kuure, Mitogen-activated protein kinase (MAPK) pathway regulates branching by remodeling epithelial cell adhesion, PLoS Genet 10 (3) (2014) e1004193.

[73] D. Yu, H. Geng, Z. Liu, L. Zhao, Z. Liang, Z. Zhang, D. Xie, Y. Wang, T. Zhang, J. Min, C. Zhong, Cigarette smoke induced urocystic epithelial mesenchymal transition via MAPK pathways, Oncotarget 8 (5) (2017) 8791-8800.

[74] L.M. Shaw, I. Rabinovitz, H.H. Wang, A. Toker, A.M. Mercurio, Activation of phosphoinositide 3-OH kinase by the alpha6beta4 integrin promotes carcinoma invasion, Cell 91 (7) (1997) 949-960.

[75] B.K. Park, X. Zeng, R.I. Glazer, Akt1 induces extracellular matrix invasion and matrix metalloproteinase-2 activity in mouse mammary epithelial cells, Cancer Res 61 (20) (2001) 7647-7653.

[76] K. Baudiss, R. de Paula Vieira, S. Cicko, K. Ayata, M. Hossfeld, N. Ehrat, A. Gomez-Munoz, H.K. Eltzschig, M. Idzko, C1P Attenuates Lipopolysaccharide-Induced Acute Lung Injury by Preventing NF-kappaB Activation in Neutrophils, J Immunol 196 (5) (2016) 2319-2326.

Chapter 2

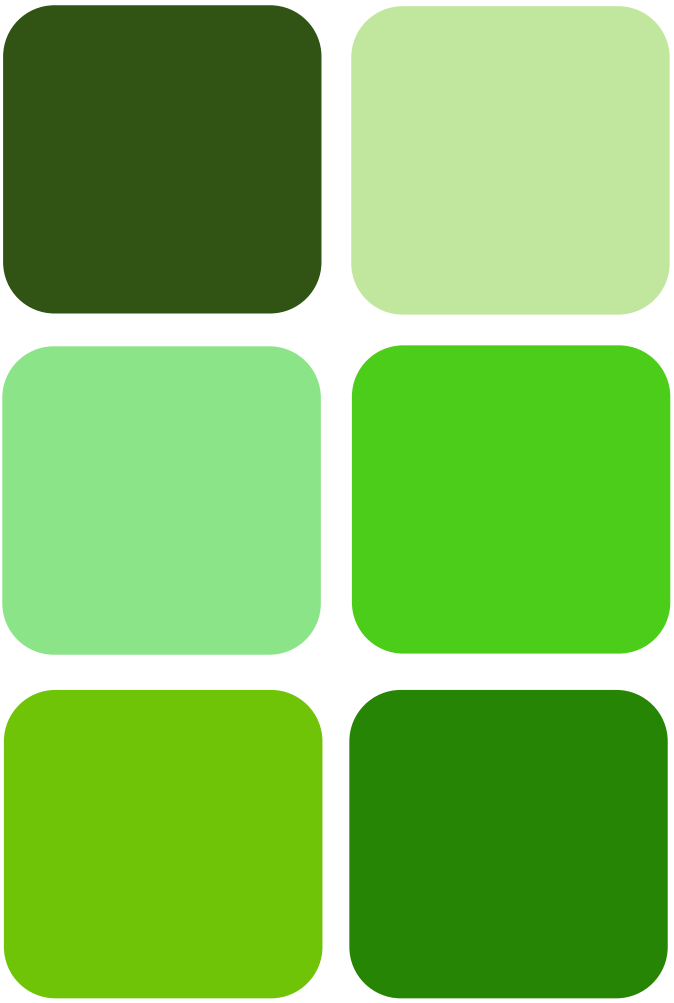

CHAPTER 2:

Implication of phosphatidylethanolamine *N*-methyltransferase in adipogenesis

1. Introduction

1.1. Adipogenesis

Over the past decades, the adipose tissue has been defined as a dynamic organ implicated in several important physiological processes such as glucose metabolism, appetite, immunological responses, inflammation, angiogenesis, blood pressure regulation and reproductive function [1, 2]. The main cells present in adipose tissue are mature adipocytes. Adipogenesis is the differentiation process of fibroblast like pre-adipocytes into mature lipid filled, insulin-responsive adipocytes. This highly controlled process can be divided into well-defined stages: (i) mesenchymal precursors, (ii) committed pre-adipocytes, (iii) growth-arrested pre-adipocytes, (iv) mitotic clonal expansion, (v) terminal differentiation and (vi) mature adipocytes. The latter stage is characterized by a large lipid droplet, which causes cell swelling so that the nucleus is displaced to the outer edge of the cell. The aberrant increase in fat mass observed in obese subjects is due to deregulation of the number (hyperplasia) and size (hypertrophy) of adipocytes.

Adipogenesis has been studied extensively because of the increasing prevalence of obesity in our society. However, the mechanisms involved in pre-adipocyte differentiation and the establishment and progression of obesity remain largely unknown. In order to attain a successful differentiation into mature adipocytes, pre-adipocytes need to achieve changes not only in their morphology but also in gene expression. Although the exact mechanisms that regulate the adipogenic process is not fully understood, some of the molecular pathways involved have been elucidated. Also,

some transcriptional factors have been identified as necessary to promote pre-adipocyte differentiation. These include peroxisome proliferator-activated receptor (PPAR), CCAAT/enhancer-binding proteins (C/EBPs), single transducers and activators of transcription (STATs), and Kruppel-like factor (KLF) proteins, as well as some fatty acids, prostaglandins and glucocorticoids.

Thus, decoding the mechanisms involved in adipogenesis is essential for understanding the processes that are implicated in the development and progression of obesity and obesity-related diseases.

1.2. Obesity

Overweight and obesity are defined as abnormal or excessive fat accumulation that may impair health. The rise of the obesity epidemic seemed to begin in most high-income countries in 1970s and, since then, most middle-income and many low-income countries have joined the global trend in obesity prevalence in adults and children. The worldwide prevalence of obesity nearly tripled between 1975 and 2016. By then, an estimated 1.9 billion adults were overweight. Of these, more than 650 million adults were obese. Overall, about 13% of the world's adult population was obese. Furthermore, it is estimated that over 340 million children aged 5-19 were overweight or obese in 2016.

Overweight and obesity are linked to more deaths worldwide than underweight. Raised body mass index (BMI) is an essential risk factor for various metabolic diseases such as hypertension [3], dyslipidemia [4], type II diabetes (T2D) and insulin resistance (IR)[5-7], non-alcoholic fatty liver disease [8, 9], cardiovascular diseases [10-13], and certain forms of cancer [14-16], which increase obesity-associated morbidity and mortality.

From a biochemical point of view, obesity is the result of an imbalance where energy intake exceeds energy expenditure over time. This energy excess leads to triglyceride accumulation, which is associated with local and systemic chronic state of low-grade adipose tissue inflammation. This inflammatory state is characterized by an increase of immune cell infiltration into obese adipose tissue and increased production and secretion of pro-inflammatory factors into the bloodstream. Adipocytes secrete a number of protein factors known as adipokines that play critical roles in the regulation of glucose and lipid metabolism and immune responses [17, 18]. Alterations in

adipokine levels and chronic inflammation in the adipose tissue exert profound effects on metabolic pathways, leading to the development of metabolic disorders [19, 20]. Therefore, understanding the mechanisms that control adipogenic differentiation and triglyceride accumulation would be an effective approach for developing new strategies for prevention and treatment of obesity-related diseases.

1.3. Differentiation of pre-adipocytes into mature adipocytes

One of the most extensively characterized and widely used cell system for studying adipogenesis is the 3T3-L1 mouse pre-adipocyte cell line. These cells are derived from Swiss 3T3 mouse embryos and require a glucocorticoid-supplemented differentiation cocktail for induction of adipogenesis [21-23]. 3T3-L1 fibroblasts undergo cell differentiation to mature adipocytes when treated with adipogenic induction medium (AIM), which consists of DMEM, 10% FBS and an adipogenic cocktail (0.5 mM 3-isobutyl-1-methylxanthine (IBMX), 1 μg/ml insulin, 0.25 μM dexamethasone and 2 μM rosiglitazone) [22-24]. IBMX is a non-competitive selective phosphodiesterase inhibitor that raises intracellular cAMP levels. Dexamethasone is a synthetic glucocorticoid receptor (GR) agonist, and rosiglitazone works as an insulin sensitizer by binding to the PPAR in fat cells making them more responsive to insulin [24]. These pro-adipogenic compounds initiate the differentiation program, which starts with the phosphorylation of cAMP Response Element-Binding protein (CREB) that will then activate the expression of CCAAT/Enhancer Binding Protein beta (C/EBP-β). C/EBP-β acquires DNA-binding activity to facilitate several rounds of post confluent mitosis, referred to as mitotic clonal expansion (MCE), a required step for terminal differentiation. When cells exit the cell cycle they suffer deep phenotypical changes leading to homogeneous population of spherical, and lipid droplet-filled cells that are morphologically and biochemically similar to *in vivo* differentiated adipocytes.

1.4. The adipogenic transcriptional network

Adipogenesis is usually described as a cascade of genetic events that can be divided into two stages. The first stage includes the transient activation of C/EBP-β and C/EBP-δ, induced by the hormonal adipogenic cocktail [25], which allows the expression of multiple cell-cycle related genes to facilitate mitotic clonal expansion (MCE), a required step for terminal differentiation. In this phase, cells lose their fibroblast morphology to acquire a round shape. C/EBP-β and C/EBP-δ are also responsible for the initiation of the second stage, where PPAR-γ and C/EBP-α will be activated. These two

factors are considered the master transcriptional regulators of the adipogenic process. PPAR-γ and C/EBP-α initiate a positive feedback to induce their own expression and also activate a large number of downstream target genes whose expression will determine the adipocyte, such as acetyl CoA carboxylase, important in the fatty acid synthesis pathway, the glucose transporter GLUT4, or the fatty acid binding proteins (FABPs). Throughout this process, small lipid droplets start to appear within the cell, which will end up merging to form large lipid droplets that will comprise almost the whole cell.

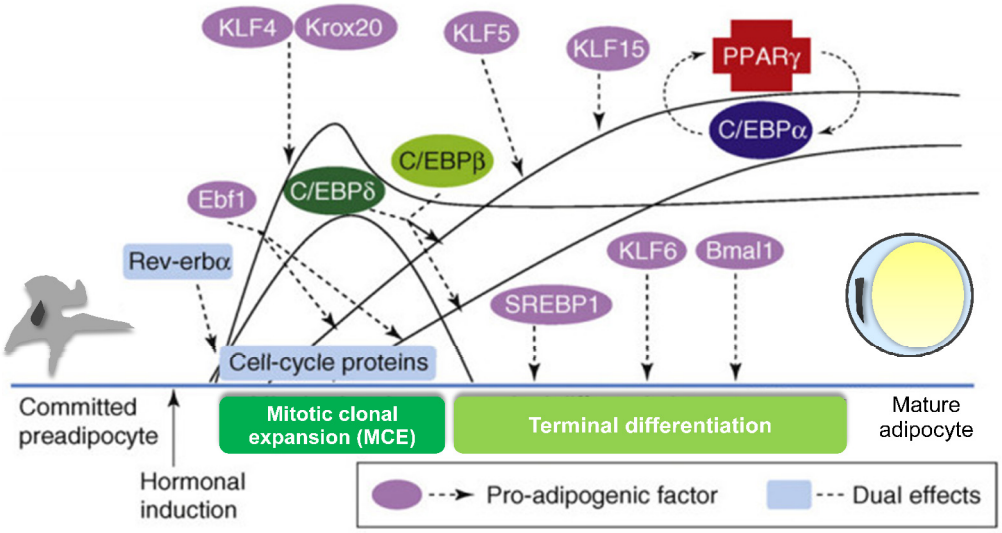

Figure 1: Transcriptional regulation of adipocyte differentiation. Once adipogenesis is induced by hormonal adipogenic cocktail, C/EBP-β and C/EBP-δ promote the activation of multiple cell cycle-related genes and delay the expression of C/EBP-α and PPAR-γ to ensure MCE phase, a required step for further terminal differentiation. When MCE phase is completed the expression of C/EBP-α and PPAR-γ as well as their downstream target genes is allowed, thereby leading to mature adipocyte formation. Adapted image from [1].

1.5. The CerK/C1P axis in adipogenesis

Sphingolipids and sphingolipid-related enzymes have emerged as key regulators of vital cellular processes including cell growth, differentiation, or cell death, and it has also been shown that some of them take part in inflammatory responses and inflammation-associated diseases including cardiovascular diseases, cancer, and obesity.

Among the sphingolipid family, ceramides have been implicated in insulin resistance leading to type II diabetes, and sphingosine and sphingosine kinase are

altered in the obese state [26, 27]. Previously, our laboratory has demonstrated that Ceramide Kinase (CerK) expression and activity increase during the differentiation of pre-adipocytes, and that CerK knock-down results in impaired adipogenesis [22]. In concordance with our previous results, it has been established that cellular ceramide levels are inversely correlated with adipocyte differentiation [28]. In addition, it has been shown that CerK deficiency improves diet-induced obesity and insulin resistance in mice [29]. Thus, these data point to a putative role of ceramide kinase in the onset and development of obesity.

More recently, our group showed that administration of exogenous C1P to cells undergoing adipocyte differentiation causes a significant reduction in the levels of TG, which was concomitant with a significant decrease in leptin release and PPAR-ɣ expression, pointing to a possible anti-adipogenic action of exogenous C1P [30].

1.6. The role of PEMT in adipogenesis

Phosphatidylethanolamine *N*-methyltransferase (PEMT) is a small integral membrane protein (~ 22 kDa isoform 1, and ~ 27 kDa isoform 2) that catalyzes the production of phosphatidylcholine (PC) via three sequential methylation of phosphatidylethanolamine (PE) using S-adenosylmethionine as a methyl donor. Despite being predominantly expressed in the liver, PEMT activity has also been demonstrated in other tissues, including the adipose tissue, in which PEMT expression was induced by feeding mice with a high fat diet (HFD) [31, 32]. A possible role of PEMT in obesity and obesity-associated disorders was first suggested by Vance and co-workers based on *in vitro* and *in vivo* assays. Interestingly, PEMT deficient mice were found to be protected against obesity and insulin resistance [33-35]. In humans, it has been established that obese subjects show transcriptional upregulation of the *Pemt* gene [36]. *In vitro*, PEMT was demonstrated to be important in lipid droplet formation and processing and to be actively involved in maintaining a stable lipid droplet phenotype in adipocytes [32]. However, the possible implication of PEMT in adipogenesis and adipocyte biochemistry has not been fully studied.

Thus, the aim of this chapter was to evaluate whether PEMT is implicated in adipocyte differentiation, and to investigate whether this enzyme is related to CerK/C1P in the process of adipogenesis.

2. RESULTS

2.1. PEMT is upregulated during adipogenesis

The implication of PEMT in adipogenesis was tested using 3T3-L1 mouse pre-adipocytes (fibroblast phenotype). Cell differentiation was induced by incubation of the pre-adipocytes with AIM for up to 9 days (see *Materials and Methods* section). Western-blotting revealed that the adipocyte markers PPAR-ɣ, perilipin-1 and adiponectin, were overexpressed during the adipogenic process (Fig. 2).

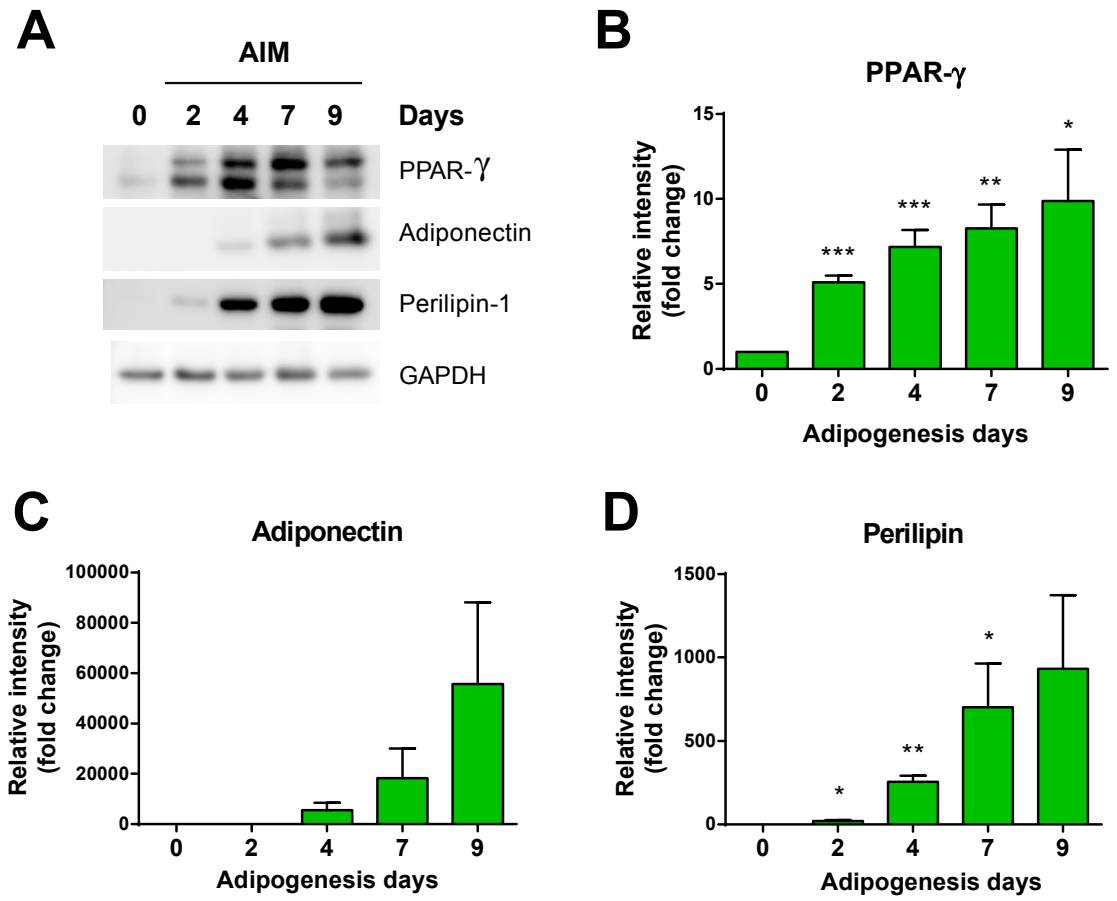

Figure 2: Adipocyte marker expression increased during pre-adipocyte differentiation. 3T3-L1 cells were seeded in 6-well plates (2 x 10^5 cells/well) in DMEM containing 10% NBCS. 48 h post confluence, cells were differentiated up to day 9 as described in *Materials and Methods*. Cells were harvested at indicated time points and protein expression was analyzed by western blotting. A) PPAR-ɣ, adiponectin and perilipin 1 expression was detected by western blotting using specific antibodies. GAPDH was used as protein loading control. Similar results were obtained in 5 independent experiments. B, C and D) Quantification of A normalized to total protein and relative to non-differentiated control. Data are expressed as arbitrary units of intensity relative to GAPDH and are the mean ± SEM of 5 different experiments.

A relevant observation was that the protein levels of PEMT were also upregulated during adipogenesis (figure 3). Maximal PEMT expression occurred at day 7. Noteworthy, the PEMT isoform that was upregulated during cell differentiation was PEMT-2, not the canonical PEMT isoform.

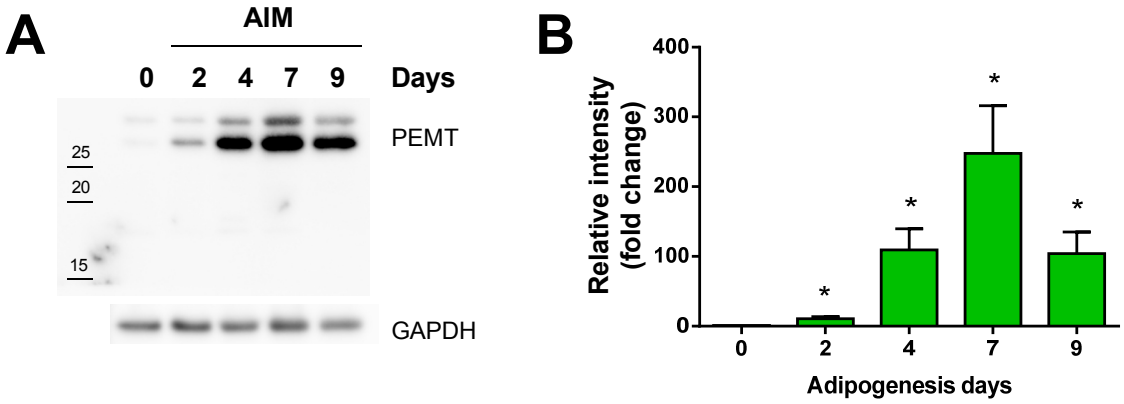

Figure 3: PEMT-2 expression increases during adipogenesis. 3T3-L1 cells were seeded in 6-well plates (2 x 10^5 cells/well) in DMEM containing 10% NBCS. 48 h post confluence, cells were differentiated up to day 9 as described in *Materials and Methods*. Cells were harvested at indicated time points and protein expression was analyzed by western blotting. A) PEMT expression was detected by western blotting using specific antibody and GAPDH was used as a protein loading control. Similar results were obtained in 5 independent experiments. B) Quantification of A normalized to total protein and relative to non-differentiated control. Data are expressed as arbitrary units of intensity relative to GAPDH and are the mean ± SEM of 5 different experiments.

2.2. PEMT contributes to lipid storage in 3T3-L1 cells

The implication of PEMT in adipogenesis was studied using specific siRNA to silence the gene encoding this enzyme (please see the *Materials and Methods* section). Protein expression was analyzed by western-blotting 4 days after induction of cell differentiation. Figure 4 shows that PEMT was efficiently silenced using this method.

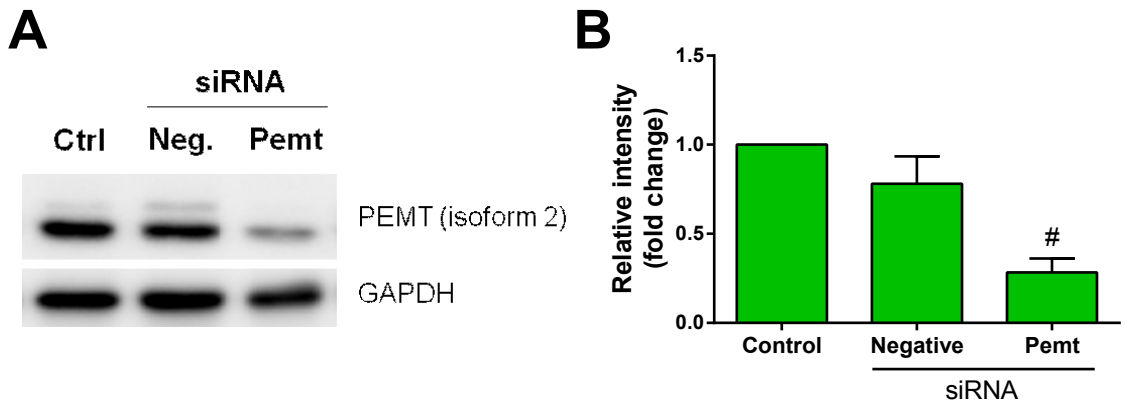

Figure 4: PEMT siRNA efficiently downregulates PEMT protein expression in 3T3-L1 cells. Cells were seeded in 6-well plates (2 x 10^5 cells/well) in DMEM containing 10% NBCS and transfected with PEMT siRNA as described in *Materials and Methods*. 48 h after gene silencing, cells were differentiated until day 4. On day 4 after induction of differentiation, cells were harvested and PEMT expression was analyzed by western blotting. A) PEMT was detected by western blotting using specific antibody and GAPDH was used as a protein loading control. Similar results were obtained in 4 independent experiments. B) Quantification of A normalized to total protein and relative to control. Data are expressed as arbitrary units of intensity to GAPDH and are the mean ± SEM of 4 different experiments. (#p‹0.05).

To test whether PEMT was involved in adipogenesis, the content of lipid droplets was determined in cells where *Pemt* was silenced with specific siRNA. The content of lipid droplets was determined at day 7 of differentiation when droplets are abundant within the cells. Lipid droplets were visualized using a conventional light microscope after staining with Oil red O and were subsequently quantified. In addition, the triglyceride (TG) content was determined using a commercial kit, as indicated in the *Materials and Methods* section. Figure 5 shows that PEMT silencing effectively blocked lipid droplet formation and triglyceride accumulation in 3T3-L1 cells, indicating that PEMT plays a key role in adipogenesis.

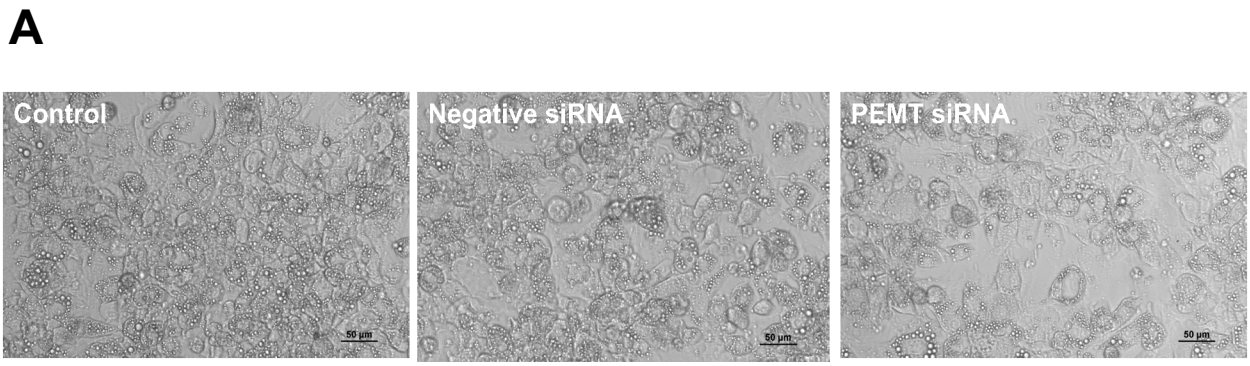

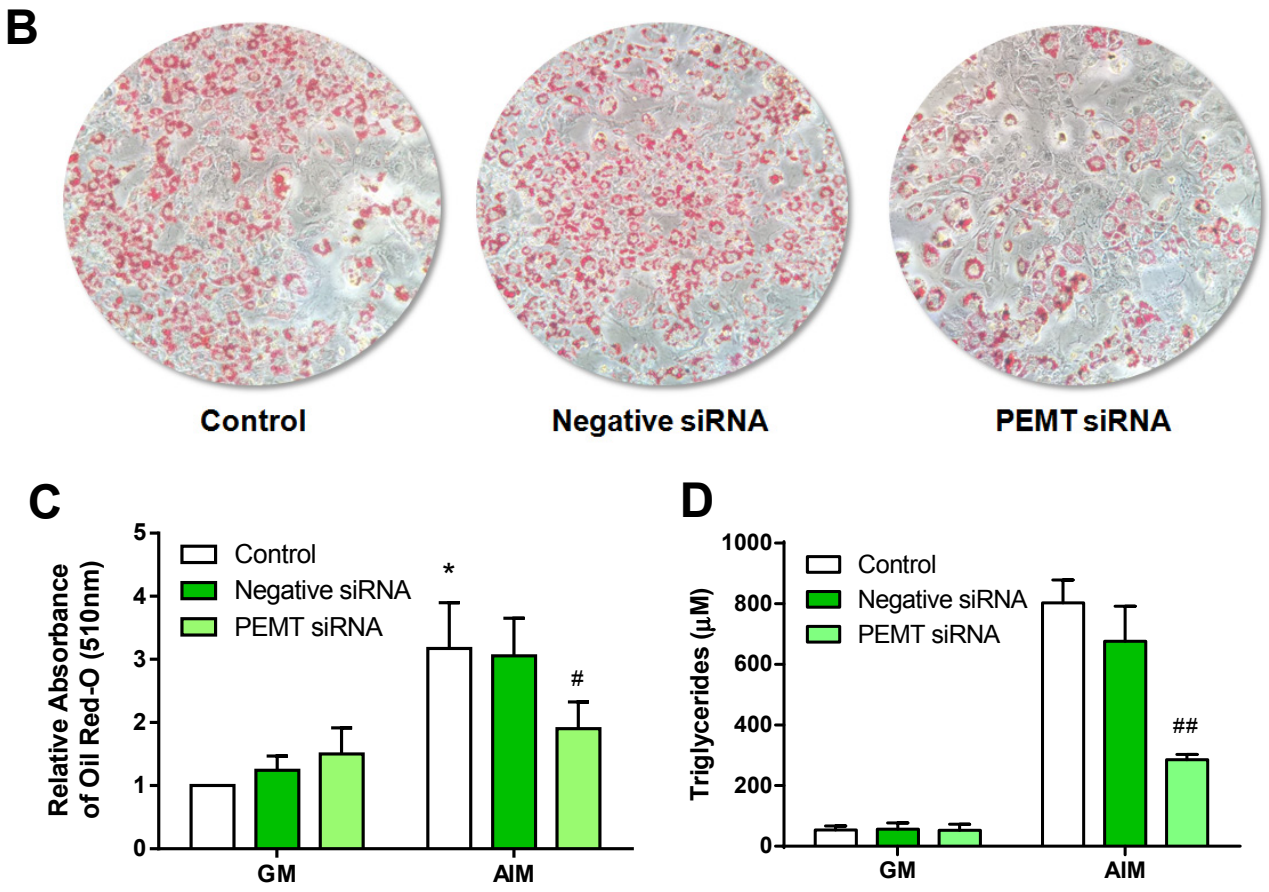

Figure 5: PEMT siRNA inhibits 3T3-L1 cell differentiation. 3T3-L1 cells were seeded in 24-well plates in DMEM containing 10% NBCS and transfected with *Pemt* siRNA as described in *Materials and Methods*. 48 hours after gene silencing differentiation was induced up to day 7th. A) On day 7 after induction of differentiation, lipid droplets were visualized and micrographs were taken. B) On day 7 after induction of differentiation, cells were stained with Oil red O as described in *Materials and Methods* and lipid droplets were visualized under a conventional light microscope. C) Lipid droplets in B were quantified measuring the absorbance of each well at 510 nm. Absorbance of empty wells without cells was subtracted to the values. Data are expressed as the means ± SEM of 8 different experiments performed in duplicate (*p‹0.05). D) On day 7 after induction of differentiation, triglycerides were measured using a commercial kit as described in *Materials and Methods*. (GM: *growth medium*; AIM: *adipogenesis induction medium*). Results are expressed as the means ± SEM of 4 different experiments performed in duplicate. (*p‹0.05).

2.3. PEMT knockdown results in reduced adipocyte marker expression.

As mentioned earlier, during the adipogenic process there is upregulation of PPAR-ɣ, adiponectin and perilipin-1. So, to further support the role of PEMT in adipocyte differentiation, the levels of these adipocyte markers were analyzed by Western-blotting after PEMT silencing. Figure 6 shows that PEMT knockdown was accompanied

by significant reduction of PPAR-ɣ, adiponectin and perilipin-1 expression thereby supporting the notion that PEMT plays a fundamental role in adipogenesis.

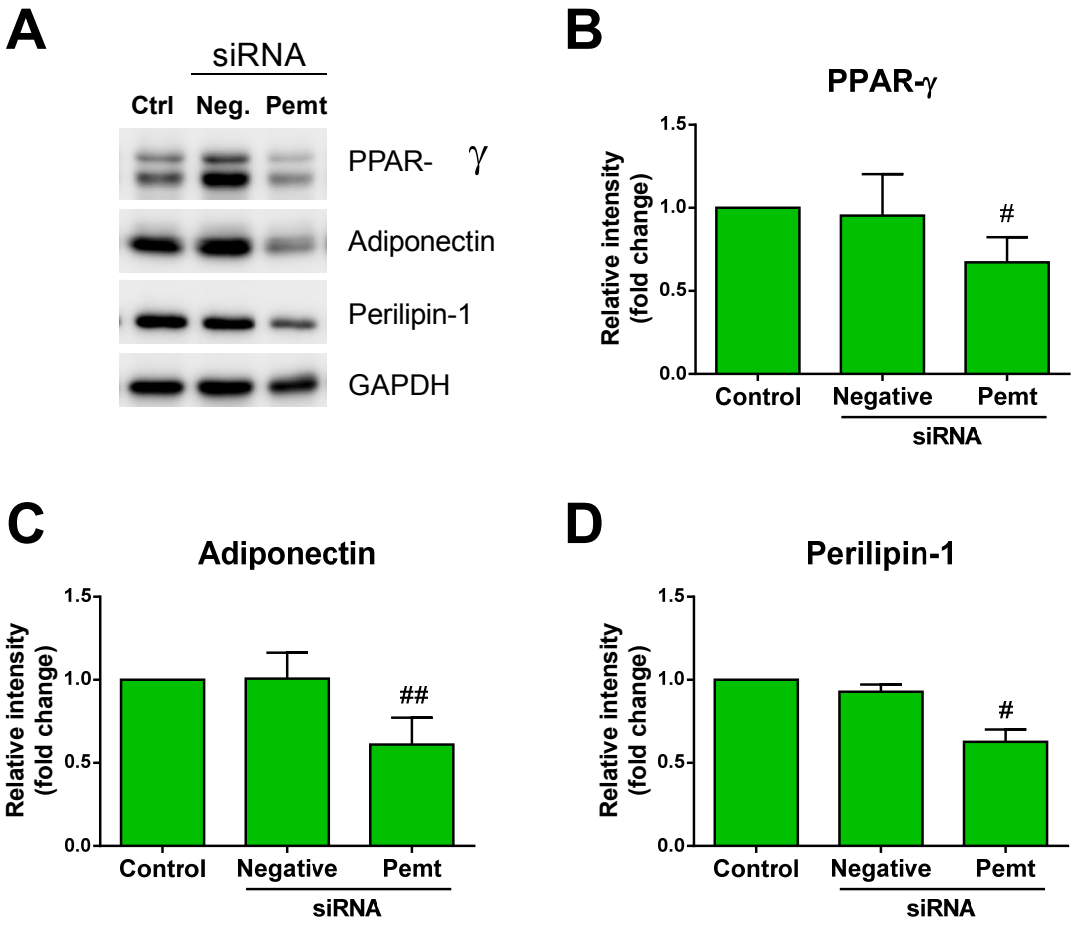

Figure 6: PEMT silencing reduces adipocyte marker expression in 3T3-L1 differentiated cells. 3T3-L1 cells were seeded in 6-well plates (2 x 10^5 cells/well) in DMEM containing 10% NBCS and transfected with PEMT siRNA as described in *Materials and Methods*. 48 h after gene silencing, cells were differentiated until day 4. On day 4 after induction of differentiation, cells were harvested and protein expression was analyzed by western blotting. A) PPAR-ɣ, adiponectin and perilipin-1 expression was detected by western blotting using specific antibodies and GAPDH was used as a protein loading control. Similar results were obtained in 4 independent experiments. B, C and D) Quantification of A normalized to total protein and relative to each control. Data are expressed as arbitrary units of intensity relative to GAPDH and are the mean ± SEM of 5 different experiments. (#p‹0.05; ##p‹0.01).

2.4. PEMT knockdown reduces leptin release

Leptin is a hormone secreted by mature adipose cells that helps to regulate energy balance and fat storage. To further confirm that PEMT plays a key role in adipogenesis,

the levels of leptin were measured in adipocytes that were treated or not with specific siRNA to silence PEMT. Figure 7 shows that PEMT silencing significantly reduced leptin release in differentiated 3T3-L1 cells, which is consistent with the implication of PEMT in adipogenesis.

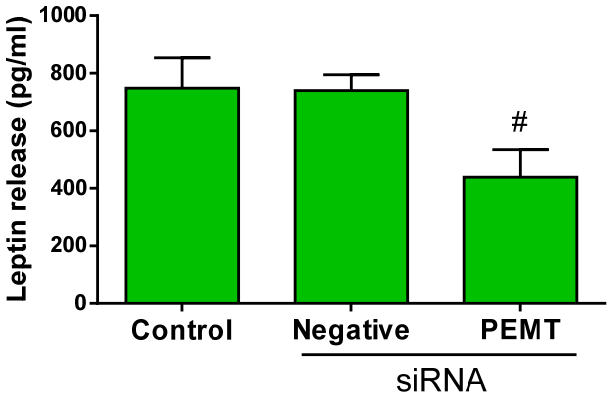

Figure 7: PEMT silencing reduces leptin release in 3T3-L1 differentiated cells. 3T3-L1 cells were seeded in 24-well plates in DMEM containing 10% NBCS and transfected with *Pemt* siRNA as described in *Materials and Methods*. 48 hours after gene silencing, differentiation was induced up to day 7. On day 7 after induction of differentiation, culture medium was collected, centrifuged and leptin concentration on the supernatant was measured using ELISA kit, as described in *Materials and Methods*. Results are the mean ± SEM of 8 different experiments performed in duplicate (#$p<0.05$).

2.5. PEMT knockdown does not alter ceramide kinase activity

Our laboratory recently showed that expression of ceramide kinase (CerK), the enzyme that produces ceramide 1-phosphate (C1P) from ceramide intracellularly, was upregulated and activated during adipogenic differentiation, and that knockdown of CerK resulted in impaired adipogenesis [22]. Therefore, it was hypothesized that PEMT expression might be related to CerK activity. To test the hypothesis, PEMT was silenced in 3T3-L1 cells and adipogenesis was induced up to day 7, when the peak of CerK expression was maximum [22]. As shown in figure 8, PEMT silencing did not alter CerK activity, indicating that if there was a connection between PEMT and CerK, PEMT would not be an upstream factor. However, the expression of PEMT is significantly decreased by C1P, as shown below, which indicates that PEMT may be a downstream effector of CerK/C1P.

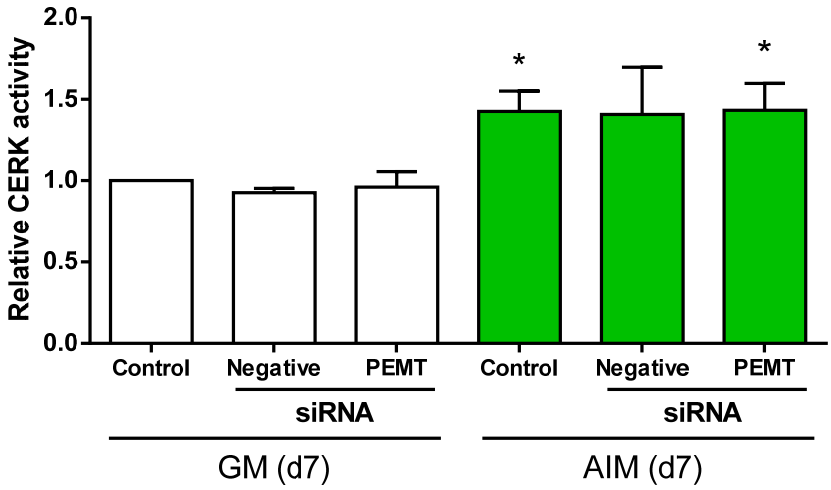

Figure 8: PEMT silencing does not alter ceramide kinase activity. 3T3-L1 cells were seeded in 6-well plates (2 x 10^5 cells/well) in DMEM containing 10% NBCS and transfected with *Pemt* siRNA as described in *Materials and Methods*. 48 hours after gene silencing, differentiation was induced up to day 7. On day 7 after induction of differentiation, cells were collected and ceramide kinase activity assay was performed as described in *Materials and Methods*. (GM: *growth medium*; AIM: *adipogenesis induction medium*). Results are the mean ± SEM of 4 different experiments (*p‹0.05).

2.6. Exogenous C1P inhibits PEMT expression and adipogenesis

Another relevant finding in this work was that C1P substantially decreased PEMT expression. We observed that treatment of cells with 20 μM C1P decreased both PEMT and PPAR-ɣ expression suggesting, that C1P may exert its anti-adipogenic role, at least in part, by interfering with PEMT expression (Figure 9).

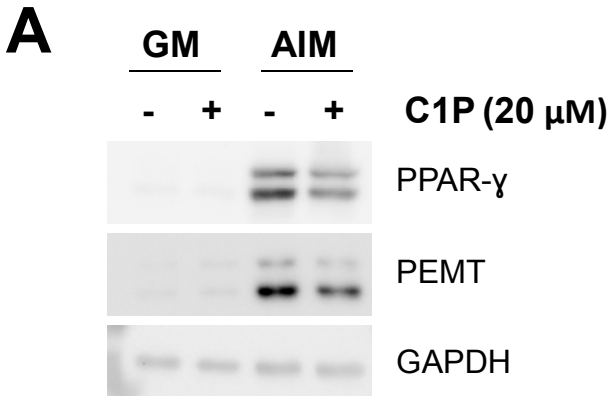

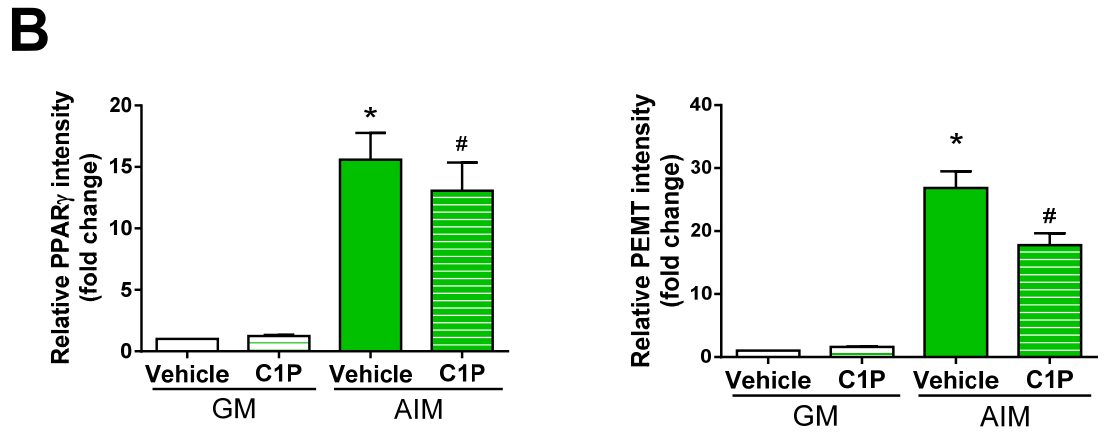

Figure 9: Exogenous C1P reduces PPAR-ɣ and PEMT expression. 3T3-L1 cells were seeded in 6-well plates (2 x 10^5 cells/well) in DMEM containing 10% NBCS. 48 h post confluence, cells were differentiated with or without the presence of 20 μM C1P up to day 4. Cells were then harvested and protein expression was analyzed by western blotting. A) PPAR-ɣ and PEMT expression was detected by western blotting using specific antibodies and GAPDH was used as a protein loading control. Similar results were obtained in 3 independent experiments. B) Quantification of A normalized to total protein and relative to each control. (GM: *growth medium*; AIM: *adipogenesis induction medium*). Data are expressed as arbitrary units of intensity relative to GAPDH and are the mean ± SEM of 3 different experiments (*p‹0.05).

2.7. PEMT is necessary for ERK and AKT deactivation during adipogenesis

Different reports, including work from our own laboratory, have previously suggested a role of MAPKs in adipogenesis.

Investigation into the mechanism by which PEMT silencing inhibited adipogenesis pointed to a possible role of ERK1-2 in this process. Figure 10 shows a sharp decrease in ERK1-2 phosphorylation throughout the differentiation process, suggesting that deactivation of these kinases is associated with adipogenesis, which was consistent with our previous work [30].

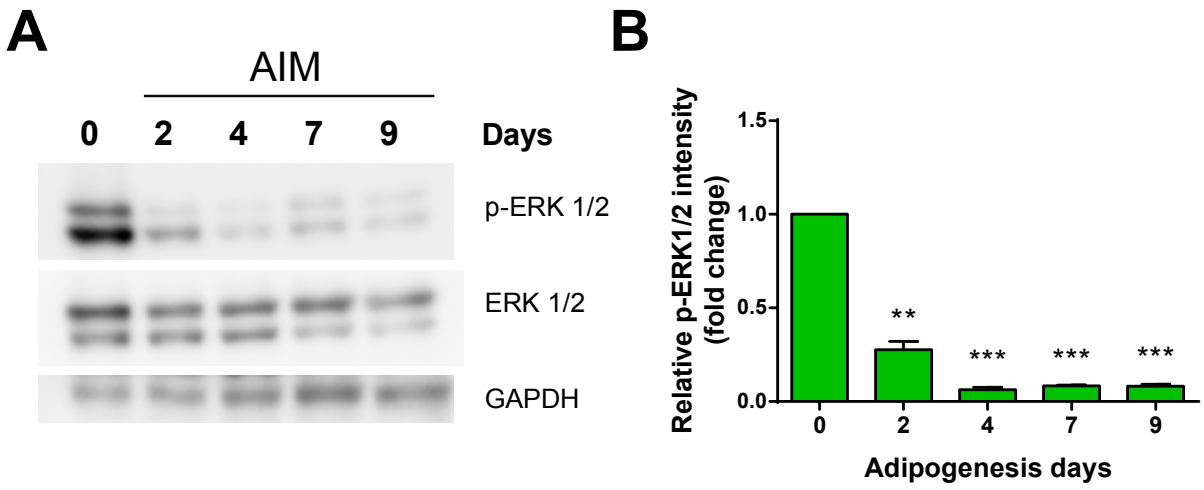

Figure 10: ERK is deactivated during adipogenesis. 3T3-L1 cells were seeded in 6-well plates (2 x 10^5 cells/well) in DMEM containing 10% NBCS. 48 h post confluence, cells were differentiated up to day 9. Cells were harvested at indicated time points and protein expression was analyzed. A) ERK and p-ERK expression was detected by western blot using specific antibodies and GAPDH was used as a protein loading control. Similar results were obtained in 3 independent experiments. B) Quantification of A normalized to total protein and relative to non-differentiated cells. Data are expressed as arbitrary units of intensity relative to GAPDH and are the mean ± SEM of 3 different experiments.

By contrast, ERK1-2 phosphorylation was increased in PEMT knockdown cells (figure 11), thereby reinforcing the notion that ERK1-2 are essential in adipogenesis and that at least part of the mechanism by which PEMT knockdown inhibits adipocyte differentiation involves the activation of these kinases.

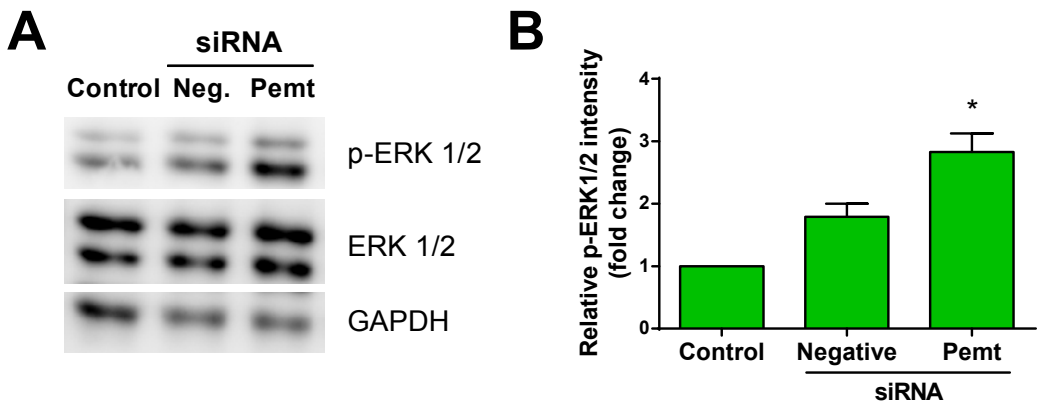

Figure 11: PEMT knockdown induces ERK activation in 3T3-L1 cells. 3T3-L1 cells were seeded in 6-well plates in DMEM containing 10% NBCS and transfected with *Pemt* siRNA as described in *Materials and Methods*. 48 hours after gene silencing, differentiation was induced up to day 4. Cells were then harvested and protein expression was analyzed by western blotting. A) ERK and p-ERK expression was detected by western blotting using specific antibodies and GAPDH was used as a protein loading control. Similar results were obtained in 4 independent experiments. B) Quantification of A normalized to total protein and relative to control. Data are expressed as arbitrary units of intensity relative to GAPDH and are the mean ± SEM of 3 different experiments. (*p<0.05).

Another kinase, the serine/threonine kinase AKT (also known as protein kinase B, PKB), is thought to have an essential role in adipocyte differentiation. As for ERK1-2, there was a marked decrease in AKT phosphorylation throughout the differentiation process (Figure 12), suggesting that deactivation of this kinase is associated with adipogenesis.

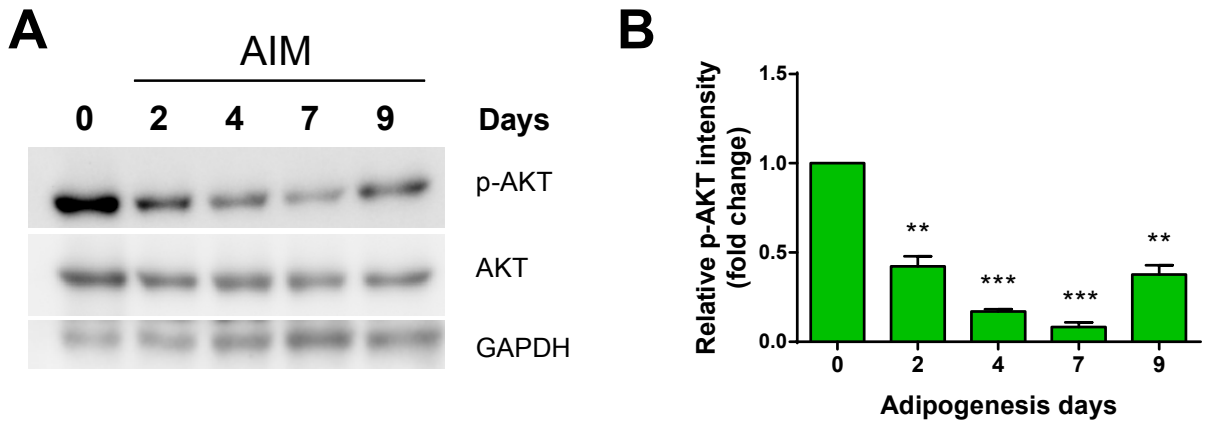

Figure 12: AKT is deactivated during adipogenesis. 3T3-L1 cells were seeded in 6-well plates (2 x 10^5 cells/well) in DMEM containing 10% NBCS. 48 h post confluence, cells were differentiated up to day 9. Cells were harvested at indicated time points and protein expression was analyzed. A) AKT and p-AKT expression was detected by western blot using specific antibodies and GAPDH was used as a protein loading control. Similar results were obtained in 3 independent experiments. B) Quantification of A normalized to total protein and relative to non-differentiated cells. Data are expressed as arbitrary units of intensity relative to GAPDH and are the mean ± SEM of 3 different experiments.

However, similarly to ERK1-2, AKT phosphorylation was increased in PEMT knockdown cells (figure 13), thereby reinforcing the notion that AKT is also essential in adipogenesis and that at least part of the mechanism by which PEMT knockdown inhibits adipocyte differentiation involves the activation of this kinase.

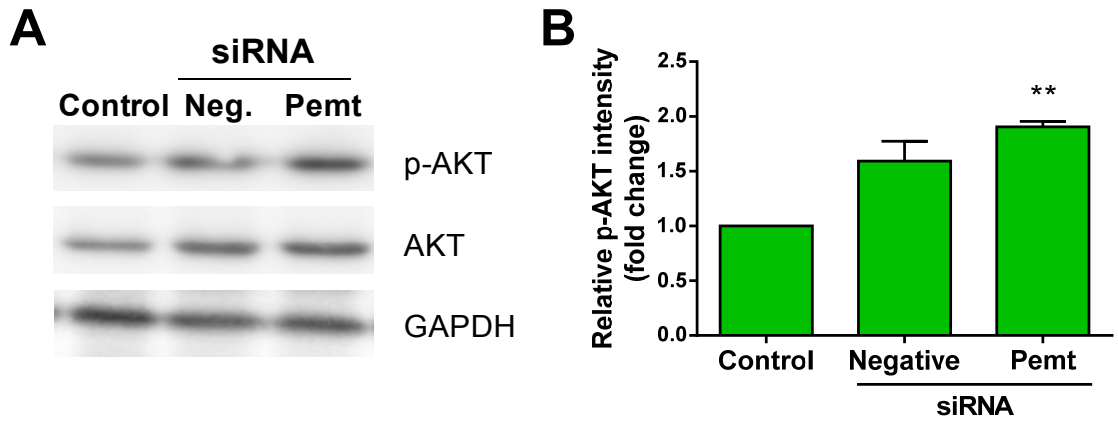

Figure 13: PEMT knockdown induces AKT phosphorylation in 3T3-L1 cells. 3T3-L1 cells were seeded in 6-well plates in DMEM containing 10% NBCS and transfected with *Pemt* siRNA as described in *Materials and Methods*. 48 hours after gene silencing, differentiation was induced up to day 4. Cells were then harvested and protein expression was analyzed by western blotting. A) AKT and p-AKT expression was detected by western blotting using specific antibodies and GAPDH was used as a protein loading control. Similar results were obtained in 3 independent experiments. B) Quantification of A normalized to total protein and relative to control. Data are expressed as arbitrary units of intensity relative to GAPDH and are the mean ± SEM of 3 different experiments. (*$p<0.05$).

3. DISCUSION

Given that adipogenesis is a key event in the development of obesity, understanding the mechanisms or molecular pathways implicated in this process may prove useful for treatment of obesity and obesity-associated diseases. Differentiation of pre-adipocytes to mature adipocytes is a multi-step process that is accompanied by highly regulated induction of CCAAT-enhancer-binding protein (C/EBP) transcription factors and the peroxisome proliferator-activated receptors family (PPAR), followed by activation of a variety of adipocyte-specific genes that lead to further differentiation [37].

The data presented in this chapter show a significant increase in PEMT-2 during pre-adipocyte differentiation. PEMT-2 expression begins to increase 2 days after the induction of adipogenesis and remains high throughout cell differentiation, suggesting that this enzyme is a key factor in this process. In fact, knockdown of the *pemt* gene resulted in impaired adipocyte differentiation, as seen by a reduced expression of adipogenic markers, as well as reduced lipid droplet formation, triglyceride content and leptin release. The data presented in this thesis, together with work from other labs, suggest that PEMT is important in obesity. PEMT deficiency was found to be protective against insulin resistance in mice [33-35], and it was observed that in human obese subjects the *pemt* gene was upregulated [36]. In particular, in *in vitro* experiments PEMT was shown to be important in lipid droplet formation and processing, and that it is actively involved in maintaining a stable lipid droplet phenotype in adipocytes [32].

This work also identifies the regulatory function of PEMT in adipocyte differentiation by modulating the post translational phosphorylation of extracellularly-regulated kinases (ERK) and AKT (also known as protein kinase B, PKB). Previous studies from our lab and others suggested a role of MAPKs in adipogenesis. However, the data seemed to be contradictory, as both ERK activation and inhibition were suggested to be important for regulation of adipogenesis. In particular, our laboratory showed that soon after the induction of cell differentiation ERK was activated by phosphorylation after 1 to 4 h, and then that activation was suppressed and remained low until the end of the adipogenic process [30]. Thus, the function of ERK in adipogenesis is thought to be timely regulated: early on, ERK had to be turned on for a proliferative step and to initiate adipocytes into the differentiation process, whilst later, ERK had to be shut-off to let the cells differentiate. In this work, we show that ERK is under regulation by PEMT, as knockdown of this enzyme increased ERK

phosphorylation, which would delay cell differentiation. Our data are in agreement with the fact that adipocyte differentiation requires, at the beginning, a precise proliferative step (mitotic clonal expansion, MCE), which takes place post-confluency. MCE is initiated by adipogenic stimuli, such as insulin, which are known to activate the ERK pathway [38]. Then, during terminal differentiation, adipocyte markers begin to be expressed, when ERK activity is returned to a low level.

AKT has also been shown to have a fundamental role in adipocyte differentiation. It was demonstrated that mouse embryonic fibroblast (MEFs) lacking AKT failed to differentiate into mature adipocytes [39], and AKT silencing was found to block differentiation of 3T3-L1 cells [40]. Moreover, the overexpression of constitutively active AKT in 3T3-L1 adipocytes was found to promote adipocyte differentiation [41]. It is known AKT phosphorylates and regulates a large variety of substrates involved in different biological processes [42], many of which could contribute to the role of AKT in driving adipocyte differentiation. Of importance, we show in this work that during adipogenesis AKT activation was suppressed and remained low until the end of the adipogenic process, and that knocking down PEMT resulted in sustained activation of AKT (and also ERK) leading to impaired expression of adipocyte-specific markers, such as PPAR-ɣ, adiponectin and perilipin 1, thus, blocking adipogenesis. According to our results, it can be hypothesized that like for ERK, both AKT early activation followed by late inhibition may be important steps for regulation of adipogenesis.

Another relevant finding in this thesis is the possible link between PEMT expression and C1P action. Our group recently showed that administration of exogenous C1P to cells that are undergoing adipocyte differentiation caused a significant reduction in the levels of TG, which was concomitant with a significant decrease in leptin concentration, pointing to a possible anti-adipogenic and anti-inflammatory action of exogenous C1P [30]. Here, we demonstrate that at least part of the mechanism by which C1P causes the repression of adipogenesis involves downregulation of PEMT. In fact, the enhancement and maintenance of high levels of ERK1-2 phosphorylation by C1P observed in our previous work correlates with our new findings showing that ERK is regulated by PEMT expression.

It can be concluded that PEMT is a novel regulator of adipogenesis with potential implications in obesity and that targeting *pemt* may result useful in the treatment of obesity-associated disorders.

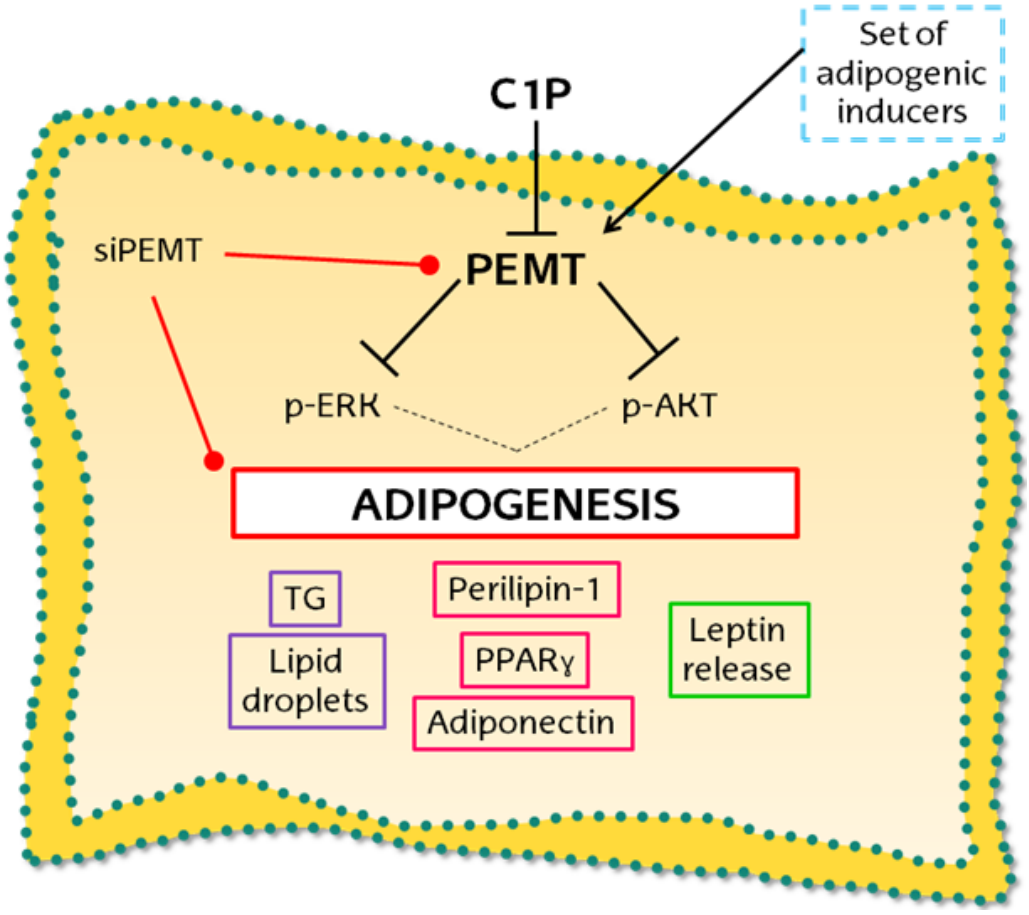

Figure 14: Working model for the role of PEMT in the adipogenic process.

4. REFERENCES

[1] M.I. Lefterova, M.A. Lazar, New developments in adipogenesis, Trends Endocrinol Metab 20 (3) (2009) 107-114.

[2] V.G. Athyros, K. Tziomalos, A. Karagiannis, P. Anagnostis, D.P. Mikhailidis, Should adipokines be considered in the choice of the treatment of obesity-related health problems?, Curr Drug Targets 11 (1) (2010) 122-135.

[3] J.A. Dorresteijn, F.L. Visseren, W. Spiering, Mechanisms linking obesity to hypertension, Obes Rev 13 (1) (2012) 17-26.

[4] R. Franssen, H. Monajemi, E.S. Stroes, J.J. Kastelein, Obesity and dyslipidemia, Med Clin North Am 95 (5) (2011) 893-902.

[5] S.E. Kahn, R.L. Hull, K.M. Utzschneider, Mechanisms linking obesity to insulin resistance and type 2 diabetes, Nature 444 (7121) (2006) 840-846.

[6] M.I. McCarthy, Genomics, type 2 diabetes, and obesity, N Engl J Med 363 (24) (2010) 2339-2350.

[7] A.W. Drong, C.M. Lindgren, M.I. McCarthy, The genetic and epigenetic basis of type 2 diabetes and obesity, Clin Pharmacol Ther 92 (6) (2012) 707-715.

[8] H.C. Masuoka, N. Chalasani, Nonalcoholic fatty liver disease: an emerging threat to obese and diabetic individuals, Ann N Y Acad Sci 1281 (2013) 106-122.

[9] E.K. Speliotes, Genetics of common obesity and nonalcoholic fatty liver disease, Gastroenterology 136 (5) (2009) 1492-1495.

[10] V.Z. Rocha, P. Libby, Obesity, inflammation, and atherosclerosis, Nat Rev Cardiol 6 (6) (2009) 399-409.

[11] G.K. Hansson, P. Libby, The immune response in atherosclerosis: a double-edged sword, Nat Rev Immunol 6 (7) (2006) 508-519.

[12] T. Tzotzas, P. Evangelou, D.N. Kiortsis, Obesity, weight loss and conditional cardiovascular risk factors, Obes Rev 12 (5) (2011) e282-289.

[13] C.M. Apovian, N. Gokce, Obesity and cardiovascular disease, Circulation 125 (9) (2012) 1178-1182.

[14] M.J. Khandekar, P. Cohen, B.M. Spiegelman, Molecular mechanisms of cancer development in obesity, Nat Rev Cancer 11 (12) (2011) 886-895.

[15] K. Basen-Engquist, M. Chang, Obesity and cancer risk: recent review and evidence, Curr Oncol Rep 13 (1) (2011) 71-76.

[16] S.D. Hursting, S.M. Dunlap, Obesity, metabolic dysregulation, and cancer: a growing concern and an inflammatory (and microenvironmental) issue, Ann N Y Acad Sci 1271 (2012) 82-87.

[17] C.A. Drevon, Fatty acids and expression of adipokines, Biochim Biophys Acta 1740 (2) (2005) 287-292.

[18] M. Giralt, R. Cereijo, F. Villarroya, Adipokines and the Endocrine Role of Adipose Tissues, Handb Exp Pharmacol 233 (2016) 265-282.

[19] P. Mancuso, The role of adipokines in chronic inflammation, Immunotargets Ther 5 (2016) 47-56.

[20] A. Guilherme, J.V. Virbasius, V. Puri, M.P. Czech, Adipocyte dysfunctions linking obesity to insulin resistance and type 2 diabetes, Nat Rev Mol Cell Biol 9 (5) (2008) 367-377.

[21] B.M. Spiegelman, C.A. Ginty, Fibronectin modulation of cell shape and lipogenic gene expression in 3T3-adipocytes, Cell 35 (3 Pt 2) (1983) 657-666.

[22] M. Ordonez, N. Presa, M. Trueba, A. Gomez-Munoz, Implication of Ceramide Kinase in Adipogenesis, Mediators Inflamm 2017 (2017) 9374563.

[23] K. Zebisch, V. Voigt, M. Wabitsch, M. Brandsch, Protocol for effective differentiation of 3T3-L1 cells to adipocytes, Anal Biochem 425 (1) (2012) 88-90.

[24] A.K. Student, R.Y. Hsu, M.D. Lane, Induction of fatty acid synthetase synthesis in differentiating 3T3-L1 preadipocytes, J Biol Chem 255 (10) (1980) 4745-4750.

[25] D.P. Ramji, P. Foka, CCAAT/enhancer-binding proteins: structure, function and regulation, Biochem J 365 (Pt 3) (2002) 561-575.

[26] P.J. Larsen, N. Tennagels, On ceramides, other sphingolipids and impaired glucose homeostasis, Mol Metab 3 (3) (2014) 252-260.

[27] M.H. Moon, J.K. Jeong, S.Y. Park, Activation of S1P2 receptor, a possible mechanism of inhibition of adipogenic differentiation by sphingosine 1phosphate, Mol Med Rep 11 (2) (2015) 1031-1036.

[28] K.M. Choi, Y.S. Lee, M.H. Choi, D.M. Sin, S. Lee, S.Y. Ji, M.K. Lee, Y.M. Lee, Y.P. Yun, J.T. Hong, H.S. Yoo, Inverse relationship between adipocyte differentiation and ceramide level in 3T3-L1 cells, Biol Pharm Bull 34 (6) (2011) 912-916.

[29] S. Mitsutake, T. Date, H. Yokota, M. Sugiura, T. Kohama, Y. Igarashi, Ceramide kinase deficiency improves diet-induced obesity and insulin resistance, FEBS Lett 586 (9) (2012) 1300-1305.

[30] M. Ordonez, N. Presa, A. Dominguez-Herrera, M. Trueba, A. Gomez-Munoz, Regulation of adipogenesis by ceramide 1-phosphate, Exp Cell Res 372 (2) (2018) 150-157.

[31] D.E. Vance, Physiological roles of phosphatidylethanolamine N-methyltransferase, Biochim Biophys Acta 1831 (3) (2013) 626-632.

[32] G. Horl, A. Wagner, L.K. Cole, R. Malli, H. Reicher, P. Kotzbeck, H. Kofeler, G. Hofler, S. Frank, J.G. Bogner-Strauss, W. Sattler, D.E. Vance, E. Steyrer, Sequential synthesis and methylation of phosphatidylethanolamine promote lipid droplet biosynthesis and stability in tissue culture and in vivo, J Biol Chem 286 (19) (2011) 17338-17350.

[33] R.L. Jacobs, Y. Zhao, D.P. Koonen, T. Sletten, B. Su, S. Lingrell, G. Cao, D.A. Peake, M.S. Kuo, S.D. Proctor, B.P. Kennedy, J.R. Dyck, D.E. Vance, Impaired de novo choline synthesis explains why phosphatidylethanolamine N-methyltransferase-deficient mice are protected from diet-induced obesity, J Biol Chem 285 (29) (2010) 22403-22413.

[34] A.A. Noga, Y. Zhao, D.E. Vance, An unexpected requirement for phosphatidylethanolamine N-methyltransferase in the secretion of very low density lipoproteins, J Biol Chem 277 (44) (2002) 42358-42365.

[35] X. Gao, J.N. van der Veen, M. Hermansson, M. Ordonez, A. Gomez-Munoz, D.E. Vance, R.L. Jacobs, Decreased lipogenesis in white adipose tissue contributes to the resistance to high fat diet-induced obesity in phosphatidylethanolamine N-methyltransferase-deficient mice, Biochim Biophys Acta 1851 (2) (2015) 152-162.

[36] N.K. Sharma, K.A. Langberg, A.K. Mondal, S.K. Das, Phospholipid biosynthesis genes and susceptibility to obesity: analysis of expression and polymorphisms, PLoS One 8 (5) (2013) e65303.

[37] Q.Q. Tang, T.C. Otto, M.D. Lane, Mitotic clonal expansion: a synchronous process required for adipogenesis, Proc Natl Acad Sci U S A 100 (1) (2003) 44-49.

[38] F. Bost, M. Aouadi, L. Caron, B. Binetruy, The role of MAPKs in adipocyte differentiation and obesity, Biochimie 87 (1) (2005) 51-56.

[39] A. Baudry, Z.Z. Yang, B.A. Hemmings, PKBalpha is required for adipose differentiation of mouse embryonic fibroblasts, J Cell Sci 119 (Pt 5) (2006) 889-897.

[40] H.H. Zhang, J. Huang, K. Duvel, B. Boback, S. Wu, R.M. Squillace, C.L. Wu, B.D. Manning, Insulin stimulates adipogenesis through the Akt-TSC2-mTORC1 pathway, PLoS One 4 (7) (2009) e6189.

[41] J. Xu, K. Liao, Protein kinase B/AKT 1 plays a pivotal role in insulin-like growth factor-1 receptor signaling induced 3T3-L1 adipocyte differentiation, J Biol Chem 279 (34) (2004) 35914-35922.

[42] C.J. Green, O. Goransson, G.S. Kular, N.R. Leslie, A. Gray, D.R. Alessi, K. Sakamoto, H.S. Hundal, Use of Akt inhibitor and a drug-resistant mutant validates a critical role for protein kinase B/Akt in the insulin-dependent regulation of glucose and system A amino acid uptake, J Biol Chem 283 (41) (2008) 27653-27667.

Chapter 3

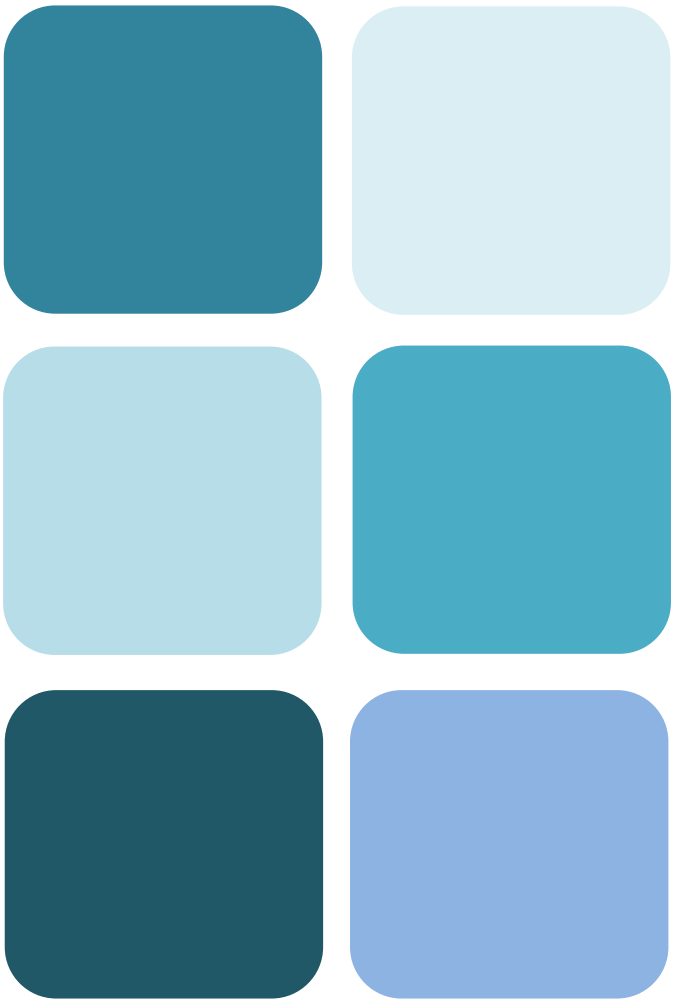

CHAPTER 3:
Implication of sphingolipid metabolites in non-alcoholic fatty liver disease in phosphatidylethanolamine *N*-methyltransferase deficient mice. Role of Vitamin E.

1. INTRODUCTION

1.1. Non-alcoholic fatty liver disease (NAFLD)

Non-alcoholic fatty liver disease (NAFLD) is increasingly recognized as the liver component of metabolic syndrome. According to recent data, it is estimated that approximately 25% of the adult population in developed countries suffers from this disease [1]. NAFLD is defined as the presence of more than 5% fat in the liver without any other liver disease etiologies and/or use of medication, and it includes a histological range from simple steatosis or fat accumulation to non-alcoholic steatohepatitis (NASH), in which along with fat there is inflammation and damage to liver tissue, and which can further progress to cirrhosis and liver cancer [2].

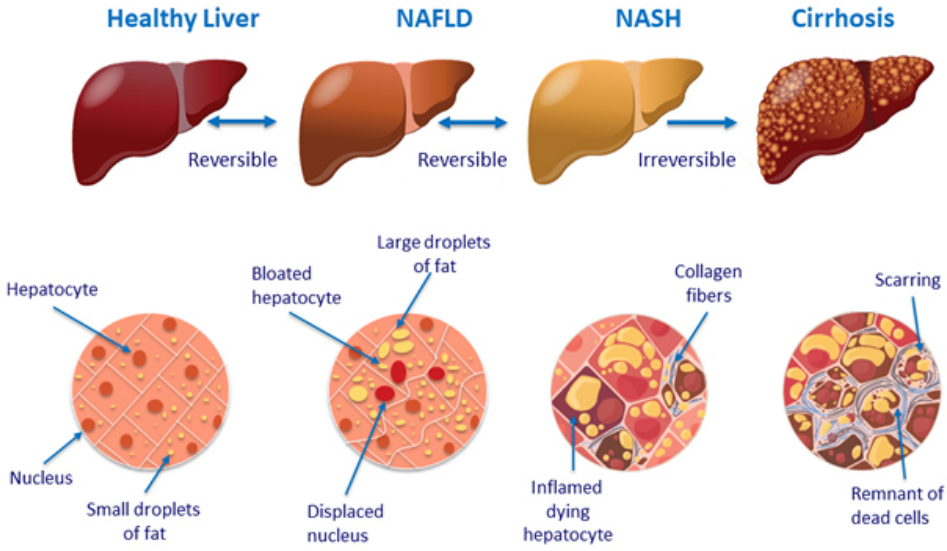

Figure 1: Progression of NAFLD. Taken from *HCV-trials* website.

NAFLD is linked to a low molar ratio of hepatic phosphatidylcholine (PC) to phosphatidylethanolamine (PE) [3-5]. PC and PE are the two main phospholipids in plasma membranes of all mammalian cells. In mice, around 70% of hepatic PC is produced via the CDP-choline pathway and the other 30% via phosphatidylethanolamine *N*-methyltransferase (PEMT) pathway, by which PE is converted to PC via three sequential methylation reactions.

1.2. The role of PEMT in NAFLD development

PEMT is important for the biosynthesis of PC in the liver, which is the quantitatively major phospholipid of hepatic endoplasmic reticulum (ER) membranes and plasma lipoproteins. PC species derived from either the CDP-choline pathway or the PEMT pathway are crucial for the assembly and secretion of very low-density lipoprotein (VLDL) particles, as deletion of either pathway results in a strong reduction of VLDL secretion [6-9]. In order to determine whether PEMT has functions other than regulation of PC biosynthesis in mammals, *Pemt*$^{-/-}$ mice were constructed [10]. The availability of this new animal model allowed to determine the implication of this enzyme in NAFLD, obesity and inflammation.

In particular, mice lacking PEMT are protected from high-fat diet (HFD)-induced obesity and insulin resistance, but develop severe NAFLD when fed a HFD. However, the molecular mechanisms implicated in these pathologies are not well understood. It has been suggested that reduced very low-density lipoprotein (VLDL) secretion is a relevant factor for development of NAFLD [8, 11, 12], but there will most likely be other mechanisms involved. In this connection, sphingolipid metabolism has been associated with the establishment and progression of NAFLD. Specifically, a major sphingolipid metabolite implicated in NAFLD is ceramide [13-16].

1.3. Ceramide metabolism in NAFLD

One of the lipid classes that have been associated with the development of NAFLD and NASH is sphingolipids and it is unknown whether sphingolipid metabolism is affected by PEMT-deficiency. Sphingolipids belong to a class of membrane lipids that play a fundamental role in membrane architecture and the regulation of key physiologic processes. Among the sphingolipid family, ceramides have been linked to cell death, insulin resistance, oxidative stress, and inflammatory processes [17-23] suggesting that ceramides may play an important role in development of fatty liver

disease [13-15]. Ceramides have been demonstrated to act on the mitochondrial electron transport chain leading to hydrogen peroxide and reactive oxygen species (ROS) generation, thereby inducing oxidative stress and promoting inflammation in different biological systems [20, 24-26]. However, whether sphingolipid metabolism might have any association with PEMT has not been investigated. Moreover, although some reports suggest a link between ceramides and NAFLD or NASH, the mechanisms involved are incompletely understood.

1.4. Vitamin E

Vitamin E (α-tocopherol) is a lipid-soluble chain breaking molecule that defends cells against radical-induced damage [27]. Vitamin E is absorbed in the intestine, transported in plasma mainly with apolipoprotein B-containing chylomicrons, and transferred to parenchymal cells in the liver. Subsequently, vitamin E is secreted from the liver, mainly in association with VLDL, in order to be distributed to other tissues [28].

Currently, there is no definitive treatment for NALFD, mainly because the precise mechanism underlying the disease and its progression is still poorly understood. Although it has been previously demonstrated that livers from HFD-fed *Pemt*$^{-/-}$ mice exhibit increased oxidative stress [9], its importance in the development of NASH has not been established.

The aim of the present study was to investigate whether supplementation of the diet with vitamin E could attenuate HFD-induced NASH in *Pemt*$^{-/-}$ mice, and whether aberrant sphingolipid metabolism is involved in the disease progression in this model.

2. RESULTS

2.1. Vitamin E supplementation reduced liver weight and improved hepatic lipid secretion in *Pemt*$^{-/-}$ mice

Recent reports have indicated that vitamin E supplementation can attenuate hepatic steatosis [28-30]. Therefore, we fed *Pemt*$^{+/+}$ and *Pemt*$^{-/-}$ mice a HFD or a HFD supplemented with 0.5g/kg vitamin E for 3 weeks to determine whether it could prevent fatty liver development in *Pemt*$^{-/-}$ mice. HFD-feeding for 3 weeks caused *Pemt*$^{-/-}$ mice to develop severe NASH [31], so this condition was sufficient to investigate the effect of vitamin E on NASH development in these mice. In addition, the concentration

of vitamin E used in the experiments results in an approximate dose of 133 IU/kg/day, which is equivalent to the recommended dose for human vitamin E supplements.

To verify that vitamin E supplementation was sufficiently absorbed, we measured vitamin E concentration in the liver, where it is stored. As shown in figure 2, vitamin E concentrations were strongly increased in livers of supplemented animals. It is noteworthy that the accumulation of vitamin E was significantly higher in *Pemt*$^{-/-}$ mice compared to *Pemt*$^{+/+}$ mice. Vitamin E is a hydrophobic molecule that is stored in lipid droplets, and it is secreted from the liver as a component of VLDL particles. The higher vitamin E concentrations in supplemented *Pemt*$^{-/-}$ mice are, thus, probably due to impaired VLDL secretion and subsequent higher hepatic lipid content in these mice.

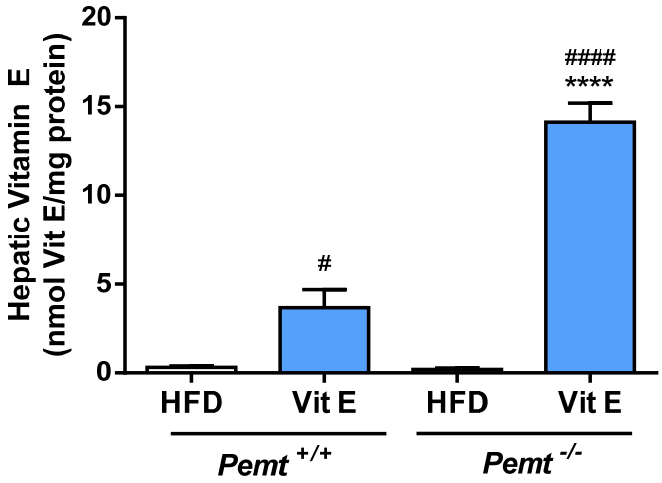

Figure 2: Vitamin E is efficiently stored in livers. After 3-week treatment with or without vitamin E, livers from *Pemt*$^{+/+}$ and *Pemt*$^{-/-}$ mice were collected and hepatic vitamin E levels were quantified by HPLC, as described previously [32], and normalized to total protein. All values are the means ± SEM (*n=5* per group). *Difference between genotypes; #difference between treatments. ($p < 0.05$).

Once proven that vitamin E treatment had worked, we analyzed livers from *Pemt*$^{+/+}$ and *Pemt*$^{-/-}$ mice after 3 weeks feeding with the HFD with or without vitamin E supplementation and found that livers from PEMT deficient animals were larger than those from *Pemt* wild type ones. Even though the liver weights did not decrease with vitamin E supplementation, body weights were normalized to *Pemt*$^{+/+}$ values, resulting in a decrease in relative liver weight upon vitamin E.

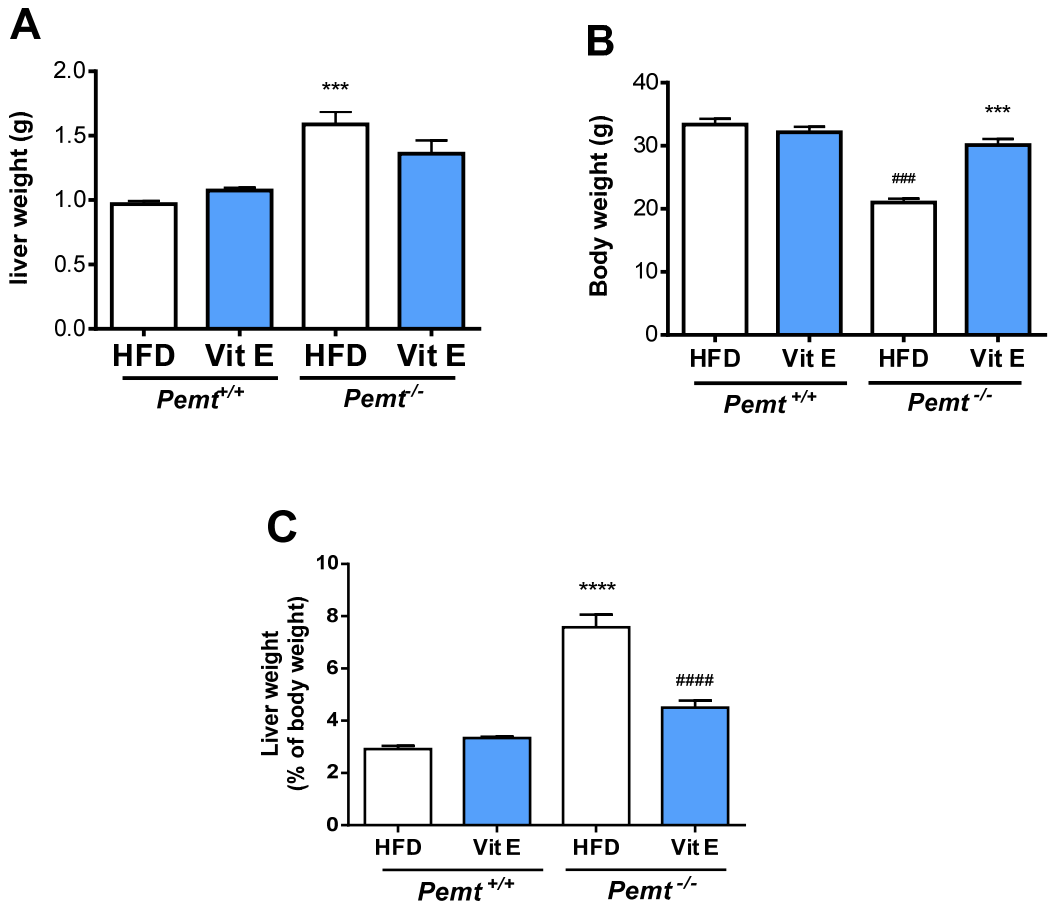

Figure 3: Vitamin E supplementation reduced liver weight in *Pemt*$^{-/-}$ mice. After 3-week treatment with or without vitamin E, each animal and livers were weighted. A) Liver weight; B) total body weight; C) liver weight relative to total body weight. All values are the means ± SEM (*n=5* per group). *Difference between genotypes; #difference between treatments. ($p< 0.05$).

As mentioned before, fatty liver is defined as the presence of more than 5% fat in the liver. Thus, we measured hepatic triglyceride content in livers from *Pemt*$^{+/+}$ and *Pemt*$^{-/-}$ mice on a HFD or HFD supplemented with vitamin E. Figure 4 shows that hepatic TG levels were 2.5-fold higher in *Pemt*$^{-/-}$ mice compared to *Pemt*$^{+/+}$ mice, and vitamin E treatment seemed to be accompanied by a slight reduction in TG concentration; however this observation did not reach statistical significance.

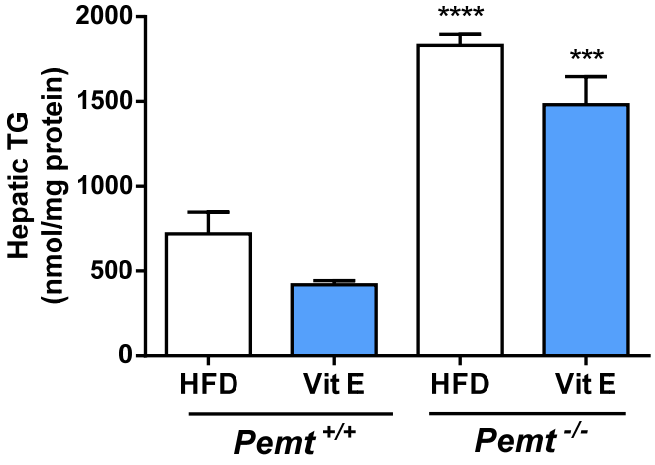

Figure 4: Vitamin E supplementation did not significantly reduce hepatic TG levels in *Pemt*$^{-/-}$ mice. After 3-week treatment with or without vitamin E, livers from *Pemt*$^{+/+}$ and *Pemt*$^{-/-}$ mice were collected and TG levels were analyzed, as described in *Materials and Methods*. Results are expressed relative to total protein content in the samples. All values are the means ± SEM (*n=5* per group). *Difference between genotypes. ($p < 0.05$).

Although we did not observe statistically significant differences in hepatic TG levels, hematoxylin-eosin staining showed large lipid droplets in liver samples of *Pemt*$^{-/-}$ mice and, even though there was a similar lipid accumulation in vitamin E treated livers, the lipid droplets appeared to be smaller after treatment with vitamin E (figure 5). This suggests that the same amount of neutral lipids is stored in a larger number of lipid droplets, which likely allow the lipids to be more accessible to fatty acid oxidation.

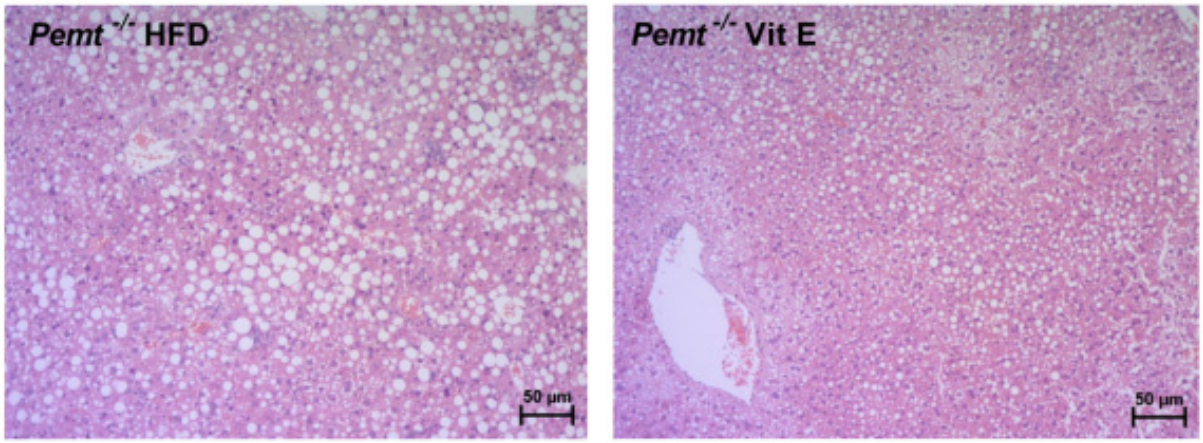

Figure 5: Hematoxylin-eosin staining in liver samples from *Pemt*$^{-/-}$ mice with or without vitamin E treatment. After 3-week treatment with or without vitamin E, livers from *Pemt*$^{-/-}$ mice were collected and stained with hematoxylin-eosin, as described in *Materials and Methods*.

Representative pictures of hematoxylin-eosin staining of liver samples from untreated and vitamin E supplemented *Pemt*$^{-/-}$ mice.

Since NALFD is linked to a low molar ratio of hepatic phosphatidylcholine (PC) to phosphatidylethanolamine (PE) [3-5], we tested to evaluate what happened with those two phospholipids after 3-week feeding with a HFD with or without vitamin E supplementation. Figure 6 shows that, although not statistically significant, hepatic PC was slightly reduced and, conversely, hepatic PE levels were increased in *Pemt*$^{-/-}$ mice. Hence, the PC:PE ratio was slightly lower in *Pemt*$^{-/-}$ mice. However, vitamin E supplementation did not change PC:PE ratio in either genotype.

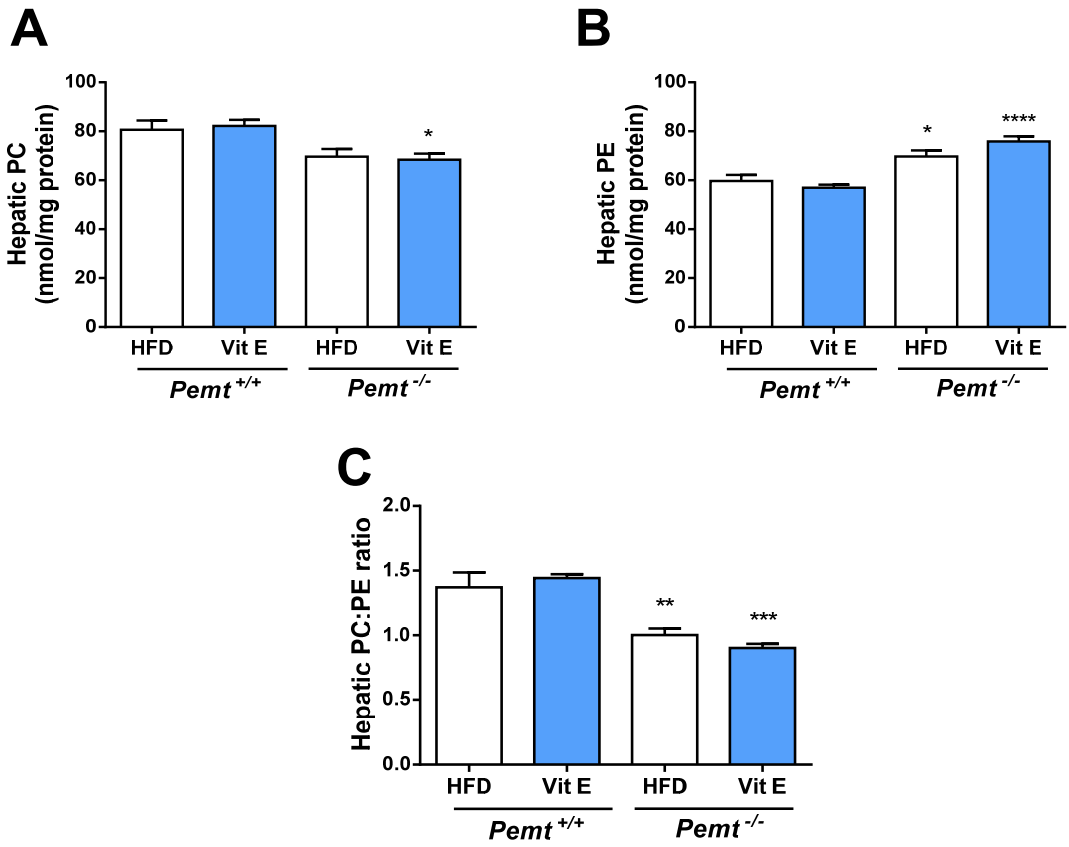

Figure 6: Vitamin E supplementation did not alter hepatic lipid profile. After 3-week treatment with or without vitamin E, livers from *Pemt*$^{+/+}$ and *Pemt*$^{-/-}$ mice were collected and PC and PE levels were determined, as described in *Materials and Methods*. A) Hepatic PC content in livers from *Pemt*$^{+/+}$ and *Pemt*$^{-/-}$ mice fed a HFD or a HFD supplemented with vitamin E. B) Hepatic PE content in livers from *Pemt*$^{+/+}$ and *Pemt*$^{-/-}$ mice fed a HFD or a HFD supplemented with vitamin E. C) PC:PE ratio in livers from *Pemt*$^{+/+}$ and *Pemt*$^{-/-}$ mice fed a HFD or a HFD supplemented with vitamin E. All values are the means ± SEM (*n=5* per group). *Difference between genotypes. ($p < 0.05$).

Even though hepatic TG concentration was not reduced by vitamin E supplementation, vitamin E was able to increase VLDL-TG secretion in *Pemt*$^{-/-}$ animals compared to those without supplementation, as demonstrated by plasma TG quantification after the inhibition of lipoprotein lipase (LPL) by Poloxamer 407 (figure 7). However, VLDL-TG secretion rates and fasting plasma TG levels were still lower in vitamin E-supplemented *Pemt*$^{-/-}$ mice compared to *Pemt*$^{+/+}$ mice.

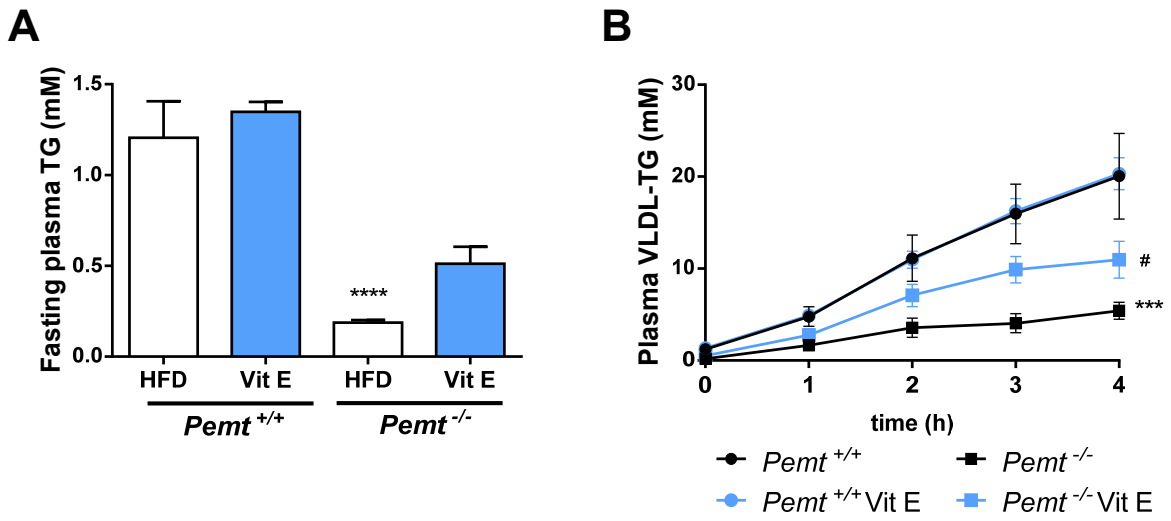

Figure 7: Vitamin E supplementation improves hepatic VLDL secretion in *Pemt*$^{-/-}$ mice. After 3-week treatment with or without vitamin E, plasma was collected and plasma TG levels were measured, as described in *Materials and Methods*. A) Plasma TG concentration in fasting conditions in *Pemt*$^{+/+}$ and *Pemt*$^{-/-}$ mice fed a HFD ± vitamin E. B) TG secretion curves after Poloxamer 407 injection. All values are the means ± SEM (*n=5* per group). *Difference between genotypes; #difference between treatments. ($p < 0.05$).

We then measured plasma ApoB-100 and ApoB-48 levels and observed no difference between the groups, indicating poorly lipidated VLDL particles, rather than fewer VLDL particles, in *Pemt*$^{-/-}$ mice. Vitamin E did not affect ApoB-100 or ApoB-48 in either genotype. Nonetheless, the observation of no changes in ApoB levels combined with an increase in VLDL-TG production suggest that vitamin E supplementation improved the lipidation of VLDL particles in *Pemt*$^{-/-}$ mice (figure 8).

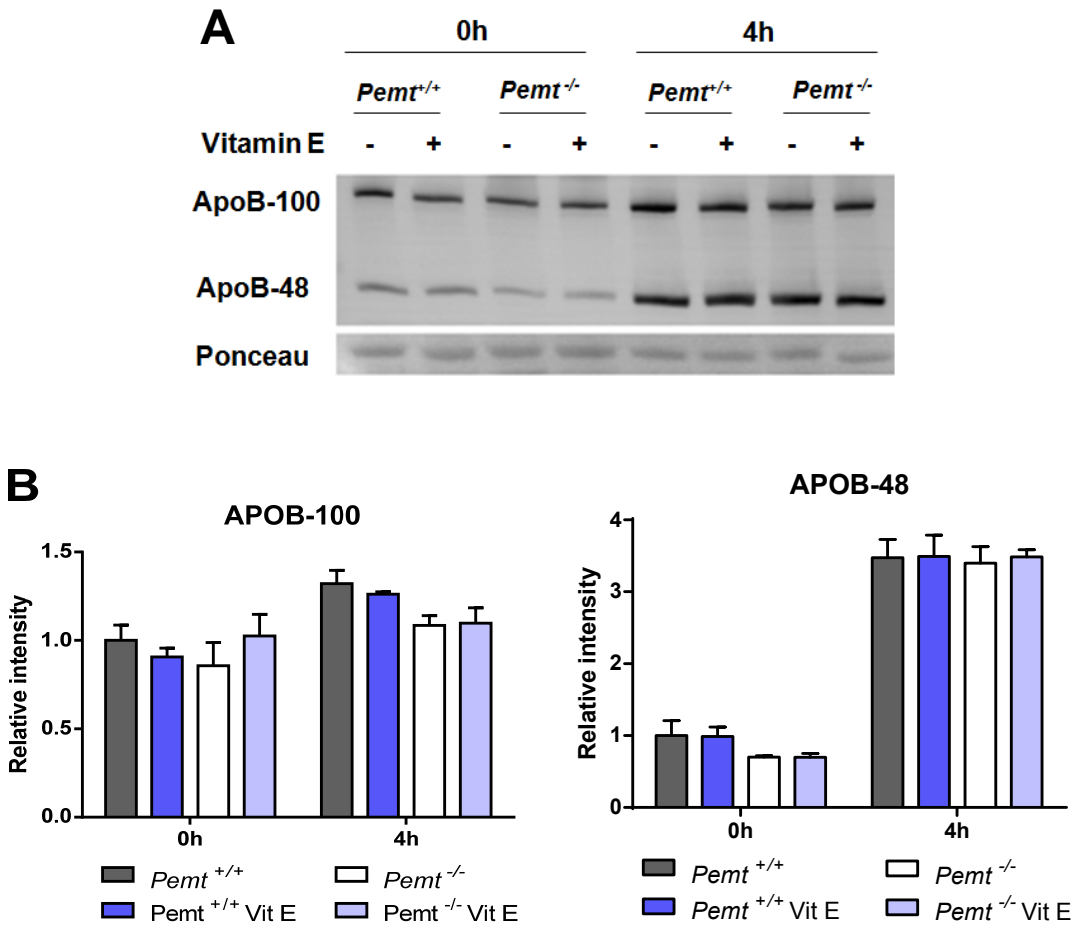

Figure 8. Vitamin E does not increase plasma ApoB levels. A) Inmunoblot of ApoB in plasma in fasting conditions and 4 hours after Poloxamer 407 injection. Ponceau staining was used as loading control. B) Quantification of A. All values are means ± SEM (*n*=4 per group).

We next measured plasma high-density lipoprotein (HDL) levels and interestingly, they were also reduced in HFD-fed *Pemt*$^{-/-}$ animals, as indicated by strongly reduced plasma total cholesterol and ApoA1 levels (Fig. 9). Vitamin E supplementation almost normalized HDL levels in *Pemt*$^{-/-}$ mice.

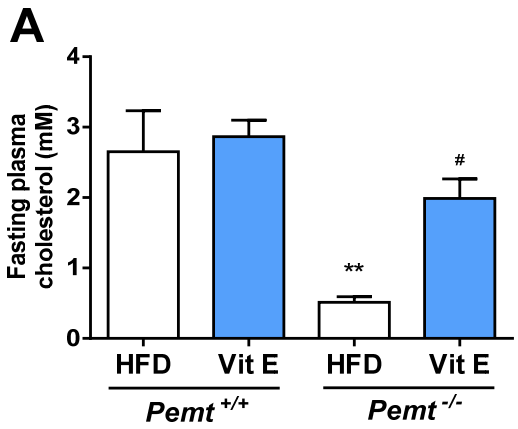

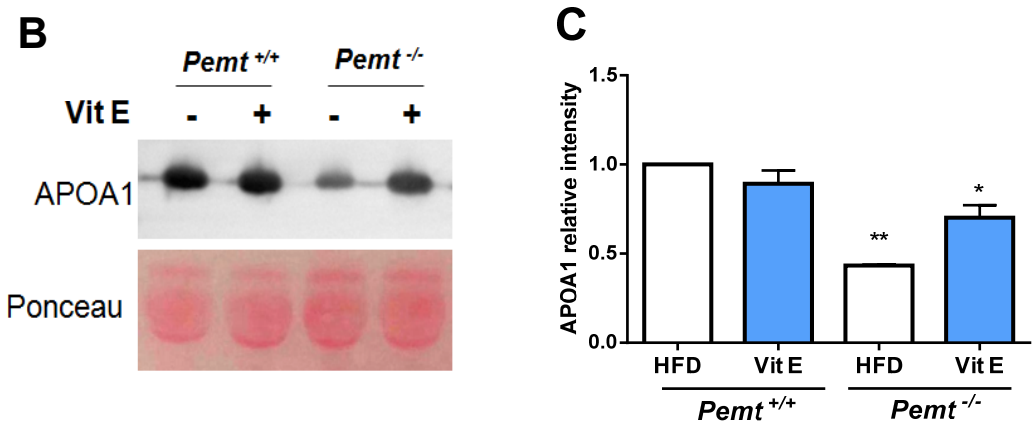

Figure 9: Vitamin E supplementation normalizes plasma HDL levels in *Pemt*$^{-/-}$ mice. After 3 weeks on a HFD with or without vitamin E, plasma was collected and cholesterol levels were measured as described in *Materials and Methods*. A) Plasma total cholesterol concentrations in fasting conditions in *Pemt*$^{+/+}$ and *Pemt*$^{-/-}$ mice fed a HFD ± vitamin E. B) Inmunoblot for APOA1 in plasma samples. Ponceau staining was used as a loading control. C) Quantification of A relative to control. All values are means ± SEM (*n=5* per group for A, *n=4* per group for B and C). *Difference between genotypes; #difference between treatments. ($p< 0.05$).

To determine whether the low plasma concentrations of HDL-cholesterol were due to increased hepatic uptake of the cholesterol-loaded high density lipoprotein, we measured the expression of hepatic SR-B1 (scavenger receptor, class B type 1), which is a multiligand membrane receptor protein that functions as a physiologically relevant HDL receptor, whose primary role is to mediate selective uptake or influx of HDL-derived cholesteryl esters into cells and tissues. Surprisingly, there was a reduction of hepatic SR-B1 levels in *Pemt*$^{-/-}$ mice, suggesting that low HDL-cholesterol levels were, at least in part, likely due to reduced hepatic production of HDL particles rather than increased uptake of HDL-cholesterol into the liver. The reduction in SR-B1 levels in *Pemt*$^{-/-}$ mice was completely restored when supplemented with vitamin E (Fig. 10).

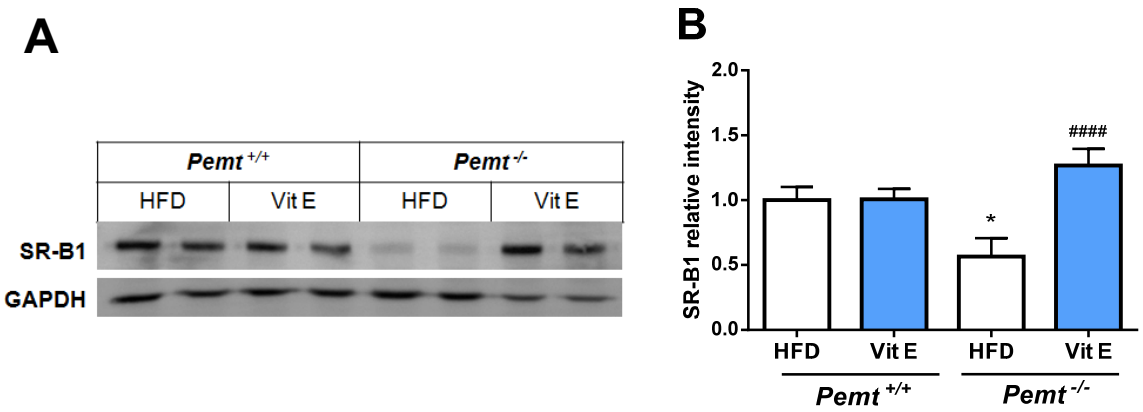

Figure 10: Vitamin E supplementation normalizes hepatic SR-B1 levels in *Pemt*$^{-/-}$ mice. After 3 weeks on a HFD with or without vitamin E, livers from all groups of animals were collected and homogenates were made as described in *Materials and Methods*. A) Inmunoblot of SR-B1 in liver samples . B) Quantification of A relative to control. All values are means ± SEM (*n*=4 per group). *Difference between genotypes; #difference between treatments. ($p < 0.05$).

2.2. Vitamin E treatment prevented hepatic oxidative stress in *Pemt*$^{-/-}$ mice

Since vitamin E is an antioxidant and oxidative stress is an important trigger for the development of NASH [33, 34], we determined the levels of oxidative stress in all groups of animals. Hepatic lipid peroxidation, an indicative of oxidative stress in liver [4, 35], was 4-fold higher in *Pemt*$^{-/-}$ mice compared to *Pemt*$^{+/+}$ mice, as indicated by higher amounts of thiobarbituric acid reactive substances (TBARS). Vitamin E supplementation completely normalized TBARS values to the levels observed in *Pemt*$^{+/+}$ mice (Fig. 11).

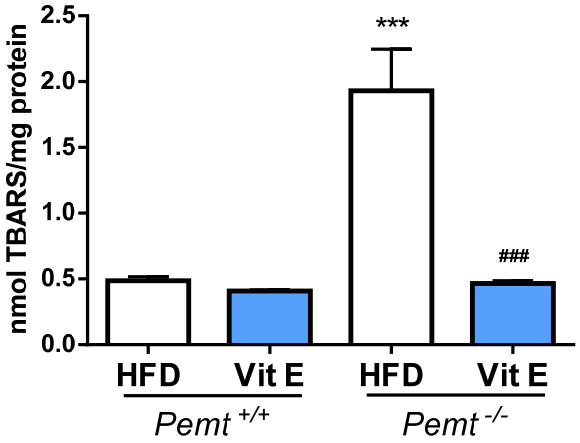

Figure 11: Vitamin E normalizes hepatic lipid peroxidation levels in *Pemt*$^{-/-}$ mice. After 3-week treatment on a HFD with or without vitamin E, hepatic concentration of thiobarbituric acid-reactive substances (TBARS), a marker of lipid peroxidation, were measured, as described in *Materials and Methods*. All values are the means ± SEM (*n=5* per group). *Difference between genotypes; #difference between treatments. ($p < 0.05$).

Similarly, the ratio of oxidized (GSSG) and reduced (GSH) glutathione (GSSH/GSH) was increased in HFD-fed *Pemt*$^{-/-}$ mice compared to *Pemt*$^{+/+}$ mice, and this increase was completely prevented by vitamin E supplementation.

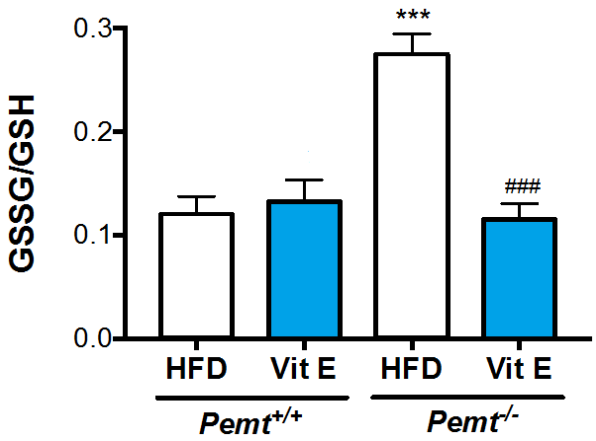

Figure 12: Vitamin E normalizes hepatic glutathione status in *Pemt*$^{-/-}$ mice. After 3-week treatment on a HFD with or without vitamin E, hepatic glutathione status was analyzed as a marker for oxidative stress, as described in *Materials and Methods*. All values are the means ± SEM (*n=5* per group). *Difference between genotypes; #difference between treatments. ($p < 0.05$).

We next sought to determine the mRNA levels of genes related to oxidative stress. We measured NADPH oxidase 2 (*Nox2*), heme oxygenase 1(*Hmox1*), and mitochondrial uncoupling protein 2 (*Ucp2*) mRNA levels. As it can be observed in figure 13, all mRNA levels were 2.5 to 4-fold increased in *Pemt*$^{-/-}$ mice samples, and they all were reduced by vitamin E.

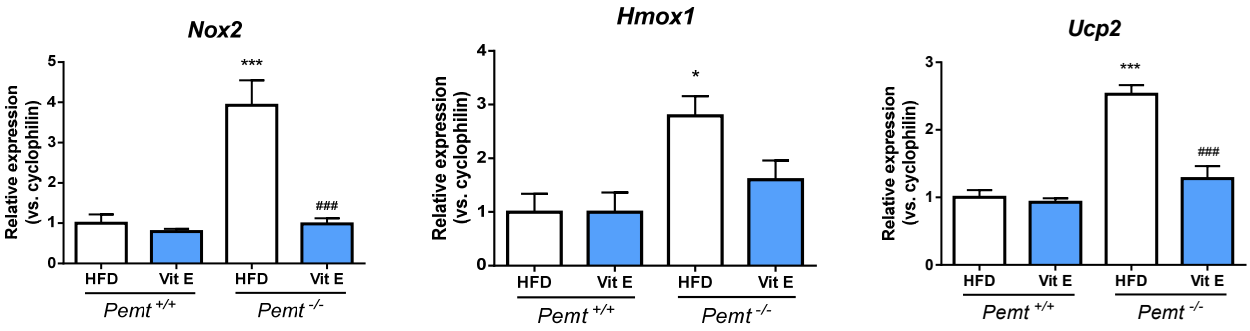

Figure 13: Vitamin E supplementation reduced oxidative stress-related gene expression in *Pemt*$^{-/-}$ mice. After 3-week treatment on a HFD with or without vitamin E hepatic expression of oxidative stress-related genes was analyzed by qPCR as described in *Materials and Methods*. mRNA levels for oxidative stress-related genes NADPH oxidase 2 (*Nox2*), Heme oxygenase 1 (*Hmox1*); and mitochondrial uncoupling protein 2 (*Ucp2*) relative to cyclophylin expression and normalized to corresponding control group. All values are the means ± SEM (*n=5* per group). *Difference between genotypes; #difference between treatments. ($p < 0.05$).

We next tested to evaluate whether the oxidative stress in *Pemt*$^{-/-}$ mice would lead to endoplasmic reticulum (ER) stress in these mice. Protein levels of CCAAT-enhancer-binding protein homologous protein (CHOP) and Binding immunoglobulin protein (BiP), and protein disulfide-isomerase (PDI), all markers of ER stress, were all elevated in livers from HFD-fed *Pemt*$^{-/-}$ mice compared to *Pemt*$^{+/+}$ mice. Dietary supplementation with vitamin E prevented the induction of these proteins, as the protein levels in vitamin E-treated Pemt-/- mice were indistinguishable from the Pemt+ /$^{+}$ controls (Fig 14). Together, this suggests that oxidative stress resulted in ER stress in livers of *Pemt*$^{-/-}$ mice, and that treatment with vitamin E prevented oxidative stress, thereby alleviating ER stress.

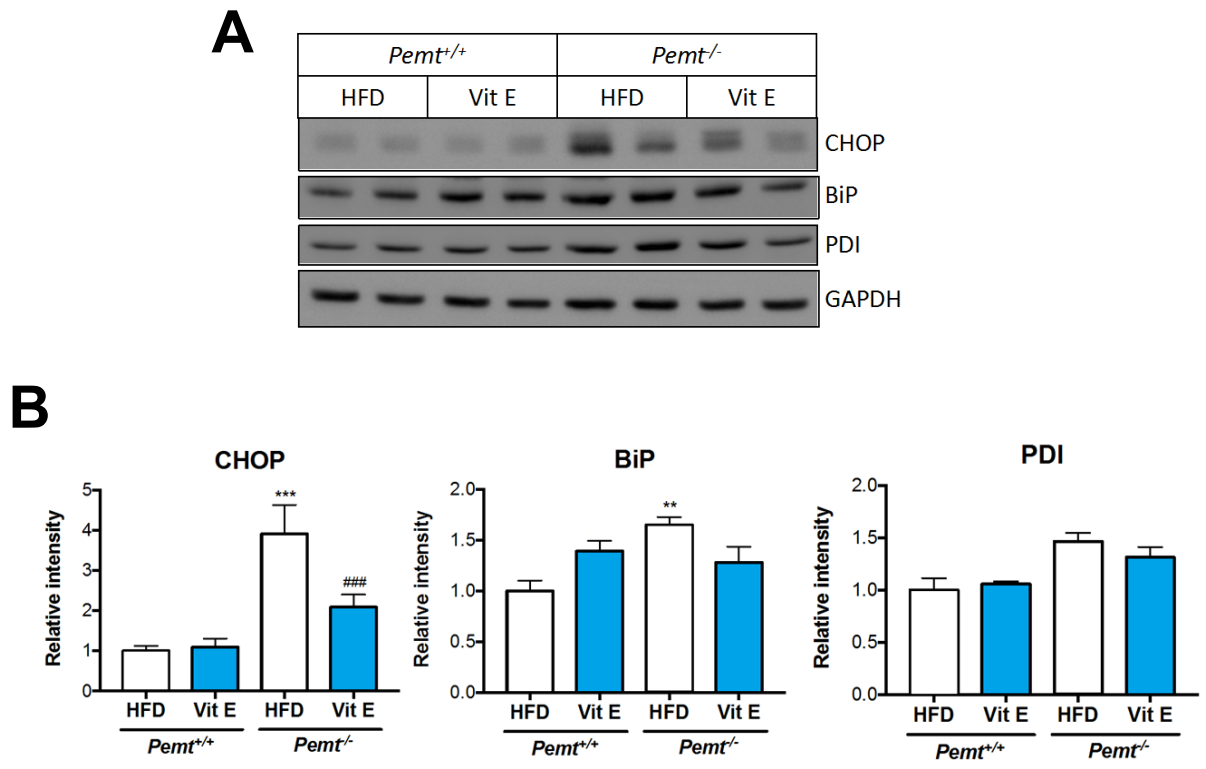

Figure 14: Vitamin E supplementation reduced oxidative stress-related protein expression in *Pemt*$^{-/-}$ mice. After 3-week treatment on a HFD with or without vitamin E, hepatic expression levels of ER stress-related proteins were analyzed by western blot, as described in *Materials and Methods*. A) Immunoblot of proteins involved in ER stress CCAAT-enhancer-binding protein homologous protein (CHOP), binding immunoglobulin protein (BiP), and protein disulfide-isomerase (PDI). GAPDH was used as a loading control. B) Quantification of A relative to the amount of loading control and normalized to the corresponding control group. All values are the means ± SEM (n=4 per group). *Difference between genotypes; #difference between treatments. (P< 0.05).

2.3. Vitamin E treatment prevented hepatic inflammation and fibrosis in *Pemt*$^{-/-}$ mice

Two important hallmarks of NASH are inflammation and fibrosis development. Therefore, we sought to evaluate the effect of vitamin E supplementation on these two processes. We first measured mRNA levels of genes *Cd68* (macrophage marker) *and Tnf-α* (inflammatory cytokine), both indicators of inflammation. Both markers were more than 5-fold increased in *Pemt*$^{-/-}$ mice fed a HFD, indicating increased number of macrophages in the liver. Vitamin E supplementation completely prevented the increase in *Cd68* and *Tnf-α* expression, indicating reduced infiltration of macrophages in the liver under this condition.

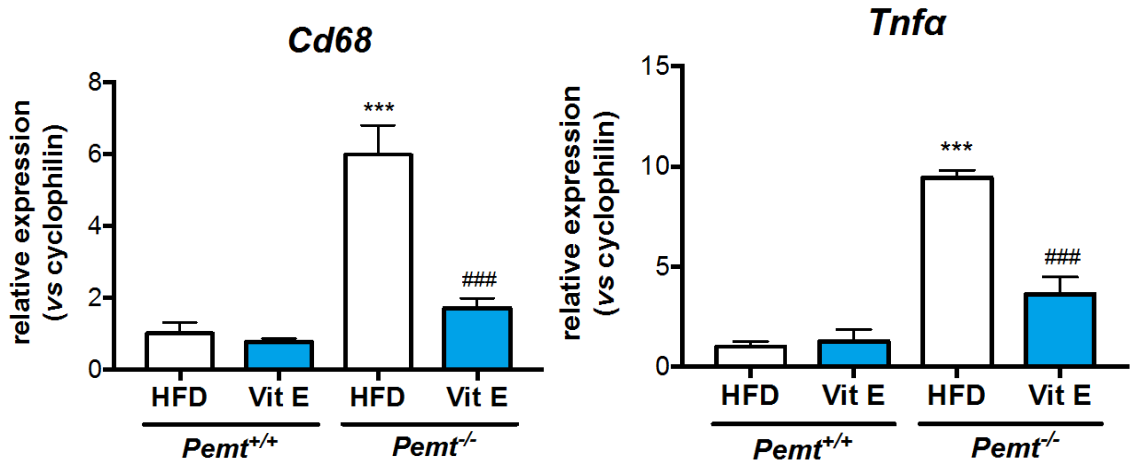

Figure 15: Vitamin E supplementation prevented hepatic inflammation in *Pemt*$^{-/-}$ mice. After 3-week treatment on a HFD with or without vitamin E, hepatic expression of inflammation-related genes was analyzed by qPCR as described in *Materials and Methods*. mRNA levels for *Cd68* and *Tnf-α* relative to cyclophilin expression and normalized to the corresponding control group. All values are the means ± SEM (*n=5* per group). *Difference between genotypes; #difference between treatments. ($p < 0.05$).

Since both oxidative stress and inflammatory cytokines can activate hepatic stellate cells, we investigated whether vitamin E supplementation could prevent the development of hepatic fibrosis in *Pemt*$^{-/-}$ mice. mRNA levels of alpha-1 type I collagen (*Col1a1*), responsible for collagen synthesis, as well as those of tissue inhibitor of metalloproteinase 1 (*Timp1*) were strongly increased in HFD-fed *Pemt*$^{-/-}$ mice and this increase was partially prevented by vitamin E supplementation.

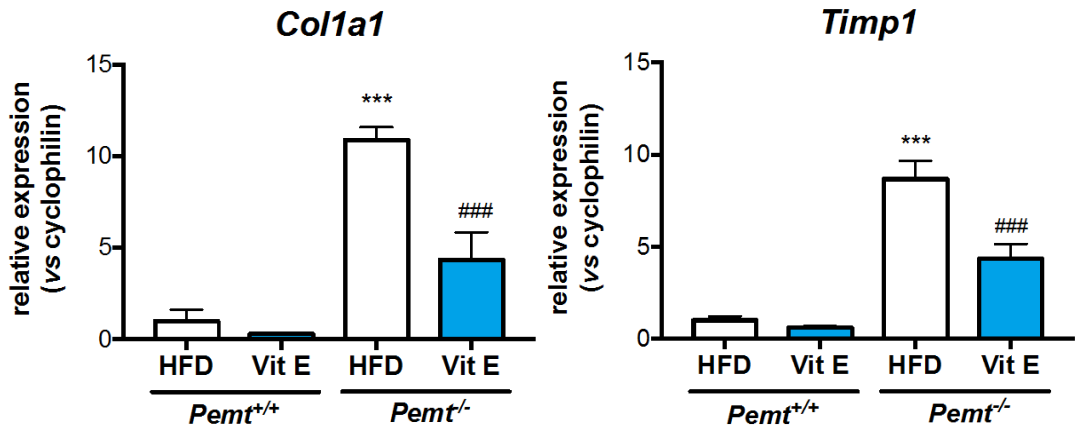

Figure 16: Vitamin E supplementation prevented hepatic fibrosis in *Pemt*$^{-/-}$ mice. After 3-week treatment on a HFD with or without vitamin E, hepatic expression of fibrosis-related genes was analyzed by qPCR as described in *Materials and Methods*. mRNA levels for Col1a1 and Timp1 relative to cyclophilin expression and normalized to the corresponding control group. All values are the means ± SEM (*n=5* per group). *Difference between genotypes; #difference between treatments. ($p < 0.05$).

Moreover, Picro-Sirius Red staining confirmed that the amount of fibrillar collagen was lower when *Pemt*$^{-/-}$ mice were fed the vitamin E-supplemented diet. Together these data indicated a protective role of vitamin E in development of NASH.

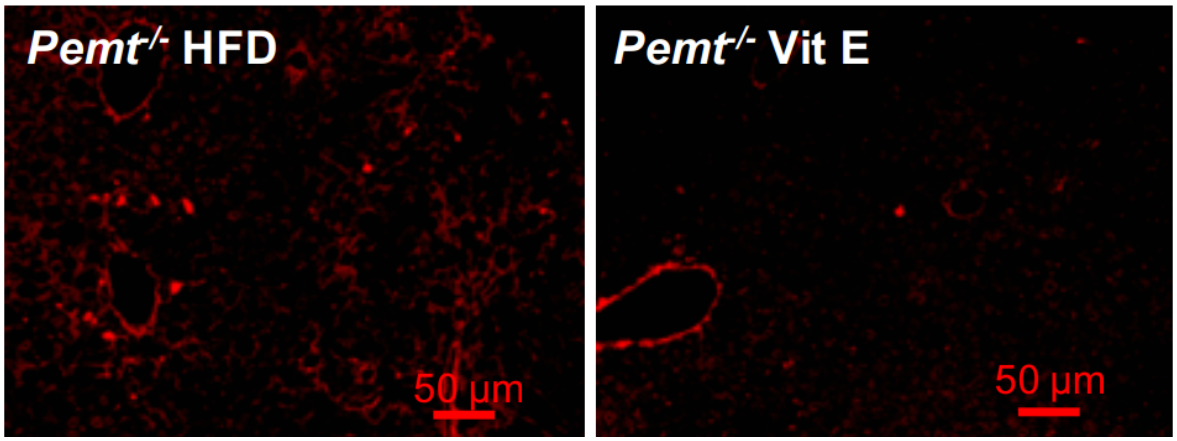

Figure 17: Vitamin E supplementation prevented hepatic fibrosis in *Pemt*$^{-/-}$ mice. After 3-week treatment on a HFD with or without vitamin E, hepatic liver samples were stained with Picro-Sirius Red, as described in *Materials and Methods*. Histological assessment of hepatic fibrosis untreated and vitamin E- supplemented *Pemt*$^{-/-}$ mice.

2.4. Ceramide metabolism is normalized in *Pemt*$^{-/-}$ mice treated with vitamin E

Due to the increasingly recognized role of ceramides and their derivatives in the development of NAFLD [13-16], we investigated ceramide metabolism in 3-week HFD-fed *Pemt*$^{-/-}$ mice that developed NASH, and determined whether vitamin E could influence the master enzymes of the different routes for ceramide synthesis and/or breakdown.

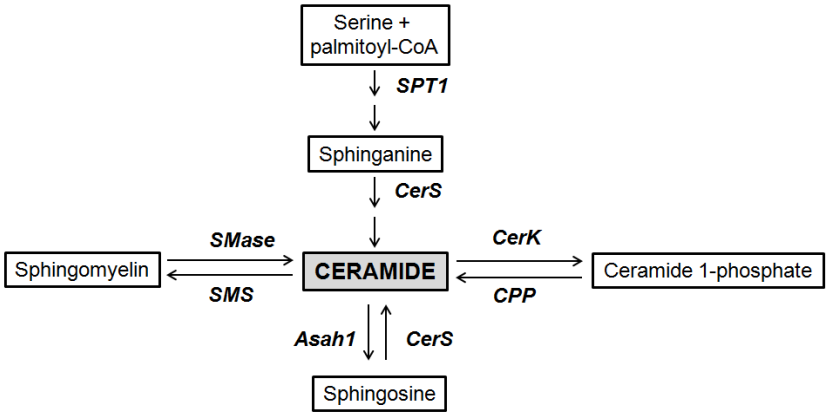

Figure 18: Schematic representation of ceramide biosynthesis pathways.

As it can be observed in figure 19, there were no changes in the mRNA levels of serine palmitoyltransferase 1 (*Spt1*), which is the rate limiting enzyme for *de novo* synthesis of ceramide, ceramide synthase 2 and 6 (*CerS2-CerS6*), which are also important regulatory enzymes in the *de novo* biosynthetic pathway of ceramides and also participate in the salvage pathway of ceramide synthesis. However, there was a slight reduction in acidic sphingomyelinase (*ASMase*) in *Pemt*$^{-/-}$ mice, which could not be reversed with vitamin E treatment. In addition, we observed that acidic ceramidase (*Asah1*), the enzyme that degrades ceramides to sphingosine, and ceramide kinase (*CerK*), the enzyme that phosphorylates ceramides to produce C1P, mRNA levels were 1.5-and 2.5-fold higher, respectively, in *Pemt*$^{-/-}$ mice, and vitamin E supplementation normalized those levels to control *Pemt*$^{+/+}$ values.

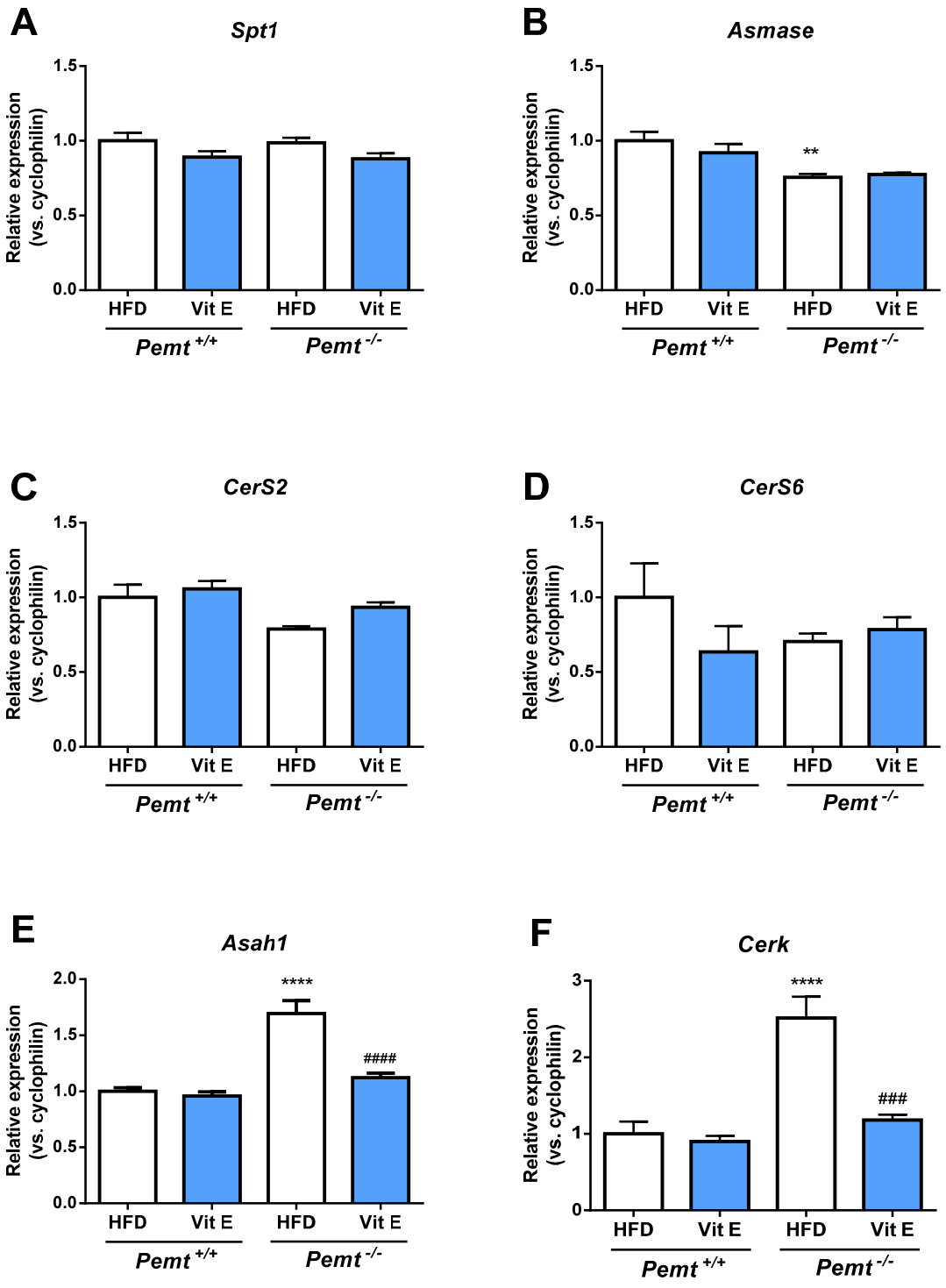

Figure 19: Ceramide metabolism master enzyme expression was normalized with vitamin E supplementation. mRNA levels after 3-week treatment on a HFD with or without vitamin E supplementation relative to cyclophilin expression of: A) *de novo* ceramide synthesis pathway enzyme SPT1 (serine palmitoyltransferase subunit 1), *C* and *D: salvage* and *de novo* synthesis pathway enzymes CERS2, CERS6 (ceramide synthase 2 and 6), *E:* SMase synthesis pathway enzyme ASMase (acid sphingomyelinase), *F:* ASAH1 (acidic ceramidase), and *G:* Ceramide 1-

phosphate converting enzyme CerK (ceramide kinase). All values are means ± SEM (n=5 per group). *Difference between genotypes; #difference between treatments. (p< 0.05).

Mass-spectrometry analysis revealed that ceramide levels were indeed elevated in livers from *Pemt*$^{-/-}$ mice, and they were reduced upon vitamin E supplementation in these mice. Similarly, sphingomyelin, sphinganine, and sphingosine were also increased in *Pemt*$^{-/-}$ mice, and vitamin E supplementation normalized them all to control levels. Interestingly, the concentration of 1-deoxy-ceramides, which are one of the most correlated biomarkers for the progression of NASH [16], were also strongly increased in *Pemt*$^{-/-}$ mice compared to *Pemt*$^{+/+}$ mice and treatment with vitamin E reduced those levels by more than 50%. By contrast, mass-spectrometry analysis did not show any significant differences in total ceramide 1-phosphate (C1P) levels or in the individual species of C1P (C16:0, C24:1, C26:0), although there was a mild increase in C26:1 C1P, but this was not significantly reduced upon vitamin E supplementation.

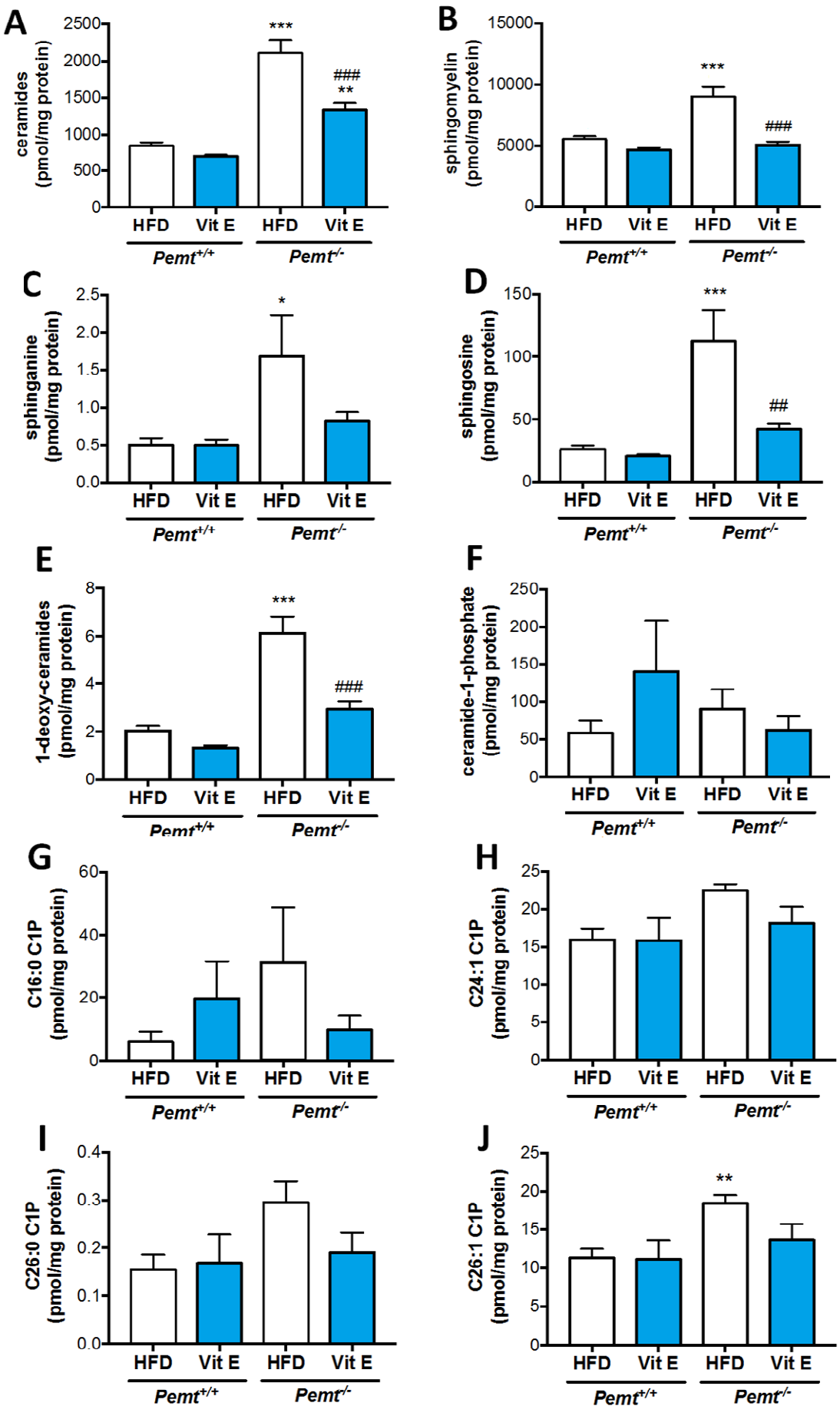
A
ceramides (pmol/mg protein)
2500
2000
1500
1000
500
0
***
###
**
HFD
Vit E
HFD
Vit E
Pemt+/+
Pemt-/-
B
sphingomyelin (pmol/mg protein)
15000
10000
5000
0
***
###
HFD
Vit E
HFD
Vit E
Pemt+/+
Pemt-/-
C
sphinganine (pmol/mg protein)
2.5
2.0
1.5
1.0
0.5
0.0
*
HFD
Vit E
HFD
Vit E
Pemt+/+
Pemt-/-
D
sphingosine (pmol/mg protein)
150
100
50
0
***
##
HFD
Vit E
HFD
Vit E
Pemt+/+
Pemt-/-
E
1-deoxy-ceramides (pmol/mg protein)
8
6
4
2
0
***
###
HFD
Vit E
HFD
Vit E
Pemt+/+
Pemt-/-
F
ceramide-1-phosphate (pmol/mg protein)
250
200
150
100
50
0
HFD
Vit E
HFD
Vit E
Pemt+/+
Pemt-/-
G
C16:0 C1P (pmol/mg protein)
60
40
20
0
HFD
Vit E
HFD
Vit E
Pemt+/+
Pemt-/-
H
C24:1 C1P (pmol/mg protein)
25
20
15
10
5
0
HFD
Vit E
HFD
Vit E
Pemt+/+
Pemt-/-
I
C26:0 C1P (pmol/mg protein)
0.4
0.3
0.2
0.1
0.0
HFD
Vit E
HFD
Vit E
Pemt+/+
Pemt-/-
J
C26:1 C1P (pmol/mg protein)
25
20
15
10
5
0
**
HFD
Vit E
HFD
Vit E
Pemt+/+
Pemt-/-

Figure 20: Ceramide metabolism is normalized in *Pemt*$^{-/-}$ mice treated with vitamin E. Quantification by mass-spectrometry of *A*: total ceramides; *B*: total sphingomyelin; *C*: total sphinganine; *D*: total sphingosine; *E*: total 1-deoxyceramides; *F*: total ceramide 1-phosphate; *G-I*: ceramide 1-phosphate species (C16:0, C24:1, C26:0, C26:1), in liver samples from *Pemt*$^{+/+}$ and *Pemt*$^{-/-}$ mice fed a HFD or a HFD supplemented with vitamin E. All values are means ± SEM (*n*=5 per group). *Difference between genotypes; #difference between treatments. ($p < 0.05$).

3. DISCUSSION

Although the mechanisms responsible for NAFLD development and progression are still poorly understood, oxidative stress could be the 'second hit' triggering the transition from steatosis to steatohepatitis, and promoting hepatic damage, inflammation and fibrosis [36, 37]. We investigated whether vitamin E could prevent the development of NASH in a mouse model of reduced PC synthesis. In summary, we observed improved VLDL-TG secretion from the liver, and normalization of cholesterol metabolism, but no reduction in hepatic TG upon vitamin E supplementation in HFD-fed *Pemt*$^{-/-}$ mice. Nevertheless, vitamin E supplementation efficiently prevented hepatic oxidative stress, inflammation and fibrosis. Moreover, we observed aberrant ceramide metabolism in *Pemt*$^{-/-}$ mice and this was restored with vitamin E supplementation. Thus, vitamin E supplementation prevented the progression from simple steatosis to steatohepatitis in mice lacking PEMT.

Previous studies in animals with fatty liver disease have demonstrated a beneficial effect of vitamin E on liver health. In mice fed a methionine- and choline-deficient diet, vitamin E treatment ameliorated steatosis, oxidative stress, hepatic apoptosis, inflammation and fibrosis [38, 39]. In obese (*ob/ob*) mice, treatment with α- or γ-tocopherol prevented lipopolysaccharide-induced NASH, but not steatosis [40], which is similar to what we observed in *Pemt*$^{-/-}$ mice. Furthermore, the progression on NAFLD caused by partial hepatectomy was also attenuated by vitamin E treatment [29]. In contrast to the studies with experimental animals, the benefits of vitamin E in humans have been less clearly delineated. Two large randomized clinical trials have been conducted to evaluate the efficacy of vitamin E to ameliorate NASH. The Pioglitazone versus Vitamin E versus Placebo for the treatment of non-diabetic Patients with Non-alcoholic Steatohepatitis (PIVENS) study investigated the effect of vitamin E (800 IU/day) in non-diabetic, non-cirrhotic adults with NASH [41]. Vitamin E compared to placebo significantly improved NASH, as it reduced steatosis, inflammation, and hepatocellular ballooning, but not fibrosis. This outcome in humans is somewhat different from our data in *Pemt*$^{-/-}$ mice, where vitamin E did reduce fibrosis, but not steatosis. The Treatment of NAFLD in Children (TONIC) study investigated vitamin E in children with NASH [42]. Resolution of NASH was significantly higher in vitamin E versus the placebo treatment group, due to reduced hepatocellular ballooning. However, vitamin E did not reduce steatosis, inflammation or fibrosis in this study. Although vitamin E seems effective in improving NASH in non-diabetic subjects, there

have not been clinical trials carried out in diabetic subjects. Considering that up to 75% of people with NASH also suffer from type 2 diabetes, this is an area that needs to be addressed.

Our study provides insights in the mechanism by which vitamin E ameliorates NASH, which might result in better-designed interventions for NASH in humans.

Oxidative stress occurs when there is an imbalance between reactive oxygen species production and antioxidant defenses. In the liver, increased oxidative stress and chronic inflammation are considered key features for the progression from simple hepatic steatosis to steatohepatitis or NASH. Several studies show a connection between the severity of NASH and the degree of oxidative stress [33, 34, 43, 44]. During hepatic steatosis, there is an increased influx of fatty acids derived from the circulation and/or from *de novo* lipogenesis, often in combination with reduced fatty acid oxidation. In NAFLD patients, mitochondrial respiratory chain complexes are often decreased, resulting in an increased production of reactive oxygen species (ROS) [45, 46]. In addition, NASH patients exhibit insufficient antioxidant defenses, such as GSH, superoxide dismutase and catalase, resulting in oxidative stress in the liver [34, 47]. Increased ROS can cause cellular damage and detrimental responses in several cell types of the liver. For instance, in Kupffer cells, oxidative stress can induce the production of cytokines, including TNF-α, TGF-β, FAS-ligand and IL-8 [48]. ROS exposure can also activate hepatic stellate cells and induce proliferation and collagen synthesis [49]. Thus, oxidative stress can cause apoptosis, inflammation and fibrosis in the liver and thereby progress from simple steatosis into NASH. The main triggers of these cellular responses are products of ROS-induced lipid peroxidation. Due to its hydrophobic nature, vitamin E is especially effective at stopping the chain reaction of lipid peroxidation. We have demonstrated here that HFD-fed *Pemt*$^{-/-}$ mice indeed exhibit increased lipid peroxidation, which could be the trigger to the development of NASH in these mice. Dietary vitamin E supplementation completely prevented lipid peroxidation. By preventing this type of oxidative stress, vitamin E likely prevented the activation of both Kupffer cells and stellate cells, thereby preventing the development of inflammation and fibrosis in livers of *Pemt*$^{-/-}$ mice.

In the past decades ceramides have emerged as intracellular signaling molecules involved in the regulation of differentiation, proliferation, and apoptosis. Recently, ceramides have also been linked to fatty liver disease development, as they can act as key lipid mediators of insulin resistance, oxidative stress, and inflammation in different

organs [13-17, 23]. In response to inflammatory signals, such as TNF-α or IL-1β, ceramide formation and release from membrane sphingomyelin is increased [24, 50]. In addition, ceramide levels can promote ROS production in the mitochondria by interfering with the electron transport chain [20, 24-26]. This increase in oxidative stress stress can then again lead to progression from NAFLD to NASH. Thus, ceramides seem to be part of a perpetual cycle in which ROS-induced cytokine production causes ceramide levels to increase, which in turn exacerbates oxidative stress and inflammation. Hence, we sought to determine whether ceramide metabolism was altered in HFD-induced NAFLD in *Pemt* $^{-/-}$ mice, and whether vitamin E could influence ceramide metabolism or ceramide-mediated events. We observed marked accumulation of ceramides in the livers of *Pemt*$^{-/-}$ mice, but no increases in the mRNA levels of the enzymes involved in ceramide synthesis (*Spt1*, *Cers2*, *Cers6* or *Asmase*). Nevertheless, inflammatory cytokines may have induced the activity of these enzymes, rather than transcription, resulting in elevated ceramide formation. Besides, given that liver is a key site for ceramide synthesis, that up to 80% of plasma ceramides are associated with VLDL/LDL particles [51, 52], and that VLDL secretion from liver is impaired in HFD-induced NAFLD in *Pemt*$^{-/-}$ mice, the majority of hepatic ceramides is likely accumulating due to impaired secretion from the liver. Interestingly, *Cerk*, the enzyme that catalyzes the production of anti-apoptotic ceramide 1-phosphate from ceramide, and *Asah1*, an enzyme that degrades ceramides to sphingosine, which has opposing effects to ceramides in some cell types [53, 54] were both overexpressed in *Pemt*$^{-/-}$ animals fed a HFD. The induction of *Cerk* and *Asah1* expression could serve to reduce ceramide levels within the cell in an attempt to limit the detrimental accumulation of ceramides in the liver. VLDL-TG secretion was partially restored in *Pemt*$^{-/-}$ mice upon vitamin E supplementation, which could be linked to the prevention of ER stress in these mice. As a result of the increase in VLDL production, ceramides would also be secreted from the liver at a higher rate. Together with the possibly reduced cytokine-mediated release of ceramides from the plasma membrane, this prevented the accumulation of ceramides and other sphingolipids in hepatocytes and normalized *Cerk* and *Asah1* expression, since their induction would no longer be needed.

Interestingly, hepatic TG concentrations in *Pemt*$^{-/-}$ mice were not lowered upon vitamin E supplementation. Even though VLDL-TG secretion in *Pemt*$^{-/-}$ mice was increased by vitamin E supplementation, it was still strongly impaired compared to *Pemt*$^{+/+}$ mice. The lipid droplets in vitamin E-supplemented *Pemt*$^{-/-}$ livers were

remarkably smaller but more abundant. Smaller lipid droplets would render the lipids more metabolically accessible and thereby also contribute to improved liver health.

It can be concluded that sphingolipid metabolism is impaired in *Pemt*$^{-/-}$ mice fed a HFD showing very high levels of ceramides, which are associated with hepatic inflammation and development of NAFLD and NASH. Through the prevention of oxidative stress, dietary vitamin E supplementation reduced hepatic inflammation and fibrosis, and it restored aberrant ceramide metabolism in this mouse model of impaired PC synthesis. Dietary vitamin E supplementation could thus be a viable therapeutic option in the continuously growing population of patients with hepatic steatosis to prevent the progression into the more detrimental stages of NAFLD. Hence, the data presented in this thesis support the therapeutic potential of vitamin E in the treatment of NASH.

4. REFERENCES

[1] Z.M. Younossi, A.B. Koenig, D. Abdelatif, Y. Fazel, L. Henry, M. Wymer, Global epidemiology of nonalcoholic fatty liver disease-Meta-analytic assessment of prevalence, incidence, and outcomes, Hepatology 64 (1) (2016) 73-84.

[2] G.C. Farrell, C.Z. Larter, Nonalcoholic fatty liver disease: from steatosis to cirrhosis, Hepatology 43 (2 Suppl 1) (2006) S99-S112.

[3] J.N. van der Veen, J.P. Kennelly, S. Wan, J.E. Vance, D.E. Vance, R.L. Jacobs, The critical role of phosphatidylcholine and phosphatidylethanolamine metabolism in health and disease, Biochim Biophys Acta 1859 (9 Pt B) (2017) 1558-1572.

[4] Z. Li, L.B. Agellon, T.M. Allen, M. Umeda, L. Jewell, A. Mason, D.E. Vance, The ratio of phosphatidylcholine to phosphatidylethanolamine influences membrane integrity and steatohepatitis, Cell Metab 3 (5) (2006) 321-331.

[5] K.K. Kharbanda, M.E. Mailliard, C.R. Baldwin, H.C. Beckenhauer, M.F. Sorrell, D.J. Tuma, Betaine attenuates alcoholic steatosis by restoring phosphatidylcholine generation via the phosphatidylethanolamine methyltransferase pathway, J Hepatol 46 (2) (2007) 314-321.

[6] R.L. Jacobs, C. Devlin, I. Tabas, D.E. Vance, Targeted deletion of hepatic CTP:phosphocholine cytidylyltransferase alpha in mice decreases plasma high density and very low density lipoproteins, J Biol Chem 279 (45) (2004) 47402-47410.

[7] R.L. Jacobs, S. Lingrell, Y. Zhao, G.A. Francis, D.E. Vance, Hepatic CTP:phosphocholine cytidylyltransferase-alpha is a critical predictor of plasma high density lipoprotein and very low density lipoprotein, J Biol Chem 283 (4) (2008) 2147-2155.

[8] A.A. Noga, Y. Zhao, D.E. Vance, An unexpected requirement for phosphatidylethanolamine N-methyltransferase in the secretion of very low density lipoproteins, J Biol Chem 277 (44) (2002) 42358-42365.

[9] J.N. van der Veen, S. Lingrell, X. Gao, A.D. Quiroga, A. Takawale, E.A. Armstrong, J.Y. Yager, Z. Kassiri, R. Lehner, D.E. Vance, R.L. Jacobs, Pioglitazone attenuates hepatic inflammation and fibrosis in phosphatidylethanolamine N-methyltransferase-deficient mice, Am J Physiol Gastrointest Liver Physiol 310 (7) (2016) G526-538.

[10] C.J. Walkey, L.R. Donohue, R. Bronson, L.B. Agellon, D.E. Vance, Disruption of the murine gene encoding phosphatidylethanolamine N-methyltransferase, Proc Natl Acad Sci U S A 94 (24) (1997) 12880-12885.

[11] R.L. Jacobs, Y. Zhao, D.P. Koonen, T. Sletten, B. Su, S. Lingrell, G. Cao, D.A. Peake, M.S. Kuo, S.D. Proctor, B.P. Kennedy, J.R. Dyck, D.E. Vance, Impaired de novo choline synthesis explains why phosphatidylethanolamine N-methyltransferase-deficient

mice are protected from diet-induced obesity, J Biol Chem 285 (29) (2010) 22403-22413.

[12] J.N. van der Veen, S. Lingrell, X. Gao, A. Takawale, Z. Kassiri, D.E. Vance, R.L. Jacobs, Fenofibrate, but not ezetimibe, prevents fatty liver disease in mice lacking phosphatidylethanolamine N-methyltransferase, J Lipid Res 58 (4) (2017) 656-667.

[13] M. Pagadala, T. Kasumov, A.J. McCullough, N.N. Zein, J.P. Kirwan, Role of ceramides in nonalcoholic fatty liver disease, Trends Endocrinol Metab 23 (8) (2012) 365-371.

[14] J.Y. Xia, W.L. Holland, C.M. Kusminski, K. Sun, A.X. Sharma, M.J. Pearson, A.J. Sifuentes, J.G. McDonald, R. Gordillo, P.E. Scherer, Targeted Induction of Ceramide Degradation Leads to Improved Systemic Metabolism and Reduced Hepatic Steatosis, Cell Metab 22 (2) (2015) 266-278.

[15] T. Kasumov, L. Li, M. Li, K. Gulshan, J.P. Kirwan, X. Liu, S. Previs, B. Willard, J.D. Smith, A. McCullough, Ceramide as a mediator of non-alcoholic Fatty liver disease and associated atherosclerosis, PLoS One 10 (5) (2015) e0126910.

[16] D.L. Gorden, D.S. Myers, P.T. Ivanova, E. Fahy, M.R. Maurya, S. Gupta, J. Min, N.J. Spann, J.G. McDonald, S.L. Kelly, J. Duan, M.C. Sullards, T.J. Leiker, R.M. Barkley, O. Quehenberger, A.M. Armando, S.B. Milne, T.P. Mathews, M.D. Armstrong, C. Li, W.V. Melvin, R.H. Clements, M.K. Washington, A.M. Mendonsa, J.L. Witztum, Z. Guan, C.K. Glass, R.C. Murphy, E.A. Dennis, A.H. Merrill, Jr., D.W. Russell, S. Subramaniam, H.A. Brown, Biomarkers of NAFLD progression: a lipidomics approach to an epidemic, J Lipid Res 56 (3) (2015) 722-736.

[17] J.A. Chavez, M.M. Siddique, S.T. Wang, J. Ching, J.A. Shayman, S.A. Summers, Ceramides and glucosylceramides are independent antagonists of insulin signaling, J Biol Chem 289 (2) (2014) 723-734.

[18] J.A. Chavez, S.A. Summers, A ceramide-centric view of insulin resistance, Cell Metab 15 (5) (2012) 585-594.

[19] B.T. Bikman, A role for sphingolipids in the pathophysiology of obesity-induced inflammation, Cell Mol Life Sci 69 (13) (2012) 2135-2146.

[20] B.T. Bikman, S.A. Summers, Ceramides as modulators of cellular and whole-body metabolism, J Clin Invest 121 (11) (2011) 4222-4230.

[21] M. Maceyka, S. Spiegel, Sphingolipid metabolites in inflammatory disease, Nature 510 (7503) (2014) 58-67.

[22] J.R. Zierath, The path to insulin resistance: paved with ceramides?, Cell Metab 5 (3) (2007) 161-163.

[23] W.L. Holland, J.T. Brozinick, L.P. Wang, E.D. Hawkins, K.M. Sargent, Y. Liu, K. Narra, K.L. Hoehn, T.A. Knotts, A. Siesky, D.H. Nelson, S.K. Karathanasis, G.K. Fontenot, M.J.

Birnbaum, S.A. Summers, Inhibition of ceramide synthesis ameliorates glucocorticoid-, saturated-fat-, and obesity-induced insulin resistance, Cell Metab 5 (3) (2007) 167-179.

[24] S. Corda, C. Laplace, E. Vicaut, J. Duranteau, Rapid reactive oxygen species production by mitochondria in endothelial cells exposed to tumor necrosis factor-alpha is mediated by ceramide, Am J Respir Cell Mol Biol 24 (6) (2001) 762-768.

[25] R. Fucho, N. Casals, D. Serra, L. Herrero, Ceramides and mitochondrial fatty acid oxidation in obesity, FASEB J 31 (4) (2017) 1263-1272.

[26] C. Garcia-Ruiz, A. Colell, M. Mari, A. Morales, J.C. Fernandez-Checa, Direct effect of ceramide on the mitochondrial electron transport chain leads to generation of reactive oxygen species. Role of mitochondrial glutathione, J Biol Chem 272 (17) (1997) 11369-11377.

[27] A. Azzi, R. Gysin, P. Kempna, A. Munteanu, L. Villacorta, T. Visarius, J.M. Zingg, Regulation of gene expression by alpha-tocopherol, Biol Chem 385 (7) (2004) 585-591.

[28] T. Pacana, A.J. Sanyal, Vitamin E and nonalcoholic fatty liver disease, Curr Opin Clin Nutr Metab Care 15 (6) (2012) 641-648.

[29] G. Karimian, M. Kirschbaum, Z.J. Veldhuis, F. Bomfati, R.J. Porte, T. Lisman, Vitamin E Attenuates the Progression of Non-Alcoholic Fatty Liver Disease Caused by Partial Hepatectomy in Mice, PLoS One 10 (11) (2015) e0143121.

[30] V. Nobili, M. Manco, R. Devito, P. Ciampalini, F. Piemonte, M. Marcellini, Effect of vitamin E on aminotransferase levels and insulin resistance in children with non-alcoholic fatty liver disease, Aliment Pharmacol Ther 24 (11-12) (2006) 1553-1561.

[31] J. Ling, T. Chaba, L.F. Zhu, R.L. Jacobs, D.E. Vance, Hepatic ratio of phosphatidylcholine to phosphatidylethanolamine predicts survival after partial hepatectomy in mice, Hepatology 55 (4) (2012) 1094-1102.

[32] C.A. Redlich, J.N. Grauer, A.M. Van Bennekum, S.L. Clever, R.B. Ponn, W.S. Blaner, Characterization of carotenoid, vitamin A, and alpha-tocopheral levels in human lung tissue and pulmonary macrophages, Am J Respir Crit Care Med 154 (5) (1996) 1436-1443.

[33] E. Albano, E. Mottaran, M. Vidali, E. Reale, S. Saksena, G. Occhino, A.D. Burt, C.P. Day, Immune response towards lipid peroxidation products as a predictor of progression of non-alcoholic fatty liver disease to advanced fibrosis, Gut 54 (7) (2005) 987-993.

[34] R.N. Hardwick, C.D. Fisher, M.J. Canet, A.D. Lake, N.J. Cherrington, Diversity in antioxidant response enzymes in progressive stages of human nonalcoholic fatty liver disease, Drug Metab Dispos 38 (12) (2010) 2293-2301.

[35] S.A. Noeman, H.E. Hamooda, A.A. Baalash, Biochemical study of oxidative stress markers in the liver, kidney and heart of high fat diet induced obesity in rats, Diabetol Metab Syndr 3 (1) (2011) 17.

[36] E. Buzzetti, M. Pinzani, E.A. Tsochatzis, The multiple-hit pathogenesis of non-alcoholic fatty liver disease (NAFLD), Metabolism 65 (8) (2016) 1038-1048.

[37] J.K. Dowman, J.W. Tomlinson, P.N. Newsome, Pathogenesis of non-alcoholic fatty liver disease, QJM 103 (2) (2010) 71-83.

[38] Y.M. Nan, W.J. Wu, N. Fu, B.L. Liang, R.Q. Wang, L.X. Li, S.X. Zhao, J.M. Zhao, J. Yu, Antioxidants vitamin E and 1-aminobenzotriazole prevent experimental non-alcoholic steatohepatitis in mice, Scand J Gastroenterol 44 (9) (2009) 1121-1131.

[39] N. Phung, N. Pera, G. Farrell, I. Leclercq, J.Y. Hou, J. George, Pro-oxidant-mediated hepatic fibrosis and effects of antioxidant intervention in murine dietary steatohepatitis, Int J Mol Med 24 (2) (2009) 171-180.

[40] M.Y. Chung, S.F. Yeung, H.J. Park, J.S. Volek, R.S. Bruno, Dietary alpha- and gamma-tocopherol supplementation attenuates lipopolysaccharide-induced oxidative stress and inflammatory-related responses in an obese mouse model of nonalcoholic steatohepatitis, J Nutr Biochem 21 (12) (2010) 1200-1206.

[41] A.J. Sanyal, N. Chalasani, K.V. Kowdley, A. McCullough, A.M. Diehl, N.M. Bass, B.A. Neuschwander-Tetri, J.E. Lavine, J. Tonascia, A. Unalp, M. Van Natta, J. Clark, E.M. Brunt, D.E. Kleiner, J.H. Hoofnagle, P.R. Robuck, Pioglitazone, vitamin E, or placebo for nonalcoholic steatohepatitis, N Engl J Med 362 (18) (2010) 1675-1685.

[42] J.E. Lavine, J.B. Schwimmer, M.L. Van Natta, J.P. Molleston, K.F. Murray, P. Rosenthal, S.H. Abrams, A.O. Scheimann, A.J. Sanyal, N. Chalasani, J. Tonascia, A. Unalp, J.M. Clark, E.M. Brunt, D.E. Kleiner, J.H. Hoofnagle, P.R. Robuck, Effect of vitamin E or metformin for treatment of nonalcoholic fatty liver disease in children and adolescents: the TONIC randomized controlled trial, JAMA 305 (16) (2011) 1659-1668.

[43] K. Begriche, A. Igoudjil, D. Pessayre, B. Fromenty, Mitochondrial dysfunction in NASH: causes, consequences and possible means to prevent it, Mitochondrion 6 (1) (2006) 1-28.

[44] Y.K. Zhang, R.L. Yeager, Y. Tanaka, C.D. Klaassen, Enhanced expression of Nrf2 in mice attenuates the fatty liver produced by a methionine- and choline-deficient diet, Toxicol Appl Pharmacol 245 (3) (2010) 326-334.

[45] M. Perez-Carreras, P. Del Hoyo, M.A. Martin, J.C. Rubio, A. Martin, G. Castellano, F. Colina, J. Arenas, J.A. Solis-Herruzo, Defective hepatic mitochondrial respiratory chain in patients with nonalcoholic steatohepatitis, Hepatology 38 (4) (2003) 999-1007.

[46] S. Dasarathy, Y. Yang, A.J. McCullough, S. Marczewski, C. Bennett, S.C. Kalhan, Elevated hepatic fatty acid oxidation, high plasma fibroblast growth factor 21, and fasting bile acids in nonalcoholic steatohepatitis, Eur J Gastroenterol Hepatol 23 (5) (2011) 382-388.

[47] A.P. Rolo, J.S. Teodoro, C.M. Palmeira, Role of oxidative stress in the pathogenesis of nonalcoholic steatohepatitis, Free Radic Biol Med 52 (1) (2012) 59-69.

[48] D. Pessayre, Role of mitochondria in non-alcoholic fatty liver disease, J Gastroenterol Hepatol 22 Suppl 1 (2007) S20-27.

[49] D. Wu, A.I. Cederbaum, Oxidative stress and alcoholic liver disease, Semin Liver Dis 29 (2) (2009) 141-154.

[50] M. Sawada, T. Kiyono, S. Nakashima, J. Shinoda, T. Naganawa, S. Hara, T. Iwama, N. Sakai, Molecular mechanisms of TNF-alpha-induced ceramide formation in human glioma cells: P53-mediated oxidant stress-dependent and -independent pathways, Cell Death Differ 11 (9) (2004) 997-1008.

[51] J.M. Haus, S.R. Kashyap, T. Kasumov, R. Zhang, K.R. Kelly, R.A. Defronzo, J.P. Kirwan, Plasma ceramides are elevated in obese subjects with type 2 diabetes and correlate with the severity of insulin resistance, Diabetes 58 (2) (2009) 337-343.

[52] A.H. Merrill, Jr., S. Lingrell, E. Wang, M. Nikolova-Karakashian, T.R. Vales, D.E. Vance, Sphingolipid biosynthesis de novo by rat hepatocytes in culture. Ceramide and sphingomyelin are associated with, but not required for, very low density lipoprotein secretion, J Biol Chem 270 (23) (1995) 13834-13841.

[53] A. Gomez-Munoz, Modulation of cell signalling by ceramides, Biochim Biophys Acta 1391 (1) (1998) 92-109.

[54] A. Gomez-Munoz, P.A. Duffy, A. Martin, L. O'Brien, H.S. Byun, R. Bittman, D.N. Brindley, Short-chain ceramide-1-phosphates are novel stimulators of DNA synthesis and cell division: antagonism by cell-permeable ceramides, Mol Pharmacol 47 (5) (1995) 833-839.

Conclusions

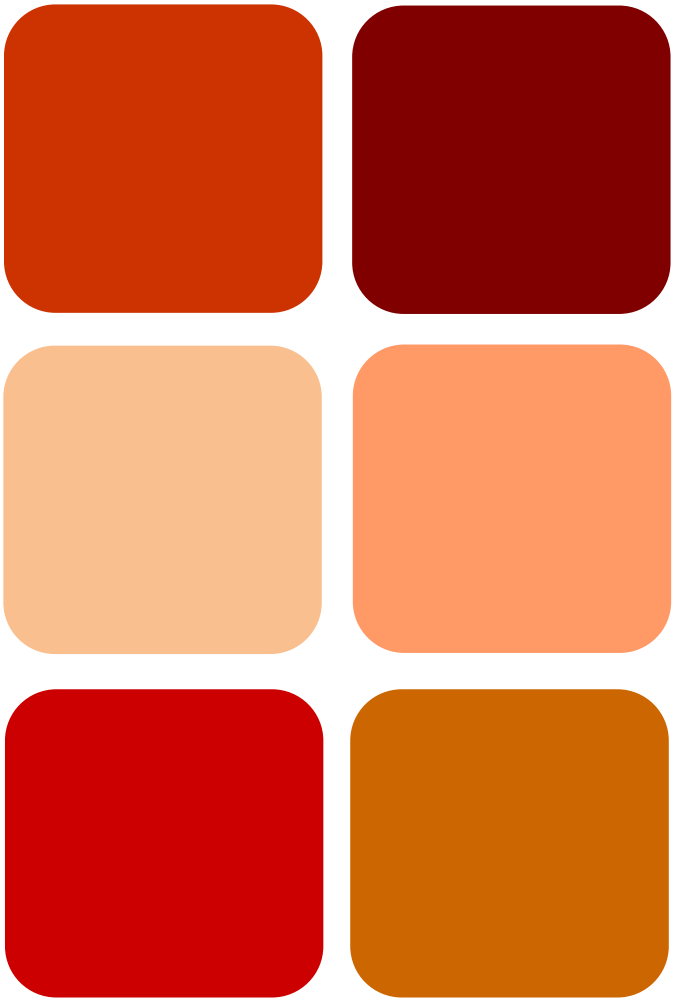

Conclusions

From the results obtained in this thesis, the following conclusions may be drawn.

1. CSE exposure promotes the release of MCP-1 from lung epithelial cells, which stimulates the migration and activation of THP-1 monocytes. ROCK1, but not ROCK2, is necessary for MCP-1 release, while AKT2, CerK and exogenous C1P elicit opposite effects.

2. CSE exposure promotes the loss of E-cadherin. The mechanism involves ERK2, but not ERK1. By contrast, the PI3K/AKT2 pathway promotes maintenance of E-cadherin.

3. PEMT is necessary for differentiation of pre-adipocytes into mature adipose cells.

4. Exogenous C1P inhibits adipogenesis through downregulation of PEMT expression.

5. *Pemt*$^{-/-}$ mice fed a HFD present abnormal sphingolipid metabolism, with elevation of ceramides, sphingomyelin, sphinganine, sphingosine, 1-deoxyceramides, and C26:1 C1P as well as higher expression of mRNAs for Asah1 and CerK.

6. Vitamin E supplementation restores Asah1 and CerK mRNA, as well as sphingolipid levels. It also improves VLDL-TG secretion, normalizes cholesterol metabolism, and reduces hepatic oxidative stress, inflammation and fibrosis, all of which would prevent the progression from simple steatosis to steatohepatitis.

Appendix

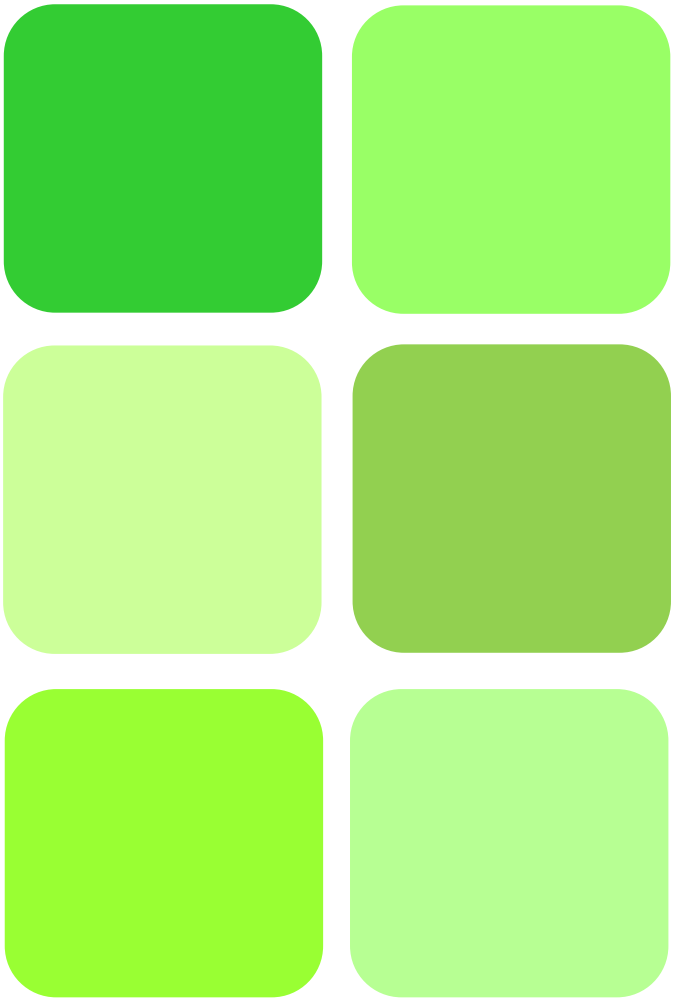

Scientific contributions

1

Phosphatidic acid inhibits ceramide 1-phosphate-stimulated macrophage migration.

Ouro A, Arana L, Rivera IG, Ordoñez M, Gomez-Larrauri A, **Presa N**, Simón J, Trueba M, Gangoiti P, Bittman R, Gomez-Muñoz A. Biochem Pharmacol. 2014 Dec 15;92(4):642-50.

Abstract

Ceramide 1-phosphate (C1P) was recently demonstrated to potently induce cell migration. This action could only be observed when C1P was applied exogenously to cells in culture, and was inhibited by pertussis toxin. However, the mechanisms involved in this process are poorly understood. In this work, we found that phosphatidic acid (PA), which is structurally related to C1P, displaced radiolabeled C1P from its membrane-binding site and inhibited C1P-stimulated macrophage migration. This effect was independent of the saturated fatty acid chain length or the presence of a double bond in each of the fatty acyl chains of PA. Treatment of RAW264.7 macrophages with exogenous phospholipase D (PLD), an enzyme that produces PA from membrane phospholipids, also inhibited C1P-stimulated cell migration. Likewise, PA or exogenous PLD inhibited C1P-stimulated extracellularly regulated kinases (ERK) 1 and 2 phosphorylation, leading to inhibition of cell migration. However, PA did not inhibit C1P-stimulated Akt phosphorylation. It is concluded that PA is a physiological regulator of C1P-stimulated macrophage migration. These actions of PA may have important implications in the control of pathophysiological functions that are regulated by C1P, including inflammation and various cellular processes associated with cell migration such as organogenesis or tumor metastasis.

2

Sphingomyelinase D/ceramide 1-phosphate in cell survival and inflammation.

Rivera IG, Ordoñez M, **Presa N**, Gomez-Larrauri A, Simón J, Trueba M, Gomez-Muñoz A. Toxins (Basel). 2015 Apr 29;7(5):1457-66.

Abstract

Sphingolipids are major constituents of biological membranes of eukaryotic cells. Many studies have shown that sphingomyelin (SM) is a major phospholipid in cell bilayers and is mainly localized to the plasma membrane of cells, where it serves both as a building block for cell architecture and as a precursor of bioactive sphingolipids. In particular, upregulation of (C-type) sphingomyelinases will produce ceramide, which regulates many physiological functions including apoptosis, senescence, or cell differentiation. Interestingly, the venom of some arthropodes including spiders of the genus Loxosceles, or the toxins of some bacteria such as Corynebacterium tuberculosis, or Vibrio damsela possess high levels of D-type sphingomyelinase (SMase D). This enzyme catalyzes the hydrolysis of SM to yield ceramide 1-phosphate (C1P), which promotes cell growth and survival and is a potent pro-inflammatory agent in different cell types. In particular, C1P stimulates cytosolic phospholipase A2 leading to arachidonic acid release and the subsequent formation of eicosanoids, actions that are all associated to the promotion of inflammation. In addition, C1P potently stimulates macrophage migration, which has also been associated to inflammatory responses. Interestingly, this action required the interaction of C1P with a specific plasma membrane receptor, whereas accumulation of intracellular C1P failed to stimulate chemotaxis. The C1P receptor is coupled to Gi proteins and activates of the PI3K/Akt and MEK/ERK1-2 pathways upon ligation with C1P. The proposed review will address novel aspects on the control of inflammatory responses by C1P and will highlight the molecular mechanisms whereby C1P exerts these actions.

3

Caged ceramide 1-phosphate (C1P) analogs: Novel tools for studying C1P biology.

Gomez-Muñoz A, Gangoiti P, Rivera IG, **Presa N**, Gomez-Larrauri A, Ordoñez M. Chem Phys Lipids. 2016 Jan;194:79-84.

Abstract

Ceramide 1-phosphate (C1P) is a bioactive sphingolipid metabolite that is produced in cells by the action of ceramide kinase (CerK) acting upon ceramide, and is also found in the circulation. C1P was first demonstrated to be mitogenic and antiapoptotic in different cell types, and was later shown to induce cell migration. Understanding the precise mechanisms by which C1P exerts its biological effects has been possible using specific photosensitive caged C1P analogues synthesized by Robert Bittman's group. These compounds are cell permeable, bypass cell plasma membrane receptors, and can be released into the cytosol upon light irradiation, thereby allowing precise determination of the intracellular mechanisms of actions of C1P. Two derivatives of N-palmitoyl-ceramide 1-phosphate have been used in most studies. In one C1P derivative the cage was 7-(N,N-diethylamino)coumarin (DECM-C1P) while in the other it was a 4-bromo-5-hydroxy-2-nitrobenzhydryl moiety (BHNB-C1P). The uncaging process released C1P in the cytosol, and this was accompanied by stimulation of cell proliferation, inhibition of apoptosis, and production of low levels of reactive oxygen species. However, intracellular accumulation of C1P did not affect chemotaxis. The caged C1P analogues allowed distinction between the extracellular events evoked by C1P, as for example through interaction with a putative cell-surface receptor, from its intracellular effects.

4

Control of inflammatory responses by ceramide, sphingosine 1-phosphate and ceramide 1-phosphate.

Gomez-Muñoz A, **Presa N**, Gomez-Larrauri A, Rivera IG, Trueba M, Ordoñez M. Prog Lipid Res. 2016 Jan;61:51-62.

Abstract

Inflammation is a network of complex processes involving a variety of metabolic and signaling pathways aiming at healing and repairing damage tissue, or fighting infection. However, inflammation can be detrimental when it becomes out of control. Inflammatory mediators involve cytokines, bioactive lipids and lipid-derived metabolites. In particular, the simple sphingolipids ceramides, sphingosine 1-phosphate, and ceramide 1-phosphate have been widely implicated in inflammation. However, although ceramide 1-phosphate was first described as pro-inflammatory, recent studies show that it has anti-inflammatory properties when produced in specific cell types or tissues. The biological functions of ceramides and sphingosine 1-phosphate have been extensively studied. These sphingolipids have opposing effects with ceramides being potent inducers of cell cycle arrest and apoptosis, and sphingosine 1-phosphate promoting cell growth and survival. However, the biological actions of ceramide 1-phosphate have only been partially described. Ceramide 1-phosphate is mitogenic and anti-apoptotic, and more recently, it has been demonstrated to be key regulator of cell migration. Both sphingosine 1-phosphate and ceramide 1-phosphate are also implicated in tumor growth and dissemination. The present review highlights new aspects on the control of inflammation and cell migration by simple sphingolipids, with special emphasis to the role played by ceramide 1-phosphate in controlling these actions.

5

Ceramide 1-phosphate regulates cell migration and invasion of human pancreatic cancer cells.

Rivera IG, Ordoñez M, **Presa N**, Gangoiti P, Gomez-Larrauri A, Trueba M, Fox T, Kester M, Gomez-Muñoz A. Biochem Pharmacol. 2016 Feb 15;102:107-119.

Abstract

Pancreatic cancer is an aggressive and devastating disease characterized by invasiveness, rapid progression and profound resistance to treatment. Despite years of intense investigation, the prognosis of this type of cancer is poor and there is no efficacious treatment to overcome the disease. Using human PANC-1 and MIA PaCa-2 cells, we demonstrate that the bioactive sphingolipid ceramide 1-phosphate (C1P) increases pancreatic cancer cell migration and invasion. Treatment of these cells with selective inhibitors of phosphatidylinositol 3-kinase (PI3K), Akt1, or mammalian target of rapamycin 1 (mTOR1), or with specific siRNAs to silence the genes encoding these kinases, resulted in potent inhibition of C1P-induced cell migration and invasion. Likewise, the extracellularly regulated kinases 1 and 2 (ERK1-2), and the small GTPase RhoA, which regulates cytoskeleton reorganization, were also found to be implicated in C1P-stimulated ROCK1-dependent cancer cell migration and invasion. In addition, pre-treatment of the cancer cells with pertussis toxin abrogated C1P-induced cell migration, suggesting the intervention of a Gi protein-coupled receptor in this process. Pancreatic cancer cells engineered to overexpress ceramide kinase (CerK), the enzyme responsible for C1P biosynthesis in mammalian cells, showed enhanced spontaneous cell migration that was potently blocked by treatment with the selective CerK inhibitor NVP-231, or by treatment with specific CerK siRNA. Moreover, overexpression of CerK with concomitant elevations in C1P enhanced migration of pancreatic cancer cells. Collectively, these data demonstrate that C1P is a key regulator of pancreatic cancer cell motility, and suggest that targeting CerK expression/activity and C1P may be relevant factors for controlling pancreatic cancer cell dissemination.

6

Regulation of cell migration and inflammation by ceramide 1-phosphate.

Presa N, Gomez-Larrauri A, Rivera IG, Ordoñez M, Trueba M, Gomez-Muñoz A. Biochim Biophys Acta. 2016 May;1861(5):402-9.

Abstract

Ceramide 1-phosphate (C1P) is a bioactive sphingolipid metabolite first shown to regulate cell growth and death. Subsequent studies revealed that C1P was a potent stimulator of cytosolic phospholipase A2 (cPLA2) with ensuing release of arachidonic acid and prostaglandin biosynthesis. The latter findings placed C1P on the list of pro-inflammatory metabolites. More recently, C1P was found to potently stimulate cell migration, an action that is associated to diverse physiological effects, as well as to inflammatory responses and tumor dissemination. The implication of C1P in inflammation has gained further interest in the last few years due to the discovery that it can exert anti-inflammatory actions in some cell types and tissues. In particular, C1P has been demonstrated to inhibit pro-inflammatory cytokine release and blockade of the pro-inflammatory transcription factor NF-κB in some cell types, as well as to reduce airway inflammation and lung emphysema. The present review is focused on novel aspects of C1P regulation of cell migration and the impact of C1P as novel anti-inflammatory agent.

7

Implication of matrix metalloproteinases 2 and 9 in ceramide 1-phosphate-stimulated macrophage migration.

Ordoñez M, Rivera IG, **Presa N**, Gomez-Muñoz A. Cell Signal. 2016 Aug;28(8):1066-74.

Abstract

Cell migration is a complex biological function involved in both physiologic and pathologic processes. Although this is a subject of intense investigation, the mechanisms by which cell migration is regulated are not completely understood. In this study we show that the bioactive sphingolipid ceramide 1-phosphate (C1P), which is involved in inflammatory responses, causes upregulation of metalloproteinases (MMP) -2 and -9 in J774A.1 macrophages. This effect was shown to be dependent on stimulation of phosphatidylinositol 3-kinase (PI3K) and extracellularly regulated kinases 1-2 (ERK1-2) as demonstrated by treating the cells with specific siRNA to knockdown the p85 regulatory subunit of PI3K, or ERK1-2. Inhibition of MMP-2 or MMP-9 pharmacologically or with specific siRNA to silence the genes encoding these MMPs abrogated C1P-stimulated macrophage migration. Also, C1P induced actin polymerization and potently increased phosphorylation of the focal adhesion protein paxillin, which are essential factors in the regulation of cell migration. As expected, blockade of paxillin activation with specific siRNA significantly reduced actin polymerization. In addition, inhibition of actin polymerization with cytochalasin D completely blocked C1P-induced MMP-2 and -9 expression as well as C1P-stimulated macrophage migration. It was also observed that pertussis toxin (Ptx) inhibited Akt, ERK1-2, and paxillin phosphorylation, and completely blocked cell migration. The latter findings support the notion that C1P-stimulated macrophage migration is a receptor mediated effect, and point to MMP-2 and -9 as possible therapeutic targets to control inflammation.

8

Implication of Ceramide Kinase in Adipogenesis.

Ordoñez M, **Presa N**, Trueba M, Gomez-Muñoz A. Mediators Inflamm. 2017;2017:9374563.

Abstract

Ceramide kinase (CerK) plays a critical role in the regulation of cell growth and survival and has been implicated in proinflammatory responses. In this work, we demonstrate that CerK regulates adipocyte differentiation, a process associated with obesity, which causes chronic low-grade inflammation. CerK was upregulated during differentiation of 3T3-L1 preadipocytes into mature adipocytes. Noteworthy, knockdown of CerK using specific siRNA to silence the gene encoding this kinase resulted in substantial decrease of lipid droplet formation and potent depletion in the content of triacylglycerols in the adipocytes. Additionally, CerK knockdown caused blockade of leptin secretion, an adipokine that is crucial for regulation of energy balance in the organism and that is increased in the obese state. Moreover, CerK gene silencing decreased the expression of peroxisome proliferator-activated receptor gamma (PPARγ), which is considered the master regulator of adipogenesis. It can be concluded that CerK is a novel regulator of adipogenesis, an action that may have potential implications in the development of obesity, and that targeting this kinase may be beneficial for treatment of obesity-associated diseases.

9

Regulation of adipogenesis by ceramide 1-phosphate.

Ordoñez M, **Presa N**, Dominguez-Herrera A, Trueba M, Gomez-Muñoz A. Exp Cell Res. 2018 Sep 26. pii: S0014-4827(18)30661-X.

Abstract

We showed previously that ceramide kinase (CerK) expression increases during adipogenesis pointing to a relevant role of intracellular C1P in this process. In the present work we demonstrate that administration of exogenous C1P inhibits the differentiation of 3T3-L1 pre-adipocytes into mature adipocytes through a mechanism involving activation of extracellularly regulated kinases (ERK) 1-2. Exogenous C1P reduced the accumulation of lipid droplets and the content of triacylglycerol in these cells, and potently inhibited the expression of the early and late adipogenic markers C/EBPβ and PPARγ, respectively. C1P also reduced the secretion of leptin, which is a crucial regulator of energy balance and appetite in the organism, and is considered to be a late marker of adipogenesis. Interestingly, all of these C1P actions were reversed by pertussis toxin, suggesting the intervention of a Gi protein-coupled receptor previously identified for C1P, in this process. Also, exogenous C1P significantly reduced CerK activity. Altogether, the data presented in this work suggest that exogenous C1P may balance adipogenesis, and that targeting CerK may be a novel way for potential applications in the treatment of obesity or other inflammation-associated diseases.

10

Vitamin E alleviates non-alcoholic fatty liver disease in phosphatidylethanolamine N-methyltransferase deficient mice.

Presa N, Clugston RD, Lingrell S, Kelly SE, Merril AH Jr, Jana S, Kassiri Z, Gomez-Muñoz A, Vance DE, Jacobs RL, van der Veen JN.

Abstract

Phosphatidylethanolamine N-methyltransferase (PEMT) converts phosphatidylethanolamine (PE) to phosphatidylcholine (PC), mainly in the liver. Pemt$^{-/-}$ mice are protected from high-fat diet (HFD)-induced obesity and insulin resistance, but develop severe non-alcoholic fatty liver disease (NAFLD) when fed a HFD, mostly due to impaired VLDL secretion. Oxidative stress is thought to be an essential factor in the progression from simple steatosis to steatohepatitis. Vitamin E is an antioxidant that has been clinically used to improve NAFLD pathology. Our aim was to determine whether supplementation of the diet with vitamin E could attenuate HFD-induced hepatic steatosis and its progression to NASH in Pemt$^{-/-}$ mice. Treatment with vitamin E (0.5 g/kg) for 3 weeks improved VLDL-TG secretion and normalized cholesterol metabolism, but failed to reduce hepatic TG content. Moreover, vitamin E treatment was able to reduce hepatic oxidative stress, inflammation and fibrosis. We also observed abnormal ceramide metabolism in Pemt$^{-/-}$ mice fed a HFD, with elevation of ceramides and other sphingolipids and higher expression of mRNAs for acid ceramidase (Asah1) and ceramide kinase (Cerk). Interestingly, vitamin E supplementation restored Asah1 and Cerk mRNA and sphingolipid levels. Together this study shows that vitamin E treatment efficiently prevented the progression from simple steatosis to steatohepatitis in mice lacking PEMT.